THE UNIVERSITY OF SYDNEY

DOCTORAL THESIS

Gravitational Waves and Fundamental Physics

Author:
Cyril Oscar LAGGER

Supervisor:
Associate Professor Archil KOBAKHIDZE

A thesis submitted in fulfillment of the requirements for the degree of Doctor of Philosophy

in the

Particle Physics Group
School of Physics - Faculty of Science

July 2019

Declaration of Authorship

I, Cyril Oscar Lagger, declare that this thesis titled, "Gravitational Waves and Fundamental Physics" and the work presented in it are my own. I confirm that:

- This work was done wholly or mainly while in candidature for a research degree at the University of Sydney.
- Where I have consulted the published work of others, this is always clearly attributed
- Where I have quoted from the work of others, the source is always given.
- I have acknowledged all main sources of help.
- The author convention for all my publications below is alphabetical.
- Chapters 1, 2, 3 and 8 are entirely my own work.
- Chapter 4 has been published as [1]. Together with the co-authors I designed the research study. Together with Adrian Manning I performed all computations and data analysis present in the article. I wrote the main part of the manuscript. Note that the results of [1] have also been presented in the essay article [2] which received an Honorable Mention in the 2017 Essay Competition of the Gravity Research Foundation.
- Chapters 5 and 6 have been published as [3] and [4]. For the coherence of this thesis, the first parts of [3, 4] have been joined together to form Chapter 5 whereas the second parts of these articles form Chapter 6. Small changes have been made to ensure the consistency of the text. Regarding [3], I designed the research study together with the co-authors. Together with Jason Yue and Adrian Manning I performed all analytic computations and data analysis. Together with Adrian Manning I numerically computed the dynamics of the phase transition and the production of gravitational waves for our model. I designed and wrote the code to solve the time-dependent bounce PDE over a lattice. I wrote the main part of the manuscript. Regarding [4], I designed the research study together with the co-authors. Together with Suntharan Arunasalam, Shelley Liang and Albert Zhou I performed all analytic computations and data analysis. Together with Shelley Liang I numerically evaluated the phenomenological predictions of our model. Together with Suntharan Arunasalam and Albert Zhou I studied and evaluated the cosmological predictions of our model.

- Chapter 7 has been published as [5]. I am the single author and I have contributed entirely to this work. Some preliminary results have been obtained during my Master thesis performed as a collaboration between the EPF Lausanne and the University of Sydney in 2015. The article [5] has been published during my PhD.

Cyril Oscar Lagger
July 2019

As supervisor for the candidature upon which this thesis is based, I can confirm that the authorship attribution statements above are correct.

Archil Kobakhidze
July 2019

Abstract

Doctor of Philosophy

Gravitational Waves and Fundamental Physics

by Cyril Oscar LAGGER

This thesis investigates the theoretical implications of gravitational waves for particle physics and cosmology. The main purpose is to show that studying gravitational waves does not only give us information about their own properties but also provides us with knowledge towards a better understanding of the structure and content of the Universe. Therefore we first give an overview of the current state of fundamental physics whose two pillars are general relativity and quantum field theory. We also emphasize the limitations of these theories and what are some of the main unsolved problems in physics. We discuss in particular where gravitational waves may come into play to shed new light on such mysteries.

After such general considerations, we move to specific research topics. More precisely, we make use of the gravitational wave signal GW150914, announced by LIGO and Virgo collaborations in 2016, to constrain the scale of non-commutative space-time. Assuming that space-time admits some quantum fuzziness, we explicitly compute the equations of motion of a binary black hole system and the associated generation of gravitational waves in the post-Newtonian formalism. Compared to general relativity, we show that leading non-commutative effects produce a correction of order $(v/c)^4$ to the motion of the system. For this correction to be consistent with the GW150914 signal, we find that the scale of non-commutativity is bounded to be below or at the order of the Planck scale. This represents an improvement of ~ 15 orders of magnitude compared to previous constraints.

Our second research area focuses on the production of gravitational waves from cosmological phase transitions. First, we show how the dynamics of the electroweak and QCD phase transitions heavily relies on the particle content of the Universe as well as their interactions. We consider two unrelated extensions of the standard model: a model implementing a non-linear realization of the electroweak gauge group and a model with hidden scale invariance involving a very light dilaton. In the first case, the Higgs vacuum configuration is altered by a cubic coupling giving the possibility to have a strong and prolonged electroweak first-order transition. In our second model, we show that the electroweak transition cannot proceed until it is triggered by a first-order QCD chiral symmetry breaking around 130 MeV. We then compute the stochastic gravitational wave background produced during these two first-order phase transitions. The non-linearly realized model predicts signals that can be detected by pulsar timing arrays such as the future SKA. Although the peak frequency of gravitational waves predicted by the scale invariant model is also expected to be in the range of pulsar timing arrays, further work is required to precisely determine their amplitude.

Finally, we investigate the backreaction of particle production on false vacuum decay. We present a formalism which makes use of the reduced density matrix of the system to quantify the impact of these particles on the decay rate of a scalar field in flat space-time. We then apply this method to a toy model potential and we exhibit different scenarios with either significant or negligible backreaction.

Acknowledgements

First and foremost, I wish to thank my supervisor Archil Kobakhidze for his guidance and support. I am particularly thankful for his dedication towards my projects and for our endless hours of discussion. He gave me the freedom and opportunity to work on multiple interesting topics and to broaden my knowledge of physics. I would also like to express my gratitude for his administrative support, notably for his help when I arrived in Australia a few years ago.

I would also like to thank my auxiliary supervisor Michael Schmidt and my collaborators Suntharan Arunasalam, Robert Foot, Shelley Liang, Adrian Manning, Jason Yue and Albert Zhou for all the work done together.

I am grateful to the entire particle physics group at the University of Sydney for the insightful discussions, meetings and Journal Clubs which have given me the chance to reinforce my general understanding of physics. This includes all the people I had the chance to meet during the last few years and notably all the students of room 342. It was great sharing this office space with you.
I would also like to thank Mikhail Shaposhnikov and the laboratory of particle physics and cosmology at EPF Lausanne for their hospitality.

I would like to acknowledge the ARC Centre of Excellence for Particle Physics at the Terascale (CoEPP) who has supported this work and also given the opportunity to strengthen the particle physics community in Australia.

Finally, I want to express a very special gratitude to my friends and to my family who never stopped encouraging me and helping me during all the various stages of my academic and personal life. In particular, thank you Anaïs for following me all around the world and keeping me sane in the process.

Contents

Chapter 1

Introduction

This thesis presents the physics of gravitational waves and how they can be used to study fundamental aspects of the Universe. It synthesizes four years of research performed at the interplay between particle physics and cosmology [1–5]. Such topics are inherently complex, both conceptually and mathematically, but our introductory Chapter tries to give an overview of the subject with as little technicality as possible. We take the time to discuss the most important concepts of fundamental physics in simple terms such that both non-physicists and physicists may have the opportunity to appreciate the motivations and the results of our research. Then Chapters 2 and 3 focus on the technical formulation of general relativity and quantum field theory, the two pillars of modern physics. This allows us to give a precise meaning to specific concepts such as gravitational waves, quantum particles or cosmological phase transitions. We can then move to the core of this thesis, namely Chapters 4 to 7 which contain a precise description of both our research methodology and results. We show in particular how gravitational waves can provide new information about the content and dynamics of the Universe. Finally, Chapter 8 concludes this report and suggests future research directions.

The essence of this work relies on a fascination to understand the reality and a desire to answer fundamental questions about its nature. What is the structure of the Universe? What is it made of? How do we explain the phenomena occurring around us? Throughout history, humankind managed to gather a considerable amount of knowledge regarding such questions, leading to conceptual, technological and social progress. In our context of interest, the discovery of the Higgs boson in 2012 [6, 7] and the observation of gravitational waves in 2015 [8] are examples of such recent milestones. On the other hand, it is clear that a lot of things related to the Universe remain obscure to us today.

Among the various lines of research that can be imagined to push our knowledge forward, we propose here that studying the properties of gravitational waves is a promising way. This is because they are, from their very definition, related to fundamental properties of the Universe. Gravitational waves are what physicists describe as some "ripples" of space-time which propagate at the speed of light. This concept originates from two very important, but far from obvious, statements. First, it tells that space and time are neither independent from each other nor absolute. Second, it says that space and time interact with the matter in the Universe. We start our discussion by exploring these ideas in more details and by looking how space, time and matter are conceived off by scientists.

1.1 The nature of space, time and matter

1.1.1 Going beyond the intuition

According to human everyday life experience, the world seems to be made of different types of *objects* capable of *moving* in a 3-dimensional *geometric substrate*. This naturally gives rise to the three distinct notions of *matter*, *time* and *space*. As such, the origin of these concepts only relies on some intuitive and anthropocentric perceptions. It is therefore important to objectively question what are their reality, properties and relationships. Historically, philosophy and physics have attached a lot of importance to this task and a lot of progress has been achieved (see e.g. [9–12]). However, this text will illustrate several times how various aspects of these concepts are still poorly understood today. The quest towards a better understanding of the fundamental properties of our Universe remains fully active and keeps motivating numerous researchers.

To establish an objective understanding of concepts such as space, time and matter, we have to ask how to go beyond the aforementioned intuitive perception of reality. This is usually achieved through the scientific method which is very briefly reminded here.[1] It starts by an in-depth and skeptical observation of selected phenomena, followed by the formulation of a set of hypothesis *induced* from this observation. This set of laws, called a model, is usually formulated in terms of mathematical equations. To be considered scientific, a model should then allow the *deduction* of predictions which can be compared to the results of a specifically designed experiment. A model is thus said to be *refutable* as any disagreement between prediction and experiment gives the opportunity to discard it.

Taken rigorously, no scientific model can ever be considered as fundamentally correct or true. There should always be the possibility for an experiment to contradict such model. It does not mean that science *per se* is unable to give any relevant information about the Universe. It is rather an ever ongoing process by which new theories emerge and, in case they are judged to provide a more accurate description, supersede previous ones. We can also think of a theory as being valid only for a specific set of phenomena and accept that it fails to describe situations occurring outside its scope. All in all, it is important to keep in mind that science is not a linear process and that at a given time in history there is often more than one theory that is able to describe the same phenomena. It is the difficult task of scientists to propose new experiments and theoretical arguments to decide which ones are the more consistent with reality. This usually leads the scientific community to define as *consensus* the models which provide the largest range of validity and have survived the most experiments.

It is not the aim of this thesis to detail the various theories that have been proposed through the history of physics to model space, time and matter. It is sufficient for our purpose to focus on how ideas evolved from *Newtonian mechanics* to the modern consensus which includes general relativity and quantum field theory. As they are the building blocks of modern physics, these models and their underlying principles are presented in this introduction in non-technical terms.

[1] The scientific method is an active subject of discussion in science and philosophy of science. Different interpretations and methodology have been defined by different authors and we refer the reader to the specialized literature (see e.g. [13, 14]) for more details.

1.1.2 Classical mechanics

Absolute space and time

Classical mechanics provides a description of many physical phenomena, such as the motion of macroscopic and astronomical objects. It has been rigorously formalized by Newton (1642-1727) more than 300 years ago in his *Philosophiæ Naturalis Principia Mathematica* [9]. In this text, he explicitly expresses what are his assumptions about the nature of time and space:

> Absolute, true and mathematical time, of itself, and from its own nature flows equably without regard to anything external, and by another name is called duration: relative, apparent and common time, is some sensible and external (whether accurate or unequable) measure of duration by the means of motion, which is commonly used instead of true time [...]
>
> Absolute space, in its own nature, without regard to anything external, remains always similar and immovable. Relative space is some movable dimension or measure of the absolute spaces; which our senses determine by its position to bodies: and which is vulgarly taken for immovable space [...] ([9, p. 77])

Two different and important concepts appear here. Newton assumes first the existence of some absolute space and time where absolute means that they are not affected by the motion and interactions of objects. However, Newton also realizes that the perception of physical events taking place in this absolute backdrop is somehow dependent on the observer. This is why he introduces some relative space and time from where originates the idea of *frame of reference*. To speak about the motion of an object, an observer has to choose some physical system (the frame) which he considers as fixed (as a reference) and relative to which any displacement will be measured.

Two observers in two different frames are therefore expected to give two different description of the same phenomenon. Typically, an object perceived as static in a first frame can be seen as moving in a second one. What sounds like some intrinsic arbitrariness has actually been the source of one the most important concepts in the history of physics, namely the *principle of relativity*. In Newtonian mechanics, this principle postulates the existence of a set of reference frames, called *inertial reference frames*, in which the laws of physics should be the same as the laws valid in absolute space and time. If such frames exist, what would their nature be? Similarly to some previous ideas [15] of Galilei (1564-1642), Newton proposes that they are all the frames moving in straight lines and at constant velocity compared to absolute space. As an example, the results of an experiment performed by an observer at the surface of the earth should be the same as the results obtained by an observer doing the same experiment in a train moving at constant velocity compared to the ground.

All these ideas can be summarized by the following set of principles underlying classical mechanics:

(P1) There exists an absolute space.

(P2) An inertial frame is any frame of reference moving in straight line at constant velocity compared to absolute space.

(P3) There exists an absolute time, which is the same in all inertial reference frames.

(P4) The laws of physics are the same in all inertial frames (*Principle of relativity*).

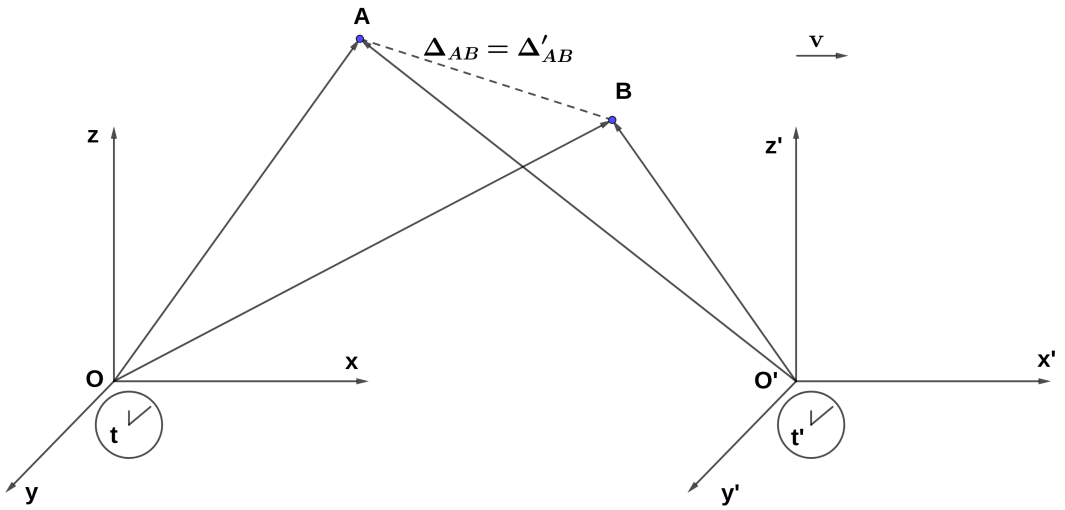

FIGURE 1.1: Two events A and B as seen from two inertial frames F and F' moving at constant velocity $\mathbf{v}$ respective to each other.

Coordinate system, Euclidean space and Galilean transformation

The previous principles can be formalized more quantitatively by introducing the concept of a *coordinate system*. As illustrated in Figure 1.1, an observer in a given frame can specify an event by its time t and its position $\mathbf{x} = (x, y, z)$, relatively to some origin O at $(t = 0, \mathbf{x} = \mathbf{0})$. This four real numbers are called the coordinates of the event.[2] It is now possible to give a precise geometrical meaning to the notion of straight line introduced by the principle **(P2)**. A straight line corresponds to the shortest path between two locations $\mathbf{x}_A$ and $\mathbf{x}_B$. Their distance (in Cartesian coordinates) is measured by the well-known formula

$$\Delta d_{AB} = \sqrt{(x_A - x_B)^2 + (y_A - y_B)^2 + (z_A - z_B)^2}. \tag{1.1}$$

The geometry associated to space in Newtonian mechanics is therefore the generalization in three dimensions of the structure of a flat plane. In mathematical terms, such a space is said to be *flat and Euclidean*. For comparison, a simple example of a non-Euclidean geometry in two dimensions would be the surface of a sphere.

Let us now imagine that two observers in two different inertial frames, F and F', describe the same set of events in their respective coordinate systems, $(t, \mathbf{x})$ and $(t', \mathbf{x}')$. From the definition of inertial frames, we can consider three types of transformations relating these two systems. The first and most obvious ones are translations, namely the case where the two frames are aligned and do not move compared to each other. They only differ by their origin of space and time: $t' = t + t_0$ and $\mathbf{x}' = \mathbf{x} + \mathbf{x}_0$, with t_0 and $\mathbf{x}_0$ some constant values. The second ones are spatial rotations which relate frames which are fixed but whose coordinate axis are not aligned. Finally, consider F and F' originally at the same location and then moving away from each other at a constant velocity $\mathbf{v}$ aligned with their x-axis, as in Figure 1.1.

[2] Note that there are generally different possible choices of coordinate systems to describe events in a given frame (Cartesian, cylindrical and spherical systems are the most common ones) and that the physics is independent of such a mathematical choice.

Their coordinates are therefore related in the following simple way:

$$\begin{cases} t' &= t \\ x' &= x - vt \\ y' &= y \\ z' &= z \end{cases} \tag{1.2}$$

These three types of transformations can be combined with each other[3] and are generically called *Galilean transformations*. They form a well-defined mathematical structure known as a *group of symmetry*. This name comes from the fact that the laws of classical mechanics stay *invariant* under such transformations (as requested by the principle **(P4)**). In particular, the distance (1.1) between two events A and B is measured to be the same in all inertial frames: $\Delta d_{AB} = \Delta d'_{AB}$. In the same way and consistently with the principle **(P3)**, time flows equally in such frames: $\Delta t_{AB} = \Delta t'_{AB}$. It is worth mentioning that all these notions which have appeared here (transformation, group, symmetry) are not only the concern of classical mechanics but are actually crucial to understand the foundations of modern physics.

The classical laws of motion and the properties of matter

Although the framework we just introduced gives a rigorous description of space, time and the perception of motion, it does not say anything about the cause of such motion. In other words, what are the laws of physics? In his Principia [9], Newton formulates three laws that we can give as follows:

(N1) In an inertial frame, a body free of any interaction will remain at rest or move in straight line at constant velocity.

(N2) Anything which changes the uniform motion of a body in an inertial frame is called a force. The sum of all the forces acting on a object is equal to the inertial mass of the object times its acceleration:

$$\mathbf{F} = m_I \mathbf{a}. \tag{1.3}$$

(N3) If a body exerts a force on an object, then the object exerts a force of equal magnitude and opposite direction on the body.

At this stage, these laws are not yet concerned with the nature of the forces. They state that whatever acts on an object modifies its velocity proportionally to some intrinsic quantity, called the inertial mass m_I. Inertial mass has to be understood here as the capacity of an object to "resist" to a change in his motion, in the sense that, acted upon by a same force, the velocity of a body with a bigger m_I will change less that the one of a body with a smaller m_I. This notion will soon become important in our discussion.

For classical mechanics to be complete, it finally remains to define what is the nature of the objects and the forces between them. What are the properties of matter? In standard mechanics, it is assumed first that objects or particles are well localized quantities at any time in a given reference frame, such that a trajectory $\mathbf{x}(t)$ can be associated to them. Then it is also assumed that objects can interact with each other, leading to the notion of force. Determining the nature of these interactions

[3] For example, if the two frames are moving with a velocity not aligned along the x-axis, the transformation can be given by a combination of a rotation and a relation of the form (1.2).

has historically been obtained through empirical observations. Intuitively, the idea is that particles have some intrinsic properties causing them to attract or repulse each other. By the end of the 18th century, two main types of forces were recognized as explaining most of the observed physical phenomena: the gravitational and electromagnetic interactions. Particles with *gravitational mass* would attract each other whereas particles with *electric charge* would either attract or repulse each other in function of the sign of the charges. The mathematical expressions of these forces are known as respectively the *Newton's law of universal gravitation* [9] and the *law of Coulomb* (1736-1806) [16, 17]:

$$\mathbf{F}_{\text{grav}} = G\frac{m_1 m_2}{r^2}\hat{\mathbf{r}} \qquad \mathbf{F}_{\text{elec}} = \kappa_e \frac{q_1 q_2}{r^2}\hat{\mathbf{r}}. \tag{1.4}$$

In both equations, r is the distance and $\hat{\mathbf{r}}$ the direction between the two objects. Both forces are therefore known as *inverse-square laws*. The other quantities are the gravitational masses m_1 and m_2 (always positive) and the electric charges q_1 and q_2 (positive or negative). They vary from one object to another. Eventually, G and κ_e are proportionality constants known as the *gravitational constant* and the *Coulomb constant*. They do not depend on the objects but rather characterize the interaction they are related to.

Predictions and limitations of classical mechanics

Predictions from classical mechanics can be obtained by combining the laws of motion **(N1)-(N3)** with Equations of the type (1.4) for the relevant forces. The comparison with various experimental tests performed during the last 300 years have provided physicists with the opportunity to precisely define the range of validity and the limitations of this theory. Among all of them, we briefly expose four of these aspects which are relevant for our following discussion.

(L1) Regarding gravitation, Newtonian mechanics predicts planetary motion around the Sun up to a good accuracy. As an example, the Kepler's laws of motion (see [18] Chapter 1) which have originally been inferred from observations only, are a mathematical consequence of Newton's laws. On the other hand, refined measurements obtained during the middle of the 19th century showed that classical mechanics does not correctly predict some small effects in the motion of planets, such as the perihelion precession of Mercury.[4] This was a a strong indication that Newtonian mechanics is not a complete theory of gravitation.

(L2) A second and more conceptual concern is that gravitation seems to play a special role in classical mechanics compared to other forces. Inertial mass in Equation (1.3) and gravitational mass in Equation (1.4) are a priori two different concepts, in the same way as inertial mass and electric charge are different notions. However, measurements (as obtained from Eötvös-type experiments [20]) show that these two types of masses have the same value up to at least very high precision. This is simple to illustrate. Imagine two different objects falling under the gravitational attraction of the earth. If they are in vacuum, no friction acts on them and the only force is given by $\mathbf{F}_{\text{grav}}$. From Equations (1.3) and (1.4), their acceleration is given as follows:

$$\mathbf{a} = \frac{m_{\text{grav}}}{m_I}\frac{G m_{\text{earth}}}{r^2}\hat{\mathbf{r}}. \tag{1.5}$$

[4] This problem was first discovered by Le Verrier (1811-1877) in 1859 [19].

If m_{grav} and m_I were different in general, different objects would fall with different accelerations. However experience says that all objects in free-fall have the same motion, suggesting that $m_{\text{grav}} = m_I$. This equality sounds surprising in Newtonian gravity as it cannot be explained from any of its principles.

(L3) Another conceptual problem is the idea of *action at a distance*. The formalism we presented above suggests that distant objects affect each other instantaneously without the existence of any mediator between them. Newton himself was actually concerned with this problem such that he wrote in his fourth letter to Bentley (25 February 1692/3) [21]: "Gravity must be caused by an Agent acting constantly according to certain laws; but whether this Agent be material or immaterial, I have left to the Consideration of my readers".

(L4) We finally mention how the study of electromagnetism has been important to shed light on the limitations of classical mechanics. In classical electrodynamics, the interaction between charged particles is described in terms of electric and magnetic *force fields*. This led Maxwell (1831-1879) to realize that light can be described as a wave of such electromagnetic fields propagating through space [22]. At this stage already, we note the particular nature of light in the sense that its wave-like behaviour does not correspond to the idea that matter is only made of well-localized particles. More importantly, it appears that the laws governing the dynamics of charged particles and electromagnetic fields, known as the Maxwell equations and Lorentz force law, are not invariant under the Galilean transformations (1.2). In other words, the laws of classical mechanics combined with Maxwell equations predict that the speed of light should change when measured in different reference frames. However, Michelson and Morley [23] published in 1887 the results of an experiment where they detected no difference for the speed of light measured in different frames. This was the indication that either Newtonian mechanics or Maxwell's formulation had to be modified.

The limitations of classical mechanics we just mentioned, among others, have been the source of a substantial reformulation of the description of space, time and matter starting around the end of the 19th century. As we shall see now, this led to the emergence of special and general relativity as well as quantum mechanics.

1.1.3 Special and general relativity

Space-time as a unified structure

A solution to reconcile Maxwell equations with the laws of motion relies on a strong change of paradigm about the nature of space and time. The theory behind it, special relativity (SR), has mainly been formalized by Einstein (1879-1955) around 1905 [24]. This theory considers the principle of relativity **(P4)** and the speed of light as fundamental concepts, but refute the idea of absolute space and time (namely the principles **(P1)** and **(P3)** of classical mechanics). The notion of inertial frame is still present but modified such that it does not make any reference to absolute space. It is simply defined as a frame in which a body with no force acting on it is not accelerating. In summary, special relativity relies on the two following axioms:

(SR1) The laws of physics are the same in all inertial frames (*Principle of relativity*).

(SR2) The speed of light in vacuum, c, is the same in all inertial frames.

The postulate **(SR2)** looks consistent with the results of the Michelson-Morley experiment. However it clearly breaks Galilean transformations and requires to abandon the idea of an absolute time independent of space. Imagine two observers in two different inertial frames. Special relativity tells that they will both measure a same light ray to move at the same speed c in their own frame. This is only possible if they measure different values for both length and time intervals and these values compensate each other to keep c constant.

Along this line of thinking, Einstein showed in his paper [24] how space and time coordinates have to transform between inertial frames to satisfy the two postulates **(SR1)**-**(SR2)**. He actually realized that these transformations were already known as those leaving the Maxwell equations of electromagnetism invariant and previously discussed a few years earlier by several physicists including Lorentz, Larmor, FitzGerald and Poincaré.[5] Special relativity appeared therefore as a promising candidate towards a unified description of the laws of motion and electromagnetism. The transformations in question include space-time translations and spatial rotations, as in classical mechanics. However, the Galilean transformations (1.2) are replaced by the so-called *Lorentz boosts* given by[6]

$$\begin{cases} t' &= \gamma\left(t - \frac{vx}{c^2}\right) \\ x' &= \gamma(x - vt) \\ y' &= y \\ z' &= z \end{cases} \tag{1.6}$$

where $\gamma = \frac{1}{\sqrt{1-\frac{v^2}{c^2}}}$ is known as the Lorentz factor. These transformations have again well-defined mathematical properties and form either the *Lorentz group* (without translations) or the *Poincaré group* (including translations). They are crucial in modern physics and will be discussed in more details in Section 3.1.1.

As expected, equation (1.6) shows that space and time coordinates are interrelated and cannot be seen as independent quantities anymore. We also notice that for $v \ll c$, we can approximate $\gamma \sim 1$ and the transformations reduce to the Galilean equation (1.2). It basically means that special relativity reduces to Newtonian mechanics when velocities of the systems under investigation are small compared to the speed of light. In other words, this has the advantage that experiments that were already consistent with classical mechanics will straightforwardly stay valid in special relativity. This is a process which occurs regularly in science. When looking for new theories of nature, it is indeed more usual to consider the current models as approximations that need to be extended rather than looking for completely new frameworks.

Minkowski space-time and causality

Special relativity introduces a lot of new concepts compared to Newtonian mechanics. There is no more absolute notion of space and time in the sense that no inertial frame can be preferred to another one. Mathematically, space and time of special relativity can be combined in a four-dimensional geometrical structure, called Minkowski (1864-1909) space-time. It differs from the Euclidean space-time mentioned earlier in the following way. In Euclidean space-time, time was the same in any frame and the spatial distance (1.1) between two events was invariant under

[5] For more details about the history of special relativity, see [25].

[6] We again assume that the two frames are moving along their x-axis.

Galilean transformations. In Minkowski space-time, this spatial distance is not invariant under Lorentz boosts.[7] The quantity which is actually conserved between two events A and B is called the space-time interval Δs_{AB} given by the following expression:[8]

$$(\Delta s_{AB})^2 = -c^2(t_A - t_B)^2 + (x_A - x_B)^2 + (y_A - y_B)^2 + (z_A - z_B)^2. \tag{1.7}$$

This formula is a direct consequence of the axioms of special relativity given above. If the two events A and B correspond to a same light ray, then $\Delta s_{AB} = 0$ which is nothing but saying that the speed of light satisfies the relation $c = \Delta d/\Delta t$ in any inertial frame (axiom **(SR2)**).

Thanks to the previous formula, special relativity allows us to clearly introduce the concept of *causality*. We speak of causality when an event has some effect on some other event. As in special relativity nothing can move faster than light, it implies that two such events cannot be separated by a time interval which is longer than the time light would take to travel between them. In other words, $\Delta s < 0$. On the other hand if Δs is positive, it means that the events never influenced each other. As a direct consequence, the concept of "action at a distance" of Newtonian mechanics is incompatible with special relativity. The idea that forces act between objects has to be completely reformulated. It is important to keep in mind that special relativity alone does not say anything about how to solve this problem and how to describe forces. In electromagnetism for example, the solution comes from the Maxwell equations which specify that electromagnetic fields play the role of the mediator of the forces between charged particles. But what about gravitation? We will see shortly that this question led to the development of general relativity.

Acceleration, general covariance and the equivalence principle

We have seen that inertial frames own a special status in both Newtonian mechanics and special relativity. We can go further and wonder what would happen if an observer O' measures some events from a *non-inertial frame*, namely a frame undergoing acceleration with respect to an inertial observer O. In such a case, the laws of motion are not constrained by the principle of relativity to be the same for O and O'. We should expect O' to witness some non-inertial effects in the behaviour of any objects. In classical mechanics, it is actually straightforward to see that if the equations of motion of an object of inertial mass m are given by $\mathbf{F} = m\mathbf{a}$ in O, then the corresponding equations in O' are $\mathbf{F}' = m\mathbf{a}'$ with $\mathbf{F}' = \mathbf{F} + \mathbf{F}_{\text{fict}}$. It means that the non-inertial observer sees the object moving as if it was under the influence of the regular force $\mathbf{F}$ plus some *fictitious* force $\mathbf{F}_{\text{fict}}$ which is only an artifact of her non-inertial motion.[9] Typical examples of fictitious forces include the Coriolis or centrifugal forces.

Such reasoning about non-inertial frames and acceleration has been important for the development of the general theory of relativity. General relativity is the theory of gravitational interaction developed mostly by Einstein between 1907 and 1915 (see e.g. [26–28][10]), subsequently to his formulation of special relativity. This theory is based on two interrelated concepts: *general covariance* and the *equivalence principle*.

[7] This means that lengths measured by two different observers are generally different.

[8] The reader familiar with special relativity will recognize our choice of signature $(-,+,+,+)$ for the metric.

[9] We emphasize that fictitious forces are not the result of any physical interactions between objects.

[10] A comprehensive collection of Einstein papers are available on https://einsteinpapers.press.princeton.edu/.

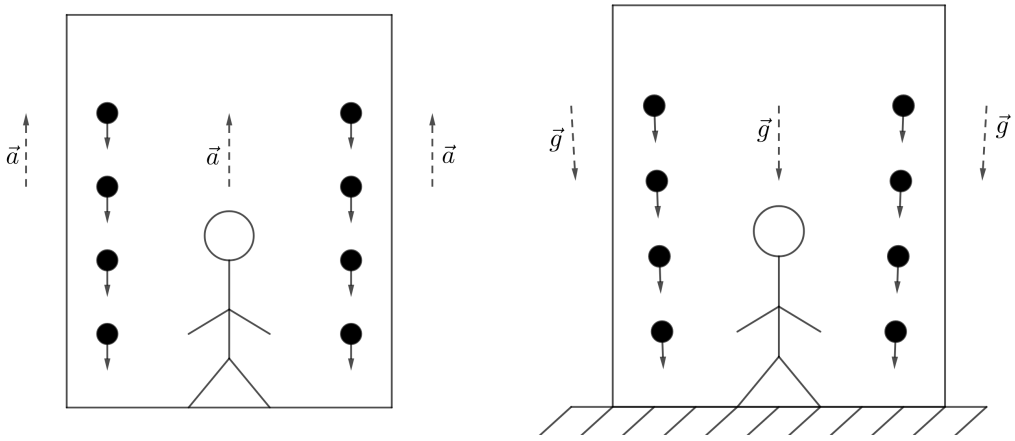

(A) Acceleration in free space (B) Gravitational field on Earth

FIGURE 1.2: Physicist observing the motion of two test masses inside a box, either moving with acceleration **a** in free space or feeling the Earth gravitational field **g**. For $||\mathbf{a}|| = ||\mathbf{g}||$, all single motions are the same locally. However, looking at relative motion of the two bodies would show the non-local nature of gravitational fields. In (B), the objects fall towards the center of the Earth rather than parallel (the effect is highly exaggerated for illustration).

General covariance, also called diffeomorphism invariance, is the idea that the laws of motion should stay the same for arbitrary observers, whether inertial or not. This extends the principle of relativity to a higher conceptual level but seems at first sight to be difficult to reconcile with the appearance of the fictitious forces we encountered above. We shall see how this difficulty is overcome in Section 2.1.

On the other hand, the equivalence principle is the way Einstein expressed his idea that the gravitational interaction is *universal*. There are actually different forms of this principle. The weak equivalence principle (WEP) states as a postulate that the two notions of inertial and gravitational masses we presented in the paragraph **(L2)** are equal. Universal therefore means that different objects placed in the same gravitational field will react and move in the same way. The other usual thought experiment illustrating the equivalence principle is the one of a physicist inside a box who is unable to see the outside world. As shown in Figure 1.2, she would not be able to detect any difference if the box were either sitting on Earth or instead accelerating at constant rate in free space. Uniform acceleration and gravitation seem therefore impossible to disentangle. It is however important to notice that this claim can only be valid locally, namely in a small enough region of space-time. Figure 1.2 also suggests that distant objects at the surface of the Earth would indeed not fall in parallel directions but towards the center of the Earth.

Since the nature of the experiment performed in the box can be arbitrary (and does not need to necessarily involve massive objects), the WEP can be rephrased in a more general form, called the Einstein equivalence principle (EEP). Following [29] page 50, the EEP says:

> In small enough regions of space-time, the laws of physics reduce to those of special relativity. It is impossible to detect the existence of a gravitational field by means of local experiments.

A very important implication of this principle is that every physical system feels gravity (including light rays). It is indeed not possible to single out a frame which

would be gravitationally free and with respect to which we could measure the acceleration of other objects due to gravity. In a way, gravitation is not a force anymore but a backdrop in which particles move. This profound change of paradigm is also well summarized by Carroll [29] page 51:

> [It] makes more sense to *define* "unaccelerated" as "free-falling", and that is what we shall do. From here we are led to the idea that gravity is not a "force" - a force is something that leads to acceleration, and our definition of zero acceleration is "moving freely in the presence of whatever gravitational field happens to be around".

From flat to curved space-time

The equivalence principle naturally leads to the idea that gravity is an unavoidable background influencing the motion of test particles. The next strong postulate of general relativity is to say that this is nothing but the fact that gravitational fields curve space-time. One of the simplest ways to depict what *curved* means is to say that the motion of free-falling particles is not given by straight lines anymore. There are now curved paths, called geodesics, which minimize the distance between events in space-time.[11]

In contrast to Newtonian mechanics and special relativity, the concept of inertial frames moving in straight lines has therefore to be abandoned. To strengthen this difference, we remind that inertial frames can be defined globally over all space-time in special relativity. This is not the case in general relativity anymore. Even if we decide to attach a frame to a free-falling particle, other free-falling particles situated at a long distance would be seen as accelerating in the original frame. This is due to the non-local effects of gravity we mentioned above and in Figure 1.2b. The best that can be done is to restrict this frame to a small region of space-time around the particle of reference. Such frames are said to be *locally inertial*. But then, how do we compare the behaviour of distant objects? This is achieved in general relativity thanks to various technical tools related to the mathematics of curved space-time. These notions are presented in detail in Section 2.1. The key notion is to be able to define unambiguously what a "distance" means in curved space-time. This will be a generalization of the space-time interval (1.7) which appeared in special relativity.

This discussion leads us to another important change of paradigm compared to classical physics. Saying that the curvature of space-time and gravitational fields are related means that matter and space-time interact with each other. In general relativity, the energy and mass content of the Universe is therefore responsible for the geometry of space-time. The mathematical equations giving this relation are known as the Einstein Field Equations presented in 1915 in [28]. There are solutions of these equations that allow physicists to predict gravitational phenomena in general relativity and therefore to asses its validity.

Since 1915, numerous phenomena have been tested with excellent accuracy. The precession of Mercury [30] (mentioned as a limitation of Newtonian mechanics **(L1)**) and the deflection of light by the Sun [31] are such early examples. The detection of gravitational waves [8] is on the other hand much more recent. On top of experimental tests, general relativity is also quite remarkable conceptually. The problem **(L3)** of action at a distance is now solved by the fact that test particles react to local changes in the geometry of space-time and not directly to distant objects. The

[11] The usual (but probably oversimplified) example is to imagine what is the shortest path between two points on a sphere. This is well-known to be given by a circular arc.

"Agent" discussed by Newton is space-time itself. As of today, no theory has been able to explain the gravitational interaction in a better way, although we shall see in Section 1.2.1 that there are still various aspects of the Universe which escape our understanding.

1.1.4 Quantum mechanics and particle physics

Our previous discussion has been rather vague regarding the nature of matter. We talked in a generic way of particles, bodies or objects without describing their properties. It is now time to look in more details at what physicists and chemists learned about the structure of matter and how this led them to the development of quantum mechanics and particle physics.

Probably the most important approach towards understanding matter has been *reductionism*: the idea that a phenomenon can be decomposed into smaller entities and explained from them. This led some ancient Greek philosophers to assume that the process should eventually stop and that all matter is made of "uncuttable" units they called atoms [32]. Whether or not really indivisible quantities exist is still unclear today. However, what is certain is that matter admits a hierarchical organization in terms of well-defined patterns at different length scales. Macroscopic objects are all made from a set of less than one hundred chemical elements, historically classified by chemists such as Lavoisier (1743-1794) and Mendeleev (1834-1907) [33]. These elements then share a similar *atomic* structure in terms of electrons "orbiting" around a nucleus made of protons and neutrons. These last two entities are made of even smaller units called quarks, belonging to a larger class of so-called *elementary particles*.[12]

We will give more details below and in Section 3.1 about elementary particles. The important thing to notice at this stage is that such a reductionist description is a priori not in contradiction with classical mechanics. Some complications may appear to describe the collective behaviour of a large number of such particles (like in a gas) but again classical theories such as thermodynamics and statistical physics can in theory overcome such problems. In practice however, several experiments around the end of the 19th century were in contradiction with classical predictions. Also, as we mentioned earlier in **(L4)**, the wave-like nature of light was asking for more understanding.

The birth of quantum mechanics

A wrong prediction of classical mechanics concerns the electromagnetic radiation of macroscopic bodies. It is indeed known that any object at a given temperature emits a spectrum of electromagnetic waves, called a *black-body spectrum*. One of the main problems was the discrepancy between the observed and predicted amount of energy that is radiated. To resolve this problem, Planck (1858-1947) proposed in 1900 that electromagnetic radiation is only emitted with discrete amounts of energy rather than with a continuous spectrum of energy [34]. He was able to reproduce the black body experiments by furthermore assuming that these packets or "quanta" of energy E were proportional to the frequency ν of the corresponding electromagnetic wave:

$$E = h\nu. \tag{1.8}$$

[12] The term *elementary* means that are no experimental evidences (yet) that these particles are made of smaller substructures.

The proportionality constant h is called the *Planck constant* as Planck managed to derive its value from the available observations. Interestingly, the idea that electromagnetic energy is carried as quanta was further supported by Einstein in 1905 [35] in order to explain the photoelectric effect, namely the fact that free electrons are emitted when light hits a material.

These considerations on electromagnetic radiation marked the birth of quantum mechanics. During its early stage, it was unclear how to conciliate the two different nature of light (corpuscular and wave-like) together. First investigations have been rather heuristic, as for example the derivation of the structure of the atom by Bohr (1885-1962). Based on a previous model from Rutherford (1871-1937) [36], he proposed in 1913 that electrons could only travel around the nucleus on specific orbits and could transition between them by emitting or absorbing discrete quanta of energy [37]. Although these empirical ideas were more and more in line with the experimental observations of that time, they were still lacking some more complete formulation. A major breakthrough came in 1923 form the matter-wave hypothesis of de Broglie (1892-1987) [38]. He postulated that not only light but all matter in general exhibits both wave-like and corpuscular properties. To each massive particle, such as an electron, it would then be possible to associate a wavelength λ given by:

$$\lambda = \frac{h}{p}\,, \tag{1.9}$$

where we find the Planck constant again and $p = mv$ is the momentum of the particle. From there originates modern quantum mechanics and the concept of wave function.

Wave function, quantum state and the uncertainty principle

Modern quantum mechanics assumes that the state of any physical system can be fully described by its wave function $\psi(t, \mathbf{x})$. Following the original idea [39] from Born (1882-1970), it can be interpreted as a probability distribution. For a single electron, the function $|\psi(t, \mathbf{x})|^2$ would then represent the probability to find this electron at a given location and time. As in Newtonian mechanics, the state of a particle is determined from its interactions with other objects. However, the equations of motion $\mathbf{F} = m\mathbf{a}$ should be modified to satisfy the wave nature of quantum particles. This was achieved in part by Schrödinger (1887-1961) who developed the concept of wave mechanics and proposed a specific equation that the wave function of a single particle of mass m should satisfy [40]:

$$i\frac{h}{2\pi}\frac{\partial}{\partial t}\psi(t, \mathbf{x}) = \left(-\frac{\hbar^2}{4\pi m}\nabla^2 + V(t, \mathbf{x})\right)\psi(t, \mathbf{x}), \tag{1.10}$$

where the *potential* $V(t, \mathbf{x})$ encompasses the information about the interactions. There is now a clear change of paradigm compared to Newtonian mechanics. The notion of a well-localized particle has been replaced by the less-intuitive concept of probability distribution. The question of how to interpret this concept, and quantum mechanics in general, has driven many passionate debates, such as between Einstein and Bohr [41], and remains not totally understood today. Putting this problem aside, quantum mechanics rapidly became popular among physicists as it was able to explain many physical phenomena (e.g. the detailed structure of the hydrogen atom) and to predict unexpected properties of matter.

In parallel to the development of wave mechanics, several physicists including Heisenberg (1901-1976) and Born realized that quantum mechanics could be formulated in a more abstract way through the notion of *states and operators* [42, 43]. Put simply, the wave function $\psi(t, \mathbf{x})$ is interpreted as the spatial representation of a more fundamental quantity called the state of the system and written $|\psi\rangle$. Any physical quantity that could be experimentally measured from this system is then obtained from the action of an operator on the state of the system. For example, measuring the energy of a particle would correspond to acting with a properly defined "energy operator $\hat{E}$" on the state of this particle. This formulation, called *matrix mechanics*, has actually been proved to be mathematically equivalent to wave mechanics. Both approaches are still used today, and depending on the context, one formulation may appear easier to use than the other.

Among the various predictions of quantum mechanics which differ from classical theories, we would like to emphasize two important concepts: the *uncertainty principle* and the *spin* of a particle. Introduced by Heisenberg in 1927 [44], the uncertainty principle states that there is an unavoidable limit to the precision with which the position and velocity of a particle can be measured. This is a direct result of matrix mechanics which actually does not only apply to position and velocity but to any pair of operators which do not *commute*. It means that if we act with two operators, say $\hat{A}$ and $\hat{B}$, on a state $|\psi\rangle$, we may see that $\hat{A}\hat{B}\,|\psi\rangle \neq \hat{B}\hat{A}\,|\psi\rangle$. In such a case, the uncertainties related to the observation of the quantities A and B are fundamentally restricted to satisfy

$$\Delta A\,\Delta B \geq \frac{h}{4\pi}\,, \tag{1.11}$$

independently of the sensitivity of the experimental device which is used. This principle is of prime importance for this thesis, as it is the source of our investigations about the quantum nature of space-time which we shall discuss in Section 1.2.3 and Chapter 4.

The second concept to emphasize, *the spin*, was introduced by Pauli (1900-1958) in 1924 as a non-classical degree of freedom of the electron to correctly account for the observed emission spectrum of some atoms [45]. It took some years to interpret the physical meaning of this new property of the electron, namely as an intrinsic form of angular momentum. It is thanks to wave and matrix mechanics that Pauli subsequently managed to formulate this notion more adequately and to introduce *spin operators*. In particular, this allowed physicists to correctly interpret the results of the Stern-Gerlach experiment performed a few years earlier [46]. This experiment is now recognized as giving the experimental evidence for the existence of spin of an electron. As we shall see below, the concept of spin actually appears to be associated not only to the electron but to any particle.

Quantum field theory and particle physics

There are many other predictions of quantum mechanics that we will not address in this thesis. From now on, we will mostly focus on how it provides the relevant framework to describe elementary particles, namely quantum field theory (QFT). We can say for simplicity that QFT originally emerged from two distinct efforts: the combination of quantum mechanics with classical fields (such as electromagnetic fields) and the combination of quantum mechanics with special relativity. Major steps in these two directions have been originally made by Dirac (1902-1984). On one hand, he proposed in 1927 a theory of quantum electrodynamics [47] where electromagnetic fields are considered as a set of quantum harmonic oscillators. In

this quantum version of Maxwell electromagnetism, the photon could then be seen as an "excitation" of the underlying fields. On the other hand, he proposed in 1928 a generalization of the Schrödinger equation[13] which was compatible with special relativity [48, 49]. Interestingly, this *Dirac equation* predicted the possible existence of anti-electrons, namely electrons with positive electric charge.[14]

The next breakthrough was to consider that these two approaches could be merged together to give a single framework describing at once all types of matter. This is the modern view of QFT where every particle (not only the photon) is seen as the excitation of a corresponding quantum field which permeates all space-time. This has been formalized by physicists including Jordan, Wigner, Fermi, Feynman and many others.[15] The key observation was that only specific types of fields would allow physicists to build laws of physics which are invariant under Lorentz transformations. It turns out that the mathematical properties of the Lorentz group require that fields be categorized in terms of a parameter which corresponds to nothing but the notion of spin previously discovered. Fields with different spin would correspond to different types of particles and transform in their own way when seen from different inertial frames. There is an even deeper consequence of this description of matter in terms of fields with different spins. It allows us to reinterpret the notion of force without the problem of action at a distance. Consider for example two electrons. QFT predicts that the repulsive force that we can observe between them is due to an exchange of photons, namely excitations that propagate through the photon field between the electrons. At the risk of slightly oversimplifying, QFT says that particles with integer spin (such as the photon) are those mediating interactions between "matter" particles with half-integer spin (such as the electron).

We can already realize from this short discussion that QFT is powerful to accommodate multiple concepts at once. An interesting question to ask at this stage is: how many different types of fields do we need to accurately describe the nature around us? In other words, how many interactions and particles exist? As of today, the best answer is given by the so-called standard model of particle physics. It describes three fundamental interactions (electromagnetic, weak and strong) which are able to accommodate almost all experimental observations in particle physics with excellent accuracy. An important milestone for this model was the discovery in 2012 of the Higgs boson by the Large Hadron Collider at CERN [6, 7]. We shall give much more details about the standard model and elementary particles in Section 3.1.

1.1.5 Cosmology

The other major research area we will consider in this thesis is *cosmology* which asks questions about the origin, evolution and fate of the Universe as a whole. It should not be surprising that this subject involves all the knowledge we have previously described regarding the nature of space, time and matter. The current paradigm of cosmology is actually strongly tied to general relativity and particle physics. Moreover, this is one of the research fields which provides the most compelling evidences that our current theories are far from complete.

[13] It is clear that the Schrödinger equation (1.10) is not invariant under the Lorentz boosts (1.6).
[14] The positron was discovered a few years later, in 1932, by Anderson [50].
[15] See e.g. [51] for an historical and conceptual presentation of field theories.

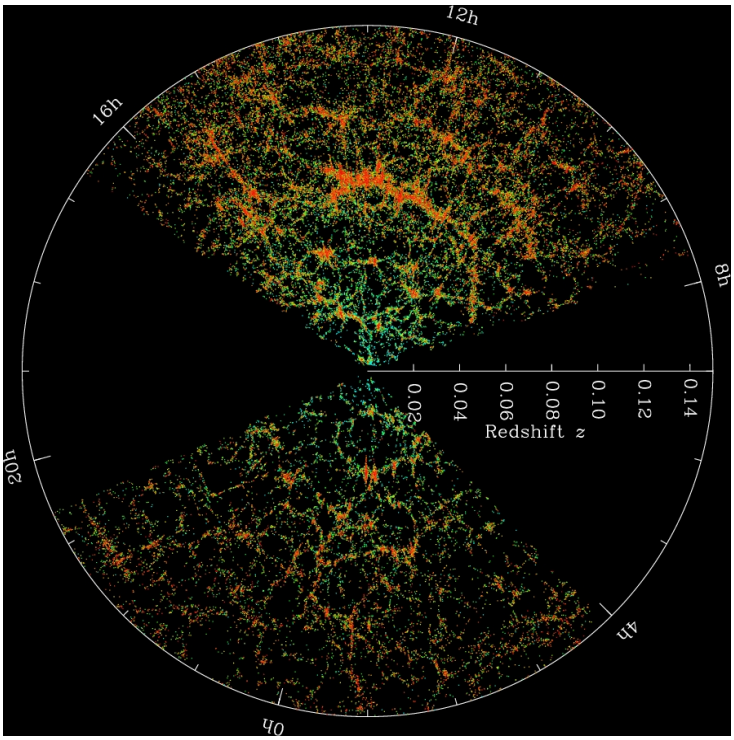

FIGURE 1.3: Map of the galaxies in the Universe based on observations from the Sloan Digital Sky Survey (SDSS). Each point is a galaxy and the Eearth is at the center. Image Credit: M. Blanton and SDSS (https://www.sdss.org/).

The cosmological principle and the expanding Universe

Talking about the chronology of the Universe requires some preliminary precautions as we remind that the notion of time depends on the observer. A rigorous approach therefore requires to find models which satisfy the laws of general relativity. Relatively soon after Einstein proposed his field equations for gravity, several physicists including Friedmann, Lemaître, Robertson and Walker (FLRW) independently derived an exact solution of these equations that can account for the structure of the Universe at very large scales [52–55]. We will present the mathematical details of this model in Section 3.2 and highlight some key features here.

The FLRW model is based on the so-called *cosmological principle* which assumes that the spatial distribution of matter is homogeneous and isotropic over large enough distances in the Universe. As illustrated in Figure 1.3, this is an assumption which seems rather justified from current experimental observations as long as we consider scales much bigger than the typical size of galaxies. This hypothesis is obviously not valid at smaller distances where inhomogeneities cannot be neglected anymore. Such considerations are very important for several astrophysical phenomena but we will not consider them in detail here.

Probably the most fascinating prediction of the FLRW model is that physical distances may expand or contract with time at a rate which depends on the density of matter in the Universe. In other words, space stretches itself in response to the energy and matter distribution. This fact has been confirmed by several astrophysical observations. Most notably, Slipher [56] and Hubble [57] both measured in the 1910s-1920s that distant galaxies are moving away from the Earth, suggesting that

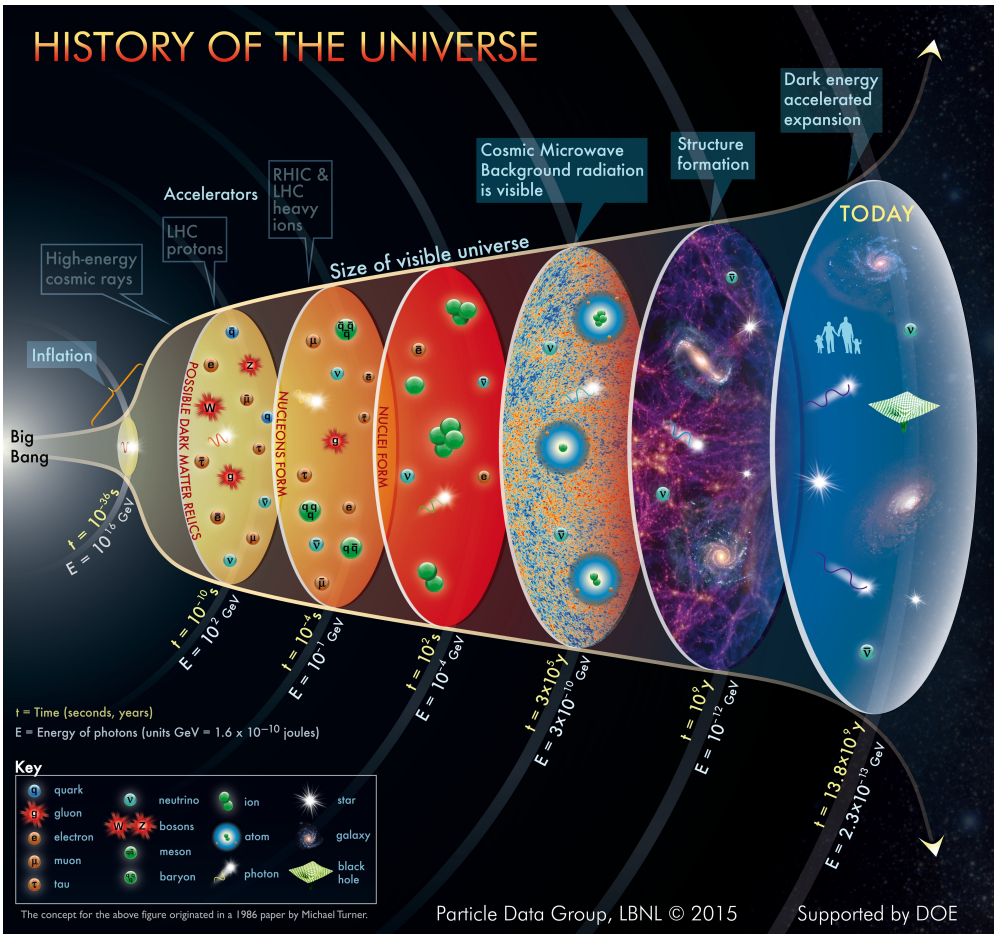

FIGURE 1.4: Artistic view of the history of the Universe. Image Credit: Particle Data Group at Lawrence Berkeley National Lab (`http://particleadventure.org/history-universe.html`).

our Universe is expanding.[16] From there originated the intuitive idea that our Universe was smaller and denser in the past. This led physicists to build the so-called Big Bang model of cosmology.

Big Bang cosmology

If we imagine that the Universe is more and more contracted as we go backwards in time, it is tempting to say that it originated from some singular event or some kind of primordial "explosion" that we can call the Big Bang. However, we emphasize that it is difficult, if not impossible, to speak about any hypothetical origin of the Universe. We have to stay pragmatic and keep in mind that the only way we can reconstruct the past of the Universe is by collecting observations which can be proved to be older and older. In short, current Big Bang cosmology does not say anything about some "first event", but it provides relevant historical information. An overview of the current state of knowledge is summarized in Figure 1.4.[17] Several of the notions shown in this picture will be described throughout this thesis.

[16] Recent results obtained from supernovae by two groups in 1998 [58, 59] actually support that the Universe is in an accelerating expansion. We shall see in Section 1.2.1 that this observation is at the origin of one of the biggest mysteries of physics. But we emphasize that an expanding Universe is in itself in total agreement with the current laws of physics (only the acceleration is problematic).

[17] Note that some concepts in Figure 1.4 are still theoretical and not confirmed experimentally.

The main tool to probe the past of the Universe is the light we detect today on Earth but that has been emitted earlier somewhere else (for example from a distant star). Interestingly, Big Bang cosmology predicts that light can only bring us so far back in time. To understand this fact, we need to have some knowledge about the state of matter when the Universe was denser and hotter. Physicists think that all matter at that stage was in the form of an interacting plasma of elementary particles. Atoms or composite particles such as protons and neutrons were not formed yet. Most importantly, photons were not able to freely propagate in the plasma, they were constantly interacting with other particles. It means that there is no way for us to detect photons of this early epoch. It was only from a particular time, when the Universe was finally diluted and cold enough, that photons could freely stream across space. So the expanding model of the Universe predicts that photons from this period constitute the earliest light we can have access to.

This prediction has actually been confirmed by the experimental detection of the cosmic microwave background (CMB) almost 60 years ago [60–62]. This observation has been very important for cosmology as it is one of the strongest evidences supporting the Big Bang scenario of an expanding Universe. Moreover, the details encoded in the CMB are of primordial importance. Although we have no direct access to earlier photons, it is still possible to use those from the CMB to help us decipher what happened before in the Universe [62]. This is why obtaining more and more precise measurements of the CMB has been very important and has motivated the construction of several detectors and telescopes such as COBE, WMAP, BICEP or PLANCK. The slice at $t = 3 \times 10^5$ years in Figure 1.4 show what the CMB looks like from recent observations.

Despite much progress in cosmology, it still remains difficult to get a precise understanding of the early Universe and its description stays somewhat speculative. It would be very helpful for physicists if there existed some type of information which was produced before the CMB and, contrarily to light, had freely propagated towards us until today. We shall see in the next Section that such a candidate does exist and that it corresponds to a particular type of gravitational waves which may be detected during the next decades. An essential part of this thesis will be dedicated to the study of this interesting phenomenon.

1.2 Gravitational waves as a probe of the Universe

The previous Section gave a broad overview of modern physics and the theories on which it is built. We now want to present how gravitational waves may be useful to improve our knowledge of the Universe. We think it is therefore important to give first a summary of what are the main problems to solve in fundamental physics. Then we take the time to explain what gravitational waves are in simple terms. In this way, the non-expert reader might have the opportunity to appreciate the relevance of gravitational waves and to understand the results of our work [1–5] which will be summarized at the end of this Section.

1.2.1 The Unknown

Our preceding discussion could give the impression that general relativity and quantum field theory provide a comprehensive description of time, space and matter. This thesis would probably not exist if that were true. We also remind that problems are needed (and welcome) for science to progress.

Fortunately, physics is currently facing a lot of interesting questions. For clarity, we propose to classify them in three categories:

(Q1) Theory and observation disagree on the results of an experiment,

(Q2) Theoretical inconsistencies exist inside a model,

(Q3) The complexity or inaccessibility of a phenomenon hinders its description.

This classification is probably not complete and rather arbitrary but it gives an overall feeling of the situation. Problems of type **(Q1)** are the most compelling ones: either the theory or the observation is wrong. Without hesitation, something else is needed. The second type is more difficult to apprehend as physicists may sometimes disagree on the meaning of theoretical inconsistencies. In some cases, evident mathematical problems occur in a model and it is clear that a reformulation or a better theory is required. In other cases, people would argue that what is considered as a problem by others may not be relevant or goes outside the scope of science (see e.g. [63, 64] for a recent discussion). The category **(Q3)** differs from the previous two in the sense that no new model is needed, but our knowledge is restricted because of our limitations to have access to all the information of a system. Such problems can typically be overcome by the development of better experiments and better computational tools. The following examples will illustrate these three groups but it is important to keep in mind that the reality is usually more complicated and that some problems may belong to various categories at the same time.

Dark matter

One of the main concerns of modern physics is related to the hypothetical existence of *dark matter*. It relies on several evidences of type **(Q1)** obtained during the last one hundred years. The study of galaxy clusters by Zwicky in the 1930s [65, 66] and then of spiral galaxies by Rubin and Ford around 1970 [67] showed some clear inconsistencies in the dynamics of such objects. For instance, the radial velocity of distant stars in a galaxy is observed to be much larger than what is predicted by the laws of gravitation (either from Newtonian mechanics or general relativity). The two main solutions proposed by physicists to explain this phenomena are either to modify gravitation or to postulate the existence of a new type of massive particles which are invisible to us (and therefore called dark matter) but would contribute to the gravitational potential of the system.

There are other observational evidences supporting the existence of dark matter or the need for a new theory of gravity [68]. The most compelling one is provided by the CMB temperature anisotropy. The patterns in the temperature spectrum of the CMB photons cannot be explained from the combination of general relativity with the standard model of particle physics. The simplest solution would be to invoke again the existence of unknown particles whose density in the Universe should roughly be five times bigger than the density of usual matter [69]. Although probably not impossible, it seems more difficult to explain the CMB anisotropy by only changing the laws of gravity and keeping the standard model as we know it [70]. But neither of these two main hypothesis has been confirmed or refuted yet. Various apparatus such as particle accelerators and telescopes are currently trying to create or detect dark matter particles. The absence of any detection at least allows physicists to put constraints on (and sometimes discard) the various theoretical models which have been proposed to solve this mystery.

Dark energy, the cosmological constant and vacuum energy

A second conundrum is known as the *dark energy* problem. As mentioned earlier, there are experimental evidences that the Universe is currently in an accelerating expansion [58, 59]. The only way to explain this observation with general relativity is to add a constant term to the Einstein equations. It is important to note that there is no mathematical problem *per se* to introduce this *cosmological constant*. Concerns arise when we try to interpret the physical nature of this term because it should correspond to a form of energy which fills space homogeneously, has a constant density and negative pressure. Compared to the usual kind of matter and energy encountered on Earth, this "fluid" seems to have rather intriguing properties. In addition, the aforementioned observations support that dark energy is currently dominant in the Universe and constitutes roughly 70% of its total energy density.

The situation becomes even more interesting when we realize that quantum field theory could *a priori* provide a natural interpretation of dark energy but fails to do so in practice. Indeed, the Heisenberg uncertainty principle tells that the lowest energy state of a quantum system is never zero. Therefore quantum fields which permeate all space-time should always have a non-zero *vacuum energy* which could in principle play the role of the cosmological constant. The problem is that it is not clear how to correctly calculate the vacuum energy from quantum field theory and that the proposed computations give results which are orders of magnitude away from the observed value (see [71] for a comprehensive review). Little is known about how to solve this problem, but as we will explain below it might be related to the existence of divergences in QFT and the fact that we are missing a quantum theory of gravity.

Quantum gravity

An intrinsic problem of quantum field theory is the appearance of infinities when trying to compute observables [72, 73]. As we shall explain in Section 3.1, there exists a technique called *renormalization* which allows us to regulate these divergences and to obtain finite predictions. This prescription stays well under control as long as the model under consideration satisfies some specific conditions. Such a theory is said to be *renormalizable*. For example, the standard model of particle physics is one such model and it predicts results in impressive agreement with high precision measurements. Note that renormalization fails to give a value of the vacuum energy which is consistent with the cosmological constant described above. It is usual to claim that this is not a problem in particle physics when gravitational effects are negligible because such measurements are only sensitive to differences in energies.

If we have insisted on the appearance of divergences in QFT in the previous paragraph, this is also because it can help us to understand a part of another problem known as *quantum gravity*. Indeed, it is well known that various difficulties arise if we try to quantize the gravitational field [74]. In particular, general relativity is a non-renormalizable theory. This means that it will not be valid to describe phenomena occurring at very small distances (typically around 10^{-35} m).[18] Intuitively, physicists would expect that space-time itself should be quantized at sufficiently small distances. Although some ideas have been proposed, such as string theory [75] or loop quantum gravity [76], there is no consensus on what reality could be

[18] We note however that general relativity, seen as an effective theory, remains a consistent low-energy quantum field theory (see [73] Chapter 22).

at such scales. As explained in Section 1.2.3, a part of this thesis is dedicated to studying this problem in more detail.

The early Universe

As explained in Section 1.1.5, it is difficult to get experimental information regarding the state of the Universe long before the CMB was formed. As long as we do not go too far back in time, it is however possible to theoretically predict various phenomena that could have happened by combining our knowledge of particle physics and general relativity. This includes cosmological phase transitions, that we shall discuss at great length in this thesis, and various interaction processes between elementary particles. The main difficulty at this stage is to find signatures that could help us to confirm the validity of such predictions. On the other hand, if we extrapolate further back in time, we will eventually reach a state of matter which is so dense that quantum gravitational effects become important. We then face the type of problems we mentioned above when discussing quantum gravity.

The positive side of having only little information regarding the early Universe is that it can be used as a playground by theoretical physicists to develop new ideas or to propose solutions to existing problems. Inflation and baryogenesis are such examples. The former process describes a hypothetical period of accelerating expansion in the very early Universe that could explain at the same time why all the photons in the CMB have a similar temperature and why some parts of the Universe are denser than others [77]. The latter process uses the idea that the Universe might have undergone out of thermal equilibrium periods to explain why there is currently more matter than antimatter in the Universe [78, 79]. We might come back to these two concepts from time to time in this thesis although we shall not focus our attention on them.

More problems

We finish our discussion about the unknown part of the Universe by mentioning that there are various other problems that we have not introduced and not detailed in this Chapter. The hierarchy problem, related to the mass of the Higgs boson, is one of them that we will consider in Section 5.1.2. Another example is related to the origin of the neutrino masses which is still not well understood [80]. It is worth mentioning at this stage that a common approach to try to solve such problems is to extend the standard model by introducing new particles or new interactions. In that case, physicists usually talk of beyond the standard model (BSM) physics.

1.2.2 Gravitational waves in a nutshell

It is now time to describe what gravitational waves (GWs) are. GWs are ripples of space-time that are predicted by general relativity. We remember from Section 1.1.3 that energy and matter in the Universe have the effect to curve space-time. So it is not too difficult to imagine that if an object is moving in the frame of an observer, she may detect changes in the curvature of space around her as a function of her time. Fortunately, the mathematical formulation of general relativity gives a very clear description of this phenomenon. It is possible to compute the properties of these waves as a function of the source which produces them and also to determine under which conditions they may be detected.

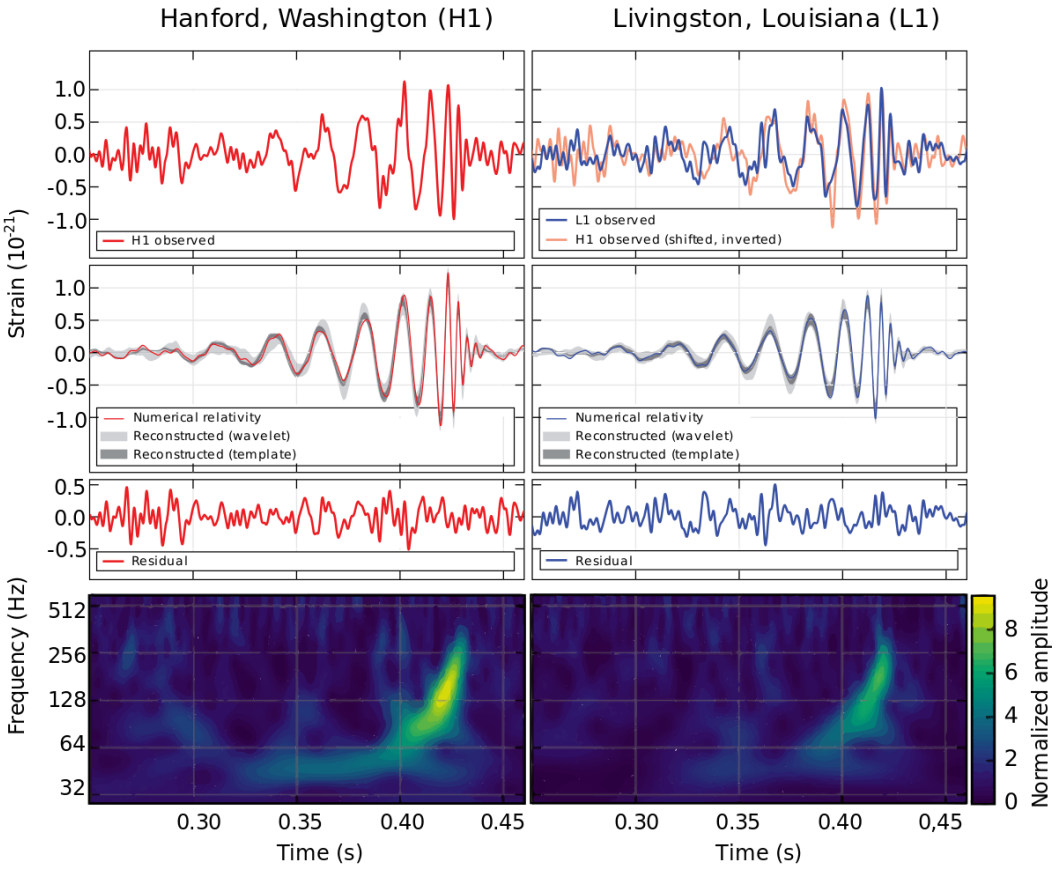

FIGURE 1.5: The gravitational wave signal GW150914 as observed by the two LIGO detectors in Hanford and Livingston. Image Credit: [8].

Historically, the concept of GWs had already been suggested a few years before general relativity was established. But it is only after the Einstein field equations appeared that serious predictions started to be made [81]. Because of the complexity of these equations, it took many years for physicists to carefully compute accurate properties of GWs and to design detectors. The first (indirect) evidence of their existence is associated to the first observation of a binary pulsar by Hulse and Taylor in 1974 [82]. A binary pulsar is a system made of two neutron stars orbiting around each other and with one body emitting some electromagnetic radiation periodically. The observation, during several years, of the radiation coming from the Hulse-Taylor pulsar showed that the orbit of the system was shrinking. This is interpreted as the fact that the system gradually loses energy from its interaction with space-time and that this energy is radiated away as GWs. The rate of decrease of the orbit of the pulsar was in excellent agreement with the predictions of general relativity [83], giving a strong evidence for the existence of GWs although they could not be detected directly.

It was only recently, in 2015, that the first direct detection of GWs was made on Earth by the LIGO/Virgo collaborations [8]. The shape of this signal, called GW150914, is given in Figure 1.5. At the time of writing this thesis, a total of eleven such signals have been confirmed by LIGO/Virgo and more observations are expected in the future. We now give a brief overview of the main characteristics of GWs. We also remind that the mathematical aspects will be treated in detail in Chapter 2.

Production mechanisms

In theory, most matter perturbations produce GWs. In practice however, the interaction between matter and space-time as given by the Einstein equations is very small such that extremely energetic processes are required to produce GWs that would have a chance to be detected. We mention here two phenomena of interest.

The first type of production has already been mentioned above and consists of the inspiralling of two very compact objects such as neutron stars or black holes. As the system evolves, it radiates more and more energy and the bodies rotate faster and faster until they collide. It is nearby the time of collision that the emitted GWs have their maximal amplitude. Seen from Earth, these waves have a typical shape which is exactly the one shown in Figure 1.5. The signal is said to be transient and directional as it comes from a particular location in the sky and only lasts for a short period of time. We will study this particular type of GWs in detail in Chapters 2 and 4.

A second production mechanism is related to the dynamics of the early Universe. As we mentioned in our cosmology Section 1.1.5, the matter at this epoch was in the form of a hot and dense plasma of elementary particles. Quantum field theory predicts that, around that time, elementary fields may undergo some phase transitions accompanied, under certain conditions, by perturbations in the energy and density of matter. This disturbance could have been strong enough to produce a *stochastic background* of GWs. This last expression means that contrary to the previous case, such GWs are not produced at a specific location in space, but everywhere at roughly the same time and with different amplitudes and frequencies. It is still not clear today if such GWs exist as we have not been able to detect them yet. Planned experiments are expected to give us more information in the next few decades. The relationship between the physics of the early Universe and these GWs will be discussed in Chapters 5 and 6.

We also mention that there are other ways to produce potentially detectable GWs, but we will not cover them in this thesis. Particularly interesting scenarios are those related to inflation [84] and cosmic strings [85, 86].

Propagation

Once produced, GWs propagate through space at the speed of light. As their interaction with matter is tiny, it can be assumed that they travel freely. This property renders GWs very interesting as it means that any information gathered from their detection gives direct information about the source which produced them. From our discussion above, this can either be the properties of a binary system, such as their masses, or some information regarding the state of matter in the early Universe. We now understand why we said earlier that GWs may provide a direct access to the state of the Universe even before the CMB.

What we just said about propagation is actually not entirely correct. The fact that the Universe is expanding will affect the properties of GWs while they travel. Typically, their wavelength will be stretched by the fact that space is itself stretching everywhere. This effect, known as *redshift*, is stronger the longer the wave travels. Similarly, the amplitude of GWs will be diluted as the Universe grows. These two effects are generally not difficult to take into account as long as we have a good understanding of the rate of expansion of the Universe.

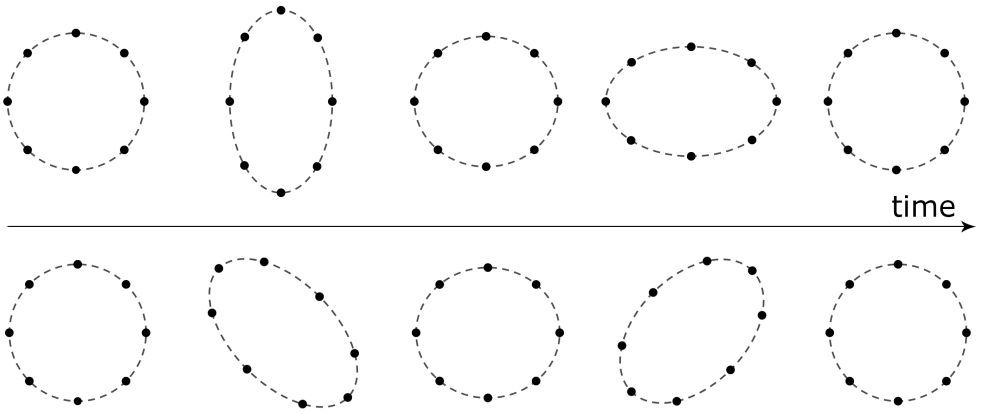

FIGURE 1.6: Generic effect of GWs on a ring of test masses. We assume here that GWs propagate in a direction perpendicular to the plane formed by the ring. General relativity predicts that the movement of the ring is given by the superposition of two effects: a "+" (plus) motion as in the upper panel and a "×" (cross) motion as in the lower panel. See Section 2.1.4 for a mathematical justification.

Detection principle

As space is stretched or contracted at the passage of GWs, the general idea to observe them is to detect changes in the distance between test masses. The typical effect that we can expect to observe is explained in Figure 1.6. To be able to measure a change of distance between the bodies, we need to be sure to use a ruler which is not itself stretched by GWs. Light is the perfect candidate as we know that its speed stays constant in any frame. A change of distance can then be noticed by measuring a change in the time taken by light to travel between the test objects. Such variations remain very difficult to detect in general and this requires to design high-precision experiments. We briefly discuss three experimental setups which differ by their geometry or choice of test masses.

We begin with earth-based laser interferometers. They are composed of two arms, a few kilometers long, into which light can propagate in vacuum. The test objects are mirrors of a few tens of kilograms placed at each extremity of the arms and in suspension such that they are isolated from Earth vibrations. By measuring the time taken by light to travel between the mirrors, physicists can notice small variations of their position that could be induced by the passage of a GW. Such detectors are typically sensitive to frequencies between 10 Hz to 10 kHz and are particularly adapted to the detection of GWs produced from black hole or neutron star binaries of a few solar masses [87]. Three such instruments are currently operational: the two LIGO detectors in the USA and the Virgo interferometer in Italy.[19] As said above, they have already confirmed the detection of eleven binary mergers similar to the one in Figure 1.5.

The second type of apparatus consists of space-based laser interferometers. Test masses of a few kilograms are placed in free-fall inside at least three spacecrafts separated from each other by a few million kilometers. Light rays are emitted between each spacecraft in order to constantly measure their relative distance and detect any potential variations. Taking into account their configuration and the length of their arms, such instruments are expected to be sensitive to much larger wavelengths than LIGO/Virgo. They could typically detect signals with frequencies around 10^{-3}

[19] A fourth (underground) interferometer, KAGRA, is currently under construction in Japan and expected to give results in a few years [88].

Hertz. Such experiments have not been built yet but several proposals are currently under investigation. The most promising project is the Laser Interferometer Space Antenna (LISA) which is planned to be operational around 2034 [89]. Among various objectives, two of its goals are to study the merger of very massive black holes and to try to detect stochastic gravitational waves produced during the early Universe. We also mention that other space-based ideas have been proposed such as the Big Bang Observer (BBO) [90] and the Deci-Hertz Interferometer Gravitational wave Observatory (DECIGO) [91].

The last detectors we present are pulsar timing arrays (PTA). We already mentioned that pulsars are neutron stars emitting periodic electromagnetic radiation. The idea is therefore to monitor the time of arrival on Earth of the pulses coming from a selected set of pulsars. In comparison with the previous types of instruments, the role of test masses is now played by the pulsars and the Earth. The lengths of the arms of this "interferometer" are then just the distances between each pulsar and the Earth. If GWs of low frequency (10^{-9} to 10^{-6} Hz) propagate in our neighbourhood, they will produce some measurable disturbance in the time of arrival of the pulses. The International Pulsar Timing Array (IPTA) [92], a collaboration of various telescopes around the world, is currently looking for such perturbations by observing roughly 30 pulsars. No GW signal has been observed yet and this allowed the collaboration to place various constraints on the properties of the stochastic GW background [93–95]. A new instrument, the Square Kilometer Array (SKA) [96], is currently under development and is expected to deliver first results in the next decade.

1.2.3 Testing the quantum nature of space-time

Now that we have an overall understanding of GWs, we can discuss their usefulness for fundamental physics. Let us first mention that the LIGO/Virgo detection has been important to confirm the existence of GWs and to strengthen the validity of general relativity. It allowed physicists to probe GR in a way which had never been possible before. Previous tests were indeed restricted to processes involving weak and almost static gravitational fields. The collision of two black holes belongs however to the regime of strong and dynamical fields and it could have led to unexpected phenomena. As we will explain in details in Section 2.2.3, it turns out that all observed signals are in good agreement with GR so far.

There are various other reasons that make the observed waveforms interesting. They can be used to study models of modified gravity [97], to confirm that GWs propagate at the speed of light [98] or even to look for dark matter in the form of primordial black holes [99]. In our papers [1, 2], we used such a signal, GW150914 to be precise, to study the quantum nature of space-time. The details of our investigation are given in Chapter 4 but we give here a summary of our approach and results.

In our brief discussion about quantum gravity, we emphasized that it is unclear how to conciliate the principles of quantum field theory with general relativity. In particular, the nature of space-time as we imagine it is expected to change at very small distances. In general relativity, the implicit assumption is that space-time is a continuous fabric and that events can be localized unambiguously from their coordinates. So it is possible, in this framework, to divide space-time indefinitely and to consider smaller and smaller distances without needing to modify the laws of gravitation. But there is a priori no reason to think that this is true. Could space-time be made of small "atoms"? Could space-time be discrete rather than continuous? Such questions indeed sound legitimate once we take quantum mechanics into account.

Non-commutative space-time

Various mathematical models of quantum space-times have been proposed. Although they differ in their formalism, most of them invoke at some point the existence of a minimal length scale. A comprehensive review discussing various of these approaches can be found in [100]. The particular model in which we are interested is named *non-commutative space-time*. The idea is that space-time becomes fuzzy below a given scale such that it is no longer possible to localize events with arbitrary accuracy. Formally, coordinates are not real numbers anymore but quantum operators that do not commute. Similarly to the position and velocity of a particle in usual quantum mechanics, this assumption results in an uncertainty principle for the coordinates. For example, if we consider the $\hat{x}$ and $\hat{y}$ coordinate operators, we will get:

$$\hat{x}\hat{y} - \hat{y}\hat{x} \neq 0\,, \qquad \Delta x\,\Delta y \gtrsim \frac{1}{2}\,l_{xy}^2\,, \tag{1.12}$$

where l_{xy} is the length at which non-commutative effect starts to take place between the x and y coordinates. Similar identities exist for all other couples of coordinates such as $\hat{t}$ and $\hat{z}$.

This idea of non-commuting coordinates was originally proposed by Heisenberg as a possible way to cure the divergences appearing in quantum field theory. The first article based on this formalism was then published in 1946 by Snyder [101]. However, maybe because renormalization proved to be efficient to deal with divergences, space-time non-commutativity has not received a lot of attention until the 1990s-2000s. This period coincides with the development of noncommutative geometry [102] and the observation that space-times with the property (1.12) can be seen as low-energy limits of certain string theories [103, 104] (see also the reviews [105, 106]).

As of today, there is still no experimental indication supporting the existence of a minimal length or the fuzziness of space/time. This is not surprising as such effects are only expected to occur at distances which are still far from the reach of current technology. Based on intuitive theoretical arguments, this distance should correspond to the length at which gravitational effects start to be comparable to other forces such as electromagnetism. This scale is known as the Planck scale and is defined from the combination of the fundamental constants appearing in gravitation (G), quantum mechanics ($\hbar$) and special relativity (c). Explicitly the Planck length and time are given by:

$$l_P = \sqrt{\frac{\hbar G}{c^3}} \approx 1.6 \cdot 10^{-35}\ \text{m} \qquad t_P = \sqrt{\frac{\hbar G}{c^5}} \approx 5.4 \cdot 10^{-44}\ \text{s}. \tag{1.13}$$

Constraint from GWs

According to several analysis [107–110], the best existing constraints on the scale of non-commutativity are roughly at the order of 10^{-20} m. It means that if non-commutativity exists, it has to appear at distances smaller than this value. Our claim in [1, 2] is that GW signals from binary black hole mergers, such as GW150914, allow us to give a more stringent bound. Our computations and results are given in full detail in Chapter 4. The approach we follow is to compute the dynamics of the two black holes with the new assumption that space-time admits non-commutativity of the form given by Equation (1.12). We are thus able to explicitly compute the dominant non-commutative effect on the phase of the GWs produced during the merger. By comparing our analytic formula to the data analysis performed by LIGO/Virgo

on the GW150914 signal [111], we can extract a constraint that the scale of non-commutativity has to satisfy in order to stay consistent with observation. Interestingly, we find that the scale cannot be much bigger than the Planck scale. More precisely, we explicitly get that

$$l_{xt}^2 \lesssim 12 \cdot l_P t_P \,, \tag{1.14}$$

and argue that similar constraints should exist for the other components ($l_{xy}, \dots$). This represents a strong improvement compared to the previous bounds we mentioned. It means that GWs give us here information that was previously not available in another form. Of course, this result does not allow us to conclude on the existence or non-existence of non-commutativity around the Planck scale or below. More precise apparatus would be needed to probe the quantum nature of space-time further.

1.2.4 Probing the history and fate of the Universe

A substantial part of the work presented in this thesis lies at the interplay between particle physics and cosmology. We are particularly interested in the large scale behaviour of quantum fields as it may involve interesting phenomena such as phase transitions, quantum tunnelling and the production of GWs. Let us discuss these concepts in more details.

Phase transitions

QFT predicts that space-time is filled by various quantum fields whose excitations are interpreted as particles. As with any physical system, these fields naturally tend to reach their state of lowest energy. In most situations, this means that the fields admit a homogeneous background value, called a *vacuum expectation value* (vev), over all space-time. It is also possible for some physical systems to have non-trivial vacuum configurations, namely to admit one or several metastable states on top of the true ground state. *Metastability* corresponds here to configurations which are not of lowest energy but in which a system will stay for a long time as long as not enough energy is provided to the system by the exterior environment.

Actually, the vacuum configuration of a dynamical system can change with time and depends on its interactions with other systems. For example, the value of the ground state can evolve or metastable states can appear or disappear. In the context of cosmology, it is of prime importance to know how the vacuum configurations of quantum fields evolved in order to understand the processes that happened during the history of the Universe. According to computations that we shall present in Chapters 3 and 5, the standard model predicts that at least two important events should have occurred during the early Universe: the electroweak phase transition and the quantum chromodynamic (QCD) phase transition. The former process corresponds to a change of vacuum state of the Higgs field and is expected to be the mechanism at the origin of the masses of the elementary particles. It should have happened roughly 20 picoseconds after the Big Bang. The latter process is expected to have occurred later (at 20 microseconds) when the quark fields acquired a non-zero vacuum expectation value (and subsequently combined together to form composite particles such as protons).

Quantum tunnelling and bubble nucleation

The two phase transitions we just described could have happened in two different ways. The picture is as follows. Initially, the field is trapped in its ground state. As the temperature of the Universe decreases, another vacuum state of lower energy forms such that the initial configuration either becomes unstable or metastable. In the first case, the field simply transitions to the new vacuum homogeneously over all the Universe at the same time. Such a transition is said to be a *crossover*. In the second case, the field will stay trapped for a while in the metastable phase until it decays to the new state through *quantum tunnelling*. This process is not homogeneous and happens via the nucleation of bubbles of the new phase (like in boiling water) which then expand and gradually convert all the Universe. This is the signature of a *first-order phase transition*.

It is possible to show that the standard model predicts the electroweak and QCD phase transitions to be crossovers [112, 113]. In that case, it would be difficult to find experimental signs that could prove that these events really happened. On the other hand, several extensions of the standard model, for example motivated by the problems discussed in Section 1.2.1, are known to predict first-order transitions. As explained below, we could have the opportunity in that case to find signatures in the form of GWs observed today on Earth. This is exactly what we investigate in detail in Chapters 5 and 6 for particular particle physics models we shall discuss in due time.

We also want to briefly emphasize that quantum tunnelling and phase transitions may play a role regarding the fate of the Universe. As we explain in Section 7.1, there is a chance for the current vacuum state of the Higgs field to be metastable. Fortunately, even if this is the case, computations show that the probability for the Universe as we know it to decay into another state is extremely small. This raises however a few interesting questions such as why the Universe has not decayed into this lowest-energy state during inflation. Motivated by all these considerations about quantum tunnelling, one of our research works has been to study if the creation of particles during tunnelling influences the decay rate of the metastable fields [5]. This is the topic of Chapter 7, which in itself is not related to the subject of GWs, but is anyway relevant for our overall discussion of fundamental physics.

Stochastic GW background from bubble collisions

The final idea we want to mention in this broad introduction is why GWs are expected to be produced during a first-order transition. This is simply because the collisions between the expanding bubbles create perturbations in the matter content of the Universe which then disturb the curvature of space-time according to general relativity. This would result in a stochastic GW background that could be detectable by the instruments we described in Section 1.2.2.

Chapter 6 shows how to compute the properties of such a GW background. Our main conclusion is that there exist extensions of the standard model that predict GWs potentially detectable by pulsar timing arrays [3, 4]. Future GW measurements (either detections or absence of detections) are therefore expected to give new information on both the dynamics of the Universe and its matter content.

Chapter 2

From General Relativity to GWs

As it has been emphasized in our Introduction, the paradigm of modern of physics relies on both the general theory of relativity and quantum field theory. They give the foundation on which are built the standard models of both cosmology and particle physics. The next two Chapters present the physics and mathematics of these theories by focusing on the aspects which are the most relevant for this thesis. Whereas the Introduction was given with minimal technicality, it is assumed from now on that the reader is familiar with modern physics. The reader interested in a more comprehensive description of these topics can refer to the textbook reviews mentioned in the text. Regarding this Chapter, see for example [29, 114] for GR and [115, 116] for GWs.

2.1 The General Theory of Relativity

Einstein's general theory of relativity, or general relativity (GR) for short, is a geometrical and classical theory which describes the gravitational interaction, namely the dynamics of massive objects. As explained in Section 1.1.3, it relies on the *equivalence principle*, *general coordinate invariance* and *curved space-time*. The general formalism summarizing these concepts is presented now. It will allow us to give a precise mathematical description of both GWs and cosmology, two key concepts of this thesis.

2.1.1 The mathematics of curved space-time

In order to write physical laws which are invariant under general coordinate transformations, we need to express physical quantities as mathematical objects satisfying well-defined transformation properties. In this sense, GR makes use of *tensors* which are abstract objects made of m upper (contravariant) and n lower (covariant) indices and transform as

$$x^\mu \to \bar{x}^\mu \quad \Rightarrow \quad T^{\mu_1\dots\mu_m}_{\nu_1\dots\nu_n} \to \bar{T}^{\mu_1\dots\mu_m}_{\nu_1\dots\nu_n} = \left(\prod_{i=1}^{m} \frac{\partial \bar{x}^{\mu_i}}{\partial x^{\rho_i}} \prod_{j=1}^{n} \frac{\partial x^{\sigma_j}}{\partial \bar{x}^{\nu_j}}\right) T^{\rho_1\dots\rho_m}_{\sigma_1\dots\sigma_n} \,. \tag{2.1}$$

The transformation rule of any quantity built from a combination of tensors is then uniquely determined by the previous equation. This is particularly useful to find expressions satisfying required transformation properties.

A major achievement of GR is its ability to express the geometrical nature of space-time and the gravitational interaction in terms of tensors. More particularly, the geometry of space-time is entirely defined by its metric tensor, $g_{\mu\nu}$, which can

be introduced as follows. Imagine a test particle in a gravitational field. According to the equivalence principle, there exists a local inertial frame, ξ^μ, at rest respectively to the particle. The line element, which gives the distance between two points separated by infinitesimal coordinate intervals $d\xi^\mu$, is therefore specified by the Minkowski metric of special relativity as $ds^2 = \eta_{\mu\nu} d\xi^\mu d\xi^\nu$.[1] However, if the trajectory of the particle is seen from a general coordinate system, $x^\mu = x^\mu(\xi)$, the line element becomes

$$ds^2 = \eta_{\alpha\beta} \frac{\partial \xi^\alpha}{\partial x^\mu} \frac{\partial \xi^\beta}{\partial x^\nu} dx^\mu dx^\nu \equiv g_{\mu\nu}(x)\, dx^\mu dx^\nu \,. \tag{2.2}$$

In other words, the metric $g_{\mu\nu}$ gives the notion of distance as measured in a general coordinate system and automatically satisfies the requirement (2.1) for being a tensor. It allows us to compute any finite distance along a path γ between two spacetime points A and B. Indeed, if the curved γ is parametrized by a scalar σ as $x^\mu(\sigma)$, with $x^\mu(\sigma_0) = x^\mu_A$ and $x^\mu(\sigma_1) = x^\mu_B$, we have

$$s_\gamma = \int_\gamma ds = \int_{\sigma_0}^{\sigma_1} \sqrt{g_{\mu\nu} \frac{dx^\mu}{d\sigma} \frac{dx^\nu}{d\sigma}} d\sigma \,. \tag{2.3}$$

It is now possible to study the motion of a test particle in the general coordinate system x^μ. In a way which reminds us about Newtonian mechanics, GR assumes that test objects travel along "shortest" trajectories, namely curves which minimize (2.3). Such trajectories $x^\mu(\sigma)$ are called *geodesics* and a straightforward variation of Equation (2.3) shows that they satisfy the following *geodesic equations*:

$$\frac{d^2 x^\mu}{d\sigma^2} + \Gamma^\mu_{\nu\rho} \frac{dx^\nu}{d\sigma} \frac{dx^\rho}{d\sigma} = 0 \,, \tag{2.4}$$

where the Christoffel symbols are defined as

$$\Gamma^\rho_{\mu\nu} = \frac{1}{2} g^{\rho\sigma} \left(\partial_\mu g_{\sigma\nu} + \partial_\nu g_{\sigma\mu} - \partial_\sigma g_{\mu\nu} \right) \,. \tag{2.5}$$

The geodesic equations are invariant under general coordinate transformations, but we note that the Christoffel symbols are not tensors as they do not satisfy Equation (2.1). In particular, it is always possible to find a coordinate system ξ^μ such that at a given point P we have $\Gamma^\rho_{\mu\nu}(P) = 0$. This frame is nothing but the local inertial frame introduced above and the vanishing of the Christoffel symbols is a mathematical consequence of the equivalence principle. The equations of motion for the particle simply reduce to $d^2\xi^\mu / d\sigma^2 \big|_P = 0$ and therefore ξ^μ is called a *local free-falling reference frame*.[2]

The word *local* is important and actually leads to the notion of curvature. It means that it is generally not possible to find a single frame in which two distinct free particles are both seen as free-falling. In other words, two free particles can accelerate towards each other when seen from the same frame. This is expressed by the geodesic deviation equations. Consider a family of geodesics $x^\mu(\sigma, \lambda)$ specified by the parameter λ. We write the tangent vector to the trajectory as $u^\mu(\sigma, \lambda) =$

[1] The metric signature is given by $(-,+,+,+)$. Greek indices range from 0 to 3 and Latin indices range from 1 to 3. We also work in natural units ($c = 1, \hbar = 1$) unless otherwise specified.

[2] We briefly mention that the geodesic equations share some similarity with the second law of Newton. The first term in (2.4) is the acceleration of the particle and the second term can be interpreted as the fictitious forces appearing in non-inertial reference frames.

$\frac{\partial x^\mu(\sigma,\lambda)}{\partial \sigma}$ and the deviation between geodesics as $v^\mu(\sigma,\lambda) = \frac{\partial x^\mu(\sigma,\lambda)}{\partial \lambda}$. It can be shown that the deviation satisfies the following equations:

$$\frac{D^2 v^\mu}{d\sigma^2} = -R^\mu_{\nu\rho\sigma}\, u^\nu u^\sigma v^\rho \,, \tag{2.6}$$

where we have introduced the intrinsic derivative D and the Riemann tensor R given by

$$\frac{Dv^\mu}{d\sigma} = \frac{dv^\mu}{d\sigma} + \Gamma^\mu_{\nu\rho} v^\nu \frac{\partial x^\rho}{d\sigma} \,, \tag{2.7}$$

$$R^\mu_{\nu\rho\sigma} = \partial_\rho \Gamma^\mu_{\nu\sigma} + \Gamma^\mu_{\alpha\rho}\Gamma^\alpha_{\nu\sigma} - (\rho \leftrightarrow \sigma). \tag{2.8}$$

The fact that $R^\mu_{\nu\rho\sigma}$ is a tensor means that the right-hand side of Equation (2.6) cannot be turned off by going to a free-falling frame. In terms of gravitational interaction, this term represents a tidal acceleration. In terms of geometry, it represents the notion of curvature of the manifold from which the Riemann tensor is built, in this case space-time.

Diffeomorphism invariance implies that coordinates are *a priori* meaningless in GR and proper care has to be taken when extracting physical observables. This is particularly true if we want to introduce causality. It cannot be defined from the "time" coordinate anymore as in special relativity. Fortunately, curved space-time seen as a Lorentzian manifold admits a mathematically well-defined causal structure. We can say that two events are causally connected if they can be joined by a curve whose tangent vectors V^μ at each point are either null ($g_{\mu\nu}V^\mu V^\nu = 0$) or timelike ($g_{\mu\nu}V^\mu V^\nu < 0$). It is then not difficult to define causal hypersurfaces generalizing the light cones of special relativity. More details about such considerations and the geometry of Lorentzian manifolds can be found in [29] Chapters 2 and 3.

2.1.2 Einstein Field Equations

The formalism we just presented allows us to interpret the motion of an object in a gravitational field as the motion of a particle in a curved space-time. The remaining question to answer is how the gravitational field, namely the massive matter content of the Universe, determines the curvature of space-time. We present an answer to this question based on a field theoretic approach. On one hand, the metric $g_{\mu\nu}(x)$ is seen as a classical field taking values at each point of a coordinate system x. On the other hand, the matter content is determined by a Lagrangian density $\mathcal{L}_M$. The dynamics and interaction between space-time and matter can therefore be given by an action $S[g_{\mu\nu}, \mathcal{L}_M]$ which has to be a scalar under general coordinate transformations. The simplest scalar than can be built from the metric is the Ricci scalar given by $R = g^{\mu\nu}R_{\mu\nu}$ where $R_{\mu\nu} = R^\sigma_{\mu\rho\nu}$ is the Ricci tensor. This gives rise to the Einstein-Hilbert action of GR:

$$S_{EH} = \int d^4x \sqrt{-g}\left(\frac{1}{16\pi G}R + \mathcal{L}_M\right) \,, \tag{2.9}$$

where $g = \mathrm{Det}(g_{\mu\nu})$ is the determinant of the metric and G the gravitational constant. The variation of the action according to the metric ($g_{\mu\nu} \to g_{\mu\nu} + \delta g_{\mu\nu}$) gives:

$$\delta S_{EH} = \frac{1}{16\pi G}\int d^4x \sqrt{-g}\left(R_{\mu\nu} - \frac{1}{2}R - 8\pi G\, T_{\mu\nu}\right)\delta g^{\mu\nu} \,, \tag{2.10}$$

where $T_{\mu\nu} = -\frac{2}{\sqrt{-g}}\frac{\partial(\sqrt{-g}\mathcal{L}_M)}{\partial g^{\mu\nu}}$ is the energy-momentum tensor associated to the matter distribution. As the variation of the metric is arbitrary, we obtain the following field equations:

$$R_{\mu\nu} - \frac{1}{2}R = 8\pi G\, T_{\mu\nu}\,. \tag{2.11}$$

This last expression is known as the *Einstein Field Equations* (EFE) and it governs the interrelated dynamics of space-time and matter. As the EFE involves symmetric 4×4 tensors, it forms a system of ten second-order partial differential equations. Studying the predictions and validity of GR requires to solve the EFE for different space-time and matter configurations. This is generally a difficult task as no exact analytic solutions of these equations are known. As we shall see, we usually resort to various kinds of approximations or numerical methods.

It is however important to realize that the complexity of the EFE can be slightly reduced once remembering that these equations are invariant under coordinate transformations. Indeed, we expect the freedom to choose any coordinate system to reduce the number of independent equations from 10 to 6. This can be seen in various ways, notably from the properties of the Riemann tensor. It is known to satisfy the following Bianchi identities:

$$\nabla_\kappa R^\mu_{\nu\rho\sigma} + \nabla_\sigma R^\mu_{\nu\kappa\rho} + \nabla_\rho R^\mu_{\nu\sigma\kappa} = 0 \quad \text{and} \quad \nabla_\mu \left(R^{\mu\nu} - \frac{1}{2}g^{\mu\nu}R \right) = 0\,, \tag{2.12}$$

where we remind that the covariant derivative of any tensor is given by

$$\nabla_\rho T^{\mu_1\ldots\mu_m}_{\nu_1\ldots\nu_n} = \partial_\rho T^{\mu_1\ldots\mu_m}_{\nu_1\ldots\nu_n} + \Gamma^{\mu_1}_{\lambda\rho} T^{\lambda\ldots\mu_m}_{\nu_1\ldots\nu_n} + \ldots - \Gamma^{\lambda}_{\nu_1\rho} T^{\mu_1\ldots\mu_m}_{\lambda\ldots\nu_n} - \ldots \tag{2.13}$$

It directly follows from Equations (2.11) and (2.12) that

$$\nabla_\mu T^{\mu\nu} = 0\,. \tag{2.14}$$

In other words, 4 of the 10 EFEs govern the dynamics of the matter system. The remaining 6 equations determine the geometry of space-time, namely 6 components of the metric $g_{\mu\nu}$. Its 4 remaining components are fixed by the choice of coordinates and we will see in the next Section how an appropriate choice can allow us to simplify the expression of the EFE. We also observe what is called the local conservation of energy-momentum. Indeed, Equation (2.14) for $T^{\mu\nu}$ reduces to $\partial_\mu T^{\mu\nu} = 0$ in a local free-falling frame. However, note that the energy and momentum of matter is in general not conserved in GR as it changes in response to the curvature and dynamics of space-time.

2.1.3 Harmonic gauge and post-Minkowskian expansion

Diffeomorphism invariance allows us to choose any coordinate system in order to solve the EFE (2.11). This so-called *gauge freedom* is very useful as it means that the coordinates can be fixed on a case by case by basis depending on the specific system we want to describe. In particular, it means that we can often take advantage of the possible symmetries of a configuration to simplify its analysis.

Unless otherwise specified, we will make use of the *harmonic gauge* throughout this thesis. As we shall see, this choice is particularly appropriate for the analysis of GWs and also to study the solution of the EFE when the metric consists of only small perturbations around a flat background. The harmonic condition on a set of

coordinates x^μ reads:

$$\Box_g x^\mu = 0\,, \tag{2.15}$$

where $\Box_g = g^{\mu\nu}\nabla_\mu\nabla_\nu$ is the covariant d'Alembertian.[3] When working in this gauge, it is more appropriate to trade the metric $g_{\mu\nu}$ for the following gravitational-field amplitude:

$$h^{\mu\nu} \equiv \sqrt{-g}g^{\mu\nu} - \eta^{\mu\nu}\,. \tag{2.16}$$

The harmonic condition (2.15) then implies

$$\partial_\mu h^{\mu\nu} = 0\,, \tag{2.17}$$

which gives four constraints on the metric, in the same way as explained below Equation (2.14). This allows us to rewrite the EFE as an inhomogeneous flat d'Alembertian equation [117]:

$$\Box h^{\mu\nu} = 16\pi G\,\tau^{\mu\nu}\,, \tag{2.18}$$

with $\Box = \eta^{\mu\nu}\partial_\mu\partial_\nu$. The source term $\tau^{\mu\nu}$ of this expression can be derived from the original EFE (2.11) and it contains the stress-energy-momentum content of both the matter and gravitational fields:

$$\tau^{\mu\nu} = |g|\,T^{\mu\nu} + \frac{1}{16\pi G}\Lambda^{\mu\nu}, \tag{2.19}$$

where $\Lambda^{\mu\nu}$ is a gravitational source term. Actually, $\tau^{\mu\nu}$ is not a tensor under general coordinate transformations[4] and its form will change under such transformations. This shall not be a problem as long as we keep to the harmonic gauge, for which the exact expression of the gravitational source is [117]

$$\begin{aligned}\Lambda^{\mu\nu} =& -h^{\alpha\beta}\partial^2_{\alpha\beta}h^{\mu\nu} + \partial_\alpha h^{\mu\beta}\partial_\beta h^{\nu\alpha} + \frac{1}{2}g^{\mu\nu}g_{\alpha\beta}\partial_\lambda h^{\alpha\sigma}\partial_\sigma h^{\beta\lambda}\\ &- g^{\mu\alpha}g_{\beta\sigma}\partial_\lambda h^{\nu\sigma}\partial_\alpha h^{\beta\lambda} - g^{\nu\alpha}g_{\beta\sigma}\partial_\lambda h^{\mu\sigma}\partial_\alpha h^{\beta\lambda} + g_{\alpha\beta}g^{\lambda\sigma}\partial_\lambda h^{\mu\alpha}\partial_\sigma h^{\nu\beta}\\ &+ \frac{1}{8}\left(2g^{\mu\alpha}g^{\nu\beta} - g^{\mu\nu}g^{\alpha\beta}\right)\left(2g_{\lambda\sigma}g_{\kappa\rho} - g_{\sigma\kappa}g_{\lambda\rho}\right)\partial_\alpha h^{\lambda\rho}\partial_\beta h^{\sigma\kappa}\,.\end{aligned} \tag{2.20}$$

Equation (2.18) accompanied with the condition (2.17) is completely equivalent to the original form of the EFE (2.11) and no approximation has been made to derive it. It is particularly adequate if we want to find solutions which are perturbations around the Minkowski metric and far away from any matter source ($T^{\mu\nu} = 0$). In the spirit of [117], this can be seen if we assume that h can be written as a formal power series in terms of the Newton's constant G:

$$h^{\mu\nu}_{\text{vac}} = \sum_{n=1}^{+\infty} G^n h^{\mu\nu}_{(n)}\,, \tag{2.21}$$

where the index "vac" means that the solution is valid in vacuum. This expansion is usually called a post-Minkowskian iteration, as each $h^{\mu\nu}_{(n)}$ coefficient corresponds to an nth-order perturbation of the metric around $\eta^{\mu\nu}$. Once this expansion is substituted in both Equation (2.18) and the harmonic condition (2.17), terms with similar

[3] The name of these coordinates comes from the fact that any function f satisfying $\Box f = 0$ is called "harmonic".

[4] Note however that $\tau^{\mu\nu}$ is invariant under Lorentz (flat space-time) transformations.

powers in G can be equated to get an iterative set of equations at each order n:

$$\begin{aligned} \Box h^{\mu\nu}_{(n)} &= \Lambda^{\mu\nu}_{(n)}[h_{(1)}, h_{(2)}, \dots, h_{(n-1)}] \,, \\ \partial_\nu h^{\mu\nu}_{(n)} &= 0 \,. \end{aligned} \tag{2.22}$$

The successive $\Lambda^{\mu\nu}_{(n)}$ can be explicitly computed by expanding the expression (2.20). Section (2.2) will show us that this approach is useful to study GWs produced by the merger of two astrophysical objects.

2.1.4 GWs from linearized gravity

We now present how GWs emerge when we consider approximate solutions of GR. As a starting point, note that $\Lambda^{\mu\nu}_{(1)} = 0$ in Equation (2.22). This suggests that the EFE should simplify greatly if we only consider linear perturbations of the metric. Let us therefore restrict our attention to a metric of the form

$$g_{\mu\nu} = \eta_{\mu\nu} + \tilde{h}_{\mu\nu}, \quad |\tilde{h}_{\mu\nu}| \ll 1 \,. \tag{2.23}$$

The gravitational-field amplitude (2.16) reads $h_{\mu\nu} = -\tilde{h}_{\mu\nu} + \frac{1}{2}\eta_{\mu\nu}\tilde{h}^\alpha_\alpha + \mathcal{O}(|\tilde{h}|^2)$, after having properly expanded the term $\sqrt{-g} = \sqrt{-\eta}\left(1 + \frac{1}{2}\tilde{h}^\alpha_\alpha\right) + \mathcal{O}(|\tilde{h}|^2)$. It is usual to introduce the "trace-reversed" amplitude

$$\bar{h}_{\mu\nu} = \tilde{h}_{\mu\nu} - \frac{1}{2}\eta_{\mu\nu}\tilde{h} \,, \tag{2.24}$$

with $\tilde{h} = \tilde{h}^\alpha_\alpha$. The EFE (2.18) and harmonic gauge condition (2.17) then become at linear order:

$$\begin{aligned} \Box \bar{h}_{\mu\nu} &= -16\pi G T_{\mu\nu} \,, \\ \partial^\nu \bar{h}_{\mu\nu} &= 0 \,. \end{aligned} \tag{2.25}$$

This is nothing but a wave equation with a source term. This tells us that the geometry of space-time can admit some wave-like dynamics, generically referred to as *gravitational waves*. Although Equation (2.25) is only valid for small metric perturbations, it is a good starting point to get an overview of the properties of GWs.

Propagation in vacuum

Let us consider the previous linear wave equation in vacuum: $\Box \bar{h}_{\mu\nu} = 0$. It is a well-known fact that it is invariant under a larger class of coordinate transformations than those imposed by the harmonic gauge. In addition to $\partial^\nu \bar{h}_{\mu\nu} = 0$ which reduces the number of independent components of the metric from 10 to 6, there is another residual gauge freedom allowing us to reduce it to only 2 components. A particularly convenient choice is the "transverse-traceless" (TT) gauge which imposes [115]

$$\bar{h}_{0\mu} = 0, \quad \bar{h}^i_i = 0, \quad \partial^j \bar{h}_{ij} = 0 \,. \tag{2.26}$$

Note that such a gauge choice is not possible in general inside the source where $\Box \bar{h}_{\mu\nu} \neq 0$.

The homogeneous equation $\Box \bar{h}_{\mu\nu} = 0$ admits plane wave solutions of the form[5] $\bar{h}^{TT}_{ij}(x) = e_{ij}(\mathbf{k}) e^{ik^\mu x_\mu}$ where $k^\mu = (|\mathbf{k}|, \mathbf{k})$ and the polarization tensor $e_{ij}(\mathbf{k})$ admits

[5] We use the superscript TT to specify that the solution is given in the TT gauge.

two independent components. Note that such plane waves propagate at the speed of light. Moreover, similarly to electromagnetism, such solutions are transverse to the direction of propagation given by $\hat{\mathbf{n}} = \mathbf{k}/|\mathbf{k}|$. Indeed, the gauge condition (2.26) implies $n^j \bar{h}_{ij} = 0$. If we define $\hat{\mathbf{n}}$ along the z-axis, the solution of the linearized EFE in vacuum with specific wave number $|\mathbf{k}|$ is given by

$$\bar{h}^{TT}_{\mu\nu}(x) = \begin{pmatrix} 0 & 0 & 0 & 0 \\ 0 & h_+ & h_\times & 0 \\ 0 & h_\times & -h_+ & 0 \\ 0 & 0 & 0 & 0 \end{pmatrix} e^{i|\mathbf{k}|(z-t)} \,, \tag{2.27}$$

where h_+ and $h_\times$ are the two degrees of freedom called the "plus" and "cross" polarization of GWs.

The most general solution of the linearized EFE in vacuum can then be written as a superposition of such plane waves with different wave vectors $\mathbf{k}$ and polarization coefficients:

$$\begin{aligned} \bar{h}^{TT}_{ij}(x) &= \int \frac{d^3k}{2\pi} \left(\mathcal{A}_{ij}(\mathbf{k})\, e^{ik^\mu x_\mu} + \mathcal{A}^*_{ij}(\mathbf{k})\, e^{-ik^\mu x_\mu} \right) \\ &= \int_0^{+\infty} df f^2 \int d^2\hat{\mathbf{n}} \left(\mathcal{A}_{ij}(f, \hat{\mathbf{n}})\, e^{-2\pi i f(t - \hat{\mathbf{n}}\mathbf{x})} + c.c. \right) \,, \end{aligned} \tag{2.28}$$

where $\mathcal{A}^i_i = 0$ and $k^i \mathcal{A}_{ij} = 0$. In the second line we have introduced the frequency f satisfying $|\mathbf{k}| = 2\pi f$. At this stage, it is not possible to determine the coefficients of this expansion from the linearized EFE in vacuum alone. Any specific solution will typically depend on the source from which it has been generated. In this thesis, we will mainly focus on two different types of sources. First, we will consider GWs emitted from two inspiralling black holes (see Section (2.2) and Chapter (4)). In such a case, the propagation of the waves is well defined along a specific direction $\hat{\mathbf{n}}_0$ such that Equation (2.28) at a particular position $\mathbf{x}_0$ (e.g. at the location of a detector) can be written as [115]

$$\bar{h}^{TT}_{ab}(t) = \int_0^{+\infty} df f^2 \left(A_{ab}(f)\, e^{-2\pi i f t} + c.c. \right) \,, \tag{2.29}$$

with $a, b = 1, 2$ the indices in the transverse plane. In addition to being well oriented along $\hat{\mathbf{n}}_0$, this type of signal is also transient meaning that it will only last for a short period of time at a given location. The second source type we will consider is from cosmological origin (see Section (3.2) and Chapter (6)). In this case, the produced signal corresponds to a stochastic background of GWs with superposition of waves propagating in multiple directions over long period of time. Therefore $\bar{h}^{TT}_{ij}$ will not reduce to a 2×2 matrix as in Equation (2.29).

Effect on test masses and detection principle

GWs are expected to be detected from their effect on test masses (namely objects moving along the geodesics of space-time but not heavy enough to produce any significant curvature by themselves). The motion of such test masses in the background of GWs can be studied from both the geodesic equations (2.4) and geodesic deviation equations (2.6) in the TT gauge. These two equations actually tell us that if some test masses are initially at rest at $\sigma = 0$, namely $dx^i/d\sigma\big|_{\sigma=0} = 0$, they will stay at rest and their coordinate separation will stay constant. This can be seen from the fact that the Christoffel symbols Γ^i_{00} vanish in the TT gauge at linear order of perturbation.

This observation does not mean that GWs have no effect on test masses but just that the coordinates in the TT gauge have been implicitly chosen such that they do not change under the passage of GWs. However, coordinates do not express physical quantities by themselves. Physical distances and times have to be extracted from the line element $ds^2 = \left(\eta_{\mu\nu} + \bar{h}^{TT}_{\mu\nu}(x)\right) dx^\mu dx^\nu$. For GWs propagating along the z axis and two test masses at $(t, x_1, 0, 0)$ and $(t, x_2, 0, 0)$, the coordinate separation $L = x_2 - x_1$ indeed remains constant, but the proper distance s is given at linear order by

$$\begin{aligned} s &= (x_2 - x_1)\left(1 + h_+ \cos(|\mathbf{k}|t)\right)^{\frac{1}{2}} \\ &\approx L\left(1 + \frac{1}{2} h_+ \cos(|\mathbf{k}|t)\right) , \end{aligned} \tag{2.30}$$

where we have used the metric (2.27). It means that the physical distance seen in the TT frame oscillates in response to the GWs. It is straightforward to generalize the previous formula to a ring of test masses. The effect of the cross and plus polarizations results in the behaviour that we described in the Introduction in Figure 1.6. We will not describe the properties of GW detectors or experimental processes in more details than what we have already written in this Section.

Generation of GWs from weak sources

The above discussion gives us information on how GWs propagate and can be detected. We now show how they are produced from the dynamics of matter. To begin with, we assume that the source is sufficiently weak such that the metric around it can be considered as flat and the linear approximation (2.23) still holds. Another useful approximation at this stage is to assume that the typical velocity v of the source is small compared to the speed of light, such that we can focus on the lowest-order solution in terms of v/c. We shall see in Section 2.2 how to go beyond such approximations.

A typical way to solve the wave equation (2.25) with a source term is by the use of retarded Green functions. This gives

$$\bar{h}_{\mu\nu}(x) = 4G \int d^3\mathbf{x}' \frac{1}{|\mathbf{x} - \mathbf{x}'|} T_{\mu\nu}\left(t - |\mathbf{x} - \mathbf{x}'|, \mathbf{x}'\right) . \tag{2.31}$$

Note that this solution directly satisfies the Harmonic gauge conditions (2.17). This is because the local conservation law (2.14) of the energy-momentum tensor reduces to the flat space-time conservation $\partial^\mu T_{\mu\nu} = 0$ at linear order. Our aim is to study the form of the previous solution at a distance $r = |\mathbf{x}|$ far away from the source. This would allow us to find the relations between the coefficients in Equations (2.27)-(2.28) and the properties of the source. Therefore we can assume that $|\mathbf{x}| \gg d$ where d is the typical radius of the source. Hence we can write $|\mathbf{x} - \mathbf{x}'| = r - \mathbf{x}' \cdot \hat{\mathbf{n}} + \mathcal{O}\left(d^2/r\right)$ where we use the notation $\hat{\mathbf{n}} = \mathbf{x}/r$. The solution (2.31) becomes

$$\bar{h}_{\mu\nu}(x) = \frac{4G}{r} \int d^3\mathbf{x}' T_{\mu\nu}\left(t - r + \mathbf{x}' \cdot \hat{\mathbf{n}}, \mathbf{x}'\right) , \quad r \gg d . \tag{2.32}$$

This expression can be further simplified if we now assume that the source is non-relativistic. To make the argument clear, let us first consider the energy-momentum

tensor in terms of its Fourier transform:

$$T_{\mu\nu}\left(t-r+\mathbf{x}'\cdot\hat{\mathbf{n}},\mathbf{x}'\right)=\int\frac{d^4k}{(2\pi)^4}\tilde{T}_{\mu\nu}(\omega,\mathbf{k})\,e^{-i\omega(t-r+\mathbf{x}'\cdot\hat{\mathbf{n}})+i\mathbf{k}\mathbf{x}'}\,. \tag{2.33}$$

For a non-relativistic source, we can expect $\tilde{T}_{\mu\nu}$ to be peaked at a characteristic frequency ω_s and that $v\sim\omega_s\,d\ll c$. Using the facts that the frequency ω of the produced GWs is expected to be of order ω_s and that $|\mathbf{x}'|<d$, we have $\omega\,\mathbf{x}'\cdot\hat{\mathbf{n}}\lesssim\omega_s\,d\ll c$. We note in passing that the wavelength of the GWs, $\lambda\!\!\!^{-}=\frac{c}{\omega}$, roughly satisfies $\lambda\!\!\!^{-}\sim\frac{c}{v}d$ and that the non-relativistic condition implies

$$v\ll c\quad\Rightarrow\quad\lambda\!\!\!^{-}\gg d\,. \tag{2.34}$$

This allows us to expand the exponential in Equation (2.33) and to write the energy-momentum tensor as a multipole expansion:

$$T_{\mu\nu}\left(t-r+\mathbf{x}'\cdot\hat{\mathbf{n}},\mathbf{x}'\right)=T_{\mu\nu}\left(t-r,\mathbf{x}'\right)+x'^i n^i\partial_t T_{\mu\nu}\left(t-r,\mathbf{x}'\right)+\ldots \tag{2.35}$$

We will come back to this expansion in the next Section. For the moment, we only keep the first term and get

$$\bar{h}_{\mu\nu}(x)=\frac{4G}{r}\int d^3\mathbf{x}'\,T_{\mu\nu}\left(t-r,\mathbf{x}'\right),\quad r\gg d,\ v\ll c\,. \tag{2.36}$$

There is one further step we can apply to get more information about this equation. The flat space-time conservation of the energy-momentum tensor, $\partial^\mu T_{\mu\nu}=0$, gives the following relations:

$$\int d^3\mathbf{x}\,T_{ij}(x)=\frac{1}{2}\frac{d^2}{dt^2}\int d^3\mathbf{x}\,x_i x_j T^{00}(x)\,. \tag{2.37}$$

Moreover, T^{00} corresponds to the mass-density ρ of the source at lowest order in v/c. We can therefore introduce the *second mass moment* $I_{ij}(t)=\int d^3\mathbf{x}\,\rho(x)x_i x_j$ and obtain the GW metric perturbation far away from a weak non-relativistic source:

$$\bar{h}_{ij}(x)=\frac{2G}{r}\ddot{I}_{ij}(t-r),\quad r\gg d,\ v\ll c. \tag{2.38}$$

We can use this formula to get a rough estimate of the amplitude of typical GWs. Imagine an astrophysical source of mass M, radius R and period P at a distance r from the Earth. The second mass moment of this system is roughly $I_{ij}\sim MR^2$ and then $\ddot{I}_{ij}\sim MR^2/P^2$. The radius is related to the mass and period from Newtonian mechanics such that we can get [114]

$$\bar{h}_{ij}\sim 10^{-21}\left(\frac{M}{M_\odot}\right)^{5/3}\left(\frac{1\,\mathrm{h}}{P}\right)^{2/3}\left(\frac{100\,\mathrm{pc}}{r}\right)\,. \tag{2.39}$$

We see that it is a small value for typical sources. This gives us an estimate of the sensitivity needed by a detector to observe such GWs.

2.2 GWs from compact binaries

We have learned from the previous Section that GWs are not the result of a specific phenomenon but rather a generic prediction of GR. Among the various types of GWs, we are particularly interested in those produced by compact binary systems, such as a binary black hole (BBH) and a binary neutron star (BNS). As explained in our Introduction, this is the kind of GWs that has been observed by LIGO/Virgo. The data obtained from these detections are crucial as they allow us to test GR and other fundamental theories of nature. We will see how this can be done in practice in this Section. In particular, this requires to compute solutions of the EFE to a much higher accuracy compared to the result we obtained in Equation (2.38).

The general dynamics of a binary system can be decomposed in three phases, each of them modelled by different methods. The first stage, the *inspiral*, describes the adiabatic co-rotation of the two objects. Their orbit gradually shrinks and circularizes as they radiate energy in the form of GWs. The equations of motion and the production of GWs can be analytically estimated through the post-Newtonian [117] and effective-one-body [118] methods. The second stage, the *merger*, starts when the two bodies reach their *innermost stable circular orbit* and then fall towards each other until they coalesce into a single object. The gravitational field is so strong that analytic approximations break down and numerical relativity is required to model this process. The last phase corresponds to the *ringdown* of the remnant body until it reaches a stable state. It is described by models based on quasi-normal modes [119]. Note that each phase can clearly be seen in Figure 1.5 that we gave in the Introduction. We also emphasize that various groups, using different techniques, have contributed to the modelling of these three phases. Relevant references can be found in the review [117] for analytic approaches and in the review [120] for numerical relativity.

The next part of the thesis will only present the inspiral phase of black hole binaries. We will therefore not discuss neutron star mergers. As such events are nevertheless very interesting, we briefly mention some of their characteristics. To the best of our knowledge, a BBH does not produce any other detectable signal on top of GWs. However, coalescing BNSs are known to also emit some electromagnetic radiation resulting from nuclear processes occurring during this extremely violent process. It means that such astrophysical events can be detected by both gravitational and electromagnetic detectors. This has actually been the case with the signal GW170817 seen by LIGO/Virgo and the corresponding gamma-ray burst GRB 170817A detected by Fermi and INTEGRAL [121]. This event marked a breakthrough for multi-messenger astronomy which is expected to be of prime importance in the future. Another interest of BNS mergers is that they can provide us with information regarding the state of matter inside neutron stars and help us to improve our understanding of fundamental interactions [122].

We now move to the detailed study of the analytic modelling of the inspiral phase of a BBH. This will allow us to understand how LIGO/Virgo collaborations have been able to test GR from GW waveforms, but this will also give us the formalism we need for our analysis of non-commutative space-time in Chapter 4. We start by a brief discussion about the nature of black holes in GR and then present the post-Newtonian formalism of Damour and Blanchet [117].

2.2.1 Schwarzschild metric and Black Holes

Black holes are an important prediction of GR that appear when we consider the metric produced by a static and spherically symmetric system of mass M. *A priori*, such a metric will also be useful to describe the geometry of space-time outside a star.

Metric outside a point mass

Only a few exact solutions of the EFE exist. They are most often found when some symmetries are involved like in our case of interest. Indeed, Birkhoff's theorem [123] states that any spherically symmetric solution of the EFE in vacuum is static and asymptotically flat. It follows that it is uniquely given by the Schwarzschild metric [124] describing the geometry outside a point mass. In a suitable coordinate system, this metric reads

$$ds^2 = -\left(1-\frac{2GM}{r}\right)dt^2 + \left(1-\frac{2GM}{r}\right)^{-1} dr^2 + r^2\left(d\theta^2+\sin^2(\theta)d\phi^2\right) . \quad (2.40)$$

where M can be identified as the mass of the central object. Although the last expression apparently admits two singularities at $r = 0$ and $r = 2GM$, it is well known that the latter one is an artifact of the coordinate system and can be removed by choosing other coordinates [29].

The first reason why this metric is interesting is that it provides a way to predict the motion of planets around a star. This can be compared to solar system observations to test GR. As the radius of the orbits of the planets around the Sun are much further away than $2GM_\odot$, the above coordinate system can be used without any problem. To date, solar system tests are in good agreement with GR [125] and we note in passing that it successfully resolves the problem **(L1)** we mentioned in our Introduction regarding the precession of Mercury.

Black Holes

The second reason why the Schwarzschild metric is interesting appears if we try to study the geometry (2.40) for values of r smaller or around $2GM$. The usual approach is to investigate the behaviour of light rays and the causal structure of this space-time. Interestingly, it turns out that light (and therefore any other particle) cannot escape the region $r < 2GM$ (see [29, 114] for more details). The stationary three-dimensional null surface $r = 2GM$ is therefore called the *horizon* of the metric and has the property that once crossed it cannot be crossed back. If such a geometry exists, no light would ever emerge from inside the horizon hence the name black hole. For later convenience, we introduce the notation $R_S = 2GM$ where R_S is called the Schwarzschild radius of the BH.

There are various evidences supporting the existence of such objects. Maybe the most convincing one has been provided very recently by the Event Horizon Telescope which was able to get a picture of a black hole surrounded by its accretion disk [126]. Another evidence actually comes from the detection of GWs by LIGO/Virgo, although this is an indirect proof of their existence. Although there are several interesting things to say about BHs, such as their production mechanisms, we will not give more details in this thesis. It will be sufficient for our subsequent analysis to know that they exist.

2.2.2 The post-Newtonian formalism

We now show how to compute the waveform of GWs produced during the inspiral of a BBH. We follow the formalism of Damour and Blanchet which is discussed at great length in the review [117] and in [115] Chapters 3 and 5. Most of the steps which are presented below will also be useful in Chapter 4 where we study the GWs produced by a BBH in non-commutative space-time.

Approximation schemes and zone decomposition

The idea behind the post-Newtonian (PN) formalism is to compute approximate solutions of the EFE as perturbative expansions in terms of the metric and velocity. Equation (2.38) would then be the lowest order term of the waveform of GWs computed in this way. Indeed, we remind that it was obtained for a weak (linearized gravity) and slowly moving ($v \ll c$) source. For a gravitationally bound two-body system, these two approximations are actually not independent. To see this, let us consider two objects of masses m_1 and m_2 and let us introduce some useful quantities:[6]

$$\begin{aligned} M &= m_1 + m_2 \\ \mu &= \tfrac{m_1 m_2}{M} \\ \nu &= \tfrac{\mu}{M} = \tfrac{m_1 m_2}{M^2} \,, \end{aligned} \tag{2.41}$$

known as the total mass, the reduced mass, and the symmetric mass ratio of the system. Then the Virial theorem tells that[7]

$$\frac{1}{2}\mu v^2 = \frac{1}{2}\frac{G\mu M}{r} \quad \Rightarrow \quad \frac{v^2}{c^2} = \frac{R_S}{2r} \,. \tag{2.42}$$

Since a weak gravitational field is equivalent to asking the Schwarzschild radius to be small compared to the radius of the system, $R_S/r \ll 1$, this is equivalent to $v \ll c$. So unless we consider systems tied by non-gravitational forces, both expansions have to be performed at the same time.

Let us now see how such perturbative expansions can be performed to solve the full EFE. We consider the exact expression (2.18) valid in the harmonic gauge. It can be formally written as a retarded integral of the form

$$h^{\mu\nu}(t, \mathbf{x}) = -\frac{4G}{c^4} \int \frac{d^3\mathbf{x}'}{|\mathbf{x} - \mathbf{x}'|} \, \tau^{\mu\nu} \left(t - \frac{|\mathbf{x} - \mathbf{x}'|}{c}, \mathbf{x}' \right) \,. \tag{2.43}$$

Compared to the linear Equation (2.31), this expression does not represent a solution for the metric as it appears on both sides of the equation, notably through τ. On the contrary, the non-linearity of the EFE is now more than manifest and we clearly see that retardation effects will occur. In particular, the metric at time t_0 and distance r_0 of the source will not only be determined by the state of the source at time $t_0 - r_0/c$ (as it would be the case in flat space-time) but also from all its previous states. This will give rise to so-called hereditary and tails effects. Another strong complication is that τ extends over all space-time and is not restricted to a compact region around the source.

[6] Note that we shall neglect the spin of BHs in our discussion. More details can be found in [117] Chapter 11.

[7] We will sometimes restore the speed of light c in our equations for clarity.

Despite these difficulties, the important observation is that retardation effects are much smaller near the source (small $|\mathbf{x}-\mathbf{x}'|$) than far away from it. This is one motivation to try to solve the EFE with different perturbative schemes in different space-time zones and then to match these solutions together. For a source of size d, the idea is to consider three zones as follows:

$$\begin{cases} \text{near zone:} & 0 < r < d \\ \text{exterior near zone:} & d < r < \mathcal{R} \\ \text{far zone:} & \mathcal{R} < r \end{cases} \tag{2.44}$$

where, for non ultra-relativistic sources, $\mathcal{R}$ can be identified with the wavelength $\lambda\!\!\!^{-}$ satisfying Equation (2.34). Reference [117] argues that the EFE can be solved pertubatively as a post-Newtonian expansion in $\frac{v}{c}$ for $r < \mathcal{R}$ and as a post-Minkowskian expansion for $r > \mathcal{R}$. The two series can then be matched together in the exterior near zone where they are both valid.

Far zone solution

We remind that the post-Minkowskian approach looks for solutions of the vacuum EFE ($T^{\mu\nu} = 0$ far from the source) of the form (2.21): $h^{\mu\nu}_{\text{vac}} = \sum_{n=1}^{+\infty} G^n h^{\mu\nu}_{(n)}$. This requires to solve iterative equations of the form (2.22). This is not a trivial task as these equations are inhomogeneous for $n \geq 2$. As exposed in Chapter 2 of [117], general solutions for each $h_{(n)}$ have been found in the form of a multipole expansion of symmetric-trace-free (STF) harmonics. This method is now known as the multipolar post-Minkowskian (MPM) approach. The generic solution can be written as

$$h^{\mu\nu}_{\text{ext}} = \sum_{n=1}^{+\infty} G^n h^{\mu\nu}_{(n)}[I_L, J_L, W_L, X_L, Y_L, Z_L] \,, \tag{2.45}$$

where the so-called *mass-type* multipole moments I_L and *current-type* multipole moments J_L encode the physical properties of the system. The other multipole moments W_L to Z_L are there to ensure the harmonic gauge condition. Regarding the notation, a STF tensor I_L is made of l spatial indices j_1 to j_l. I_L is also invariant under the exchange of any pair of indices and it has a vanishing trace. Actually, any expansion in terms of STF tensors is equivalent to an expansion in terms of the more usual spherical harmonics.

Theorem 4 of [117] then states that the metric (2.45), valid in harmonic coordinates $(t, \mathbf{x})$, can be conveniently expressed far away from the source in terms of the so-called radiative coordinates $(T, \mathbf{X})$ as a series in $1/R$ (for $R \to +\infty$ and fixed retarded time, $U = T - R/c = \text{const}$). Rather than the metric itself, we are more interested in the energy flux $\mathcal{F}$ carried away by GWs far away from the source. Equation (68a) in [117] tells us that it is given by:

$$\mathcal{F} = \sum_{l=2}^{+\infty} \frac{G}{c^{2l+1}} \left(\frac{(l+1)(l+2)}{(l-1)l!(2l+1)!!} \frac{dU_L}{dT} \frac{dU_L}{dT} + \frac{4l(l+2)}{c^2(l-1)(l+1)!(2l+1)!!} \frac{dV_L}{dT} \frac{dV_L}{dT} \right) \,, \tag{2.46}$$

where U_L and V_L are the mass and current radiative moments encompassing the information coming from the source. As explained in Section 3.3 of [117], they are related in a complicated way to the moments I_L and J_L introduced above. We also see that $\mathcal{F}$ is directly written as a post-Newtonian series. Actually, looking at the form of $\mathcal{F}$ order by order in c shows that the flux is made of both instantaneous and retarded terms (called tails effects). This is not a surprise taking into account our

previous discussion below Equation (2.43). For clarity, it is useful to write the flux as a sum of terms of different nature in the following way:

$$\mathcal{F} = \mathcal{F}_{inst} + \mathcal{F}_{tail} + \mathcal{F}_{tail-tail} \,, \tag{2.47}$$

where $\mathcal{F}_{inst}$ is the so-called instantaneous flux, namely the flux produced only by the source multipole moments, and $\mathcal{F}_{tail}$ is composed of tail integrals coming from non-linear multipole interactions between source and radiative moments (see Sec. 3.2 in [117]). We give here the leading-order expression of the instantaneous part of the flux in terms of the source moments. It will be useful for us in Chapter 4 and reads:

$$\mathcal{F}_{inst} = \frac{G}{c^5}\left\{\frac{1}{5}\frac{d^3I_{ij}}{dt^3}\frac{d^3I_{ij}}{dt^3} + \frac{1}{c^2}\left(\frac{1}{189}\frac{d^4I_{ijk}}{dt^4}\frac{d^4I_{ijk}}{dt^4} + \frac{16}{45}\frac{d^3J_{ij}}{dt^3}\frac{d^3J_{ij}}{dt^3}\right) + \mathcal{O}\left(\frac{1}{c^4}\right)\right\} . \tag{2.48}$$

At this stage, the multipole moments are still arbitrary tensors. They can only be determined from the source properties. This will be achieved once the general metric solution (2.45) is matched to the near zone solution. We note in passing that the first term in the above formula is nothing but a generalization of the well-known Einstein quadrupole formula. It could have been derived from the lowest-order solution (2.38) found under the linear approximation.

Near zone solution

In the near zone, the EFE has to be solved by taking into account the energy-momentum tensor of the source. This is achieved in the post-Newtonian formalism by looking for solutions of the form

$$h^{\mu\nu} = \sum_{n=2}^{+\infty}\frac{1}{c^n}h_n^{\mu\nu} \quad \text{with} \quad \tau^{\mu\nu} = \sum_{n=-2}^{+\infty}\frac{1}{c^n}\tau_n^{\mu\nu} \,. \tag{2.49}$$

This provides the following set of equations:

$$\Delta h_m^{\mu\nu} = 16\pi G\,\tau_{m-4}^{\mu\nu} + \partial_t^2\, h_{m-2}^{\mu\nu} \,. \tag{2.50}$$

They can be solved order by order in $m \geq 2$ and eventually lead to a generic expression for the metric at arbitrary PN order. It is sufficient for us to present the 2PN result which is given by [117]

$$\begin{aligned} g_{00} &= -1 + \frac{2}{c^2}V - \frac{2}{c^4}V^2 + \mathcal{O}\left(\frac{1}{c^6}\right) \\ g_{0i} &= -\frac{4}{c^3}V_i + \mathcal{O}\left(\frac{1}{c^5}\right) \\ g_{ij} &= \delta_{ij}\left(1 + \frac{2}{c^2}V + \frac{2}{c^4}V^2\right) + \frac{4}{c^4}\hat{W}_{ij} + \mathcal{O}\left(\frac{1}{c^6}\right) \,. \end{aligned} \tag{2.51}$$

V, V_i and W_{ij} are different retarded potentials that depend on the source. Note that other potentials will appear if we consider higher-order terms in the metric. The potential V actually contains all the information we shall need in this thesis. It is

given in terms of a retarded integral as follows:

$$V(\mathbf{x},t) = \Box^{-1}_{\rm ret}\left[-4\pi G\sigma\right] \equiv G\sum_{k=0}^{+\infty}\frac{(-1)^k}{k!}\left(\frac{\partial}{c\,\partial t}\right)^k\int d^3\mathbf{x}'|\mathbf{x}-\mathbf{x}'|^{k-1}\sigma(\mathbf{x}',t)\,, \tag{2.52}$$

where the matter source appears through the quantity $\sigma = \frac{T^{00}+T^{ii}}{c^2}$. Note that in the general PN formalism, some of the integrals in the definition of the retarded d'Alembertian may diverge at high PN orders and require the use of regularization techniques. This problem will however not occur at the order we shall consider in the rest of this thesis.

The previous formula tells us that if we know the energy-momentum tensor of the source, we can iteratively compute the retarded potentials and deduce the explicit form of the metric (2.51). Things are actually more complicated in practice as the energy-momentum tensor usually depends on the metric. In general, metric and matter act and backreact on each other and so we also need to know what would be the motion of the source according the metric. This can be done by computing the geodesic equations of particles moving in this geometry. These equations can be found from the local conservation of the energy-momentum tensor:

$$\nabla_\nu T^{\mu\nu} = 0 \quad \Rightarrow \quad \partial_\nu\left(\sqrt{-g}\,g_{\lambda\mu}T^{\mu\nu}\right) = \frac{1}{2}\sqrt{-g}\,\partial_\lambda g_{\mu\nu}T^{\mu\nu}\,. \tag{2.53}$$

For a test particle of velocity $v = (c, v^i)$, it is possible to rewrite the previous equation in the form [117]

$$\frac{dP^i}{dt} = F^i\,, \tag{2.54}$$

where the *linear momentum density* P and the *force density* F are given by

$$P^i = c\frac{g_{i\mu}v^\mu}{\sqrt{-g_{\alpha\beta}v^\alpha v^\beta}}, \quad F^i = \frac{c}{2}\frac{\partial_i g_{\mu\nu}v^\mu v^\nu}{\sqrt{-g_{\alpha\beta}v^\alpha v^\beta}}\,. \tag{2.55}$$

Explicit expressions for P and F in terms of the retarded potential V, V_i, ... can be found by inserting the metric (2.51) in these two equations. In summary, we now have all the information regarding how the metric influences the motion of the bodies and how the bodies are responsible for this metric. The only missing information is the specific form of an energy-momentum tensor as function of the physical parameters of the source. We will see how this can be done for a BBH. Before that, we show how the far zone and near zone results can be combined together.

Matching prescription

The space-time zone decomposition (2.44) suggests that the solutions of the metric found in the far and near zones are simultaneously valid in the exterior near zone. The existence of this latter region is well-justified as long as the radiation wavelength $\lambda\!\!\!^{-}$ stays bigger than the size of the source d. This is the case for non-relativistic sources as emphasized in Equation (2.34). However, this assumption seems less valid if we consider relativistic bodies, as it will be the case for us. Indeed, we can expect a BBH to have a high velocity and to create a strong gravitational field in its surroundings. Fortunately, it can be shown that the zone decomposition formalism still holds even for such objects. The justification can be found in [115] Section 5.5.

We do not give the details of the matching procedure here. The important thing to remember is that it allows us to relate the multipole moments I_L and J_L to the source properties. If we introduce the retarded time $u = t - r/c$, Theorem 6 of [117] gives the relation[8]

$$I_L(u) = \mathcal{FP} \int d^3\mathbf{x} \int_{-1}^{1} dz \left(\delta_l \hat{x}_L \Sigma - \frac{4(2l+1)}{c^2(l+1)(2l+3)} \delta_{l+1} \hat{x}_{iL} \frac{d\Sigma_i}{dt} + \frac{2(2l+1)}{c^4(l+1)(l+2)(2l+5)} \delta_{l+2} \hat{x}_{ijL} \frac{d^2\Sigma_{ij}}{dt^2} \right) (u + zr/c, \mathbf{x}) \,, \tag{2.56}$$

and similar expressions for J_L and $W_L, \dots Z_L$. This integral involves some source quantities defined as

$$\Sigma = \frac{\tau^{00} + \tau^{ii}}{c^2}, \quad \Sigma_i = \frac{\tau^{0i}}{c}, \quad \Sigma_{ij} = \tau^{ij}. \tag{2.57}$$

Once the (near-zone) pseudo-tensor $\tau^{\alpha\beta}$ is itself post-Newtonian expanded, Equation (2.56) gives explicit expressions of the moments in terms of the source parameters. This task rapidly becomes very complicated as the PN order increases. Fortunately for us, we shall only encounter expressions that stay relatively tractable in this Chapter and Chapter 4. The lowest order part of (2.56) is actually quite simple as it reduces to

$$I_{ij} = \int d^3\mathbf{x}\, \hat{x}_{ij} \sigma + \mathcal{O}\left(\frac{1}{c^2}\right) \,, \tag{2.58}$$

where σ has been introduced above. Note that we have also made use of the STF notation in the sense that $\hat{x}_{ij} = x_i x_j - \delta_{ij}/3$.

Binary black hole in circular orbit

Let us define an energy-momentum tensor describing a BBH without spin. The system is fully characterized by the two masses m_1 and m_2 of each BH. In practice, we shall mostly work with the reduced mass μ and symmetric mass ratio ν given by Equation (2.41). The usual approach is to model this system by describing the BHs as point-particles. The energy-momentum tensor is therefore given by [127]

$$T^{\mu\nu}(t, \mathbf{x}) = m_1 \gamma_1(t) v_1^\mu(t) v_1^\nu(t) \delta^3(\mathbf{x} - \mathbf{y}_1(t)) + 1 \leftrightarrow 2 \,, \tag{2.59}$$

with $\mathbf{y}_i(t)$ the positions, and $v_i^\mu(t) = \left(c, \frac{d\mathbf{y}_i(t)}{dt}\right)$ the velocities of the two bodies $i = 1, 2$. The factor γ_1 (and similarly γ_2) is expressed from the metric as

$$\gamma_1 = \frac{1}{\sqrt{g_1 (g_{\alpha\beta})_1 \frac{v_1^\alpha v_1^\beta}{c^2}}} \,. \tag{2.60}$$

This description in terms of point-particles actually comes with a price. If we directly insert the expression (2.59) into the metric, this one will be infinite because

[8] The symbol $\mathcal{FP}$ stands for *finite part*. It means that in general some divergences may appear when trying to compute the integral, see [117] for more details.

of the delta functions describing the position of the bodies. Fortunately, it is possible to resolve this problem by using the so-called Hadamard regularization which is described in [128].[9]

It is now possible to combine all the elements we have described above to determine the motion of the two BHs in the geometry they induce. We do not present the details of such computations here as we will repeat them in Chapter 4. We only give the most relevant results at 2PN order. Since the orbit of a binary system tends to circularize as it radiates GWs [130, 131], we assume that the objects are in quasi-circular motion. In this case, the 2PN relative acceleration of the system, expressed in terms of the relative position $\mathbf{y}(t) = \mathbf{y}_1(t) - \mathbf{y}_2(t)$, reduces to

$$\mathbf{a}_{circ} = -\Omega^2 \mathbf{y} + \mathcal{O}\left(\frac{1}{c^5}\right) , \tag{2.61}$$

where the angular frequency Ω is given by

$$\Omega^2 = \frac{GM}{r^3}\left[1 + (-3+\nu)\gamma + \left(6 + \frac{41}{4}\nu + \nu^2\right)\gamma^2\right] + \mathcal{O}\left(\frac{1}{c^5}\right) . \tag{2.62}$$

Note that we have introduced the following post-Newtonian parameter:

$$\gamma = \frac{GM}{c^2 r} = \mathcal{O}\left(\frac{1}{c^2}\right) . \tag{2.63}$$

It is interesting to note that the equations of motion (2.61) can be derived from a generalized Lagrangian $L_{GR}^{2PN}[\mathbf{y}(t), \mathbf{v}(t), \mathbf{a}(t)]$ which depends on the acceleration [132]. This Lagrangian admits various conserved quantities including the following conserved energy:

$$E = -\frac{\mu c^2 x}{2}\left[1 + \left(-\frac{3}{4} - \frac{1}{12}\nu\right)x + \left(-\frac{27}{8} + \frac{19}{8}\nu - \frac{1}{24}\nu^2\right)x^2\right] + \mathcal{O}\left(\frac{1}{c^5}\right) , \tag{2.64}$$

where we have introduced the frequency parameter

$$x = \left(\frac{GM\Omega}{c^3}\right)^{\frac{2}{3}} = \mathcal{O}\left(\frac{1}{c^2}\right) . \tag{2.65}$$

The word *conservation* has to be understood here in the sense of the post-Newtonian expansion. It means that the time derivative of E will be at least of order $\mathcal{O}\left(\frac{1}{c^5}\right)$. Of course, it is clear that the total energy of the system cannot be conserved because of the emission of GWs. In particular, it is well-known that this energy admits radiation-reaction terms starting from 2.5PN order [117].

The balance equation

The energy loss we just mentioned is responsible for the adiabatic decrease of the distance r between the two bodies. It is therefore a key ingredient to infer the waveform of the emitted GWs. One way to evaluate this radiation would be to compute the higher-order terms of the energy (2.64). However, as explained in [117], we would need to compute radiation-reaction terms of order $(2.5 + x)$PN to get the correct

[9] Note also that the metric and its determinant in (2.60) are evaluated at the location of the bodies, namely, $(g_{\alpha\beta})_1 \equiv g_{\alpha\beta}(\mathbf{y}_1(t))$. This is only valid as long as we compute quantities up to 2.5PN order [129]. At order 3PN or higher, g_1 has to be replaced by $g(t, \mathbf{x})$.

equations of motion at order xPN. Since state-of-the-art knowledge of E is currently limited to 4PN [133], this approach seems rather limited.

There exists another method which has been proved to be successful. The idea is to identify the energy loss in the near zone with the flux $\mathcal{F}$ of GWs far away from the source. We can obtain the information we are looking for by postulating the following balance equation:

$$\frac{dE}{dt} = -\mathcal{F}, \tag{2.66}$$

where E is the energy in the near zone. We indeed remind that we have obtained a general expression for $\mathcal{F}$ given by Equations (2.47) and (2.48). It turns out that $\mathcal{F}$ is currently known to 4PN order [133] and for illustration we give here its $2PN$ expression:

$$\begin{aligned}\mathcal{F} =& \frac{32c^5}{5G}\nu^2 x^5 \left[1 + \left(-\frac{1247}{336} - \frac{35}{12}\nu\right) x + 4\pi x^{3/2}\right. \\ &\left. + \left(-\frac{44711}{9072} + \frac{9271}{504}\nu + \frac{65}{18}\nu^2\right) x^2 + \mathcal{O}\left(\frac{1}{c^5}\right)\right].\end{aligned} \tag{2.67}$$

It is possible to combine Equations (2.64), (2.66) and (2.67) together and to solve for $x(t)$, namely $\Omega(t)$. In other words, the balance equation allows us to compute the evolution of the orbital frequency. We can therefore completely predict the dynamics of the inspiralling phase up to a given PN order.

GW waveform

The information about the dynamics of the BBH allows us to find the properties of the emitted GWs. Let us start with a generic GW signal of amplitude $A(t)$ and phase $\Phi(t)$:

$$h(t) = 2A(t)\cos\Phi(t)\,. \tag{2.68}$$

For data analysis purposes, it is actually convenient to work in the frequency-domain. As the Fourier transform cannot be computed analytically in general, it is estimated according to the stationary phase approximation (SPA), which gives [134]

$$\tilde{h}(f) = \frac{\sqrt{2\pi}A(t_f)}{\sqrt{\ddot{\Phi}(t_f)}} e^{i\psi(f)}, \quad \psi(f) = 2\pi f t_f - \pi/4 - \Phi(t_f). \tag{2.69}$$

The parameter t_f is the time when the GW frequency $d\Phi(t)/dt$ is equal to the Fourier frequency f. The next step is to relate the frequency-domain phase $\psi(f)$ to the orbital phase of the binary system. It is indeed known [117] that the GW frequency $d\Phi(t)/dt$ is twice the orbital frequency Ω. Thus, after a straightforward computation, we obtain the frequency-domain GW phase as the following PN expansion:[10]

$$\psi_I(f) = 2\pi f t_c - \phi_c - \frac{\pi}{4} + \frac{3}{128\nu}\sum_{j=0}^{4}\varphi_j\left(\frac{\pi MGf}{c^3}\right)^{(j-5)/3}, \tag{2.70}$$

[10] The subscript I reminds us that this formula is only valid during the inspiral stage.

waveform regime			median		GR quantile		$\log_{10} B^{\mathrm{GR}}_{\mathrm{model}}$	
	parameter	f−dependence	single	multiple	single	multiple	single	multiple
early-inspiral regime	$\delta\hat{\varphi}_0$	$f^{-5/3}$	$-0.1^{+0.1}_{-0.1}$	$1.4^{+3.3}_{-3.0}$	0.94	0.21	1.9 ± 0.1	
	$\delta\hat{\varphi}_1$	$f^{-4/3}$	$-0.4^{+0.0}_{-0.9}$	$-0.6^{+17.7}_{-18.0}$	0.94	0.52	1.3 ± 0.3	
	$\delta\hat{\varphi}_2$	f^{-1}	$-0.35^{+0.3}_{-0.35}$	$-3.2^{+19.3}_{-15.2}$	0.97	0.60	1.2 ± 0.2	
	$\delta\hat{\varphi}_3$	$f^{-2/3}$	$0.2^{+0.2}_{-0.2}$	$2.6^{+13.8}_{-15.7}$	0.04	0.41	1.2 ± 0.1	
	$\delta\hat{\varphi}_4$	$f^{-1/3}$	$-2.0^{+1.6}_{-1.8}$	$0.5^{+17.3}_{-18.2}$	0.98	0.49	0.3 ± 0.1	2.1 ± 0.6
	$\delta\hat{\varphi}_{5l}$	$\log(f)$	$0.8^{+0.6}_{-0.55}$	$-1.5^{+19.1}_{-16.3}$	0.02	0.55	0.7 ± 0.1	
	$\delta\hat{\varphi}_6$	$f^{1/3}$	$-1.5^{+1.1}_{-1.1}$	$-0.6^{+18.2}_{-17.2}$	0.99	0.53	0.4 ± 0.1	
	$\delta\hat{\varphi}_{6l}$	$f^{1/3}\log(f)$	$8.9^{+6.8}_{-6.8}$	$-2.4^{+18.7}_{-15.2}$	0.02	0.57	-0.2 ± 0.1	
	$\delta\hat{\varphi}_7$	$f^{2/3}$	$3.7^{+2.6}_{-2.75}$	$-3.4^{+19.3}_{-14.8}$	0.02	0.59	-0.0 ± 0.2	
intermediate regime	$\delta\hat{\beta}_2$	$\log f$	$0.1^{+0.4}_{-0.3}$	$0.15^{+0.6}_{-0.5}$	0.29	0.35	1.2 ± 0.1	2.2 ± 0.1
	$\delta\hat{\beta}_3$	f^{-3}	$0.1^{+0.5}_{-0.3}$	$-0.0^{+0.8}_{-0.6}$	0.38	0.56	0.6 ± 0.1	
merger–ringdown regime	$\delta\hat{\alpha}_2$	f^{-1}	$-0.1^{+0.4}_{-0.4}$	$-0.0^{+1.0}_{-1.15}$	0.68	0.51	1.1 ± 0.1	
	$\delta\hat{\alpha}_3$	$f^{3/4}$	$-0.5^{+2.0}_{-1.5}$	$-0.0^{+4.4}_{-4.4}$	0.67	0.50	1.3 ± 0.1	2.1 ± 0.1
	$\delta\hat{\alpha}_4$	$\tan^{-1}(af+b)$	$-0.1^{+0.5}_{-0.6}$	$-0.0^{+1.2}_{-1.1}$	0.61	0.55	1.2 ± 0.1	

FIGURE 2.1: Results of the gIMR analysis performed by LIGO/Virgo on the GW150915 signal. The details of the Bayesian analysis as well as the exact meaning of each column are explained in [111].

with t_c and ϕ_c being the time and phase at coalescence. All the interesting information is contained in the coefficients of this formula:

$$\begin{aligned} \varphi_0 &= 1 \\ \varphi_1 &= 0 \\ \varphi_2 &= \frac{3715}{756} + \frac{55}{9}\nu \\ \varphi_3 &= -16\pi \\ \varphi_4 &= \frac{15293365}{508032} + \frac{27145}{504}\nu + \frac{3085}{72}\nu^2 \\ &\dots , \end{aligned} \tag{2.71}$$

where we only give results up to 2PN for simplicity. Expressions up to 3.5PN can be found in [117].

As expected, these coefficients are completely determined from the two masses of the BBH. Such a result therefore represents a strong prediction of GR. It is clear that being able to experimentally measure the phase of a GW signal directly provides us with information about the nature of the source and about the validity of GR.

2.2.3 The GW150914 detection

We end this Chapter by briefly commenting on the GW150914 detection. The first interest of the analytic formulae we derived in the previous section is that they allow us to build templates that can be used to match potential signals in the detectors. These analytic predictions are however only valid during the inspiral stage and numerical relativity is needed to correctly model the merger and ringdown part of the event. In practice, the LIGO/Virgo collaborations used two main waveform models that combine the analytic PN results and numerical relativity: the effective-one-body (EOB) formalism [118, 135] and the IMRPhenom model [136–138], where IMR stands for Inspiral-Merger-Ringdown.

It is also interesting to understand how LIGO/Virgo used the GW150914 signal to test for deviations from GR in [111].[11] Their idea is to define a generalized IMR model (gIMR) by introducing a set of new parameters, $\delta\varphi_j$, describing potential deviations from the GR coefficients (2.71). In practice, the IMRPhenom template is modified by replacing the phase φ_j with $\varphi_j(1+\delta\varphi_j)$. The deviations $\{\delta\varphi_j\}$ are then allowed to vary (one at a time or all at once) in order to fit the observation with the gIMR template. Bounds on each of these parameters are then inferred from Bayesian analysis. The constraints they obtained from GW150914 are summarized in Table I of [111] that we have reproduced in Figure 2.1. Their conclusion is that GW150914 is consistent with the prediction of GR.

It is important to notice that the same analysis can be applied to constrain or test other models beyond GR. This is what we propose to do in Chapter 4. We shall make use of the post-Newtonian formalism presented in this Section to predict the waveform of a BBH in the background of non-commutative space-time. Our objective will be to derive some analytic corrections to the coefficients (2.71) and then to use the results in Figure 2.1 to place a bound on the scale of non-commutativity.

[11] Note that other and more recent GW signals have also been used for this purpose and give similar results.

Chapter 3

Particle Physics and Cosmology

This Chapter presents the point of view of modern physics on the structure of matter and its interactions. The underlying mathematical formalism on which all this description is built is quantum field theory (QFT) as we explained in our introductory Chapter. We show how the intuitive ideas we discussed at that time can be mathematically formalized and how this gives rise to quantitative predictions. First, we focus our attention on how QFT and symmetry principles allow us to categorize elementary particles and their interactions in the so-called standard model (SM) of particle physics. Then we move to the study of the early Universe which requires knowledge about both cosmology and finite temperature QFT. All these topics are covered in great details in several textbooks and lecture notes. In particular, we refer to [72, 73] for QFT, [139] for the Standard Model, [140, 141] for thermal QFT and [142, 143] for the early Universe.

3.1 The Standard Model of Particle Physics

3.1.1 Quantum Field Theory

There are various ways to introduce and present quantum field theory. It is a vast topic which has been developed over many years and it is obviously not our objective to give a comprehensive overview of such a formalism. The approach we follow in this Section is to give first a summary of the fundamental principles on which QFT is built and then we move to more advanced topics which are useful for our subsequent discussion.

General principles

Quantum field theory originates from the ambition to build a quantum theory of particles satisfying the following principles at once: unitarity, locality, Poincaré invariance, causality, and stability. Let us see how this works step by step. As a quantum theory of particles, the fundamental quantities on which QFT is built are all possible *particles states* (forming a Hilbert space $\mathcal{H}$), and an Hamiltonian H specifying the interactions and the time evolution of the states. It is convenient to classify the states by the number of particles they contain and to write them as follows:

- vacuum state: $|\Omega\rangle$
- one-particle state: $|\mathbf{p}, k\rangle$
- two-particle state: $|\mathbf{p}_1, k_1; \mathbf{p}_2, k_2\rangle$
- ...

where $\mathbf{p}$ is the momentum of a particle and k a generic index encompassing all other properties this particle might have. The full Hilbert space is then the tensor product between each subspace $\mathcal{H}_N$ made of all N-particle states: $\mathcal{H} = \mathcal{H}_0 \otimes \mathcal{H}_1 \otimes \dots$ Physical behaviours and observables are then extracted by acting on these particle states with carefully defined operators (such as the Hamiltonian H). In practice, this can be formalized in two different ways: either through canonical quantization (namely with operators expressed as a linear combination of creation and annihilation operators) or through the path integral formalism.

At this point, there is still nothing more than usual quantum mechanics: QFT only appears when we try to impose the aforementioned principles. Since the aim is to build a relativistic quantum theory, it is judicious to work in a Lagrangian formalism where space and time are treated on the same footing rather than with an Hamiltonian. Therefore we consider that a theory is described in terms of an action of the form

$$S = \int L(t)dt. \tag{3.1}$$

If needed, the Hamiltonian H can be recovered from the Legendre tranform of the Lagrangian L. We can now consider the content and consequences of each principle one by one:

- Unitarity:
  Conservation of probability over time imposes the evolution operator $U = e^{-iHt}$ to be unitary. This is equivalent to require the Hamiltonian to be Hermitian, $H = H^\dagger$, or the action S to be real.

- Locality:
  An efficient way to resolve the problem of action at a distance from classical mechanics (see **(L3)**) is to require that physical degrees of freedom at each point in space at a given time are independent. This is mathematically satisfied if the Hamiltonian and Lagrangian are expressed as

  $$H = \int d^3\mathbf{x}\, \mathcal{H}(\mathbf{x}, t), \quad L = \int d^3\mathbf{x}\, \mathcal{L}(\mathbf{x}, t), \quad S = \int d^4\mathbf{x}\, \mathcal{L}(\mathbf{x}, t), \tag{3.2}$$

  where the Lagrangian and Hamiltonian densities $\mathcal{H}$ and $\mathcal{L}$ are evaluated at a *unique* space-time location. The notion of *field* appears naturally: these densities return an operator at each space-time point. In full generality, a Lagrangian density can then be seen as a functional over a set of operator fields, generically written A_α, and their space-time derivatives: $\mathcal{L} = \mathcal{L}(x, A_\alpha(x), \partial_\mu A_\alpha(x), \dots)$.

- Poincaré invariance:
  QFT requires the action (3.1) to be invariant under translations and Lorentz transformations. The first condition implies that the Lagrangian density $\mathcal{L}$ does not depend explicitly on x: $\mathcal{L} = \mathcal{L}(A_\alpha(x), \partial_\mu A_\alpha(x), \dots)$. Then Lorentz invariance imposes some specific conditions on the fields A_α. In particular, if some of these fields are not scalar but return multiple values at each space-time point, they have to combine in a certain way which ensures that the action S remains a Lorentz scalar. It is then judicious to choose as fundamental fields those which transform in representations of the Lorentz group.

- Causality:
  Causality means here that a measurement performed at x should not affect a measurement at y if the events x and y are not causally connected. So any two

field operators $\mathcal{O}_1$ and $\mathcal{O}_2$ have to commute when evaluated at space-like separations: $[\mathcal{O}_1(x), \mathcal{O}_2(y)] = 0$, if $(x-y)^2 < 0$. As all operators $\mathcal{O}$ are built from the fields $A_\alpha(x)$, the causality condition directly imposes some constraints on the properties of these fields.

- Stability:
  The vacuum state of any quantum theory is defined as the lowest-energy state. It therefore requires the spectrum of the Hamiltonian to be bounded from below. This generally requires the Lagrangian to be a functional of at most one time derivative. Otherwise, the Hamiltonian would become linear in at least one variable and not be bounded from below (see [144] for a detailed discussion). In practice, this is roughly equivalent to asking $\mathcal{L} = \mathcal{L}(A_\alpha(x), \partial_\mu A_\alpha(x))$.

These principles are leading us to consider the fields $A_\alpha(x)$ as the quantities of prime importance for the description of particles and their interactions. There are two main steps which remain to be achieved before we can claim to have built a consistent model. First, we have to define which types of fields and which types of interactions are really allowed by the above principles. The answer is given by a set of mathematical concepts and rules which have been formalized during the last decades and form the content of QFT. Second, we have to explicitly specify which fields and interactions, among the allowed possibilities, we think are the best to explain experimental observations. This is equivalent to asking the Lagrangian density to be completely specified and then to be able to compute predictions from it.

Field, spin and gauge invariance

As is well explained in [73] Chapter 8, it is a non trivial task to combine unitarity and Poincaré invariance. On one hand, the above principles ask for particles to transform under unitary and irreducible representations of the Poincaré group. On the other hand, no such representations are finite-dimensional. The solution proposed by QFT is to embed particles into fields which transform in finite-dimensional representations of the Lorentz group. Although these representations are themselves non-unitary, it is still possible to combine the fields in such a way that the final theory exhibits unitarity. This has various profound ramifications.

First, representation theory of the Lorentz group provides the theoretical foundation for the notion of spin. It is well known that the Lorentz algebra is $su(2) \oplus su(2)$, such that its finite irreducible representations are characterized by two half-integers (j_1, j_2) and have dimension $(2j_1+1)(2j_2+1)$. Then, every such representation engenders several representations of $SO(3)$ with spins $j = j_1 + j_2, j_1 + j_2 - 1, \ldots, |j_1 - j_2|$. There is therefore a clear relation between the spin of a particle and the representation to which belongs the field describing it. Table 3.1 gives the fields which are usually used to describe elementary particles. We also express how they transform under a Lorentz transformation of the form $x^\mu \mapsto \Lambda^\mu{}_\nu \, x^\nu$. We remind that the generic transformation rule is given by $\Phi_a(x) \mapsto M_a{}^b(\Lambda)\Phi_b(\Lambda^{-1}x)$.

Another important consequence of the principles of QFT is the spin-statistics theorem which states that particles of integer spin satisfy Bose-Einstein statistics and particles of half-integer spin satisfy Fermi-Dirac statistics. This is a requirement which is necessary if we want the theory to be stable and if we want the theory to predict Lorentz invariant observables (see [73] Chapter 12, for more details). It follows that scalar fields and vector fields are used to describe bosons of spins 0 and 1 respectively, whereas spinor fields are used to describe fermions of spin 1/2.

(j_1, j_2)	Dimension	Field type	Notation	$M_a{}^b(\Lambda)$
$(0,0)$	1	scalar	ϕ	1
$(1/2,0)$	2	left-handed spinor	ψ_L	$e^{\frac{1}{2}(i\theta_j-\beta_j)\sigma_j}$
$(0,1/2)$	2	right-handed spinor	ψ_R	$e^{\frac{1}{2}(i\theta_j+\beta_j)\sigma_j}$
$(1/2,0)\oplus(0,1/2)$	4	Dirac spinor	$(\psi_L,\psi_R)^T$	$e^{-\frac{i}{2}\theta_{\mu\nu}S^{\mu\nu}}$
$(1/2,1/2)$	4	vector	A_μ	$\Lambda_\mu{}^\nu$

TABLE 3.1: Main representations of the Lorentz group with their corresponding field types. Λ corresponds to a generic Lorentz transformation with three rotation angles θ_j and three boost angles β_j which can be embedded in the matrix $\theta_{\mu\nu}$. Here σ_j are the Pauli matrices which can also be embedded in the matrix $S^{\mu\nu}$ in the standard way.

It is not too complicated, from the previous considerations, to know how to combine scalar and spinor fields together to build an interacting Lagrangian in agreement with the principles of QFT. However, some difficulties arise when we consider massless spin 1 particles. Such states have two degrees of freedom but are embedded into vector fields, A_μ, which have four degrees of freedom. The solution proposed by QFT to bypass this problem is to invoke *gauge invariance*. The extra degrees of freedom are removed from the fact that the Lagrangian is symmetric under a redefinition of the vector fields of the form

$$A_\mu(x) \mapsto \omega(x)A_u(x)\omega^{-1}(x) + \omega(x)\partial_\mu\omega^{-1}(x)\,, \tag{3.3}$$

where $\omega(x)$ corresponds to an element of a (compact) Lie group G at each spacetime point x. It means that massless spin 1 particles are actually identified with an equivalence class of vector fields. It follows that the unique kinetic Lagrangian for A_μ which stays invariant under (3.3) is of the form $\mathcal{L} = -\frac{1}{4}F_{\mu\nu}^2$ with the field strength $F^{\mu\nu} = \partial_\mu A_\nu - \partial_\nu A_\mu + [A_\mu, A_\nu]$. For the full Lagrangian to be gauge invariant, we still need to specify how scalars and spinors transform under the group G and which types of interactions are allowed. This can be done by considering each field Φ_a as transforming under a specific group representation $T(\omega)$ of G and by replacing derivative terms $\partial_\mu\Phi_a$ in the Lagrangian by covariant derivatives:

$$\Phi_a(x) \mapsto T(w(x))\Phi_a(x) \qquad D_\mu\Phi_a = \left[\partial_\mu + T(A_\mu)\right]\Phi_a\,, \tag{3.4}$$

where $T(A_\mu)$ is the corresponding representation of the Lie algebra of the group G.

It is interesting to note that gauge invariance imposes a lot of restrictions on the general structure of the Lagrangian. This is advantageous as it reduces the number of possibilities that have to be considered when trying to build a theory corresponding to a given set of phenomena. We will actually see that such restrictions are so strong that, at first sight, they seem to contradict with the existence of massive spin 1 bosons.

Symmetries and conserved charges

We are at a stage where the notion of symmetry seems to play a more and more important role in QFT. It is therefore important to briefly clarify the different types of situations we can encounter and what are their consequences. Consider a continuous[1] transformation (typically given by a Lie group) with parameters $\alpha = \{\alpha_i\}$:

$$\begin{cases} x'^\mu &= f^\mu(x,\alpha) \\ \Phi'_a(x') &= F_a(\Phi(x),\alpha) \end{cases} \tag{3.5}$$

This is a symmetry if $\mathcal{L}(\Phi'_a(x'), \partial'_\mu \Phi'_a(x'))d^4x' = \mathcal{L}(\Phi_a(x), \partial_\mu \Phi_a(x))d^4x$. In particular, the equations of motions will be the same before and after the transformation.

A typical example is given by the Lorentz transformations which act on both space-time and fields. Actually, most of the other symmetries we shall encounter only act on the fields ($x'^\mu = x^\mu$) and are therefore called *internal*. Another common distinction is made between global transformations with α being the same parameters over all space-time and local symmetries with $\alpha = \alpha(x)$. Gauge symmetries are typical examples of local transformations. Note also that if a theory is invariant under a local symmetry, it is automatically invariant under the corresponding global symmetry.

Continuous symmetries are important in QFT because Noether's theorem [145] states that there is a conserved current related to each of them[2]: $\partial_\mu J^\mu = 0$. This implies in particular that the *charge* $Q = \int d^3x J_0$ is conserved with time: $\partial_t Q = 0$. Such conserved operators are very useful as they allow us to classify particle states in a time-independent way. They also provide us with an interpretation of how interactions work in QFT: gauge fields mediate interactions between matter fields which are charged under the corresponding gauge group.[3] Each charge is associated to the representation of the gauge group to which the field belongs to.

The generating functional

We have almost all concepts in hand to describe the content of the SM. But first, we want to understand how observables can be computed in QFT. Let us assume we know the exact form of a Lagrangian $\mathcal{L}(\Phi_a, \partial_\mu \Phi_a)$, where the Φ_a are all the fields in the model whatever their spin. There are various observables we can infer from $\mathcal{L}$ and compare to experimental results. Probably the most popular and well-described phenomena are scattering processes where particles, initially free, interact with each other over a short distance and during a brief period of time. This typically includes collisions of particles inside accelerators or the decay of unstable particles. Other phenomena of interest are those related to the large scale dynamics of quantum fields over the history of the Universe. This is relevant for various mechanisms such as spontaneous symmetry breaking and phase transitions. It turns out that the path integral formalism of QFT provides a way to describe these two processes at the same time. We remind how this works.

For simplicity (and this will be sufficient for us), we consider the dynamics of a single scalar field with Lagrangian $\mathcal{L}(\phi)$ and vacuum state $|\Omega\rangle$. The quantities we want to compute are the vacuum expectation value of the field, $\langle\Omega|\phi(x)|\Omega\rangle$ and the n-point functions $G^{(n)}(x_1,\ldots,x_n) = \langle\Omega|T\{\phi(x_1)\cdots\phi(x_n)\}|\Omega\rangle$. Also known as the

[1] Discrete symmetries may also be relevant but are not discussed here.

[2] This statement is true as long as the the fields satisfy their equations of motion.

[3] Noether's theorem indeed holds for global symmetries and therefore also applies to gauge transformations.

correlation functions or Green functions, we remind that these expressions are written in the Heisenberg picture and $T\{\dots\}$ is the time-ordered product. The vacuum expectation value is indeed a relevant quantity to describe the global behaviour of the field in the Universe. The correlation functions are also of prime interest as they determine the elements of the scattering matrix S through the Lehmann-Symanzik-Zimmermann (LSZ) reduction formula [73].

Following the path integral formalism, these quantities can be derived from the vacuum amplitude in presence of an external source field $J(x)$:

$$Z[J] = \langle\Omega|\Omega\rangle_J = \int D\phi \exp\left[iS[\phi] + i\int d^4x\, J(x)\phi(x)\right], \tag{3.6}$$

We remind that the fields entering in the integral are classical fields and not operators anymore. $Z[J]$ is similar to the partition function of statistical mechanics and thus we expect it to completely specify the system under consideration. Indeed, it allows us to obtain the correlation functions by taking functional derivatives as follows:

$$(-i)^n \frac{1}{Z[0]} \left.\frac{\delta^n Z}{\delta J(x_1)\cdots\delta J(x_n)}\right|_{J=0} = \langle\Omega|T\{\phi(x_1)\cdots\phi(x_n)\}|\Omega\rangle, \tag{3.7}$$

and in particular

$$-i\frac{1}{Z[0]} \left.\frac{\delta Z}{\delta J(x)}\right|_{J=0} = \langle\Omega|\phi(x)|\Omega\rangle. \tag{3.8}$$

$Z[j]$ is therefore called the *generating functional for the correlation functions*. In other words, if we can compute Z according to the formula (3.6), we can predict any scattering experiment and the vacuum expectation value of the field.

It is almost always impossible to find an exact expression for Z and we have to resort to approximation methods. Perturbation theory is the most common approach, but it is only valid when the considered interactions are weak. To make this statement clearer, consider the Hamiltonian associated to $\mathcal{L}$ and let us write it as $\mathcal{H} = \mathcal{H}_0 + \mathcal{H}_I$ where the first term corresponds to the free theory and the second one encompasses the interactions. If we assume for simplicity that the interaction Hamiltonian is a functional of the field, $\mathcal{H}_I = \mathcal{H}_I[\phi(x)]$, then we can formally rewrite the generating functional as

$$Z[j] = e^{-i\int_{-\infty}^{+\infty} dt\, \mathcal{H}_I[-i\delta/\delta j(x)]} Z_0[j]. \tag{3.9}$$

$Z_0[J]$ is the generating functional of the free theory and it is well-known that it can be explicitly computed (see e.g. [73] Section 14.3). For a weakly-interacting theory, we can then approximate $Z[J]$ by only keeping the leading terms after expanding the exponential in (3.9). Each Green function $G^{(n)}(x_1,\dots,x_n)$ can therefore be computed as a perturbative series as well. The computation of the terms of these series can be performed with the help of Feynman diagrams.

We consider that the reader is familiar with the Feynman rules and we do not give more details about their implementation. What is of prime importance for us is to have introduced a formalism which is similar to statistical mechanics. It will allow us to properly discuss the concepts of spontaneous symmetry breaking and thermal field theory.

Renormalizability

There is a last important concept of QFT we want to mention. The computation of Green functions usually leads to the appearance of ultraviolet (UV) divergences. Diagrams containing loops are generically infinite. As we explained in Section 1.2.1, an entire machinery, known as renormalization, has been implemented to deal with this problem. The idea is to absorb these infinities into the bare parameters of the original Lagrangian which then become dependent on the so-called renormalization scale.

In a given theory, as long as only a finite number of diagrams diverge, it is possible to eliminate them with an equal number of parameters of the Lagrangian. Once this is done, observables can be computed unambiguously such that the model is said to be predictive or *renormalizable*. Not all Lagrangians are renormalizable and it is not difficult to exhibit models which contain an infinite number of divergent amplitudes. It turns out that *renormalizability* is a quite restrictive condition as it asks the Lagrangian to only contain operators with mass dimensions ≤ 4. Given a set of fields, there is therefore only a limited choice of interactions we can build if we want to keep the Lagrangian renormalizable.

It is important to keep in mind that non-renormalizable theories can also be predictive in their low-energy regime. Such models have an infinite number of divergent diagrams and would therefore require an infinite number of parameters to cancel them. The point is that each successive higher-order operator in a Lagrangian has a higher and higher mass dimension. Its effects are therefore more and more suppressed at low-energy scales. As long as we are interested in low-energy processes, it is possible to extract predictions from such models by only considering their leading operators. This process is widely used in particle physics under the name of the Effective Field Theory (EFT) approach. This prescription obviously breaks down whenever we reach higher energy scales and it is said that the theory requires a UV completion to correctly describe this regime. More details about such concepts can be found in [73] Chapters 22-23 and [139, 146].

We note in passing that GR, as a field theory, is non-renormalizable. As seen as an EFT, it can nevertheless predict quantum effects (typically tiny) which are valid at energy scales well below the Planck scale: $E \ll M_P$. As discussed in Section 1.2.1, it is however well-known that a UV completion of GR is needed in order to describe gravitational effects at distances close to the Planck length. We shall discuss various aspects at the frontier between quantum mechanics and GR in Chapter 4.

3.1.2 The content of the Standard Model

The standard model is a theory of particles describing three of the four forces that have been observed in nature: the strong, weak and electromagnetic interactions. It does not give a framework to describe gravity which is the concern of GR as we investigated in Chapter 2. The main idea of the SM is that fermions of spin $1/2$ make up matter and that their interactions are dictated by the exchange of gauge bosons. The gauge principle gives the natural framework to interpret each interaction as being related to a specific group of symmetry and this restricts at the same time the general structure that the SM Lagrangian can take. We shall see that an extra particle, the Higgs boson, is added to the theory in order to accommodate the observed masses of some of the gauge bosons and fermions.

Fields	$SU_c(3) \times SU_L(2) \times U_Y(1)$	(j_1, j_2)	Content
G^α_μ	$(\mathbf{8}, \mathbf{1}, 0)$	$(\frac{1}{2}, \frac{1}{2})$	8 gluons
W^a_μ	$(\mathbf{1}, \mathbf{3}, 0)$	$(\frac{1}{2}, \frac{1}{2})$	3 bosons
B_μ	$(\mathbf{1}, \mathbf{1}, 0)$	$(\frac{1}{2}, \frac{1}{2})$	1 boson
$l^i_L = (\nu^i_e, e^i_L)^T$	$(\mathbf{1}, \mathbf{2}, -\frac{1}{2})$	$(\frac{1}{2}, 0)$	6 LH leptons
e^i_R	$(\mathbf{1}, \mathbf{1}, -1)$	$(0, \frac{1}{2})$	3 RH leptons
$q^i_L = (u^i_L, d^i_L)^T$	$(\mathbf{3}, \mathbf{2}, \frac{1}{6})$	$(\frac{1}{2}, 0)$	6 LH quarks
u^i_R	$(\mathbf{3}, \mathbf{1}, \frac{2}{3})$	$(0, \frac{1}{2})$	3 RH quarks
d^i_R	$(\mathbf{3}, \mathbf{1}, -\frac{1}{3})$	$(0, \frac{1}{2})$	3 RH quarks
H	$(\mathbf{1}, \mathbf{2}, \frac{1}{2})$	$(0, 0)$	1 Higgs boson

TABLE 3.2: Field content of SM including their representations under G_{SM} and the Lorentz group.

The SM elementary particles

The standard model is described by the following gauge group:

$$G_{\text{SM}} = SU_c(3) \times SU_L(2) \times U_Y(1). \tag{3.10}$$

The group $SU_c(3)$ of quantum chromodynamics [147–149] dictates the behaviour of particles sensitive to the strong interaction. This interaction is mediated by eight massless gluons, G^α_μ ($\alpha = 1, \ldots, 8$), and acts on particles which carry a charge called *color*. On the other hand, the Glashow-Weinberg-Salam theory [150–152] unifies the electromagnetic and weak interactions under the electroweak gauge group $SU_L(2) \times U_Y(1)$ with gauge bosons W^a_μ ($a = 1, 2, 3$) and B_μ. The subscript L means that only left-handed fermions transform under $SU(2)$ whereas Y is the weak hypercharge. We will see below how these two interactions become distinct after spontaneous symmetry breaking and how the usual electric charge and photon emerge.

On top of these gauge bosons, the SM contains several spin $1/2$ particles. There are two main categories of such fermions: the six leptons (electron, muon, tau and the corresponding neutrinos) which are insensitive to the strong interaction and the six quarks (up, down, charm, strange, top and bottom) which are colored. Under the effect of the strong force, the quarks are usually combined together and form composite particles called hadrons such as mesons and baryons. We can further classify the 12 elementary fermions according to two criteria. First, the leptons and quarks are decomposed into three families which carry the same quantum numbers under the gauge group G_{SM}. Second, the left-handed spinors representing these particles are doublets under $SU_L(2)$, whereas the right-handed fields are singlet under this group. We also note that there are no right-handed neutrinos in the SM. All this classification is summarized in Table 3.2 for clarity. We can see that this Table already contains an extra particle of spin 0, the Higgs boson. It forms a doublet H under $SU_L(2)$ and we will understand its relevance after having built the SM Lagrangian.

The SM Lagrangian

The Lagrangian $\mathcal{L}_{\rm SM}$ provides the information regarding the dynamics and the interactions of the fields we described above. It satisfies the various principles we have discussed in the first part of this Chapter, in particular gauge invariance and renormalizability. The kinetic term for the gauge bosons and the fermions can be written as follows:

$$\mathcal{L}_{\rm kin} = \sum \left(-\frac{1}{4} F_{\mu\nu}^2 - \bar{\psi} i \gamma^\mu D_\mu \psi \right) , \tag{3.11}$$

where the summation is implicit over all spinors and all field strengths $F_{\mu\nu}$ corresponding to the gauge bosons. Various interactions are actually present in (3.11) if we look in more details at the field strengths and covariant derivatives:

$$\begin{aligned} G_{\mu\nu}^\alpha &= \partial_\mu G_\nu^\alpha - \partial_\nu G_\mu^\alpha + g_3 f^\alpha{}_{\beta\gamma} G_\mu^\beta G_\nu^\gamma \\ W_{\mu\nu}^a &= \partial_\mu W_\nu^a - \partial_\nu W_\mu^a + g_2 \epsilon^a{}_{bc} W_\mu^b W_\nu^c \\ B_{\mu\nu} &= \partial_\mu B_\nu - \partial_\nu B_\mu \\ D_\mu &= \partial_\mu - i g_1 Y B_\mu - \tfrac{i}{2} g_2 W_\mu^a \sigma_a - \tfrac{i}{2} g_3 G_\mu^\alpha \lambda_\alpha , \end{aligned} \tag{3.12}$$

where it is understood that the Pauli and Gell-Mann matrices σ_a and λ_α only act on the fields which are doublets under $SU_L(2)$ respectively triplets under $SU_c(3)$. We see that the coupling constants g_1, g_2 and g_3 dictate the strength of the interactions between gauge bosons and gauge bosons and between gauge bosons and fermions.

The next step is to include terms in the Lagrangian that can accommodate the experimentally measured masses of the fermions and electroweak gauge bosons. This is not straightforward because gauge invariance forbids intuitive terms such as $m^2 B^\mu B_\mu$ or $m \bar{\psi}_L \psi_R$. The solution rests on the introduction of the Higgs doublet H and the following Lagrangian:

$$\begin{aligned} \mathcal{L}_{\rm Higgs} = &- \left(D_\mu H\right)^\dagger \left(D^\mu H\right) - \lambda \left(H^\dagger H - \mu^2/2\lambda \right)^2 \\ &- \left(y_l \bar{l}_L H e_R + y_d \bar{q}_L H d_R + y_u \bar{q}_L \tilde{H} u_R + \text{h.c} \right) , \end{aligned} \tag{3.13}$$

where $\tilde{H}$ is the conjugate Higgs doublet and the covariant derivatives only involve the electroweak bosons. The second line introduces the so-called Yukawa interactions between the Higgs and the fermions. We also note that this Lagrangian contains a mass term for the Higgs which is not forbidden by gauge invariance. The SM Lagrangian $\mathcal{L}_{\rm SM} = \mathcal{L}_{\rm kin} + \mathcal{L}_{\rm Higgs}$ is now complete and we can explain how the masses of fermions and gauge bosons emerge in this picture.

The Higgs mechanism

The first thing to realize is that if the Higgs field takes a non-zero vacuum expectation value, the Yukawa interactions will result in a set of mass terms for the fermions. It is then possible to adjust the Yukawa couplings (y_l, y_d, y_u) to accommodate the observed fermion masses. The situation is more complicated for the gauge bosons. One solution rests on the idea of spontaneous symmetry breaking and the Higgs mechanism [50, 153–155]. Note that this is not the only possible prescription that can be used. We shall indeed present another mechanism, beyond the SM, in Section 5.1.1.

A global continuous symmetry G is said to be spontaneously broken if the theory under investigation has a ground state which is not invariant under this symmetry,

but only under a subgroup H of G. Goldstone's theorem [156, 157] then states that there should exist at least as many spinless and massless particles as the number of generators that are broken when we reduce G to H. Although this is an interesting fact on its own, it does not solve the original problem as these massless scalars cannot be identified with particles of the SM. The Higgs mechanism occurs when we apply the idea of spontaneous symmetry breaking not to a global symmetry but to the local symmetry given by the electroweak gauge group. In this case, the would-be Goldstone bosons disappear from the spectrum and give a mass to some of the electroweak gauge bosons during the process.

In practice, the ground state of the electroweak sector of the SM can be chosen as $W^a_\mu = B_\mu = 0$ and $H = (0, v/\sqrt{2})^T$ with $v = \mu/\sqrt{\lambda}$. This breaks $SU_L(2) \times U_Y(1)$ down to the subgroup $U_{\text{em}}(1)$ with generator $Q = T^3 + Y$. If we expand the Lagrangian around the vev v of the Higgs and properly redefine the gauge fields, the expected mass terms appear and are given as follows:

$$\begin{aligned} A_\mu &= s_W W^3_\mu + c_W B_\mu & M^2_A &= 0 \\ Z_\mu &= c_W W^3_\mu - s_W B_\mu & M^2_Z &= \tfrac{1}{4}(g_1^2 + g_2^2)v^2 \\ W^\pm_\mu &= \tfrac{1}{\sqrt{2}}(W^1_\mu \mp i W^2_\mu) & M^2_W &= \tfrac{1}{4} g_2^2 v^2 \end{aligned} \tag{3.14}$$

where $c_W = \frac{g_2}{\sqrt{g_1^2+g_2^2}}$ and $s_W = \frac{g_1}{\sqrt{g_1^2+g_2^2}}$. We note that the charge Q can then be associated with the usual electric charge and A_μ corresponds to the photon. On the other hand, the weak interaction is mediated by the massive W and Z bosons.

3.1.3 The effective action

We have seen that spontaneous symmetry breaking plays an important role in the SM and that this mechanism relies on the existence of a non-zero vacuum expectation value of the Higgs field. We have to keep in mind that the value $v = \mu/\sqrt{\lambda}$ has been extracted from the classical Higgs potential $V(H)$ in (3.13) but that the true value of $\langle H \rangle$ also includes quantum corrections. In the case of a hot and dense Universe, thermal corrections would also play an important role. We will have to take such effects into account to discuss the physics of phase transitions in Chapter 5. Therefore, we introduce now the formalism allowing us to compute such corrections.

Functional method

The main idea is to find a functional whose minimum would directly give us the vev of the field including all quantum corrections. Such a functional is called the *effective action* and it can be built from the generating functional $Z[J]$ we introduced in Equation (3.6). As emphasized in [72] Section 11.3, the way to derive the effective action has some strong analogy with statistical mechanics.

Let us consider the theory of a single scalar field ϕ. We first introduce the generating functional of connected Green functions $W[J]$ satisfying

$$e^{iW[J]} = Z[J]. \tag{3.15}$$

The functional derivative of $W[J]$ gives the vev of ϕ in presence of the source J:

$$\frac{\delta W[J]}{\delta J(x)} = \langle \Omega | \phi(x) | \Omega \rangle_J \equiv \bar{\phi}(x) \,, \tag{3.16}$$

where we have introduced the classical field $\bar{\phi}$. The idea is now to find a functional of this classical field which would reduce to the classical potential $V(\phi)$ when quantum corrections are absent. Such a potential exists and is given by the Legendre transform of $W[J]$:

$$\Gamma[\bar{\phi}] = W[J] - \int d^4x \, \bar{\phi}(x) J(x) \,, \tag{3.17}$$

which indeed satisfies

$$\frac{\delta \Gamma[\bar{\phi}]}{\delta \bar{\phi}} = -J \quad \Rightarrow \quad \left. \frac{\delta \Gamma[\bar{\phi}]}{\delta \bar{\phi}} \right|_{J=0} = 0 \,. \tag{3.18}$$

As $Z[J]$ and $W[J]$, $\Gamma[\bar{\phi}]$ is also a generating functional. It can be expanded as

$$\Gamma[\bar{\phi}] = \sum_{n=0}^{+\infty} \frac{1}{n!} \int d^4x_1 \dots d^4x_n \, \bar{\phi}(x_1) \dots \bar{\phi}(x_n) \Gamma^{(n)}(x_1, \dots, x_n) \,, \tag{3.19}$$

where $\Gamma^{(n)}$ are the one-particle irreducible (1PI) Green functions. To get to our result of interest, it is also useful to expand Γ in terms of momenta as follows:

$$\Gamma[\bar{\phi}] = \int d^4x \left(-V_{\text{eff}}(\bar{\phi}) + \frac{1}{2} \partial_\mu \bar{\phi} \, \partial^\mu \bar{\phi} \, Z(\bar{\phi}) + \dots \right) . \tag{3.20}$$

The terms in this integral are now functions of $\bar{\phi}$ instead of functionals. The first one, called the effective potential, is actually the full quantum potential we were looking for. In the case of a translation invariant theory, $\bar{\phi}$ becomes a constant and the minimum condition (3.18) becomes

$$\frac{dV_{\text{eff}}(\bar{\phi})}{d\bar{\phi}} = 0 \,, \tag{3.21}$$

which is satisfied for a non-zero value of $\bar{\phi}$ in case of spontaneous symmetry breaking. In other words, the knowledge of V_{eff} would allow us to precisely compute the vev of the field ϕ including all quantum corrections. This cannot be done exactly for most theories, but we note from Equation (3.19) that V_{eff} is the sum of all 1P1 Feynman diagrams with vanishing external momenta. It can therefore at least be estimated by perturbative approaches.

The one-loop effective potential

Coleman and Weinberg proposed in [158] to compute V_{eff} according to a loop expansion. The first term of the series is given by the sum of all tree-level diagrams, the second by summing all diagrams with one loop, etc. We note that this is not the same approach as the usual perturbative expansion in terms of a small coupling constant. As explained in [158], the advantage of the loop expansion is to preserve the vacuum structure of the potential. Moreover, it is not worse than the perturbative expansion as the set of n-loops diagrams include all diagrams of power n and less in the coupling parameters.

It is sufficient for us to consider the leading quantum corrections, namely to focus on the one-loop potential. After summing all 1PI diagrams with 1 loop and vanishing external momenta, we can get the well-known formula

$$V_{\text{1-loop}}(\bar{\phi}) = \frac{1}{2}\int \frac{d^4p}{(2\pi)^4} \ln\left(p^2 + m^2(\bar{\phi})\right) \ , \tag{3.22}$$

where the field-dependent mass is given by the second derivative of the tree-level potential as $m^2(\phi) = d^2V_0(\bar{\phi})/d\bar{\phi}^2$. We note that the integration in Equation (3.22) is performed over Euclidean four-momentum with $p^0 = ip_E$. In other words, we have performed a Wick rotation towards Euclidean time $\tau = it$. This 1-loop formula is sometimes called the Coleman-Weinberg potential.

The above result can easily be extended to include the effects of fermions and gauge bosons or additional scalar fields. We also emphasize that this expression is divergent and requires renormalization. We do not discuss these details here as they will be illustrated in practice several times in this thesis. However, we want to make a final conceptual comment. The original motivation of Coleman and Weinberg in their article was to study if radiative corrections alone could be at the origin of spontaneous symmetry breaking. In other words, starting from a tree-level potential V_0 which admits a single minimum at $\bar{\phi} = 0$, could $V_0 + V_{\text{1-loop}}$ exhibit a non-zero minimum? The answer is yes for certain types of models. This is particularly interesting for classical potentials of the form $\lambda\phi^4$ which have no mass term. We shall make use of this mechanism in Chapter 5 when considering a scale-invariant extension of the SM.

3.2 Cosmology and the early Universe

The description of the dynamics of the Universe as a whole requires to combine concepts from both general relativity and particle physics. Thanks to the previous Sections, we now have the tools required for such an investigation. We will focus our attention on the notions which are needed to understand the mechanism of phase transitions.

3.2.1 The expanding Universe

The FLRW metric and the continuity equation

Our first aim is to describe the behaviour of the Universe at large scales by solving the Einstein Field Equations of GR. As discussed in Section 1.1.5, we assume that the cosmological principle holds and we look for a metric which is spatially homogeneous and isotropic but evolves in time. Based on these symmetry arguments, the geometry of interest is given the Friedmann-Lemaître-Robertson-Walker metric [52–55]

$$ds^2 = -dt^2 + a^2(t)\left[\frac{dr^2}{1-\kappa r^2} + r^2\left(d\theta^2 + \sin^2(\theta)d\phi^2\right)\right] \ , \tag{3.23}$$

which is written in spherical coordinates. The curvature parameter κ can be $+1, 0$ or -1 for a closed, flat or respectively open Universe. The time dependence of the metric is encompassed in the so-called *scale factor* $a(t)$ which has to be determined from the EFE.

We need to specify the energy-momentum tensor describing the matter content of the Universe. A good approximation at large scales is to assume that it is described by a perfect fluid of energy density $\rho(x)$ and pressure $p(x)$ such that

$$T_{\mu\nu} = (\rho + p)U_\mu U_\nu + p g_{\mu\nu} \,, \tag{3.24}$$

where U_μ is the four-velocity of the fluid in the frame of the observer. Without even solving the EFE, we can already use the covariant conservation of the energy momentum tensor, $\nabla^\mu T_{\mu\nu}$, to get a continuity equation of the form

$$\dot{\rho} + 3\frac{\dot{a}}{a}(\rho + p) = 0 \,. \tag{3.25}$$

The properties of the fluid therefore depend on the scale factor, but they are of course also determined by the underlying behaviour and nature of the particles in the Universe. This dependence can be encompassed in the equation of state (EOS) relating energy density and pressure as $p = \omega\rho$. In most situations, ω is considered independent of time. This parametrization is advantageous as it allows us to solve the continuity equation as a function of ω. This gives

$$\rho \propto a^{-3(1+\omega)} = \begin{cases} a^{-3} & \text{if } \omega = 0 \quad \text{(matter)} \\ a^{-4} & \text{if } \omega = 1/3 \quad \text{(radiation)} \\ a^{0} & \text{if } \omega = -1 \quad \text{(vacuum energy)} \end{cases} \tag{3.26}$$

where we have given the most important types of "fluids" which are matter, radiation and vacuum energy. This shows how each of them evolves if the Universe is expanding or contracting. Whereas the latter one does not correspond to any known type of fluid, it is important to accommodate current observations as we shall mention below.

The Friedmann equations

More information about the dynamics of the Universe can be obtained from the EFE. Starting from the metric (3.23) and energy-momentum tensor (3.24), they can be rewritten as the two independent Friedmann equations

$$H^2 \equiv \left(\frac{\dot{a}}{a}\right)^2 = \frac{8\pi G}{3}\rho - \frac{\kappa}{a^2} \,, \tag{3.27}$$

$$\frac{\ddot{a}}{a} = -\frac{4\pi G}{3}(\rho + 3p) \,, \tag{3.28}$$

where we have introduced the Hubble parameter $H = \dot{a}/a$. For a flat Universe ($\kappa = 0$) dominated by a single fluid, we can immediately see how the scale factor evolves in time from Equations (3.26) and (3.27):

$$\rho = \begin{cases} t^{2/3} & \text{if } \omega = 0 \quad \text{(matter dominated)} \\ t^{1/2} & \text{if } \omega = 1/3 \quad \text{(radiation dominated)} \\ e^{Ht} & \text{if } \omega = -1 \quad \text{(vacuum dominated)} \end{cases} \tag{3.29}$$

We have to keep in mind that the reality may be more complicated, in particular if different types of fluids contribute almost equally to the total energy density and pressure. Usually we have $\rho = \sum_i \rho_i$ where i labels the different contributions such as matter, radiation, vacuum, etc.

It is possible to rewrite the first Friedmann equation in a way which is convenient to compare with observations. We first define the critical energy density today as $\rho_{\text{crit}} = 3H_0^2/(8\pi G)$ and use it to define the dimensionless abundances today $\Omega_i = \rho_i(t_0)/\rho_{\text{crit}}$. If we only consider radiation ($i = r$), matter ($i = m$), curvature ($i = \kappa$) and vacuum energy ($i = \Lambda$), it is straightforward to rewrite (3.27) as

$$\frac{H^2}{H_0^2} = \Omega_r a^{-4} + \Omega_m a^{-3} + \Omega_\kappa a^{-2} + \Omega_\Lambda \,, \tag{3.30}$$

where we have fixed $a_0 = 1$, the scale factor today. If we can measure the different Ω_i in some way, we can then use this equation backwards in time to infer the state of the Universe in the past.

Observations

Different types of observations support that the Universe is currently in an accelerating expansion [58, 59] and that a substantial part of the matter energy density is made of dark matter [159]. In terms of cosmological parameters, this corresponds to [160]

$$\Omega_r \approx 5.4 \times 10^{-5} \quad \Omega_m \approx 0.31 \quad |\Omega_\kappa| \lesssim 0.01 \quad \Omega_\Lambda \approx 0.692 \,, \tag{3.31}$$

where $\Omega_m = \Omega_b + \Omega_c$ with

$$\Omega_b \approx 0.05 \qquad \Omega_c \approx 0.26 \,. \tag{3.32}$$

We have decomposed the pressureless matter density into the baryon density Ω_b and cold dark matter density Ω_c. It is interesting to note that the two dominant components, Ω_Λ and Ω_c, are still far from being understood today, as we explained in Section 1.2.1.

3.2.2 Thermal history and phase transitions

The cosmological parameters (3.31-3.32) combined with the Friedmann Equation (3.30) tell us that the Universe was denser at earlier times. The paradigm of the hot Big Bang cosmological model is to postulate that sufficiently far in the past all matter was made of a hot plasma of interacting elementary particles. As the Universe was expanding, the plasma diluted, interaction rates decreased and various phenomena occurred leading to the formation of massive particles, baryons, nuclei, atoms, stars, etc [142]. In this thesis, we are primarily interested in two events: the electroweak and chiral phase transitions. Their description requires some knowledge of thermal field theory that we present now.

Thermodynamics and the thermal effective potential

At a sufficiently high temperature (usually $T \gtrsim 100$ GeV in the SM), all elementary particles are relativistic such that the Universe is radiation dominated and in local thermal equilibrium. Standard thermodynamics results give the radiation energy density as follows:

$$\rho_r(T) = \frac{\pi^2}{30} g_\star(T) T^4. \tag{3.33}$$

The number of relativistic degrees of freedom $g_\star$ depends on temperature. Intuitively, its value decreases when the temperature drops below the mass of a given

particle species such that it becomes non-relativistic. It can therefore be predicted from particle physics considerations. We remind for example that $g_\star = 106.75$ in the SM above 100 GeV.

Among the variety of thermodynamic processes occurring during the early Universe, we focus now our attention on the concept of symmetry restoration. As an example, thermal field theory predicts that $SU_L(2) \times U_Y(1)$ was unbroken at high enough T such that fermions and gauge bosons of the SM were massless. In other words, thermal corrections can modify the shape of the Higgs effective potential such that it only admits a single vev at zero field value. A similar process is expected for the chiral symmetry, with the vev of the quark-antiquark condensates being zero a high enough temperature. We can therefore expect that something interesting happened between this early period and now regarding the dynamics of the Higgs field and condensates.

Thermal corrections to the effective potential V_{eff} can be obtained from thermal field theory. As in usual statistical mechanics, the fundamental quantity of interest to describe a system at finite temperature is the partition function $\mathcal{Z}(T) = \text{Tr}(\exp(-\beta\hat{H}))$ with $\beta = 1/T$. As described in [140, 141], one way to compute this partition function in QFT is to see that it is a generalization of the generating functional $Z[0]$ defined in (3.6). The prescription is to go to Euclidean time $\tau = it$, change the Lagrangian as $\mathcal{L}_E = -\mathcal{L}(\tau = it)$ and time integrate it over the interval $\tau \in [0, \beta]$:

$$\mathcal{Z}(T) = \int D\phi \exp\left[-\int_0^\beta d\tau \int d^3x\, \mathcal{L}_E(\phi)\right]. \tag{3.34}$$

We can now find the thermal effective potential $V_{\text{eff}}(\bar{\phi}, T)$ from the exact same prescription that gave $V_{\text{eff}}(\bar{\phi})$ in Section 3.1.3. We build the functional $\mathcal{Z}[J](T)$ by adding a current $J(x)$ to (3.34). Then the thermal effective action $\Gamma[\bar{\phi}](T)$ is given by the Legendre transform of $W[J](T) = -i \ln \mathcal{Z}[J](T)$. From translation invariance, we again obtain that

$$\left.\frac{\delta\Gamma[\bar{\phi}](T)}{\delta\bar{\phi}}\right|_{J=0} = 0 \quad \Rightarrow \quad \frac{\partial V_{\text{eff}}(\bar{\phi}, T)}{\partial\bar{\phi}} = 0\,. \tag{3.35}$$

The thermal effective potential can then be estimated from the loop expansion and Feynman rules. The 1-loop result is given by [141]

$$V_{\text{1-loop}}(\bar{\phi}, T) = \frac{1}{2\beta}\sum_{n=-\infty}^{n=+\infty}\int \frac{d^3\mathbf{p}}{(2\pi)^3} \ln\left(\left(\frac{2\pi n}{\beta}\right)^2 + \mathbf{p}^2 + m^2(\bar{\phi})\right), \tag{3.36}$$

where the field-dependent mass is defined in the same way as in Section 3.1.3. This formula can be simplified and it is interesting to note that it can be written as the sum of the 1-loop Coleman-Weinberg potential (3.22) and a second term which carries all the temperature dependence:

$$V_{\text{1-loop}}(\bar{\phi}, T) = V_{\text{1-loop}}(\bar{\phi}) + \frac{1}{2\pi^2\beta^4}\int_0^{+\infty} dx\, x^2 \ln\left[1 - \exp\left(-\sqrt{x^2 + \beta^2 m^2(\bar{\phi})}\right)\right]. \tag{3.37}$$

This result can be generalized to take into account the effects of fermions or gauge bosons.

It is interesting to note that the temperature-dependent term does not suffer from UV divergences, only the first term does. However, relativistic thermal field theory usually leads to the appearance of infrared divergences which can be interpreted as

a sign of the failure of the perturbative expansion [140, 141]. According to [161], the one loop effective potential (3.37) is expected to stop being valid once the temperature is such that symmetry restoration happens. Fortunately, the perturbative expansion can be improved by identifying the diagrams that give rise to the infrared divergences and then by summing over them at all orders. This technique is known as *Daisy resummation* from the specific name of the divergent diagrams. Taking this problematic into account, it is usual the rewrite the one-loop thermal potential as follows [162–165]:

$$V(\bar{\phi}, T) = V_0(\bar{\phi}) + V_{\text{1-loop}}(\bar{\phi}, T) + V_{Daisy}(\bar{\phi}, T) \,. \tag{3.38}$$

Appendix A.1 gives an example of how Daisy corrections can be computed in practice.

The dynamics of first-order phase transitions

We finish this Chapter by briefly discussing how cosmological first-order PTs take place. Note that most technical details will be given in Chapter 5 directly. Let us keep considering the classical background field $\bar{\phi}$ that we have introduced above. Its cosmological behaviour can be inferred from its free energy density, $\mathcal{F}(\bar{\phi}, T) = V(\bar{\phi}, T)$, identified as the effective potential (3.38). For clarity let us also introduce the following set of temperatures: $\tilde{T} > T_c > T_n > T_p$.

At temperatures satisfying $T > \tilde{T}$, $\mathcal{F}(\bar{\phi}, T)$ admits a single minimum at $\bar{\phi} = v_T^{(+)}$, called the symmetric phase of the field. As the Universe expands and its temperature gets to $\tilde{T}$, a second minimum forms at $\bar{\phi} = v_T^{(-)}$. This new vacuum state is called the broken phase and it initially admits a free energy density which is higher than that of the symmetric phase. As the temperature keeps decreasing, the free energy density of this broken phase diminishes until it reaches a value similar to the free energy density of the symmetric phase. At that time, the two vacua are degenerate and the corresponding temperature is called $T = T_c$, the *critical* temperature. For $T < T_c$, the free energy density of the broken phase keeps decreasing such that the field at $v_T^{(+)}$ becomes metastable. QFT therefore predicts that the field may decay into the more energetically favorable sate at $v_T^{(-)}$. Once the decay probability becomes high enough, bubbles of true vacuum nucleate and start to expand in the surrounding symmetric phase. We can thus define the nucleation temperature T_n corresponding to the temperature at which most of the bubbles are produced. Finally, the last temperature T_p corresponds to the percolation temperature, namely the time when a significant part of the Universe has been converted to the new stable phase. This is at that instant that most of the bubbles are expected to collide.

The last paragraph gives a rough picture of what is expected to happen during a first-order PT. It is important to keep in mind that the dynamics can be significantly different from one particle physics model to another. We will have the opportunity to confirm this statement in Section 5.2.

Chapter 4

Constraining non-commutative space-time with GW150914

The three previous chapters have given a detailed overview of many important aspects of fundamental physics and GWs. We now start the second part of this thesis and engage in unknown territories. As emphasized in Section 1.2, our focus is on the quantum nature of space-time and the dynamics of the early Universe ; two subjects about which little is known. We now have all the technical tools in hands to support our main claim that GWs provide relevant information about these topics. The current Chapter shows in particular how to use the signal GW150914 to constrain the scale of non-commutative space-time [1, 2].

We first formalize more rigorously the ideas we introduced in Section 1.2.3 about quantum fuzziness. We adopt a mathematical model where space-time coordinates are promoted to operators satisfying the canonical commutation relations

$$[\hat{x}^\mu, \hat{x}^\nu] = i\,\theta^{\mu\nu}, \tag{4.1}$$

where $\theta^{\mu\nu}$ is a real and constant anti-symmetric tensor. Through $\theta^{\mu\nu}$, a new fundamental scale is introduced, which measures quantum fuzziness of space-time, similar to the Planck constant $\hbar$ that measures fuzziness of the phase space in the conventional quantum mechanics. To mention the context of this work, various aspects of non-commutative field theories have been investigated in the past; see references [105, 106] and references therein. On one side, it was observed that quantized space-times represent the low-energy field-theoretic limit of string theory in the background of an anti-symmetric B-field [103, 104]. On an other side, based on different treatments of non-commutative gauge symmetry, two different formulations of the non-commutative Standard Model of particle physics have been proposed in [166, 167] and [168, 169]. Some limits on the non-commutative scale have been obtained from various particle physics processes, including low-energy precision measurements [107, 108] and processes involving Lorentz symmetry violation [109, 110]. In addition, inflationary observables can be used to constrain space-time non-commutativity [170, 171]. Careful considerations [110] show that the scale of non-commutativity is limited from these studies to be smaller than the inverse $\sim TeV$ scale.

In addition, several versions of non-commutative theories of gravitation have been suggested in references [172–177]. However, non-commutativity in all these formulations shows only at the second order of the non-commutative scale [178, 179], and thus the bounds from the purely gravitational sector are expected to be less restrictive. Bearing this in mind, we consider the effect of non-commutativity on GWs through the non-commutative corrections to the classical matter source

and ignore non-commutative corrections to gravity itself, which is highly model-dependent and presumably subdominant or even nonexistent as in the string theory formulation.

Under this assumption, it has already been shown in [180] that the lowest-order non-commutative corrections to the matter source produce a second-order post-Newtonian modification of the Schwarzschild metric. We extend this analysis here to compute the non-commutative corrections to the waveform of the gravitational waves produced during the inspiraling phase of a binary BH (BBH) system. We closely follow the post-Newtonian formalism of Damour and Blanchet that we have introduced in Section 2.2.2 and proceed in the following way. In Section 4.1, we derive the non-commutative corrections to the energy-momentum tensor describing the BBH. In Section 4.2, we compute the equations of motion of this system including lowest-order, namely 2PN, noncommutative modifications. The energy flux radiated by the BBH is then derived in Section 4.3. Section 4.4 is devoted to the calculation of the phase of the waveform and to its comparison with the LIGO GW150914 observation.

4.1 Non-commutative corrections to the energy-momentum tensor

In our review of the post-Newtonian formalism, Equation (2.59) showed how the energy-momentum tensor of a BBH can be approximated by point masses in GR. For clarity, we remind the formula here:

$$\begin{aligned} T^{\mu\nu}_{GR}(\mathbf{x},t) &= m_1\gamma_1(t)v_1^\mu(t)v_1^\nu(t)\delta^3(\mathbf{x}-\mathbf{y}_1(t)) + 1 \leftrightarrow 2, \\ \gamma_1 &= \left(g_1(g_{\alpha\beta})_1\frac{v_1^\alpha v_1^\beta}{c^2}\right)^{-1/2}, \end{aligned} \tag{4.2}$$

with m_i the masses, $\mathbf{y}_i(t)$ the positions, and $v_i^\mu(t) = \left(c, \frac{d\mathbf{y}_i(t)}{dt}\right)$ the velocities of the two bodies $i = 1, 2$. We remind that the point-mass approximation induces divergences that can be cured thanks to the Hadamard regularization [128]. We also mentioned that the metric can be evaluated at the point mass location, $(g_{\alpha\beta})_i = g_{\alpha\beta}(\mathbf{y}_i(t))$ instead of $g_{\alpha\beta}(\mathbf{x},t)$, as long as we are interested in the equations of motion below 3PN order. Since the lowest-order non-commutative corrections will occur at 2PN order in our equations of motion, we can safely use the above formula in our approach.

In order to compute non-commutative corrections to the energy-momentum tensor (4.2), we follow the effective field theory formalism which has been used to compute quantum corrections [181] and non-commutative corrections [180] to classical BHs. In this approach, the Schwarzschild BHs are sourced by a massive real scalar field ϕ. To build a quantum field theory in non-commutative space-time, it is possible to work with the usual commuting coordinates x^μ instead of the operators $\hat{x}^\mu$ if we replace the product of two space-time-dependent functions by the following Moyal product [182]:

$$f(x)\star g(x) = f(x)g(x) + \sum_{n=1}^{+\infty}\left(\frac{i}{2}\right)^n \frac{1}{n!}\theta^{\alpha_1\beta_1}\cdots\theta^{\alpha_n\beta_n}\,\partial_{\alpha_1}\cdots\partial_{\alpha_n}f(x)\,\partial_{\beta_1}\cdots\partial_{\beta_n}g(x). \tag{4.3}$$

The noncommutative energy-momentum tensor for a real scalar field ϕ (in natural units) can then be written as

$$\begin{aligned} T^{\mu\nu}_{NC}(x) &= \frac{1}{2}\left(\partial^\mu\phi \star \partial^\nu\phi + \partial^\nu\phi \star \partial^\mu\phi\right) - \frac{1}{2}\eta^{\mu\nu}\left(\partial_\rho\phi \star \partial^\rho\phi - m^2\phi\star\phi\right) \\ &= \partial^\mu\phi\,\partial^\nu\phi - \frac{1}{2}\eta^{\mu\nu}\left(\partial_\rho\phi\,\partial^\rho\phi - m^2\phi^2\right) - \frac{1}{8}\theta^{\alpha_1\beta_1}\theta^{\alpha_2\beta_2}\Big(\partial_{\alpha_1}\partial_{\alpha_2}\partial^\mu\phi\partial_{\beta_1}\partial_{\beta_2}\partial^\nu\phi \\ &\quad - \frac{1}{2}\eta^{\mu\nu}\partial_{\alpha_1}\partial_{\alpha_2}\partial_\rho\phi\partial_{\beta_1}\partial_{\beta_2}\partial^\rho\phi + \frac{1}{2}\eta^{\mu\nu}m^2\partial_{\alpha_1}\partial_{\alpha_2}\phi\partial_{\beta_1}\partial_{\beta_2}\phi\Big) + \cdots\,, \end{aligned} \tag{4.4}$$

where we only keep the lowest-order non-commutative corrections. Note that the first two terms correspond to the usual energy-momentum tensor of a massive scalar field. We then quantize the field in flat space-time as explained in Section 3.1.1:

$$\hat\phi(x) = \int \frac{d^3\mathbf{p}}{(2\pi)^3\sqrt{2\omega_p}}\left(\hat a(\mathbf{p})e^{-ipx} + \hat a^\dagger(\mathbf{k})e^{ipx}\right), \tag{4.5}$$

where

$$\left[\hat a(\mathbf{p}), \hat a^\dagger(\mathbf{p}')\right] = (2\pi)^3\delta^3(\mathbf{p}-\mathbf{p}'), \quad \hat a(\mathbf{p})\,|0\rangle = 0, \quad \hat a^\dagger(\mathbf{p})\,|0\rangle = |\mathbf{p}\rangle\,. \tag{4.6}$$

The expectation value of the energy-momentum tensor (4.4) between two arbitrary states $|p_1\rangle$ and $|p_2\rangle$ becomes at tree level:

$$\langle p_2| : \hat T^{\mu\nu}_{NC}(x) : |p_1\rangle = \frac{e^{-i\,\mathbf{q}\cdot\mathbf{x}}}{2P^0}\left(2P^\mu P^\nu - \frac{1}{2}q^\mu q^\nu + \frac{1}{2}\eta^{\mu\nu}\mathbf{q}^2\right)\left(1 - \frac{1}{8}\left(\theta^{\alpha\beta}P_\alpha q_\beta\right)^2\right), \tag{4.7}$$

where we have defined $P = \frac{1}{2}(p_1+p_2)$, and $q = p_1 - p_2$, and we have chosen a frame in which $q^0 = 0$. Taking the Fourier transform of the previous formula, we obtain the position-space expression

$$\begin{aligned} &\int \frac{d^3\mathbf{q}}{(2\pi)^3}e^{i\,\mathbf{q}\cdot\mathbf{y}}\,\langle p_2| : T^{\mu\nu}_{NC}(x) : |p_1\rangle = \\ &\frac{1}{2P^0}\left(2P^\mu P^\nu + \frac{1}{2}\eta^{\mu m}\eta^{\nu n}\frac{\partial}{\partial x^m}\frac{\partial}{\partial x^n} - \frac{1}{2}\eta^{\mu\nu}\frac{\partial}{\partial x_i}\frac{\partial}{\partial x^i}\right)\left(1 + \frac{\theta^{\alpha k}\theta^{\beta l}P_\alpha P_\beta}{8}\frac{\partial}{\partial x^k}\frac{\partial}{\partial x^l}\right)\delta^3(\mathbf{x}-\mathbf{y}). \end{aligned} \tag{4.8}$$

We now interpret the previous formula as the energy-momentum tensor of a point-like particle of mass m with momentum P^μ and position $\mathbf{y}(t)$, which we call $T_{NC,P}$. This expression can be further simplified once we restore the dimensions. Using the usual relativistic relation $P^\mu = m\gamma_L v^\mu$, where γ_L is the Lorentz factor, we have

$$\begin{aligned} T^{\mu\nu}_{NC,P}(\mathbf{x},t) &= m\gamma_L v^\mu v^\nu\,\delta^3(\mathbf{x}-\mathbf{y}(t)) + \frac{m^3\gamma_L^3G^2}{8c^4}v^\mu v^\nu\Theta^{kl}\partial_k\partial_l\,\delta^3(\mathbf{x}-\mathbf{y}(t)) \\ &\quad + \left(\eta^{\mu m}\eta^{\nu n}\partial_m\partial_n - \eta^{\mu\nu}\partial_i\partial^i\right)\left(\frac{\hbar^2}{4m\gamma_L} + \frac{m\gamma_L\hbar^2G^2}{32c^4}\Theta^{kl}\partial_k\partial_l\right)\delta^3(\mathbf{x}-\mathbf{y}(t)), \end{aligned} \tag{4.9}$$

where we have introduced[1]

$$\Theta^{kl} = \frac{\theta^{0k}\theta^{0l}}{l_P^2t_P^2} + 2\frac{v_p}{c}\frac{\theta^{0k}\theta^{pl}}{l_P^3t_P} + \frac{v_pv_q}{c^2}\frac{\theta^{kp}\theta^{lq}}{l_P^4}, \tag{4.10}$$

in terms of the Planck length l_P and time t_P. The second line of Equation (4.9) is

[1] Note that the components θ^{0i} and θ^{ij} have different units.

proportional to $\hbar^2$, meaning that it will be negligible in front of the first two terms since we are considering astrophysical objects with $m \gtrsim M_\odot$. On the other hand, Equation (4.10) tells us that in a post-Newtonian expansion $\Theta^{kl} = \frac{\theta^{0k}\theta^{0l}}{l_P^2 t_P^2} + \mathcal{O}\left(\frac{1}{c}\right)$. We will only keep this dominant term, since we are looking for the lowest-order non-commutative corrections to the waveform of the GWs produced by the BBH. From the two previous considerations, we can therefore simplify the energy-momentum tensor as follows:

$$T^{\mu\nu}_{NC,P}(\mathbf{x},t) \approx m\gamma_L v^\mu v^\nu\, \delta^3(\mathbf{x}-\mathbf{y}(t)) + \frac{m^3\gamma_L^3 G^2}{8c^4} v^\mu v^\nu \frac{\theta^{0k}\theta^{0l}}{l_P^2 t_P^2}\partial_k\partial_l\, \delta^3(\mathbf{x}-\mathbf{y}(t)). \quad (4.11)$$

We remind the reader that the previous expression has been derived in flat space-time. By identifying γ_L with γ_1 defined by Equation (4.2), the first term in Equation (4.11) reproduces exactly the GR energy-momentum tensor (4.2) for a single point mass. On the other hand, we do not need to generalize the second term to curved space-time since we are only interested in the lowest-order non-commutative corrections. By the same argument, we can also replace the Lorentz factor (in the second term) by its Newtonian value $\gamma_L = 1 + \mathcal{O}\left(\frac{1}{c^2}\right)$. This allows us to define the BBH energy-momentum tensor with its lowest-order non-commutative corrections as follows:

$$\begin{aligned} T^{\mu\nu}(\mathbf{x},t) =& m_1\gamma_1(t) v_1^\mu(t) v_1^\nu(t)\delta^3(\mathbf{x}-\mathbf{y}_1(t)) \\ &+ \frac{m_1^3 G^2\Lambda^2}{8c^4} v_1^\mu(t) v_1^\nu(t)\theta^k\theta^l\partial_k\partial_l\, \delta^3(\mathbf{x}-\mathbf{y}_1(t)) + 1 \leftrightarrow 2\,, \end{aligned} \quad (4.12)$$

where we have simplified the notation by introducing $\Lambda\,\theta^i \equiv \theta^{0i}/(l_P t_P)$, with θ^i representing the components of a three-dimensional unit vector $\boldsymbol{\theta}$, $\theta^i\theta^i = 1$. In this way $\sqrt{\Lambda}$ corresponds to the time-component scale of non-commutativity relative to the Planck scale and will be the scale of non-commutativity we aim to constrain. As we argue in Section 4.4, the bounds on other components, θ^{ij}, are expected to be similar. We note in passing that θ^{0i} is sometimes considered to be vanishing within effective field theories, because of the apparent violation of unitarity (see, however, an alternative unitary formulation of non-commutative field theory with nonzero θ^{0i} in [183]). The potential violation of unitarity in the effective theory is not relevant for our calculations, and we simply assume that the issue is resolved in a full theory. Nonzero θ^{0i} also appears in unitary theories with lightlike non-commutativity, $\theta_{\mu\nu}\theta^{\mu\nu} = 0$, which are known to have a consistent string theory completion [184].

4.2 2PN equations of motion

4.2.1 General orbit

In order to infer the waveform of the GWs produced by a BBH, we require the equations of motion of the two bodies. Since we are neglecting noncommutative corrections to Einstein field equations (EFEs), we can follow the approach we have described in Section 2.2 and invoke the covariant conservation of the energy-momentum tensor (2.53):

$$\partial_\nu\left(\sqrt{-g}\, g_{\lambda\mu} T^{\mu\nu}\right) = \frac{1}{2}\sqrt{-g}\,\partial_\lambda g_{\mu\nu} T^{\mu\nu}. \quad (4.13)$$

The difference with GR is that we will now insert the expression (4.12) for the energy-momentum tensor in the previous formula. We obtain again geodesic equations

of the form (2.54), namely $\frac{dP_1^i}{dt} = F_1^i$ (for the body 1), where the linear momentum density $\mathbf{P}_1$ and force density $\mathbf{F}_1$ are this time given by

$$P_1^i = \gamma_1 \left(g_{i\mu}\right)_1 v_1^\mu + \frac{m_1^2 G^2}{8c^4}\Lambda^2\theta^k\theta^l \left(\partial_k\partial_l g_{i\mu}\right)_1 v_1^\mu \tag{4.14}$$

$$F_1^i = \frac{1}{2}\gamma_1 \left(\partial_i g_{\mu\nu}\right)_1 v_1^\mu v_1^\nu + \frac{m_1^2 G^2}{16c^4}\Lambda^2\theta^k\theta^l \left(\partial_k\partial_l\partial_i g_{\mu\nu}\right)_1 v_1^\mu v_1^\nu. \tag{4.15}$$

As usual, the equations of motion of the second body are obtained by replacing the index 1 by 2 in the above formulas. Note that the expressions inside $(\cdots)_1$ have to be evaluated at the location of the body 1, $\mathbf{y}_1(t)$.

The previous equations describe the motion of the two point masses in the background of the metric $g_{\mu\nu}(\mathbf{x}, t)$, which is itself generated by these two particles. The general form of this metric in the near zone of the system was given in Equation (2.51). At the order required for our analysis, it reads

$$\begin{aligned} g_{00} &= -1 + \frac{2}{c^2}V + \mathcal{O}\left(\frac{1}{c^4}\right) \\ g_{0i} &= \mathcal{O}\left(\frac{1}{c^3}\right) \\ g_{ij} &= \delta_{ij}\left(1 + \frac{2}{c^2}V\right) + \mathcal{O}\left(\frac{1}{c^4}\right) \end{aligned} \tag{4.16}$$

where V is the retarded potential (2.52) given by[2]

$$V(\mathbf{x}, t) = G\sum_{k=0}^{+\infty}\frac{(-1)^k}{k!}\left(\frac{\partial}{c\,\partial t}\right)^k \int d^3\mathbf{x}' |\mathbf{x} - \mathbf{x}'|^{k-1}\sigma(\mathbf{x}', t), \quad \sigma = \frac{T^{00} + T^{ii}}{c^2}. \tag{4.17}$$

The matter source σ includes now non-commutative corrections from the expression (4.12). Keeping the leading modification, we can rewrite it explicitly as

$$\sigma(\mathbf{x}, t) = m_1\gamma_1\left(1 + \frac{v_1^2}{c^2}\right)\delta^3(\mathbf{x} - \mathbf{y}_1(t)) + \frac{m_1^3 G^2\Lambda^2}{8c^4}\theta^k\theta^l\partial_k\partial_l\,\delta^3(\mathbf{x} - \mathbf{y}_1(t)) + 1 \leftrightarrow 2. \tag{4.18}$$

It is worth observing that V cannot be straightforwardly computed by inserting Equation (4.18) in Equation (4.17) since σ depends on V itself through γ_1 and γ_2. So σ and V are usually computed iteratively in each PN order. Fortunately, in our case of interest the lowest-order non-commutative correction to V is simply computed by inserting the second term of Equation (4.18) into the $k = 0$ term of the series (4.17). In other words, we have

$$V(\mathbf{x}, t) = V_{GR}^{2PN}(\mathbf{x}, t) + \frac{3m_1^3 G^3\Lambda^2}{8c^4 r_1^3}\theta^k\theta^l\hat{n}_{1kl} + \mathcal{O}\left(\frac{1}{c^5}\right) + 1 \leftrightarrow 2 \tag{4.19}$$

where V_{GR}^{2PN} is the GR expression for the potential V up to 2PN order, which can be explicitly found in Equation (B1a) of [185]. We have also defined $r_1 = |\mathbf{x} - \mathbf{y_1}|$, $\mathbf{n}_1 = (\mathbf{x} - \mathbf{y}_1)/r_1$, and the STF quantity $\hat{n}_{1kl} = n_{1k}n_{1l} - \delta_{kl}/3$.

We can now compute the 2PN expression of the linear momentum densities $\mathbf{P}_1$, $\mathbf{P}_2$ and force densities $\mathbf{F}_1$, $\mathbf{F}_2$. The first step is to introduce the metric (4.16) into

[2]Note that there is no problem of divergence regarding the retarded d'Alembertian at the PN orders we are considering.

Equations (4.14)-(4.15):

$$P_1^i = v_1^i + \frac{1}{c^2}\left(P_1^{1PN}\right)^i + \frac{1}{c^4}\left(P_1^{2PN}\right)^i + \mathcal{O}\left(\frac{1}{c^5}\right) \tag{4.20}$$

$$F_1^i = (\partial_i V)_1 + \frac{1}{c^2}\left(F_1^{1PN}\right)^i + \frac{1}{c^4}\left(F_1^{2PN}\right)^i + \frac{m_1^2 G^2 \Lambda^2}{8c^4}\theta^k\theta^l\left(\partial_k\partial_l\partial_i V\right)_1 + \mathcal{O}\left(\frac{1}{c^5}\right) \tag{4.21}$$

and similarly for $\mathbf{P}_2$ and $\mathbf{F}_2$. The terms P^{xPN} and F^{xPN} represent some 1PN and 2PN expressions involving the retarded potential V and some other higher-order retarded potentials [see Equations (146)-(147) and Equation (152) in [117]]. The point is that non-commutative corrections to these terms appear above 2PN order in the final expression for $\mathbf{P}$ and $\mathbf{F}$ and are irrelevant in this study. Similarly, we observe that non-commutative corrections to $\mathbf{P}$ start at 3PN order and thus can be neglected, explaining their absence in Equation (4.20).

Thus only $\mathbf{F}$ admits 2PN-order corrections, which originate from both the first and fourth terms of Equation (4.21). Consider first $(\partial_i V)_1$ in which we replace V by its expression (4.19). Considering only the non-commutative term, we have

$$(\partial_i V_{NC})_1 = \left(-\frac{15m_1^3 G^3\Lambda^2}{8c^4 r_1^4}\theta^k\theta^l\hat{n}_{1ikl} + 1 \leftrightarrow 2\right)_1 = -\frac{15m_2^3 G^3\Lambda^2}{8c^4 r^4}\theta^k\theta^l\hat{n}_{ikl} \tag{4.22}$$

where $r = |\mathbf{y}_1 - \mathbf{y}_2|$, $\mathbf{n} = (\mathbf{y}_1 - \mathbf{y}_2)/r$, and $\hat{n}_{ikl} = n_i n_k n_l - \frac{1}{5}\left(n_i\delta_{lk} + n_k\delta_{il} + n_l\delta_{ik}\right)$. At the second equality, we have used the Hadamard regularization described in [128]. Indeed, the first term in brackets is divergent when evaluated at the location of particle 1 since $r_1(\mathbf{y}_1(t)) = 0$. The second 2PN non-commutative correction to $\mathbf{F}_1$ comes from the fourth term in Equation (4.21) with V replaced by its Newtonian value $V = Gm_1/r_1 + Gm_2/r_2 + \mathcal{O}\left(\frac{1}{c^2}\right)$. We find after regularization:

$$\frac{m_1^2 G^2\Lambda^2}{8c^4}\theta^k\theta^l\left(\partial_k\partial_l\partial_i V\right)_1 = -\frac{15m_1^2 m_2 G^3\Lambda^2}{8c^4 r^4}\theta^k\theta^l\hat{n}_{ikl}. \tag{4.23}$$

By adding the two contributions (4.22) and (4.23), we have the final 2PN correction to the force density $\mathbf{F}_1$ as follows:

$$\left(F_1^i\right)_{NC}^{2PN} = -\frac{15m_2(m_1^2 + m_2^2)G^3\Lambda^2}{8c^4 r^4}\theta^k\theta^l\hat{n}_{ikl} \tag{4.24}$$

and similarly for the second body.

We now have all the ingredients to compute the acceleration of the first body in harmonic coordinates from their geodesic equations (2.54). The calculation is performed iteratively at each PN order. The Newtonian part of dP_1^i/dt gives $dv_1^i/dt = a_1^i$, which is directly compared to the Newtonian part of F_1^i. Then when the higher-order terms of P_1 are derived (e.g., dP_1^{1PN}/dt), each explicit acceleration that appears is order-reduced by its previous lower-order expression. Since there are no 2PN non-commutative corrections to P_1^i, it is straightforward to see that the only modification to the 2PN-order acceleration directly comes from the term (4.24), namely,

$$a_1^i = (a_1^i)_{GR}^{2PN} - \frac{15m_2(m_1^2 + m_2^2)G^3\Lambda^2}{8c^4 r^4}\theta^k\theta^l\hat{n}_{ikl} + \mathcal{O}\left(\frac{1}{c^5}\right). \tag{4.25}$$

The GR acceleration $(a_1^i)_{GR}^{2PN}$ is given explicitly in Equation (203) of [117] and has been computed iteratively following the procedure above. The acceleration of the

second body is obtained by replacing the index 1 by 2 in the previous expression.

4.2.2 Relative motion

For the rest of the Chapter, we will consider only the relative motion of the two point masses. So in addition to r and $\mathbf{n}$, we introduce the relative velocity $\mathbf{v} = \mathbf{v}_1 - \mathbf{v}_2$ and acceleration $\mathbf{a} = \mathbf{a}_1 - \mathbf{a}_2$. The expressions will also simplify by using the reduced mass μ and the symmetric mass ratio ν given in Equation (2.41). From (4.25), we directly deduce the relative acceleration

$$a_i = (a_i)^{2PN}_{GR} - \frac{15M^3(1-2\nu)G^3\Lambda^2}{8c^4r^4}\theta^k\theta^l\hat{n}_{ikl} + \mathcal{O}\left(\frac{1}{c^5}\right). \tag{4.26}$$

As in GR, this acceleration can be derived from a Lagrangian. Indeed, we see that

$$L = L^{2PN}_{GR} + \frac{3M^3\mu(1-2\nu)G^3\Lambda^2}{8c^4r^3}\theta^k\theta^l\hat{n}_{kl} + \mathcal{O}\left(\frac{1}{c^5}\right) \tag{4.27}$$

reproduces the equations of motion (4.26). Note that the non-commutative part of this Lagrangian is not Lorentz invariant. However it still admits the following conserved energy:

$$E = E^{2PN}_{GR} - \frac{3M^3\mu(1-2\nu)G^3\Lambda^2}{8c^4r^3}\theta^k\theta^l\hat{n}_{kl} + \mathcal{O}\left(\frac{1}{c^5}\right) \tag{4.28}$$

where E^{2PN}_{GR} is given in Equation (205) of [117]. Indeed, a direct computation[3] shows that $dE/dt = \mathcal{O}\left(\frac{1}{c^5}\right)$.

In order to have a better understanding of the effect of the non-commutative terms in the acceleration and the energy, we can use the following identities:

$$\theta^k\theta^l\hat{n}_{ikl} = n_i\left(\mathbf{n}\cdot\boldsymbol{\theta}\right)^2 - \frac{1}{5}n_i - \frac{2}{5}\theta_i\left(\mathbf{n}\cdot\boldsymbol{\theta}\right), \tag{4.29}$$

$$\theta^k\theta^l\hat{n}_{kl} = \left(\mathbf{n}\cdot\boldsymbol{\theta}\right)^2 - \frac{1}{3}. \tag{4.30}$$

In this form, we can see that the constant vector $\boldsymbol{\theta}$ acts like a preferred direction and will influence the motion of the BBH. In particular, we expect the orbital plane of the two point masses to precess because of the term $\theta_i\left(\mathbf{n}\cdot\boldsymbol{\theta}\right)$. On the other hand, the motion drastically simplifies if the orbital plane is perpendicular to this preferred direction as all the terms with $\mathbf{n}\cdot\boldsymbol{\theta}$ vanish. We argue now that we can restrict our attention to this simpler case since we are only looking for a bound on the parameter $\sqrt{\Lambda}$ and not a precise value.

There is of course no reason for the BBH that produced the GW150914 signal to satisfy this property. However it is important to observe that there are no orbital configurations for which each of the two expressions (4.29) and (4.30) are constantly zero, since $\boldsymbol{\theta}$ is time independent and $\mathbf{n}$ varies with time. In other words, the contributions $-\frac{1}{5}n_i$ in the acceleration and $-\frac{1}{3}$ in the energy cannot be entirely canceled, they will only be modulated by the angular-dependent terms. Consequently, we expect the non-commutative corrections to the GW waveform to be of the same order

[3] The time derivative of the second term in Equation (4.28) is canceled by the Newtonian part of dE^{2PN}_{GR}/dt in which the acceleration has to be replaced by Equation (4.26).

of magnitude with or without these terms. Hence we will use the following expressions for the relative acceleration and energy of the BBH:

$$a_i = (a_i)_{GR}^{2PN} + \frac{3M^3(1-2\nu)G^3\Lambda^2}{8c^4r^4}n_i + \mathcal{O}\left(\frac{1}{c^5}\right) \tag{4.31}$$

$$E = E_{GR}^{2PN} + \frac{M^3\mu(1-2\nu)G^3\Lambda^2}{8c^4r^3} + \mathcal{O}\left(\frac{1}{c^5}\right). \tag{4.32}$$

4.2.3 Quasicircular orbit

The previous equations further simplify if we assume that the two objects are in quasicircular orbit. This assumption is well justified since it has been shown in GR that the orbit of a BBH tends to circularize under the emissions of GWs [130, 131]. This is particularly true at the time when the GWs of the system enter the sensitivity band of the LIGO detector. It is important to note that this result has been directly derived from Einstein's quadrupole formula, which describes radiation of GWs at the lowest (Newtonian) order of the PN expansion. As we will explain in the next section, non-commutative corrections to the radiation formula appear at 2PN order, meaning that they are subdominant compared to the circularization effect. Therefore, even in non-commutative space-time, we expect to observe binaries with negligible eccentricity. Of course, precession of the orbital plane could still occur due to the angular-dependent terms in Equation (4.29). However, we shall not consider these terms for the reasons explained above.

With these approximations, we can assume that r is constant, apart from the gradual inspiraling that will ultimately cause the two bodies to merge. As explained in Section 2.2, this effect appears at 2.5PN order in the equations of motion [185] and we actually have $\dot{r} = \mathcal{O}\left(\frac{1}{c^5}\right)$. So we obtain again a simple expression for the circular orbit acceleration

$$\mathbf{a}_{circ} = -\Omega^2\mathbf{y} + \mathcal{O}\left(\frac{1}{c^5}\right). \tag{4.33}$$

where the angular frequency Ω is modified as

$$\Omega^2 = \frac{GM}{r^3}\left[1 + (-3+\nu)\gamma + \left(6 + \frac{41}{4}\nu + \nu^2 - \frac{3}{8}(1-2\nu)\Lambda^2\right)\gamma^2\right] + \mathcal{O}\left(\frac{1}{c^5}\right), \tag{4.34}$$

as a function of the post-Newtonian parameter $\gamma = GM/(c^2r)$. Note that the non-commutative term, proportional to Λ^2, comes directly from the second part of Equation (4.31). In order to write the energy (4.32) of the two particles in circular orbit, we note that the norm v of the relative velocity can be expressed as $v^2 = r^2\Omega^2 + \mathcal{O}\left(\frac{1}{c^{10}}\right)$. This implies in particular that the energy will contain two 2PN-order non-commutative corrections: one obvious contribution from the second term in Equation (4.32) and another one from the Newtonian part of E_{GR}^{2PN}, once v^2 is expressed in terms of Ω^2 given by (4.34). Adding these two contributions to the GR expression, we find

$$E_{circ} = -\frac{\mu c^2\gamma}{2}\left[1 + \left(-\frac{7}{4} + \frac{1}{4}\nu\right)\gamma + \left(-\frac{7}{8} + \frac{49}{8}\nu + \frac{1}{8}\nu^2 + \frac{1}{8}(1-2\nu)\Lambda^2\right)\gamma^2\right] + \mathcal{O}\left(\frac{1}{c^5}\right). \tag{4.35}$$

For later convenience, we want to express the energy as a function of the frequency-related parameter $x = \left(\frac{GM\Omega}{c^3}\right)^{\frac{2}{3}}$. In order to achieve this relationship, we need to know how γ depends on Ω (or x). We must therefore take the inverse of Equation (4.34). We find

$$\gamma = x\left[1 + \left(1 - \frac{1}{3}\nu\right)x + \left(1 - \frac{65}{12}\nu + \frac{1}{8}\Lambda^2(1-2\nu)\right)x^2\right] + \mathcal{O}\left(\frac{1}{c^5}\right). \tag{4.36}$$

By replacing γ in Equation (4.35), we finally obtain

$$\begin{aligned} E = &-\frac{\mu c^2 x}{2}\left[1 + \left(-\frac{3}{4} - \frac{1}{12}\nu\right)x + \left(-\frac{27}{8} + \frac{19}{8}\nu - \frac{1}{24}\nu^2 + \frac{1}{4}\Lambda^2(1-2\nu)\right)x^2\right] \\ &+ \mathcal{O}\left(\frac{1}{c^5}\right), \end{aligned} \tag{4.37}$$

which reduces to Equation (2.64) when $\Lambda \to 0$. In Section 4.4, we shall compare this expression to the energy radiated in GWs.

4.3 Energy loss

In this section, we investigate the lowest-order non-commutative corrections to the energy radiated in GWs by the BBH. As we have seen in Section 2.2.2, it is usual to assume the energy balance equation (2.66), $\frac{dE}{dt} = -\mathcal{F}$, between the variation of energy in the near zone of the BBH and the flux in the far zone. Since we have neglected non-commutative corrections to the EFEs, the GR strategy to compute the flux in terms of radiative multipole moments is still valid in our case. The only modification to this procedure is to the source (4.12) itself. We remind that the general form of the flux at 2PN order is $\mathcal{F} = \mathcal{F}_{inst} + \mathcal{F}_{tail}$. Since the tail part of the flux starts at 1.5PN order, non-commutative corrections will appear above 2PN order in this term. Hence we only need to compute corrections to the quadrupole part of the instantaneous term which was given by Equation (2.48):

$$\mathcal{F}_{inst} = \frac{G}{c^5}\left[\frac{1}{5}\frac{d^3 I_{ij}}{dt^3}\frac{d^3 I_{ij}}{dt^3} + \mathcal{O}\left(\frac{1}{c^2}\right)\right]. \tag{4.38}$$

Non-commutative effects appear in the mass quadrupole moments which at lowest order reduce to (2.58): $I_{ij} = \int d^3\mathbf{x}\,\hat{x}_{ij}\sigma + \mathcal{O}\left(\frac{1}{c^2}\right)$. We first perform the integral over the second term (non-commutative part) of σ given by Equation (4.18):

$$\begin{aligned} \int d^3\mathbf{x}\,\hat{x}_{ij}\sigma_{NC} &= \frac{m_1^3 G^2\Lambda^2}{8c^4}\theta^k\theta^l\left(\partial_k\partial_l\hat{x}_{ij}\right)\big|_{\mathbf{x}=\mathbf{y}_1(t)} + 1 \leftrightarrow 2 \\ &= \frac{(m_1^3 + m_2^3)G^2\Lambda^2}{4c^4}\left(\theta_i\theta_j - \frac{1}{3}\delta_{ij}\right). \end{aligned} \tag{4.39}$$

We directly observe that this term does not depend on time, meaning that this contribution will vanish in the instantaneous flux (4.38). Therefore the only nonvanishing 2PN non-commutative correction to $\mathcal{F}$ appears when we derive the Newtonian part of I_{ij}. Indeed, after two time derivations the expression will contain an acceleration that has to be replaced by the formula (4.25), itself containing a 2PN correction. We now explicitly compute this correction assuming a circular orbit as we discussed in the previous section. In terms of the relative position $\mathbf{y}(t)$ of the two point masses,

the quadrupole moment becomes

$$I_{ij} = \mu \left(y_i y_j - \frac{1}{3}\delta_{ij} r^2 \right) + \mathcal{O}\left(\frac{1}{c^2}\right). \tag{4.40}$$

In taking the time derivative, the second term within the brackets vanishes since $\dot{r} = \mathcal{O}\left(\frac{1}{c^5}\right)$. The first term gives $d^3 y_i y_j / dt^3 = \dot{a}_i x_j + 3 a_i v_j + (i \leftrightarrow j)$. Inserting the non-commutative term of the acceleration (4.31) (and its time derivative), we find the following 2PN non-commutative correction:

$$\left.\frac{d^3}{dt^3} I_{ij}\right|_{NC} = \frac{3\mu M^3 (1-2\nu) G^3 \Lambda^2}{2 c^4 r^5} (y_i v_j + v_i y_j). \tag{4.41}$$

Adding this term to the 2PN expression for the quadrupole mass moment in GR given in Equation (C2a) of [186], we obtain:

$$\begin{aligned} \frac{d^3}{dt^3} I_{ij} = &- \frac{8 G \nu M^2}{r^3} \left(\frac{y_i v_j + v_i y_j}{2} \right) \left[1 - \frac{\gamma}{42} (149 - 69\nu) \right. \\ &\left. + \frac{\gamma^2}{1512} \left(7043 - 7837\nu + 3703\nu^2 - 567\Lambda^2 (1-2\nu) \right) \right] + \mathcal{O}\left(\frac{1}{c^5}\right). \end{aligned} \tag{4.42}$$

The contribution from this quadrupole moment to the instantaneous flux is given by Equation (4.38). Using the fact that in a circular orbit, $\mathbf{v}^2 = \Omega^2 r^2 + \mathcal{O}\left(\frac{1}{c^{10}}\right)$ and $\mathbf{x} \cdot \mathbf{v} = \mathcal{O}\left(\frac{1}{c^5}\right)$, we have $(y_i v_j + v_i y_j)^2 = 2 r^4 \Omega^2 + \mathcal{O}\left(\frac{1}{c^5}\right)$, where the angular frequency is given by Equation (4.34). It follows straightforwardly that the lowest-order non-commutative correction to the flux is

$$\mathcal{F}_{NC} = \frac{32 c^5}{5G} \nu^2 \gamma^5 \left[-\frac{9}{8} \Lambda^2 (1-2\nu) \gamma^2 \right]. \tag{4.43}$$

The complete flux at 2PN order is computed by adding the previous term to the GR flux given in Equation (4.16) of [186]. Note that the derivation of this latter expression requires higher-order multipole moments in Equation (4.38) that we have not discussed in this Chapter since the non-commutative corrections to these terms will appear above 2PN in the final flux. As stated in Equation (2.47), tail effects are also important and will produce a 1.5PN contribution to $\mathcal{F}$. Taking all these contributions into account and after expressing γ through x thanks to (4.36), the final 2PN result including non-commutative corrections reads

$$\begin{aligned} \mathcal{F} = &\frac{32 c^5}{5G} \nu^2 x^5 \left[1 + \left(-\frac{1247}{336} - \frac{35}{12}\nu \right) x + 4\pi x^{3/2} \right. \\ &\left. + \left(-\frac{44711}{9072} + \frac{9271}{504}\nu + \frac{65}{18}\nu^2 - \frac{1}{2}\Lambda^2 (1-2\nu) \right) x^2 + \mathcal{O}\left(\frac{1}{c^5}\right) \right]. \end{aligned} \tag{4.44}$$

4.4 Constraint on $\sqrt{\Lambda}$ from the orbital phase

4.4.1 BBH orbital phase

We can now use the balance equation (2.66) to derive the secular decrease of the orbital radius r and the rate of change of the orbital frequency Ω. This will allow us to compute the evolution of the orbital phase of the BBH. For convenience, we

introduce the following time variable:

$$\Theta \equiv \frac{\nu c^3}{5GM}(t_c - t) = \mathcal{O}\left(c^8\right), \tag{4.45}$$

where t_c represents the instant of coalescence of the two point masses. Then the balance equation can be rewritten as

$$\frac{dE}{dx}\frac{dx}{d\Theta} = \frac{5GM}{\nu c^3}\mathcal{F}, \tag{4.46}$$

where $E(x)$ and $\mathcal{F}(x)$ are respectively given by Equations (4.37) and (4.44). We recall that these quantities have been derived for a quasicircular orbit where the angular-dependent non-commutative terms in (4.29)-(4.30) have been omitted. This expression provides a differential equation for the frequency parameter $x(\Theta)$, which can be directly solved (in the PN expansion sense), giving

$$\begin{aligned} x =& \frac{1}{4}\Theta^{-1/4}\left[1 + \left(\frac{743}{4032} + \frac{11}{48}\nu\right)\Theta^{-1/4} - \frac{1}{5}\pi\Theta^{-3/8}\right. \\ &\left. + \left(\frac{19583}{254016} + \frac{24401}{193536}\nu + \frac{31}{288}\nu^2 + \frac{10}{256}\Lambda^2(1-2\nu)\right)\Theta^{-1/2} + \mathcal{O}\left(\frac{1}{c^5}\right)\right]. \end{aligned} \tag{4.47}$$

This equation is nothing but the explicit temporal evolution of the angular frequency Ω. It is then straightforward to find the orbital phase ϕ of the BBH. Indeed, we have

$$\frac{d\phi}{dt} = \Omega \quad \Rightarrow \quad \frac{d\phi}{d\Theta} = -\frac{5}{\nu}x^{3/2}. \tag{4.48}$$

Integrating Equation (4.48) with respect to x [given in (4.47)] explicitly gives $\phi(\Theta)$. For data analysis purposes, it is more useful to express the phase in the frequency domain. So by inverting Equation (4.47), we can find $\Theta(x)$, allowing us to write the frequency-dependent phase evolution at 2PN precision:

$$\begin{aligned} \phi =& -\frac{x^{-5/2}}{32\nu}\left[1 + \left(\frac{3715}{1008} + \frac{55}{12}\nu\right)x - 10\pi x^{3/2}\right. \\ &\left. + \left(\frac{15293365}{1016064} + \frac{27145}{1008}\nu + \frac{3085}{144}\nu^2 + \frac{25}{4}\Lambda^2(1-2\nu)\right)x^2 + \mathcal{O}\left(\frac{1}{c^5}\right)\right], \end{aligned} \tag{4.49}$$

up to a constant of integration. We check that in the limit $\Lambda \to 0$, the two previous equations for x and ϕ reduce to their GR expressions (316) and (318) in [117].

It is now straightforward to use the previous results to predict the phase of the GWs detected on earth, far away from the source. We remind that this is done through the stationary phase approximation (SPA) which gives the frequency domain GW phase expression (2.70). As non-commutative corrections appear at 2PN-order, the first coefficient that will be modified is φ_4. From (4.49), we find

$$\varphi_4 = \frac{15293365}{508032} + \frac{27145}{504}\nu + \frac{3085}{72}\nu^2 + \frac{25}{2}\Lambda^2(1-2\nu). \tag{4.50}$$

In standard space-time ($\Lambda = 0$), we recover the same coefficients as in Equation (2.71). We also recall that in GR, the phase is known up to 4PN order and includes the coefficients φ_5 to φ_8, which we have ignored for our current purposes. We would expect non-commutative corrections to these terms as well, but their computation

would be significantly more involved and are unnecessary to impose an initial constraint on $\sqrt{\Lambda}$. Also note that spin effects are usually included in the phase coefficients since it is known that spin-orbit and spin-spin terms appear from 1.5PN and 2PN order, respectively, in the equations of motion of a BBH (see Chapter 11 of [117] and references therein). But for the same reason as above, we do not consider these effects here.

4.4.2 GW150914 signal and constraint

We have shown in Section 2.2.3 how LIGO/Virgo used the GW150914 signal to test for deviations from GR. In order to find a robust constraint on the non-commutative scale $\sqrt{\Lambda}$, we would have to perform a similar analysis, namely adding Λ as a new parameter of the gIMR model and inferring it from a statistical analysis. However, an estimated bound can be computed using a significantly simpler method. From Equation (2.71), we define the fractional non-commutative deviation from GR as

$$\delta\varphi_4^{NC} = \frac{\varphi_4^{NC}}{\varphi_4^{GR}} = \frac{1270080\,(1-2\nu)}{4353552\nu^2 + 5472432\nu + 3058673}\Lambda^2. \tag{4.51}$$

We then want to compare this correction to the value $\delta\varphi_4$ computed by LIGO/Virgo for GW150914. In order to do so we need the symmetric mass ratio ν of the BBH. However, it is important to realize that the masses of the BHs, $m_1 = 36.2^{+5.2}_{-3.8}M_\odot$ and $m_2 = 29.1^{+3.7}_{-4.4}M_\odot$ (in the source frame with 90% credible regions), have been derived by LIGO [8] from matched filtering based on GR templates. So if non-commutative corrections had been taken into account in those templates, we would expect slight deviations in the reported masses. Fortunately, this correction would have little significance on the constraint for $\sqrt{\Lambda}$. Indeed, by definition the symmetric mass ratio ν ranges between 0 (test-mass limit) and 1/4 (equal masses limit), which implies from Equation (4.51) that

$$\delta\varphi_4^{NC} \in [1.35, 4.15]\cdot 10^{-1}\Lambda^2 \tag{4.52}$$

for any BBH. In other words, the indeterminacy in the masses has less than one order of magnitude impact on any constraints we can impose on Λ. Using the central values for m_1, m_2 given above, we have $\delta\varphi_4^{NC} = 1.37\cdot 10^{-1}\Lambda^2$.

In Table I of [111], LIGO computed that the deviation from GR of the fourth coefficient is given by $\delta\varphi_4 = -2.0^{+1.6}_{-1.8}$ when only $\delta\varphi_4$ is allowed to vary, and $\delta\varphi_4 = 0.5^{+17.3}_{-18.2}$ when all the coefficients can vary. Considering the worst case scenario and asking that $|\delta\varphi_4^{NC}| \lesssim |\delta\varphi_4|$, we derive the following estimated constraint:

$$|\delta\varphi_4^{NC}| \lesssim 20 \Rightarrow \sqrt{\Lambda} \lesssim 3.5\,. \tag{4.53}$$

Recalling that $\Lambda \equiv |\theta^{0i}|/(l_P t_P)$, the previous result means that the temporal part of the non-commutative tensor is constrained be around the Planck scale.

Although we have not explicitly considered the spatial components θ^{ij} of the non-commutative tensor in this analysis, we would expect a similar constraint on them. From the energy-momentum tensor (4.9) and Equation (4.10), it is clear that these terms would appear at 2.5PN and 3PN order in the equations of motion of the BBH (and in the energy flux). So we expect the coefficient φ_6 of the GW phase (2.70) to admit non-commutative terms proportional to $|\theta^{ij}|^2/l_P^4$. These terms would then be constrained as we just did, since LIGO/Virgo computed [111] that the deviation

from GR of φ_6 is similar to $\delta\varphi_4$, namely, $\delta\varphi_6 = -0.6^{+18.2}_{-17.2}$. It also shows that the time-like and space-like components of $\theta^{\mu\nu}$ can be constrained independently from each other as they appear at different PN orders.

4.5 Chapter summary

In this Chapter we have derived, to lowest-order, an analytic deviation from GR that would be present in the phase of gravitational radiation emitted from a BBH merger, should non-commutative space-time be manifest in nature. This deviation is dependent on the scale at which non-commutative space-time becomes prevalent. We showed that (to lowest order) this phase deviation comes at 2PN order from a term proportional to $\Lambda^2 \equiv |\theta^{0i}|^2/(l_P t_P)^2$ and can be compared to the waveforms observed in the detection of GWs from BBH at LIGO, GW150914. By comparing the Bayesian analysis of allowed deviations from GR, which the LIGO and Virgo collaborations have completed using the GW150914 signal, we have constrained Λ up to the order of the Planck scale.

In deriving this constraint, we have made a number of well-justified approximations. First, we assumed that non-commutative effects contribute mainly to the energy-momentum tensor and ignored any corrections to the Einstein field equations. We expect these latter corrections to induce higher derivatives in the perturbed field equations and hence to be suppressed for low frequencies. Secondly, we have removed some angular-dependent terms in the non-commutative corrections to the equations of motion. As explained, these terms will only modulate the non-commutative corrections on the GW phase and hence have little effect on the overall bound that we placed on the scale of non-commutativity. Further, we assumed a circular orbit of the BHs, which is justified by the fact that emitted gravitational radiation removes angular momentum from a BBH and hence circularizes it. Finally, we assumed that the BHs had no spin and we used the masses estimated by the LIGO and Virgo collaborations for the GW150914 signal. We did not calculate these parameters assuming non-commutative space-time. This is because deviations of the masses of the binaries and spin effects play a very small role in constraining Λ (as emphasized in Section 4.4).

Ultimately we have found that if non-commutative space-time is realized, its scale has to be of the order of the Planck scale in order to fit with the current measurements of gravitational waves from BBH mergers. Our bound (4.53) on Λ is indeed equivalent to

$$|\theta^{0i}| \lesssim 12 \cdot l_P t_P \tag{4.54}$$

This result is the most stringent limit to date on non-commutative space-time and represents a significant improvement compared to previous constraints from particle physics considerations. This shows that GWs can indeed give us useful information about fundamental physics.

Chapter 5

Cosmological phase transitions beyond the Standard Model

We now enter into the second research topic covered in this thesis. Our objective is to learn about the dynamics of the early Universe and potentially new physics by studying the production of GWs from cosmological phase transitions (PTs). Such an investigation can be decomposed in four steps: the choice of a particle physics model of interest, the description of the dynamics of PTs that can occur for this model, the prediction for the existence and properties of associated GWs and finally the comparison with existing or future data from experiments. This Chapter focuses on the first two steps whereas Chapter 6 will discuss the part related to the GWs. Together they contain the results of our research that we obtained in our articles [3, 4].

We remind that there are various reasons to build models beyond the Standard Model. By introducing new fields or new interactions between fields, it may be possible to explain phenomena such as the existence of dark matter, the origin of the matter anti-matter asymmetry or the hierarchy problem. A lot of such models have been proposed during the last few decades and it is not straightforward to know which ones would provide the best description of nature. It is therefore important to find as many ways as possible to constrain them and test them from experimental evidences. Complementary to accelerator investigations such as those with the LHC, GWs from PTs can be considered as one of these tools. As emphasized in Section 1.2.4, the electroweak and QCD PTs are likely to be crossovers in the SM such that no production of GWs is expected during these events. On the other hand, several BSM extensions do predict one or the other of these transitions to generate GWs with interesting experimental signatures. Typically, first-order PTs produce a stochastic background of GWs from the collision of true vacuum bubbles and their interaction with the surrounding hot plasma of elementary particles [187–191].

This thesis considers two specific BSM scenarios that are described in the next Section. We present their main phenomenological properties as well as their relevance to solve existing problems of the SM. We shall then see that they give rise to very interesting (and different) types of PTs. We also emphasize that the general dynamics of the PTs we will discuss in Section 5.2 are not limited to these models and that they could also take place in other situations.

5.1 Beyond the Standard Model physics

5.1.1 A non-linearly realized electroweak gauge group

The idea of the first model we consider is to change the description of the electroweak sector of the SM. We explained in Section 3.1.2 how fermions and gauge bosons can get their masses through the Higgs mechanism and spontaneous symmetry breaking of the gauge group $SU_L(2) \times U_Y(1)$. There exist however other alternatives to this scenario. Here we present a theory where the electroweak gauge group is non-linearly realized and the Higgs boson does not need to be a singlet under this group anymore. Callan, Coleman, Wess and Zumino (CCWZ) formalized the idea of working with non-linear realizations of groups instead of usual linear representations in [192, 193]. This formalism has then be applied to the electroweak group by several authors as an alternative to the SM [194–196]. We give a brief overview of the approach and invite the reader to look either at the original articles or to the Section 1.2.1 of [197] for more details.

Non-linear realization

In the SM, electroweak gauge bosons acquire a mass from the modes that would be Goldstone bosons if the symmetry where global rather than local. These modes are contain in three of the four real components of the Higgs doublet. In the CCWZ approach however, we consider instead that the Goldstone modes are those which parametrize the coset group $G_c = SU_L(2) \times U_Y(1)/U_Q(1) \cong SU(2)$. We write these such three fields $\pi^i(x)$ and we embed them in a matrix as follows:

$$\Sigma(x) = e^{\frac{i}{v}\pi^i(\sigma^i - \mathbb{I}\delta^{i3})} \qquad D_\mu\Sigma = \partial_\mu\Sigma + ig_2\frac{\sigma^i}{2}W^i_\mu\Sigma + ig_1\Sigma\frac{\sigma^3}{2}B^i_\mu \tag{5.1}$$

where we recognize the Pauli matrices σ^i for $i \in \{1,2,3\}$. The CCWZ prescription then tells us that such fields transform according to

$$\Sigma(x) \mapsto e^{-i\beta}e^{-i\alpha^i\frac{\sigma^i}{2}}\Sigma(x)e^{\frac{\beta'}{2}(\mathbb{I}-\sigma^3)} \tag{5.2}$$

where we have acted on the left with an element of $SU_L(2) \times U_Y(1)$ and on the right with the inverse of an element of $U(1)_Q$ (whose unbroken generator is $\frac{1}{2}(Y + \sigma^3)$).

If we were now trying to build a Lagrangian describing the low energy of the electroweak sector, it would typically contain a term of the form $\frac{v^2}{4}\,\mathrm{Tr}\left(D_\mu\Sigma D^\mu\Sigma^\dagger\right)$. By expanding around the vacuum $\Sigma = \mathbb{I}$ we would recover the usual mass terms for the $W^\pm$ and Z bosons, and this without the need of a Higgs field. It means that the resonance $h(125)$ observed at the LHC [6, 7] is not required to be a doublet under the electroweak gauge group. It is particularly interesting to consider the case where this resonance is associated to a singlet under the SM gauge group. In this case, interactions that were forbidden in the SM can now be present. Although several of these interactions are severely constrained by electroweak precision measurements or flavour physics, some of them are still compatible with data and can give rise to interesting BSM phenomena as we will illustrate below. We note that this approach is rather economic as it does not postulate the existence of new particles.

Higgs potential with a cubic coupling

Motivated by our present discussion, let us consider the Higgs boson as a singlet $\rho(x) \sim (\mathbf{1},\mathbf{1})_0$ under the SM gauge group. The SM Higgs doublet can then be identified as

$$H(x) = \frac{\rho(x)}{\sqrt{2}} e^{\frac{i}{2}\pi^i(x)(\sigma^i - \mathbb{I}\delta^{i3})} \begin{pmatrix} 0 \\ 1 \end{pmatrix}, \qquad i \in \{1,2,3\} \tag{5.3}$$

in terms of the would-be Goldstone modes $\pi^i(x)$ we introduced above. The physical Higgs h then corresponds to the fluctuation of ρ around the electroweak vacuum expectation value $v = 246$ GeV such that $\rho = v + h$. Among the various BSM interactions we can build from ρ, cubic Higgs-Higgs and CP violating Higgs-Top couplings are particularly interesting. As described in [196], they can indeed drive a strong first-order PT and accommodate the observed baryon asymmetry through electroweak baryogenesis. It was further shown in [198] that the cubic Higgs coupling alone is sufficient to account for a first-order PT and to produce a stochastic background of GWs sizable enough to be observed by LISA. As the continuation of these two articles, we will show in Section 5.2.1 that there is a range of values of this cubic coupling for which the electroweak PT admits a very interesting dynamics.

We now give the details of our model of interest. All the SM configurations are assumed, with the exception of the Higgs potential which now admits an anomalous cubic coupling:

$$V^{(0)}(\rho) = -\frac{\mu^2}{2}\rho^2 + \frac{\kappa}{3}\rho^3 + \frac{\lambda}{4}\rho^4. \tag{5.4}$$

This tree-level potential explicitly depends on the three parameters μ, κ and λ. However, the relations $\frac{dV}{d\rho}\Big|_{\rho=v} = 0$ and $\frac{d^2V}{d\rho^2}\Big|_{\rho=v} = m_h^2 \approx (125\,\text{GeV})^2$ allow the model to be controlled by a single free parameter, which is chosen to be κ. Taking the example at tree level, the above relations can be solved analytically giving:

$$\mu^2 = \frac{1}{2}\left(m_h^2 + v\kappa\right), \qquad \lambda = \frac{1}{2v^2}\left(m_h^2 - v\kappa\right). \tag{5.5}$$

The same process can be used to express μ and λ as a function of κ consistently at each order of perturbation theory, at least numerically. In this thesis, we shall solve the relations at one-loop level. In order to describe the behaviour of the Higgs field in the early Universe, we then require the one-loop finite temperature potential. As described in Section 3.2.2, it reads:

$$V(\rho,T) = V^{(0)}(\rho) + V^{(1)}_{CW}(\rho) + V^{(1)}(\rho,T) + V_{Daisy}(\rho,T), \tag{5.6}$$

where $V^{(0)}$ is the potential (5.4) and the other terms are given in Appendix A.1.

For each value of κ, the potential (5.6) can be numerically computed and the thermal behaviour of the Higgs field can be analyzed. In particular we will be able to predict the dynamics of the electroweak PT in Section 5.2.1 and the associated production of GWs in Section 6.2.1. To be consistent, it is important to note that constraints on κ can be extracted from collider experiments. The typical probe is the trilinear coupling $\lambda_3 = d^3V/d\rho^3 = 6\lambda v + 2\kappa$ which is actually non-vanishing in the SM: $\lambda_3^{\text{SM}} = 3m_h^2/v$. However, current constraints on deviations from λ_3^{SM} are weak and are expected to be only at the order of $25\% - 50\%$ accuracy at the high-luminosity LHC [199].

5.1.2 The Standard Model with hidden scale invariance

The second BSM theory we consider is based on the concept of scale invariance. Scale invariance provides an attractive framework to address the problems related to the origin of mass and to the hierarchy of mass scales. In this framework, quantum fluctuations result in an overall mass scale via dimensional transmutation, while dimensionless couplings are responsible for generating mass hierarchies. The dimensionless couplings in the low-energy sector of the theory are only logarithmically sensitive to the high-energy sector and can be naturally small in the technical sense [200–202]. If high-energy and low-energy sectors interact via feeble interactions, the breaking of scale invariance in the higher energy sector would proliferate in the low-energy sector resulting in a stable mass hierarchy between the two (see e.g. [203, 204]). Such a scenario can be even better motivated from the fact that conformal invariance is indeed an essential symmetry in string theory that is believed to provide a consistent ultraviolet completion of all fundamental interactions including gravity.

Higgs-dilaton model

A minimal extension of the SM which incorporates spontaneously broken scale invariance as a low energy effective theory has been recently proposed in [205]. In this approach, non-linearly realized scale invariance is introduced by promoting physical mass parameters (including the ultraviolet cut-off Λ) to a dynamical dilaton field. The dilaton field develops a large vev via the quantum mechanical mechanism of dimensional transmutation. The dilaton-Higgs interactions then trigger the electroweak symmetry breaking and generate a stable hierarchy between the Higgs and dilaton vevs. As a result of the spontaneous breaking of anomalous scale symmetry, the dilaton develops a mass at two loop level, which can be as small as $\sim 10^{-8}$ eV (for a dilaton vev of the order the Planck scale, $\sim M_P \sim 10^{19}$ GeV). In addition, the Higgs-dilaton potential displays a nearly flat direction. Before we show how to derive such results, we emphasize that the formalism of hidden scale invariance is rather generic and can be applied to other effective field theory models, with essentially the same predictions regarding the light dilaton and the Higgs-dilaton potential [206].

Let us now be specific and consider the SM as an effective low energy theory valid up to an energy scale Λ, as introduced in [205]. In the Wilsonian approach, the ultraviolet cut-off Λ is a physical parameter that encapsulates physics (e.g. massive fields) which we are agnostic of. The Higgs potential defined at this ultraviolet scale reads:

$$V(H^\dagger H) = V_0(\Lambda) + \lambda(\Lambda)\left[H^\dagger H - v^2(\Lambda)\right]^2 + ..., \tag{5.7}$$

where H is the electroweak doublet Higgs field and V_0 is a field-independent constant (bare cosmological constant parameter). The ellipsis stands for all possible dimension > 4 (irrelevant), gauge invariant operators, $\left(H^\dagger H\right)^n$, $n = 3, 4....$ The other bare parameters are the dimensionless couplings $\lambda(\Lambda)$ and a mass dimension parameter $v(\Lambda)$, namely the bare Higgs vev. In principle, this potential has an infinite number of nonrenormalizable operators and Λ-dependent parameters must fully encode the physics beyond the SM. In practice, however, we usually deal with a truncated theory, which is valid in the low-energy domain only.

We assume now that a fundamental theory maintains spontaneously broken scale invariance, such that all mass parameters have a common origin. To make this symmetry manifest in our effective theory, we promote all mass parameters to a

dynamical field χ, the dilaton, as follows:

$$\Lambda \to \Lambda \frac{\chi}{f_\chi} \equiv \alpha\chi, \;\; v^2(\Lambda) \to \frac{v^2(\alpha\chi)}{f_\chi^2}\chi^2 \equiv \frac{\xi(\alpha\chi)}{2}\chi^2, \;\; V_0(\Lambda) \to \frac{V_0(\alpha\chi)}{f_\chi^4}\chi^4 \equiv \frac{\rho(\alpha\chi)}{4}\chi^4 \,, \tag{5.8}$$

where f_χ is the dilaton decay constant. Then, Equation (5.7) turns into the Higgs-dilaton potential

$$V(H^\dagger H, \chi) = \lambda(\alpha\chi)\left[H^\dagger H - \frac{\xi(\alpha\chi)}{2}\chi^2\right]^2 + \frac{\rho(\alpha\chi)}{4}\chi^4 \,. \tag{5.9}$$

Quantum scale anomaly

The potential (5.9) is manifestly scale invariant up to the quantum scale anomaly, which is engraved in the χ-dependence of the dimensionless couplings[1]. Indeed, the Taylor expansion around an arbitrary fixed scale μ reads:

$$\lambda^{(i)}(\alpha\chi) = \lambda^{(i)}(\mu) + \beta_{\lambda^{(i)}}(\mu)\ln(\alpha\chi/\mu) + \beta'_{\lambda^{(i)}}(\mu)\ln^2(\alpha\chi/\mu) + ..., \tag{5.10}$$

where $\lambda^{(i)} \equiv (\lambda, \xi, \rho)$ and

$$\beta_{\lambda^{(i)}}(\mu) = \left.\frac{\partial\lambda^{(i)}}{\partial\ln\chi}\right|_{\alpha\chi=\mu} , \tag{5.11}$$

are the renormalization group (RG) β-functions for the respective coupling $\lambda^{(i)}$ defined at a scale μ, while $\beta'_{\lambda^{(i)}}(\mu) = \left.\frac{\partial^2\lambda^{(i)}}{\partial(\ln\chi)^2}\right|_{\alpha\chi=\mu}$, etc. For convenience, we fix the renormalization scale at the cut-off scale Λ, which is defined through the dilaton vev as $\langle\chi\rangle \equiv v_\chi$, i.e. $\mu = \Lambda = \alpha v_\chi$. Note that while the lowest order contribution in β-functions is one-loop, i.e. $\sim \mathcal{O}(\hbar)$, the n-th derivative of β is nth order in the perturbative loop expansion, $\sim \mathcal{O}(\hbar^n)$.

The extremum condition $\left.\frac{dV}{d\chi}\right|_{H=\langle H\rangle,\chi=\langle\chi\rangle} = 0$ together with the phenomenological constraint on vacuum energy $V(v, v_\chi) = 0$, lead to the following relations:

$$\rho(\Lambda) = 0 \,, \;\; \beta_\rho(\Lambda) = 0 \,. \tag{5.12}$$

One of the above relations can be used to define the dilaton vev (dimensional transmutation) and another represents the tuning of the cosmological constant. The second extremum condition $\left.\frac{dV}{dH}\right|_{H=\langle H\rangle,\chi=\langle\chi\rangle} = 0$ simply sets the hierarchy of vevs:

$$\xi(\Lambda) = \frac{v^2}{v_\chi^2} \,. \tag{5.13}$$

In the classical limit when all the quantum corrections are zero, i.e., $\beta_{\lambda^{(i)}} = \beta'_{\lambda^{(i)}} = ... = 0$, the above vacuum configuration represents a flat direction of the Higgs-dilaton potential (5.9). The existence of this flat direction is, of course, the direct consequence of the assumed classical scale invariance. In this approximation, the dilaton is the massless Goldstone boson of spontaneously broken scale invariance. The flat direction is lifted by quantum effects and, as we will see later on, by thermal

[1] In this we differ substantially from the so-called quantum scale-invariant SM [207]. In their approach, the SM is extrapolated to an arbitrary high energy scale and regularized by invoking dilaton-dependent renormalization scale, $\mu = \mu(\chi)$

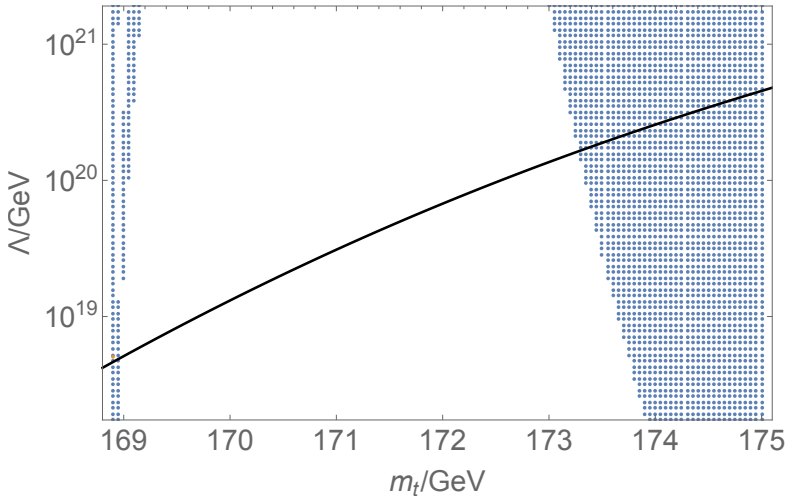

FIGURE 5.1: Plot of the allowed range of parameters (shaded region) with $m_\chi^2(v) > 0$, i.e., the electroweak vacuum being a minimum. The solid line displays the cut-off scale Λ as function of the top-quark mass m_t for which the conditions in Equation (5.12) are satisfied.

effects in the early universe. Note, however, that the dilaton develops a (running) mass in our scenario at two-loop level [205] (see also [208]),

$$m_\chi^2 \simeq \frac{\beta'_\rho(\Lambda)}{4\xi(\Lambda)} v^2 \,, \tag{5.14}$$

while the tree-level Higgs mass is given to a high accuracy by the standard formula: $m_h^2 \simeq 2\lambda(\Lambda)v^2$. Note that $\beta'_\rho \propto \xi^2$ and hence the dilaton is a very light particle, $m_\chi/m_h \sim \sqrt{\xi}$.

Phenomenology

To verify whether the above scalar field configurations correspond to a local minimum of the potential one must evaluate the running masses down to low energy scales. The relations in Equation (5.12) provide non-trivial constraints here. In Figure 5.1, we have presented our analysis based on solutions of the relevant (one-loop) RG equations (see the appendix section in Reference [205] for more details). The shaded region in the $\Lambda - m_t$ plane corresponds to a positive dilaton mass squared (minimum of the potential) and the solid curve shows the cut-off scale Λ as a function of the top-quark mass m_t for which the conditions in Equation (5.12) are satisfied. Hence, within the given approximation, we find that the model is phenomenologically viable for $m_t \lesssim 169$ GeV and $m_t \gtrsim 173$ GeV with the cut-off scale accordingly predicted to be $\Lambda \lesssim 10^{19}$ GeV and $\gtrsim 10^{21}$ GeV respectively. We note that the upper values are within the allowed experimental range for the top quark mass, $m_t = 173.34 \pm 0.27(\text{stat}) \pm 0.71(\text{syst})$ GeV [209]. Assuming $v_\chi \approx \Lambda$ ($\alpha \approx 1$), the dilaton mass for the Planck scale cut-off is predicted to be $m_\chi \approx 10^{-8}$ eV. This prediction for the ultraviolet scale Λ, however, should be taken as indicative only. Indeed, besides high-loop corrections, the actual matching conditions (threshold effects) between low energy couplings and couplings in the ultraviolet completion of the SM may affect the above predictions significantly (see, e.g., examples in Reference [210]). However, these details of the evaluation of coupling constants at high energy scales

are not essential for the purpose of the study of the electroweak PT that we will conduct in Section 5.2.2. In what follows we will always assume $\Lambda = M_P \approx 10^{19}$ GeV in our numerical calculations.

We mention that the most stringent bound on such a light dilaton ($m_\chi \sim 10^{-8}\, eV$) comes from the constraints on long-ranged Yukawa-like fifth force. According to experiments on violation of the gravitational inverse square law, the strength of this force is typically quoted to be at least two orders of magnitude smaller than the strength of the corresponding gravitational interaction [211]. This constraint can be satisfied by adjusting the dilaton-Ricci scalar coupling [212], which we will not discuss explicitly here.

Another important observation is that the potential energy densities evaluated at the origin and at the electroweak minimum are equal, $V(0,0) \simeq V(v, v_\chi)$. This is readily seen for the potential evaluated at the cut-off scale Λ: see Equations (5.9) and (5.12)-(5.13). Then, since the vacuum energy density does not depend on the renormalization scale [213], the trivial and electroweak vacuum states must be degenerate at any given low energy scale. This will have an important consequence for our subsequent study of cosmological PT in this model.

5.2 On the dynamics of phase transitions

5.2.1 Prolonged electroweak phase transition

We now study a special case of PTs that can occur in the model of Section 5.1.1 based on the non-linear realization of the electroweak gauge group. As show in Equation (5.4), the Higgs potential admits a cubic term at tree-level. In other words, a barrier exists between the two different phases of the Higgs field from the electroweak scale down to zero temperature. Since the barrier will never vanish, a first-order PT can occur a priori at arbitrarily low T, unless the Higgs field stays trapped in its metastable state. We therefore expect to predict PTs with a significant amount of supercooling.

Interestingly, we shall see that this model exhibits a range of parameters for which the PT is long-lasting, meaning that most of the true vacuum bubbles are nucleated around $T_n \sim 50$ GeV but collide well below the electroweak scale, as low as $T_p \sim [0.1, 10]$ GeV. Precise results will depend on the exact equation of state of the Universe which is complicated to compute in this context. The most important point to mention is that vacuum energy is expected to dominate over radiation energy below a given temperature, potentially leading to an inflationary stage. However, we shall argue that such a scenario is unlikely to happen in this model as a significant amount of bubbles are produced early enough (during the radiation dominated era) and subsequently act as a source of inhomogeneity which prevents inflation from occurring. Therefore, this scenario differs from previous studies of a certain class of scale-invariant models, such as [214–216], in which the nucleation of true vacuum bubbles occurs at very low temperatures, namely after inflation started. To avoid any confusion, we stress that the scale-invariant model we introduced in Section 5.1.2 will give rise to an even more different PT dynamics. This should convince us that the cosmological history of the Universe can indeed be substantially sensitive to new physics.

Decay probability

We gave a sketch of how a usual PT occurs in Section 3.2.2 in terms of the critical, nucleation and percolation temperatures. We now show how to explicitly compute such quantities starting from the one-loop finite temperature $V(\rho, T)$ given by Equation (5.6). We remind that it is completely specified by the value of the cubic coupling κ which is the only free parameter of the model.

The first process to describe is the tunnelling of the Higgs field between the two vacua. It is characterized by the decay probability Γ per unit time per unit volume. Quantum fluctuations drive this process at zero temperature [217, 218] while thermal fluctuations dominate at finite T [219, 220]. Therefore, Γ is expressed as a function of the temperature of the Universe and can be written in the semiclassical approximation as follows:

$$\Gamma(T) \approx A(T) e^{-S(T)} \tag{5.15}$$

where $A(T)$ is a prefactor of mass dimension 4 and $S(T)$ is the Euclidean action $S[\rho, T]$ evaluated along the bounce trajectory ρ_B. In full generality, the Euclidean action is the functional over the Higgs field ρ defined as [221]:

$$S[\rho, T] = 4\pi \int_0^\beta d\tau \int_0^\infty dr\, r^2 \left[\frac{1}{2} \left(\frac{d\rho}{d\tau} \right)^2 + \frac{1}{2} \left(\frac{d\rho}{dr} \right)^2 + \tilde{\mathcal{F}}(\rho, T) \right], \tag{5.16}$$

where $\tau = -it$ is the Euclidean time, $\beta = \frac{1}{T}$ and $\tilde{\mathcal{F}}(\rho, T) := V(\rho, T) - V\left(v_T^{(+)}, T\right)$ is the free energy density normalised according to its value in the unbroken phase. The bounce trajectory $\rho_B(\tau, r)$ is the solution which minimises the Euclidean action and thus satisfies the following equation of motion:

$$\frac{\partial^2 \rho}{\partial \tau^2} + \frac{\partial^2 \rho}{\partial r^2} + \frac{2}{r} \frac{\partial \rho}{\partial r} - \frac{\partial \tilde{\mathcal{F}}}{\partial \rho}(\rho, T) = 0, \tag{5.17}$$

with the boundary conditions

$$\left. \frac{\partial \rho}{\partial \tau} \right|_{\tau = 0, \pm\beta/2} = 0, \qquad \left. \frac{\partial \rho}{\partial r} \right|_{r=0} = 0, \qquad \lim_{r \to \infty} \rho(r) = v_T^{(+)}. \tag{5.18}$$

The specific shape of the bounce $\rho(\tau, r)$ depends on the temperature [220]. At zero or low temperature, it reduces to an $O(4)$ symmetric solution $\rho(\tilde{r})$ with $\tilde{r} = \sqrt{\tau^2 + r^2}$, while at high temperature it is given by an $O(3)$-symmetric and time-independent solution $\rho(r)$. The temperature scale that allows us to distinguish between these regimes is given by the mass scale of the problem or equivalently by the size R_0 of the $O(4)$ symmetric bubble at $T = 0$. In both the limits $T \ll R_0^{-1}$ and $T \gg R_0^{-1}$, the action (5.16) simplifies as follows:

$$S[\rho, T] \approx \begin{cases} S_4[\rho, T] & = 2\pi^2 \displaystyle\int_0^\infty d\tilde{r}\, \tilde{r}^3 \left[\frac{1}{2} \left(\frac{d\rho}{d\tilde{r}} \right)^2 + \tilde{\mathcal{F}}(\rho, T) \right], T \ll R_0^{-1} \\ \frac{1}{T} S_3[\rho, T] = & \dfrac{4\pi}{T} \displaystyle\int_0^\infty dr\, r^2 \left[\frac{1}{2} \left(\frac{d\rho}{dr} \right)^2 + \tilde{\mathcal{F}}(\rho, T) \right], T \gg R_0^{-1} \end{cases} \tag{5.19}$$

In these limits, the equations of motion for the bounce become:

$$\frac{d^2\rho}{dr^2} + \frac{\alpha}{r}\frac{d\rho}{dr} - \frac{\partial\tilde{\mathcal{F}}}{\partial\rho}(\rho, T) = 0, \qquad \left.\frac{d\rho}{dr}\right|_{r=0} = 0, \qquad \lim_{r\to\infty}\rho(r) = v_T^{(+)} \tag{5.20}$$

with $\alpha = 2$ for $T \gg R_0^{-1}$ and $\alpha = 3$ with r replaced by $\tilde{r}$ for $T \ll R_0^{-1}$. The prefactor $A(T)$ in equation (5.15) also admits different forms in the low and high temperature limits:

$$A(T) \approx \begin{cases} \dfrac{1}{R_0^4}\left(\dfrac{S_4(T)}{2\pi}\right)^2 & , T \ll R_0^{-1} \\ T^4\left(\dfrac{S_3(T)}{2\pi T}\right)^{3/2} & , T \gg R_0^{-1} \end{cases} \tag{5.21}$$

The difference in these expressions comes from the fact that the $O(4)$-symmetric bounce has 4 zero-modes contributing a factor $[S/(2\pi)]^{1/2}$ each, while the $O(3)$-symmetric solution only has 3 zero-modes.

In the case of a rapid PT occurring around the electroweak scale $T_{EW} \sim 100$ GeV, the high-temperature formula provides a good approximation. However, it is not clear a priori how T_p and R_0 will scale if the transition occurs with a significant amount of supercooling. In particular if $T_p \lesssim R_0^{-1}$, approximating S by S_3/T might not be accurate anymore, requiring the use of the exact expression (5.16) (or S_4 at even lower temperature). For this reason, we compare how each of the three different actions $S(T)$, $S_4(T)$ and $S_3(T)$ behaves as a function of the temperature. To do this, the bounce equations of motion must be solved numerically. In the low and high temperature regime, (5.20) is an ODE and can be integrated using the shooting method[2]. On the other hand, the space-time dependent equation (5.17) is a PDE and thus more difficult to address. Following [221, 222], we discretize space-time over a lattice. The PDE and the boundary conditions reduce then to a set of non-linear algebraic equations located at each point of the lattice. This set of equations is solved according to the Newton's method: starting from a guess solution we build a new solution which minimises the error and iterate until the error becomes small enough. For this method to converge, the choice of the guess is important. In our case, we use the zero-temperature $O(4)$ solution, found from the shooting method, as a guess to solve (5.17) at $T = 0 + \Delta T$. This solution is then used to solve the problem at $T^{(n+1)} = T^{(n)} + \Delta T$ recursively. The numerical solutions will be presented below.

Bubble dynamics and energy

Given the nucleation probability $\Gamma(T)$ discussed above, we can now describe the dynamics of a first-order PT. We apply the general formalism provided in [223]. We consider an expanding Universe with scale factor $a(t)$ and Hubble rate $H = \dot{a}/a$. The probability $p(t)$ for a given point of spacetime to be in the symmetric phase at

[2]Note that there is no bounce solution when the two vacua are exactly degenerate at T_c and that tunnelling occurs only for $T < T_c$. Numerically, the shooting method provides solutions only for a wide enough energy separation between the vacua, namely for $T \leq T_\star < T_c$. Although tunnelling solutions can exist for $T_\star < T < T_c$ and be estimated through the thin-wall approximation, they are negligible for the PT as Γ is more and more suppressed as the vacua are more and more degenerate (see e.g. Section IV in [217]).

time t is then given by [223]:

$$p(t) = \exp\left[-\underbrace{\frac{4\pi}{3}\int_{t_c}^{t} dt'\Gamma(t')a^3(t')r^3(t,t')}_{:=\mathcal{I}(t)}\right], \tag{5.22}$$

where $\mathcal{I}(t)$ corresponds to the volume occupied by the true vacuum bubbles[3]. Indeed, bubbles which have nucleated at $t' < t$ with probability $\Gamma(t')$ would have then grown until t reaching a (coordinate) radius $r(t,t')$ given by:

$$r(t,t') = \int_{t'}^{t} dt'' \frac{v(t'')}{a(t'')}, \tag{5.23}$$

with $v(t)$ being the bubble wall velocity. In the previous equation, we have neglected the initial radius of the bubble which rapidly becomes negligible compared to the expanding size.

The condition that the PT completes can be translated to the condition that $p(t) \to 0$ for $t > t_c$, where we remind that t_c is the time corresponding to the critical temperature T_c. As we are ultimately interested in the production of gravitational waves from bubble collisions, we are looking for the transition time corresponding to the period of maximum bubble collisions. This period can be estimated by the percolation time t_p [224, 225]. According to numerical simulations performed with spheres of equal size, percolation occurs when approximately 29% of space is covered by bubbles [226]. As suggested by [224, 225], we thus define t_p from the condition $p(t_p) \approx 0.7$.

Knowing the collision time, we can then look for the distribution of number of bubbles at that time as a function of their size. From (5.23), a bubble formed at time t_R will have a physical size $R(t,t_R) = a(t)r(t,t_R)$ at time t. The number density of such bubbles is then given by [223]:

$$\frac{dN}{dR}(t,t_R) = \Gamma(t_R)\left(\frac{a(t_R)}{a(t)}\right)^4 \frac{p(t_R)}{v(t_R)}. \tag{5.24}$$

For $t = t_p$, the peak of this distribution gives us the size $\bar{R}$ of the majority of the bubbles which are colliding. Equivalently, it also provides the time $t_{\bar{R}}$ when most of these bubbles have been produced. We call this moment the nucleation time t_n (rather than $t_{\bar{R}}$) and it can be explicitly computed via:

$$\frac{d}{dt_R}\left(\frac{dN}{dR}(t_p,t_R)\right)\bigg|_{t_R=t_n} = 0. \tag{5.25}$$

As we shall see in Section 6.1, $\bar{R} := R(t_p,t_n)$ is the key parameter to determine the peak frequency of the GW spectrum produced by bubble collisions.

Another important parameter, related to the amplitude of the GW spectrum, is the kinetic energy stored in the bubble walls. This kinetic energy comes from the vacuum energy released during the transition from the unbroken phase to the broken phase of the scalar field ρ. In order to derive this quantity, we briefly remind the basic thermodynamic properties of this field. As described above, its

[3]Note that the exponentiation of $\mathcal{I}$ in (5.22) corrects the fact that regions with overlapping bubbles have been counted twice in $\mathcal{I}$.

free energy is given by the effective potential, $\mathcal{F}(\rho, T) = V(\rho, T)$, and this allows us to define the pressure $p = -\mathcal{F}$ and the energy density $\epsilon(\rho, T) = \mathcal{F} - T\frac{d\mathcal{F}}{dT}$. The released vacuum energy density is associated with the following latent heat: $\tilde{\epsilon}(T) = \epsilon(v_T^{(+)}, T) - \epsilon(v_T^{(-)}, T)$. During the transition, this latent heat is converted into the formation of the bubbles (surface energy and kinetic energy of the walls) and into the reheating and fluid motion of the plasma. Following the notation of [227], we write κ_ρ the fraction of energy which goes into the kinetic energy of the bubbles (i.e. the scalar field ρ). As a result, the kinetic energy of a bubble is given by $\tilde{\epsilon}$, the portion of space it has converted and κ_ρ. For bubbles produced at t_n, their kinetic energy at the percolation time t_p is then

$$E_{\text{kin}} = 4\pi\kappa_\rho \int_{t_n}^{t_p} dt \frac{dR}{dt}(t, t_n) R^2(t, t_n)\tilde{\epsilon}(t) \tag{5.26}$$

where we have taken into account the fact that the latent heat varies with time (namely temperature). In the case of a short PT or a slowly varying $\tilde{\epsilon}$, the above equation reduces to $E_{\text{kin}} = \frac{4\pi}{3}\kappa_\rho \bar{R}^3\tilde{\epsilon}$ as we should expect.

In order to explicitly compute $\bar{R}$ and E_{kin}, we need to determine the bubble growth which depends on the velocity $v(t)$ and the scale factor $a(t)$ according to Equation (5.23). We discuss the details of the evolution of the background Universe below. Regarding the velocity, it is usually a difficult task to calculate precisely $v(t)$ as its depends on the interaction between the bubble wall and the plasma. However, it has been shown that for PTs with a sufficient amount of supercooling the produced bubbles typically reach velocities near the speed of light [227–229].[4] We shall then assume $v \sim 1$.

Equation of state

In order to carefully describe the dynamics of a long-lasting PT, the expansion of the Universe cannot be neglected and this requires to determine the scale factor $a(t)$. In the same way, it is also important to know how the temperature of the Universe, $T(t)$, evolves during the process. Both these quantities depend on the equation of state (EOS) of the different components of the Universe and which of them dominate. We discussed in Section 3.2.1 how the scale factor behaves when the Universe is dominated by a single component with EOS $p = w\epsilon$. It is given by $a(t) \propto t^\gamma$ with $\gamma = \frac{2}{3(w+1)}$ ($w \neq -1$). For $w < -1/3$ ($\gamma > 1$), it follows that the Universe undergoes an accelerated expansion (power-law inflation). In the same way, the case $w = -1$ (vacuum domination) also leads to an accelerating phase with $a(t) \propto e^{Ht}$ (exponential inflation).

In the general scenario of electroweak PT, bubbles nucleate near the electroweak scale, $T_{EW} \sim 100$ GeV, and percolate rapidly. During such a process, the Universe is radiation dominated with

$$p = \frac{1}{3}\epsilon, \qquad a(t) \propto t^{1/2}, \qquad t = \underbrace{\left(\frac{45M_p^2}{16\pi^3 g_\star}\right)^{1/2}}_{:=\zeta} \frac{1}{T^2}, \tag{5.27}$$

[4] Before the recent article [229] appeared, it was also usual to assume $\kappa_\rho \sim 1$ for supercooled PTs. This assumption now seems less justified and we shall comment on it when discussing the production of GWs in Section 6.1.

with $M_P \sim 1.22 \times 10^{19}$ GeV the Planck mass and $g_\star \sim 100$ the effective number of relativistic degrees of freedom in the symmetric phase. However, this equation of state might not be valid in the case of strong supercooling or for a prolonged transition. The reason comes from the fact that as the Universe cools down, the vacuum energy density of the scalar field which remains in the unbroken phase starts dominating over the radiation energy density, $\epsilon_{\rm rad} = \pi^2 g_\star T^4/30$, possibly leading to the phase of inflation described above.

In order to have a general understanding of transitions with such a behaviour, we introduce the time t_e of radiation-vacuum equality satisfying $\epsilon_{\rm vac}(t_e) = \epsilon_{\rm rad}(t_e)$.[5] In the standard case, $t_n \lesssim t_p \ll t_e$, and the vacuum energy is released into the bubbles before it could dominate. Then, scenarios with an inflationary background have been considered for some classes of scale-invariant models in [214–216]. In such cases, most of the bubbles nucleate after radiation-vacuum equality, namely $t_e < t_n \lesssim t_p$. On the other hand, the process we want to describe here (prolonged PT) is different from the two previous ones in the sense that $t_n < t_e < t_p$, namely bubbles are produced before vacuum energy would dominate and percolation requires a long time to complete. We now address this type of transition in more detail.

The large separation between nucleation and percolation comes from a decay probability Γ weaker than in the standard case, such that less bubbles are produced per unit volume and more time is required for them to collide. Let us clarify this reasoning by assuming that all bubbles are nucleated at t_n such that $\Gamma(t) = \bar{\Gamma}(t_n)\delta(t - t_n)$. The exponent in Equation (5.22) becomes $\mathcal{I}(t) = \frac{4\pi}{3}\bar{\Gamma}(t_n)a^3(t_n)r^3(t,t_n)$ and this clearly shows how a larger radius (i.e. longer time) compensates for a weaker nucleation probability. However, this last expression also indicates than the transition might never complete if the Universe is in accelerating expansion, since in such a case $r(t,t_n)$ is bounded[6] when $t \to \infty$. In other words, there is the possibility for the bubbles to not grow fast enough in order to reach each other and to collide.

However, we now argue that such a scenario (with no percolation) is unlikely to occur as long as enough bubbles are produced during the radiation dominated period, namely before t_e. Indeed, as bubbles nucleate, vacuum energy is converted into kinetic energy of the wall motion such that the energy budget at the time t_e is not simply dominated by vacuum energy density even if the bubbles have not yet collided. Actually, the bubbles are acting as inhomogeneity in the background of the expanding space-time and this renders difficult to naively estimate what would be the corresponding dynamics of the Universe. According to several studies including numerical simulations [230–232] (see [233] for a recent review), it has been shown that small-field inflation is very unlikely to proceed with inhomogeneous initial conditions. We shall then assume in the following part of our study that for a sufficient number of bubbles produced at t_n, the Universe expansion will not accelerate around t_e and that percolation does occur at a given time $t_p > t_e$.

An exact description of the evolution (namely a precise value of γ) would require numerical simulations which are beyond the scope of this study. As we expect no acceleration because of the previous argument, we have $\gamma < 1$ and so we assume for simplicity that the Universe remains radiation dominated during the entire process ($\gamma = 1/2$). Deviation of the value of γ in the range $[0,1]$ would change the estimation

[5] For simplicity, we assume here that the Universe is dominated by a single component at a time and that the transition is sharp between radiation and vacuum domination.

[6] This can easily be seen explicitly. Assuming $a(t) \propto t^{1/2}$ for $t < t_e$ and $a(t) \propto t^\gamma$ for $t > t_e$, Equation (5.23) (with $v \sim 1$) gives $r(t,t_n) \propto 2(t_e^{1/2} - t_n^{1/2}) + t_e^{\gamma-1/2}(t^{1-\gamma} - t_e^{1-\gamma})/(1-\gamma)$, such that when $t \to \infty$ $r(t,t_n) \to +\infty$ if $\gamma < 1$ and $r(t,t_n) \to (2 + 1/(\gamma-1))t_e^{1/2} - 2t_n^{1/2}$ if $\gamma > 1$.

of the parameters describing the transition, in particular $\bar{R}$ and $E_{\rm kin}$, but not the qualitative picture. Moreover, we expect such a deviation to be compensated by a shift in the value of the initial conditions describing the underlying particle physics model (the parameter κ in Equation (5.4) in our case).

Under the aforementioned assumptions ($\gamma \sim 1/2$, $v \sim 1$) and using Equation (5.27), we can simplify Equations (5.22), (5.23) and (5.26) and write them in terms of temperature rather than time. Regarding the evolution of the temperature, we also recall that for a strong transition the dominant part of the vacuum energy is transformed into kinetic energy of the bubble walls meaning that we can neglect heating of the plasma. In the same way, the kinetic energy is subsequently transformed into GW energy through bubble collisions such that again heating is negligible. We eventually obtain the following key equations:

$$\begin{aligned} R(T,T') &= \frac{2\zeta}{T}\left(\frac{1}{T}-\frac{1}{T'}\right) \\ p(T) &= \exp\left[-\frac{64\pi}{3}\zeta^4\int_T^{T_c} dT' \frac{\Gamma(T')}{T'^6}\left(\frac{1}{T}-\frac{1}{T'}\right)^3\right] \\ E_{\rm kin} &= 32\pi\,\kappa_\rho\,\zeta^3\int_{T_p}^{T_n} dT \frac{1}{T^3}\left(2-\frac{T}{T_n}\right)\left(\frac{1}{T^2}-\frac{1}{TT_n}\right)^2 \tilde{\epsilon}(T)\,, \end{aligned} \tag{5.28}$$

where we remind that ζ has been defined in Equation (5.27). It is now possible to numerically evaluate the previous expressions and to derive the key parameters T_n, T_p, $\bar{R}$ and $E_{\rm kin}$ defining the PT.

It is worth mentioning how the above formalism simplifies in the case of a quick PT, which is the main situation investigated in the literature. In that case, the PT is assumed to proceed rapidly around the temperature $\tilde{T}_n$ when at least one bubble has been produced per Hubble volume, namely $\int_{\tilde{T}_n}^{T_c} dT \frac{\Gamma(T)}{H^4(T)T} \sim 1$. In this context, $\tilde{T}_n$ is called the nucleation temperature and replaces our expression T_n derived from Equation (5.25). Then the decay probability can be expanded around that instant as $\Gamma(t) \approx \Gamma(\tilde{t}_n)e^{\beta(t-\tilde{t}_n)}$, where β^{-1} gives the time scale of the transition. As such a PT is not expected to proceed too far below the electroweak scale, we have $\Gamma(T) \approx A(T)e^{-S_3(T)/T}$ and hence:

$$\frac{\beta}{H(\tilde{T}_n)} = \tilde{T}_n \frac{d}{dT}\left(\frac{S_3(T)}{T}\right)\bigg|_{T=\tilde{T}_n}. \tag{5.29}$$

The characteristic size and energy of the bubbles are then expected to be $\tilde{R} = v\beta^{-1}$ and $\tilde{E}_{\rm kin} = \frac{4\pi}{3}\tilde{R}^3\epsilon(\tilde{T}_n)$ respectively.

Numerical solutions

We give the numerical results of the previous formalism applied to the model described by the potential (5.4) and (5.6). We first mention that the range of parameter $\kappa \in [-1.85, -1]m_h^2/v$ has already been investigated in [198]. In that case, the PT occurs quickly and can be described by a rapid PT (as explained in the last paragraph above). It results in the production of a GW spectrum potentially detectable by LISA. However, for $\kappa < -1.85m_h^2/v$, the transition lasts longer and we require the more general prescription that we just outlined.

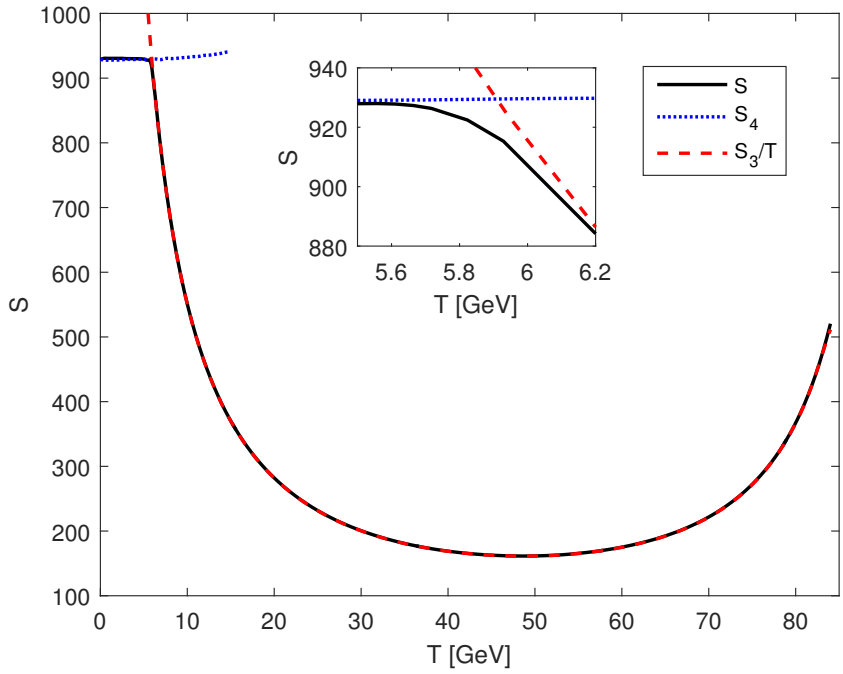

FIGURE 5.2: Thermal behaviour of the Euclidean action for $\kappa = -1.9 m_h^2/v$. The black solid line corresponds to the action $S(T)$, Equation (5.16), whose spacetime dependent bounce solution (5.17) has been solved over a lattice through Newton's method. The blue dotted line (resp. red dashed line) is the low (resp high) temperature approximation $S_4(T)$ (resp. $S_3(T)/T$) given by Equation (5.19).

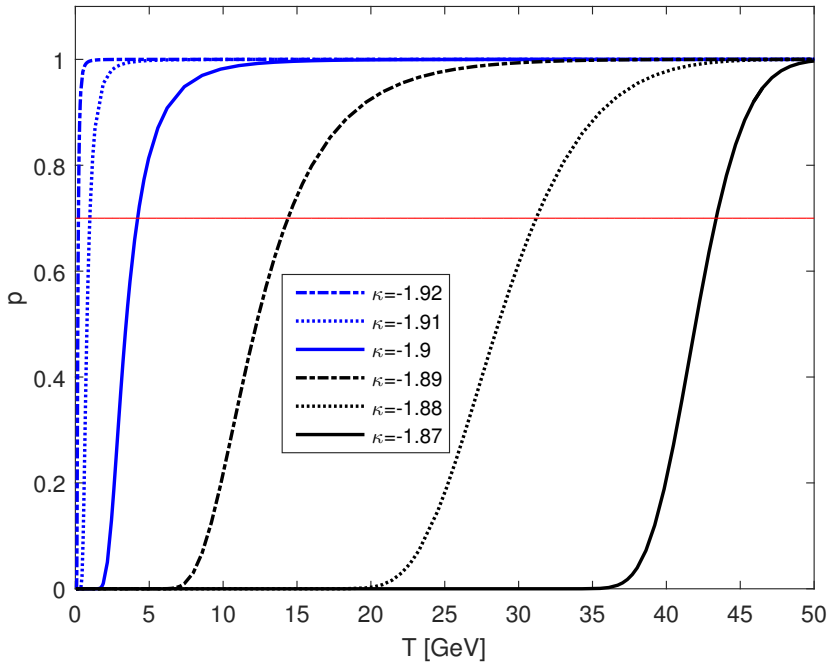

FIGURE 5.3: Thermal evolution of the probability $p(T)$ for $\kappa = [-1.92, -1.87] m_h^2/v$. The intersection between the curves and the red solid line $p(T) = 0.7$ gives the percolation temperature.

$\kappa\ [m_h^2/\lvert v\rvert]$	T_c GeV	T_n GeV	T_p GeV	$(\bar{R}H_p)^{-1}$	α
-1.87	98.3	48.9	43.4	8.79	0.57
-1.88	98.0	48.9	31.2	2.76	1.88
-1.89	97.7	49.0	14.4	1.41	37.8
-1.9	97.4	48.7	4.21	1.09	$5.09 \cdot 10^3$
-1.91	97.1	48.6	0.977	1.02	$1.73 \cdot 10^6$
-1.92	96.8	48.5	0.205	1.00	$8.80 \cdot 10^8$

TABLE 5.1: Key parameters describing the PT for $\kappa = [-1.92, -1.87]m_h^2/v$. This range of κ values has been selected in prevision of its relevance for GW production.

First, we show in Fig. 5.2 how the Euclidean action behaves as a function of temperature, for $\kappa = -1.9m_h^2/v$. It appears that the action $S(T)$ given by Equation (5.16) is not only well approximated by $S_4(T)$ at $T \ll R_0^{-1} \approx 6$ GeV and $S_3(T)/T$ at $T \gg R_0^{-1}$, but is also close to R_0^{-1}. In other words, $\min\{S_4, S_3/T\}$ provides a good approximation of the action over the entire range of temperatures considered, as also suggested in [220]. This observation is important from a computational point of view as it means we can avoid solving the time-dependent PDE (5.17) which is computationally expensive. Moreover, we observe that the action becomes, and stays, large at low temperatures ($S \sim S_4 \sim 930$), meaning that its effect on the PT dynamics is exponentially suppressed (see for example (5.15)).

Second, $p(T)$ is computed from $\Gamma(T)$ according to Equation (5.28). The results for several key values of κ are given in Fig. 5.3. As expected, the PT can be identified as a rapid change in $p(T)$ from 1 to 0. The corresponding nucleation and percolation temperatures are given in Table 5.1. We observe that $T_n \sim 49$ GeV for each κ. This is due to the fact that most of the bubbles are produced when the action $S_3(T)/T$ reaches its minimum, whose location only slightly changes with κ. On the other hand, we notice that T_p varies through several orders of magnitude. This is because the number density of bubbles produced at the nucleation time changes as a function of κ. This confirm the expectation that as the decay probability decreases, more time is needed for the transition to complete. We have verified that these results are consistent with our assumption that most bubbles are produced before vacuum energy dominates. Indeed, vacuum-radiation equality would occur at $T_e \sim 35.5$ GeV for this range of κ, if no bubbles were produced earlier. This confirms $T_n > T_e$.

The remaining task is to compute the characteristic bubble size $\bar{R}$ and the kinetic energy E_{kin} of the bubbles at the percolation temperature. For later convenience, we rescale them compared to the Hubble radius and radiation energy density at this time. To this end, Table 5.1 uses the dimensionless parameters $(\bar{R}H_p)^{-1}$ and $\alpha = \epsilon_{\text{kin}}/(\kappa_\rho \epsilon_{\text{rad}}(T_p))$ with $\epsilon_{\text{kin}} = E_{\text{kin}}/\bar{R}^3$. In this way, we can easily compare our results with those mentioned in the literature (as $v \sim 1$, $(\bar{R}H_p)^{-1}$ takes the role of β/H given by Equation (5.29)).[7]

[7]Note that Equation (5.29) could clearly not have been applied in this scenario as β would have been negative for temperatures below the minimum of S_3/T.

Analysis

Table 5.1 contains all the information we need about the PT to predict the GWs spectrum that is produced during such an event. This will be presented in detail in the next Chapter. At this stage, we can already extract interesting information from our numerical results. As expected, Table 5.1 confirms that there exist some parameters for which the PT completes well below the electroweak scale. Lower values of percolation temperature are also possible for lower values of κ, but they are constrained from various considerations. First, the obvious lower bound $T_p \gtrsim 1$ MeV is given by nucleosynthesis constraints. Second, we shall see in the next Chapter that the GW spectrum for $\kappa \lesssim -1.92 m_h^2/v$ is already excluded from current PTA surveys.

Another observation from Table 5.1 is that the two quantities $(\bar{R}H_p)^{-1}$ and $\frac{\alpha}{\alpha+1}$ approach 1 for lower and lower values of κ. The fact that $(\bar{R}H_p)^{-1} \to 1$ means that bubbles are almost of horizon size when they collide and that they never become of super-horizon size because H^{-1} also increases linearly with time. Note also that the increase in α for lower κ is mainly due to $\alpha \propto T_p^{-4}$ rather than to the change of kinetic energy stored in the bubbles.

Finally, we note that at temperatures around $T \sim 100$ MeV, the QCD PT, which is believed to be second-order in the SM, takes place. As discussed in [234], a $q\bar{q}$ condensate with non zero vacuum expectation value is thus expected to form and to contribute to the thermal potential (5.6) via a linear term in the Higgs field. This effect has no significant influence on this model since the cubic term in the tree-level potential (5.4) induces a large barrier which is not affected by such a linear term. This will however be a very important ingredient to understand the PT dynamics that occur in the scale invariant model we introduced in Section 5.1.2 and to which we return now.

5.2.2 QCD-induced electroweak phase transition

We finished our discussion about the extension of the SM with hidden scale invariance by observing that the electroweak vacuum of the Higgs-dilaton potential is degenerate with the vacuum at the origin: $V(0,0) \simeq V(v, v_\chi)$. This has an important ramification for the cosmological PT in this model: the critical temperature of the electroweak PT, T_c, defined as the temperature where the two minima are degenerate, is $T_c = 0$. Hence, the premature conclusion is disastrous for our model: no electroweak PT is possible. However, we argue that as the universe cools down QCD chiral symmetry breaking happens such that the quark-antiquark condensate triggers the electroweak symmetry breaking and the Higgs field relaxes in its electroweak symmetry breaking vacuum configuration.

Witten has pointed out a long time ago [234] that in the SM with Coleman-Weinberg radiative electroweak symmetry breaking, the cosmological electroweak PT is strongly first-order. The electroweak PT is aided by the QCD quark-antiquark condensate and hence occurs at low temperatures, namely around the temperature of the QCD chiral PT. See also the follow up work which also introduces the dilaton field [235]. Although these models are no longer phenomenologically viable, one may consider their extensions which exhibit the same features for some range of parameters [236]. We now show how this can be implemented in our model of interest with hidden scale invariance.

The finite temperature Higgs-dilaton potential

The first step to perform is to compute the finite temperature corrections to the tree-level Higgs-dilaton potential (5.9). We have to be careful before trying to directly apply the standard formalism we introduced in Section 3.2.2 and used in our previous model. A notable difference comes from the presence of the dilaton-dependent dynamical cut-off in this case. The standard quadratic divergent term $\propto \Lambda^2$, which are renormalized away within the standard calculations, and quartic (field-independent) divergent terms $\propto \Lambda^4$, which are typically ignored altogether, become now $\propto \chi^2$ and $\propto \chi^4$.

We explicitly show in Appendix A.2 how to derive the finite temperature potential taking these considerations into account. We state that purely quantum (temperature independent) corrections of the sort χ^2 and χ^4 can be absorbed in the redefinition of the tree-level couplings in Equation (5.9). Then the temperature independent logarithmic terms $\propto \ln\chi^2$ do exactly reproduce the standard zero temperature Coleman-Weinberg quantum corrections in our calculations. We remind that such quantum corrections explicitly break scale invariance and give rise to the dilaton mass at two-loop level. Therefore, in the early universe they are subdominant compared to the thermal corrections (especially along the classical flat direction), which also break scale invariance explicitly. Thus, we can safely ignore the quantum corrections in what follows.

For the purpose of illustrating how the PT dynamics proceeds, it is convenient to look at the leading high-temperature expansion of the effective thermal potential we obtained in Appendix A.2. It reads:

$$\begin{aligned} V_T(h,\chi) &= \frac{\lambda(\Lambda)}{4}\left[h^2-\frac{v^2}{v_\chi^2}\chi^2\right]^2 + c(h)\pi^2T^4 - \frac{\lambda(\Lambda)}{24}\frac{v^2}{v_\chi^2}\chi^2T^2 \\ &+ \frac{1}{48}\left[6\lambda(\Lambda)+6y_t^2(\Lambda)+\frac{9}{2}g_1^2(\Lambda)+\frac{3}{2}g_2^2(\Lambda)\right]h^2T^2+\cdots \end{aligned} \tag{5.30}$$

where h is the neutral, CP-even component of the Higgs doublet, $H=\left(0,h/\sqrt{2}\right)^{\mathrm{T}}$ and $c(h)$ is a number of relativistic degrees of freedom, which are in thermal equilibrium at T. The parameter $c(h)$ has implicit h dependence, through the relation $m_i(h)<T$, where $m_i(h)$ are h-dependent masses for SM fields. Only dominant thermal fluctuations of heaviest SM fields ($i=W^\pm,Z,h,t$) are taken into account and the relations (5.12) and (5.13) are employed when deriving Equation (5.30).

To proceed further, we first eliminate the dilaton field by solving its equation of motion, $\partial V_T/\partial\chi=0$, which implies at leading order:

$$\chi^2 \approx \frac{v_\chi^2}{v^2}\left(h^2+\frac{T^2}{12}\right)\,. \tag{5.31}$$

Note that if we set the temperature to zero, the above equation displays the flat direction of the zero temperature classical potential. Hence, the T^2 term is the leading contribution from thermal fluctuations that breaks scale invariance explicitly. Plugging (5.31) back into (5.30), we obtain the finite temperature potential in terms of the

Higgs field only:

$$V_T(h,\chi(h)) = \left[c(h)\pi^2 - \frac{\lambda(\Lambda)}{576}\right] T^4 + \frac{1}{48}\left[4\lambda(\Lambda) + 6y_t^2(\Lambda) + \frac{9}{2}g_1^2(\Lambda) + \frac{3}{2}g_2^2(\Lambda)\right] h^2T^2 + \cdots . \quad (5.32)$$

As expected in this approximation, the temperature independent terms vanish due to the flatness of the classical potential. We verified numerically that $4\lambda(\Lambda) + 6y_t^2(\Lambda) + \frac{9}{2}g_1^2(\Lambda) + \frac{3}{2}g_2^2(\Lambda) > 0$ and therefore the curvature of the effective potential (5.32) at the origin $h = 0$ is positive. Hence, $h = 0$ is a minimum of the effective potential and is separated from another local minimum, which corresponds to the electroweak symmetry breaking configuration of the Higgs field, by the temperature dependent barrier. Furthermore, this barrier persists down to $T = 0$ due to the two (and higher) loop quantum corrections. As discussed earlier, the two vacuum states are degenerate in energy. We stress again that this generic prediction of the model is largely independent of its ultraviolet completion and would imply that the Universe is stuck in the trivial symmetric minimum.

QCD effects as a trigger of the electroweak PT

The above picture is actually altered as the universe cools down to temperatures where QCD interactions become strong and various composite states start to form. As the universe remains in the symmetric phase $h = 0$, all quarks (and other SM particles) are massless at that epoch. Hence, the $SU(6)_L \times SU(6)_R$ chiral symmetry in the quark sector must be exact and it gets spontaneously broken once the QCD quark-antiquark condensate forms. Part of the $SU(6)_L \times SU(6)_R$ chiral symmetry is actually gauged and represents $SU(2) \times U(1)$ electroweak symmetry. Therefore, the quark-antiquark condensate also breaks the electroweak symmetry and results in generation of small masses for the $W^\pm$ and Z gauge bosons. The finite temperature quark-antiquark condensate, $\langle\bar{q}q\rangle_T$ has been computed within the chiral perturbation theory with N massless quarks in [237]:

$$\langle\bar{q}q\rangle_T = \langle\bar{q}q\rangle \left[1 - (N^2-1)\frac{T^2}{12Nf_\pi^2} - \frac{1}{2}(N^2-1)\left(\frac{T^2}{12Nf_\pi^2}\right)^2 + \mathcal{O}\left((T^2/12Nf_\pi^2)^3\right)\right], \quad (5.33)$$

where $\langle\bar{q}q\rangle \approx -(250\text{ MeV})^3$ is the zero temperature condensate and $f_\pi \approx 93$ MeV is the pion decay constant. From Equation (5.33) we can infer that for $N = 6$ the critical temperature of the chiral symmetry breaking PT, defined by $\langle\bar{q}q\rangle_{T_c} = 0$, is equal to $T_c \approx 132$ MeV. The condensate (5.33) would generate a linear term in the effective potential through the quark-Higgs Yukawa interactions: $y_q\langle\bar{q}q\rangle_T h/\sqrt{2}$, where y_q is the Yukawa coupling of $q-$type quark. It should be stressed that while all terms in the effective potential Equation (5.32) diminish as T decreases, the magnitude of the linear term increases. The extremum condition is modified as:

$$y_q\langle\bar{q}q\rangle_T/\sqrt{2} + \frac{\partial V_T}{\partial h} = 0\,, \quad (5.34)$$

and it is clear that the local minimum shifts from the origin $h = 0$ to non-zero values of h.

The evolution of this local minimum can be analyzed more precisely by employing the full thermal potential given in Appendix A.2 rather than its high-temperature

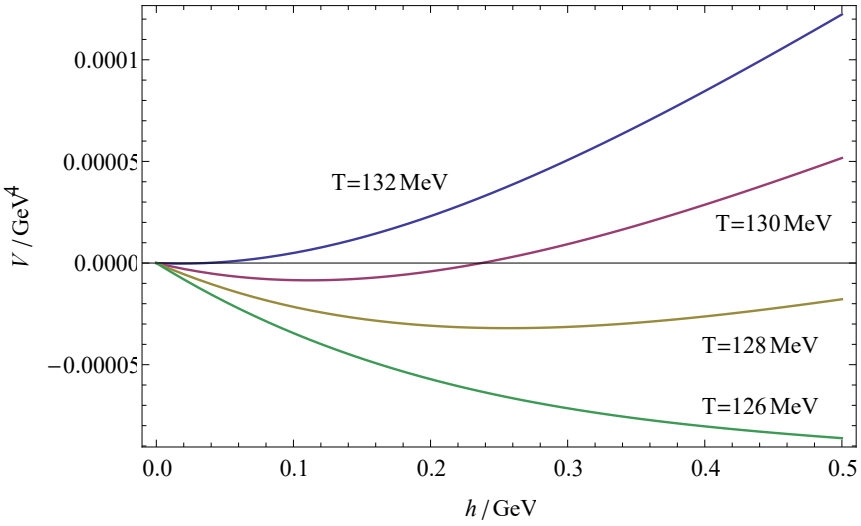

FIGURE 5.4: $V_T(h) - V_T(0)$ for different temperatures below the chiral PT and h near the origin.

expansion. We numerically find that just below the critical point of the chiral PT at T_c, the QCD condensate term is small and a non-zero minimum, h_0 does emerge near $h = 0$. This is shown in Figure 5.4. This minimum is separated by a potential barrier from another local minimum that later evolves into the electroweak vacuum. This minimum exists for 127 GeV $\leq T \leq$ 132 GeV. In this range of temperatures, the top quark remains relativistic with $\frac{m_t(h_0)}{T} \lesssim 1$. Below this range of temperatures, the contribution from $|\langle\bar{q}q\rangle_T|$ becomes large enough such that the local minimum near the origin no longer occurs, indeed the first term in Equation (5.34) becomes larger than the second term. Subsequently, the Higgs field quickly runs down classically the slope from near the origin towards the true electroweak breaking vacuum.

Cosmological implications

The first thing we notice is that the Higgs field configuration during the PT is smooth and homogeneous, and does not proceed through $h-$bubble nucleation. However, since the QCD PT precedes the electroweak one, all the six flavours of quarks are massless during that process. There are theoretical arguments [238], which are supported by numerical calculations [239], which suggest that the QCD PT with $N \geq 3$ massless quarks is first-order. So we should expect the production of GWs related to the dynamics of QCD bubbles formed during this transition.

We will show in the next Chapter that we can roughly estimate the properties of such GWs. However, we can already realize that any precise prediction would require more knowledge regarding the QCD PT than what we have presented at this stage. Indeed, we remind that computing the production of GWs from a first-order PT requires to determine the shape of the thermal potential along which tunnelling takes place. Here we only have specified the Higgs-dilaton potential, as in Equations (5.30) or (5.32), but not the potential for the quark-antiquark along which the first-order transition occurs. Also, we have implicitly assumed that the $\bar{q}q$ and Higgs transitions proceed independently one after the other. This seems justified from the fact the temperatures corresponding to the condensate formation, $T \sim 132$ MeV, and to the Higgs rolling, $T \sim 127$ MeV, are rather separated. However, a more careful analysis would be necessary to completely confirm this assumption.

We therefore understand that getting a more precise picture of the overall scenario requires to build and analyze a mutlti-field potential of the kind $V_T(h, \chi, \bar{q}q)$. This would allows us to clearly see if the QCD and electroweak PTs are distinct or entangled (for example as taking place along a particular direction in field space). We could also compute the bubble formation rate in details. We mention that such a task is currently under investigation and is expected to appear in a forthcoming publication. In this thesis, we will keep to our above assumptions and only extract order of magnitude estimates.

On top of GWs that we describe in Section 6.2.2, another interesting phenomenon we note in passing is the production of primordial black holes associated with a first-order QCD PT [240]. The mass of a horizon size black hole can be estimated to be of the order of solar mass, $M_{BH} \sim 1/(H(T_c)G) \sim M_P^3/T_c^2 \sim 10^{65}$ eV $\sim M_\odot$. These are large enough black holes to survive the Hawking evaporation until the present epoch and thus can contribute to the total dark matter density. Finally, we also mention that the model may provide a natural framework for the so-called cold baryogenesis [241].

5.3 Chapter summary

A substantial amount of content has been presented in this Chapter and it is judicious to summarize our main results. We have introduced two different particle physics models which have the potential to accommodate certain limitations of the SM. Our main interest has been to study the type of PTs that can occur during the early Universe for such theories. We remind for clarity that our ultimate motivation behind this investigation is to predict new observables (such as GWs) that could allow us to refute or consolidate the veracity of such models.

First, we discussed a modification of the SM where the electroweak gauge group is non-linearly realized. Considering the Higgs field as a singlet under the full gauge group, we argued that the Higgs potential can admit a cubic coupling κ at tree-level. We found an interesting range of values of κ for which the electroweak PT completes at a temperature significantly below the electroweak scale. This analysis required to study the behaviour of the nucleation probability of true vacuum bubbles at low temperature and to take into account the expansion of the Universe. Regarding the former point, we compared the usual low and high temperature expressions of the Euclidean action to a more general formula based on a time-dependent bounce solution. We observed that the two approximate equations actually provide a good estimate of the action over the entire range of valid temperatures. Regarding the latter point, we argued that we can consider the Universe as radiation-dominated all along the process without changing the general behaviour of the PT. A better estimation of the exact equation of state and scale factor during the PT would however slightly increase the accuracy of the relation between the parameter κ and the predicted properties of the transition given in Table 5.1. These are those values we shall use in the next Chapter to characterize the GWs produced during the transition.

Second, we studied the minimal SM with hidden scale invariance. The model predicts a light dilaton which very feebly couples to the SM fields. The Higgs-dilaton potential exhibits two degenerate minima at zero temperature, therefore the electroweak PT can only be triggered by the QCD chiral symmetry PT at $T \lesssim 132$ MeV. We found that the Higgs field configuration changes smoothly during this transition, while the chiral symmetry breaking is likely to be first-order. We pointed out that the exact description of the dynamics of the QCD-EW transition requires to define a

thermal potential which involves the dilaton, the Higgs field and the $\bar{q}q$ condensates at once. Although this task is currently still under investigation, this does not prevent us to extract order of magnitude predictions. In particular, stable primordial BHs of mass $\sim M_{\odot}$ are expected to be produced during the PT. GW signals will also be predicted in Section 6.2.2 once we learn how to characterize them.

Chapter 6

GW background from phase transitions

In Chapter 5, we have described two particle physics models which exhibit first-order cosmological phase transitions. We now want to present the results we obtained in [3, 4] regarding the production of GWs associated to these events. Our main objective is to predict the spectrum of such GWs as a function of the parameters of the models in order to obtain constraints on these parameters from current or future GW experiments. This requires to understand the different mechanisms which are responsible for the production of GWs during a first-order PT and then to be able to estimate the typical frequency and amplitude of such signals.

Although no stochastic GW background has been detected yet, the study of cosmological phase transitions is a promising research area. Indeed, we shall see that the peak frequency of a stochastic GW background produced by a PT near the electroweak scale, $T_{\mathrm{EW}} \sim 100$ GeV, is expected to lie in the millihertz range, which coincides with the projected sensitivity of the future LISA space-based interferometer [227]. This has motivated a series of investigations into the production of GWs in various BSM models, see e.g. [198, 224, 225, 242–252]. Most of these studies focus on the usual electroweak PT, but as we emphasized in our previous Chapter it is possible to find scenarios whose dynamics differ substantially from the regular case. The predicted GW spectrum is therefore expected to be quite different as well.

Let us give an overview of how the characteristic frequency and amplitude of the spectrum are derived from the dynamics of the PT. They depend on a few key parameters: the duration of the transition, the size of the colliding bubbles, the bubble-wall velocity, the fraction of vacuum energy transferred into the bubble-walls and the interaction between the expanding bubbles and the surrounding plasma. In the aforementioned studies, these quantities are computed under the assumption that the PT occurs on a time scale much shorter than the Hubble time. The instant at which most of the bubbles are nucleated is thus very close to the time when they collide and cover a significant volume of the Universe. Our analysis of the prolonged electroweak PT in Section 5.2.1 tells us however that this assumption is not justified in that case since there is a non-negligible amount of time between nucleation and collision. We expect the GW background to be predominantly produced by large bubbles colliding much later than in a typical electroweak PT previously discussed in the literature. A range of lower peak frequencies should then be observed in such a scenario. Regarding the QCD-induced electroweak PT that we described in Section 5.2.2, we already mentioned that it will be difficult to estimate the GW spectrum at this stage. This is because we do not have access yet to the potential along which the first-order chiral PT takes place. Nevertheless, we shall at least be able to give an estimate of the associated GW signal and argue that it is an interesting scenario to further investigate.

6.1 Stochastic GW background

Saying that bubbles of true vacuum nucleate, expand and collide is equivalent to saying that the corresponding background scalar field varies in space and time. The Einstein equations therefore tell us that the energy-momentum tensor of this field is a source of curvature perturbations. Moreover, a substantial amount of energy released during the PT can be transferred into the surrounding fluid in the form of turbulence or coherent motion (sound waves). This is also a source of GWs since the fluid couples to the metric as well. An entire area of research is then devoted to investigate how to solve the EFE in those cases, either analytically or numerically. We will not present the details of the various approaches which have been proposed but we focus instead on how they can be applied to obtain predictions. More information can be found for example in [116] Chapter 22.

A stochastic GW background is usually described in terms of its contribution to the energy density of the Universe per frequency interval:

$$h_0^2 \Omega_{GW}(f) = \frac{h_0^2}{\rho_c} \frac{d\rho_{GW}}{d(\ln f)}, \tag{6.1}$$

where f is the frequency, ρ_{GW} the GW energy density, $\rho_c = 3H_0^2/(8\pi G)$ is the critical energy density today and h_0 the dimensionless Hubble rate. The energy density of GWs depends on the metric perturbation $h_{\mu\nu}$ which satisfies the EFE, namely [253]

$$\rho_{GW} = \frac{1}{8\pi G} \langle \partial_t h_{\mu\nu} \partial_t h^{\mu\nu} \rangle \qquad \partial_\alpha \partial^\alpha h_{\mu\nu} \sim 8\pi G T_{\mu\nu} \,, \tag{6.2}$$

with $T_{\mu\nu}$ the energy momentum tensor describing the sources. As previously mentioned, the production of GWs from a first-order phase transition originates from three sources: the collisions of bubbles walls [187–191, 254, 255], sound waves in the plasma formed after collision [256–259] and magnetohydrodynamics turbulence in the plasma [260–264]. As these three contributions should approximately linearly combine [227], the total energy density can be written as

$$h_0^2 \Omega_{\rm GW} \simeq h_0^2 \Omega_{col} + h_0^2 \Omega_{sw} + h_0^2 \Omega_{\rm MHD} \,. \tag{6.3}$$

How much each of these terms contributes to the total energy density depends on the details of the transition and the underlying particle physics model.

We expect the GW spectrum to be mainly produced around the percolation temperature t_p of the phase transition with a characteristic frequency f_p. The amplitude of this signal then decreases as $a^{-4}(t)$ up to today while its frequency redshifts as $a^{-1}(t)$. In other words, the energy density stored in the GWs and the peak frequency today are given by [191]:

$$\begin{aligned} f_0 &= f_p \frac{a(t_p)}{a(t_0)} &&= 1.65 \times 10^{-7} \text{ Hz} \left(\frac{f_p}{H_p}\right) \left(\frac{T_p}{1 \text{ GeV}}\right) \left(\frac{g_*}{100}\right)^{1/6} \\ \Omega_{GW,0} &= \Omega_{GW} \left(\frac{a(t_p)}{a(t_0)}\right)^4 \left(\frac{H_p}{H_0}\right)^2 &&= 1.67 \times 10^{-5} h_0^{-2} \left(\frac{100}{g_*}\right)^{1/3} \Omega_{GW} \,, \end{aligned} \tag{6.4}$$

where $g_\star$ is the number of relativistic degrees of freedom introduced in Section 3.2.2 Equation (3.33).

Explicit formula

We now want to estimate the peak frequency and amplitude of each contribution in Equation (6.3). We can first investigate the collision term from dimensional analysis. We expect the peak frequency to scale with the inverse size of the bubbles at their collision, namely $f_p \sim (\bar{R})^{-1}$. Regarding the amplitude, we first have $\Omega_{col} = \rho_{GW}/\epsilon_{tot}$ where ϵ_{tot} is the total energy density of the Universe at the percolation time. The energy density of GWs is given by Equation (6.2). We can expect that $\partial_\alpha \sim \bar{R}^{-1}$ (the characteristic size of bubbles) and $T_{\mu\nu} \sim \epsilon_{\text{kin}}$ (the kinetic energy density stored in the bubbles). This implies $\rho_{GW} \sim 8\pi G \bar{R}^2 \epsilon_{\text{kin}}^2$. Substituting G from the Friedmann equation $H_p^2 = \frac{8\pi G}{3}\epsilon_{tot}$, we get:

$$\Omega_{col} \sim (\bar{R}H_p)^2 \frac{\epsilon_{\text{kin}}^2}{\epsilon_{tot}^2} \sim (\bar{R}H_p)^2 \kappa_\rho^2 \frac{\alpha^2}{(1+\alpha)^2}. \tag{6.5}$$

where we remind that $\alpha = \epsilon_{\text{kin}}/(\kappa_\rho \epsilon_{\text{rad}})$ is an indicator of the amount of energy from the PT which is transferred either into the wall motion of the bubbles or into the cosmic fluid.

In reality, Ω_{col} also depends on the bubble wall velocity v. Several studies have actually provided more accurate expressions for the GW spectrum from bubble collisions, beyond the simple dimensional analysis. They usually rely on the envelope approximation and numerical simulations [190, 191, 254], although some analytic formula have also been suggested [255, 265]. Using the results of [254], the spectrum today can be described as follows:

$$h_0^2 \Omega_{col}(f) = 1.67 \times 10^{-5} \left(\frac{100}{g_*}\right)^{1/3} \left(\frac{\beta}{H_p}\right)^{-2} \kappa_\rho^2 \left(\frac{\alpha}{1+\alpha}\right)^2 \left(\frac{0.11 v^3}{0.42 + v^2}\right) S(f), \tag{6.6}$$

where:

$$\begin{aligned} S(f) &= \frac{3.8 (f/f_0)^{2.8}}{1 + 2.8 (f/f_0)^{3.8}}, \\ f_0 &= 1.65 \times 10^{-7} \left(\frac{T_p}{1\ \text{GeV}}\right) \left(\frac{g_*}{100}\right)^{1/6} \left(\frac{\beta}{H_p}\right) \left(\frac{0.62}{1.8 - 0.1v + v^2}\right) \text{ Hz}. \end{aligned} \tag{6.7}$$

In these expressions β is the time scale of the transition. It is usually given by Equation (5.29) for a rapid PT but we emphasized that this formula is not valid for a long-lasting transition. Therefore we shall instead substitute $\beta \sim v\bar{R}^{-1}$ in Equation (6.6-6.7) in agreement with the dimensional estimate given by Equation (6.5).

Formulae of the kind (6.6)-(6.7) have been obtained for the contributions from sound waves and turbulence as well. They can be found in the literature, namely in [256–259] and [260–264] respectively. We do not present them here since we shall not use them in our subsequent computations for reasons we shall justify below.

6.2 GWs beyond the Standard Model

6.2.1 GWs from a prolonged phase transition

We now want to compute the GW spectrum produced during the long-lasting and supercooled PT detailed in Section 5.2.1. We remind that the dynamics is determined by the cubic coupling κ which appears in the Higgs tree-level potential 5.4. The numerical results presented in Table 5.1 for $\kappa = [-1.92, -1.88] m_h^2/v$ confirm that the

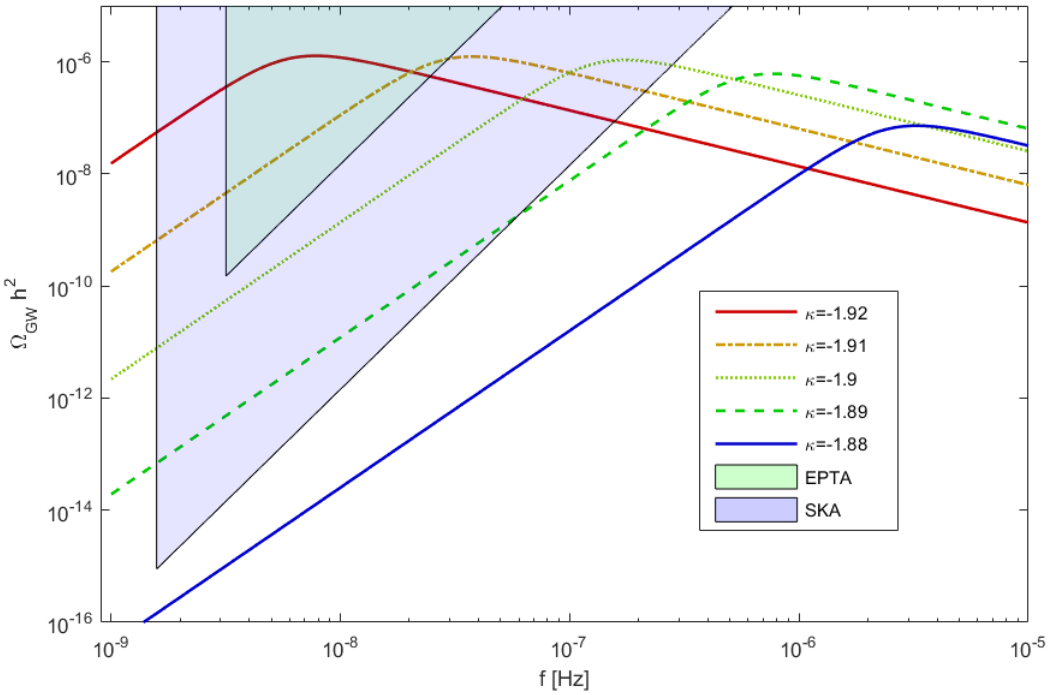

FIGURE 6.1: Lines: GW spectra estimated from Equations (6.6-6.7) and the parameters of Table 5.1 for $\kappa = [-1.92, -1.88] m_h^2/v$. Green shaded area: current exclusion limits from EPTA [93]. Blue shaded area: planned detection sensitivity of SKA [266].

electroweak PT is very strong and release a lot of energy for this parameter range. The GW results we will present therefore assume that the the collision term Ω_{col} is dominant:

$$h_0^2 \Omega_{\rm GW} \simeq h_0^2 \Omega_{col}. \tag{6.8}$$

As explained in [227], this is based on the idea that the bubbles are in a runaway configuration. The amount of converted vacuum energy is such that the energy deposited in the plasma saturates and the majority goes into accelerating the bubble wall. This is equivalent to saying that $v \sim 1$ and $\kappa_\rho \sim 1$.[1] We shall discuss the validity of this assumption below.

It is now straightforward to evaluate Equations (6.6)-(6.7) for the parameters given in Table 5.1. It appears that the peak frequency f_0 can be as low as $\sim 10^{-9} - 10^{-7}$ Hz and thus lies in the detection range of PTA experiments. In Fig. 6.1, we compare the GW spectrum for several values of κ and the current status of PTA detectors. Three collaborations have published limits on the amplitude of a stochastic GW background: the European Pulsar Timing Array (EPTA) [93], the Parkes Pulsar Timing Array (PPTA) [94] and the North American Nanohertz Observatory for Gravitational waves (NANOGrav) [95]. All these three limits are of similar amplitudes and thus we only display the EPTA results[2]. The sensitivity area should be improved in the future by the Square Kilometre Array (SKA) [96] whose expected detection range is also given in Fig. 6.1 [266].

[1] Note that the same approach has been followed and described in detail in [198] (see their Section 4) for our model of interest given in Section 5.1.1 (but for a parameter range of κ for which the PT is fast and corresponds to the typical electroweak scenario).

[2] Note that the exclusion line is computed as explained in [266].

Discussion of the results

It is clear that the model we investigated predicts GWs detectable by the aforementioned detectors and consequently we argue that this demonstrates a new method for probing first-order electroweak PTs. We might be tempted now to define the range of κ values which is not yet excluded by EPTA and which could be tested by SKA. Although Fig. 6.1 gives us a rough estimate around $\kappa \sim -1.9 m_h^2/v$, we have to keep in mind that there are a few limitations in our computation that may need to be improved in order to get more accurate predictions.

First, we remind that these results rely on our assumption of a radiation dominated period. As explained in Section 5.2.1, the exact equation of state describing the Universe during the transition is expected to be more complicated with the potential effect of changing the value of the parameters entering in the GW spectrum. This would however not change the general behaviour that we observed. Second, it is important to realize that the GW formulae (6.6)-(6.7) have been derived under the assumption of a short-lasting PT. It is not clear a priori if these fitted formula accurately describe a long-lasting transition with large bubbles. Obtaining more precise results would require new numerical simulations of bubble collisions without the assumption that the PT completes in a time less than the Hubble time. Lattice simulations beyond the envelope approximation, such as for example [267], could shed new light on this question.

Probably the main remaining concern is related to the assumption of runaway bubbles with $\kappa_\rho \sim 1$. This hypothesis actually seemed to be well justified at the time when the results in Figure 6.1 have been computed [3]. However the recent paper [229] now argues that next-to-leading order friction effects between the bubble wall and the plasma prevent the bubble to run away. They conclude that for strong PT, the velocity can still almost reach the speed of light, $v \sim 1$, but that the wall would carry less energy such that Ω_{sw} and $\Omega_{\rm MHD}$ would be the dominant contribution to $\Omega_{\rm GW}$ instead of the collision term. Assuming that this claim is true, it would then be important to add the sound wave and turbulence effects in our Figure 6.1. The amplitude of the signal coming from the collision term would therefore be reduced ($\kappa_\rho < 1$) but we expect the total amplitude to have roughly the same order of magnitude as the curves in Figure 6.1. The parameter α of the PT is indeed not modified by such considerations.[3]

Although it is clear that these limitations need to be addressed in the future, we argue that they should not change the general behaviour we observed, namely the possibility to detect a first-order electroweak PT with pulsar timing arrays. In our model of interest, the aforementioned corrections are indeed expected to be compensated by a small shift in the value of the parameter κ around the value of $-1.9 m_h^2/v$ which is indicated in Figure 6.1. Nevertheless, we realize that the detection of such GWs would provide interesting information regarding deviations from the SM Higgs trilinear coupling which can only be poorly constrained from collider experiments [198, 199]. At a more general level, we also expect other particle physics theories (e.g. models with a barrier in the tree-level Higgs potential) to exhibit supercooled and long-lasting PT with the production of low-frequency GWs.

[3] A very recent analysis of supercooled PTs taking these elements into account has been performed in [268]. Their Figure 8 shows for example how each term contributes to $\Omega_{\rm GW}$.

6.2.2 GWs from hidden scale invariance

We want to estimate the characteristics of the GWs produced during the first-order chiral PT discussed in Section 5.2.2. First, note that during the whole PT the universe is dominated by radiation since the energy difference between the two vacua is due to the difference in thermal energy (the $\propto c(h)T^4$ term in Equation (5.32)), which vanishes as $T \to 0$. Therefore the peak frequency (observed today) of the waves produced at $T_c \approx 132$ MeV can be estimated as:

$$f_0 \sim H(T_c)\frac{T_0}{T_c} \sim \frac{T_c T_0}{M_P} \sim 10^{-8}\ \text{Hz} \tag{6.9}$$

where $T_0 \approx 10^{-4}$ eV. As already mentioned, a stochastic GW background with such frequencies can potentially be detected by means of pulsar timing arrays (see also [269] for the specific case of a QCD PT).

This is of course a very rough approximation for the frequency as we are missing the information regarding the dynamics of the QCD bubbles. In the same way, we cannot estimate the amplitude of the signal unless we specify the potential for the quark-antiquark condensates. However the estimate (6.9) motivates us to look into the predictions of this model in more detail. This task is currently under investigation and should result in a forthcoming publication containing more information regarding the expected GW signal.

6.3 Chapter summary

We are now at the end of our investigation that we started in Chapter 5 regarding the production of gravitational waves from cosmological phase transitions. In particular, we have studied the production of GWs during a strongly supercooled electroweak phase transition. Considering a particle physics model based on a non-linear realization of the electroweak gauge group, we carefully computed the dynamics of the Higgs field during such a transition. We argued that the collisions of large bubbles (of the order the horizon size) induced a large amplitude stochastic GW background in the frequency range $10^{-9} - 10^{-7}$ Hz which can be probed by pulsar timing arrays. We derived this prediction from both dimensional arguments and the use of previous numerical simulations of colliding bubbles. Although it is clear from these analyses that our model of interest predicts a GW spectrum in the sensitivity band of PTA detectors, more refined simulations would be needed to improve the accuracy of our results. In particular, a better estimation of the exact equation of state and the inclusion of sound waves and fluid turbulence would increase the accuracy of the relation between GW predictions and specific values of the parameter κ of the particle physics model we considered. We have also estimated the peak frequency of GWs produced during a first-order chiral PT that is predicted to happen in an extension of the SM with scale invariance. Again, the signal is expected to have a frequency as low as $\sim 10^{-8}$ Hz. Future computations will be able to improve the accuracy of this prediction.

In summary, we provided examples of non-trivial PTs that can be detected with pulsar timing arrays. This enlarges the way of probing first-order cosmological PT in addition to previous proposals with space-base interferometers such as LISA. This also increases the prospects of new generation PTA detectors like SKA.

Chapter 7

Backreaction of particle production on false vacuum decay

We showed in Chapter 5 that quantum tunnelling is a key ingredient of first-order cosmological phase transitions. False vacuum decay is actually an interesting process on its own and we propose to investigate some of its aspects in more details in this Chapter. In particular, we present the results we obtained in [5] regarding the backreaction of particle production on the decay rate of a metastable scalar field at zero temperature. In the 1980s, Rubakov proved that the fluctuations generated during the tunnelling of a metastable field produce a spectrum of real particles [270, 271]. This observation was then confirmed by other groups using different formalisms [272, 273]. We propose to review and extend Rubakov's work to evaluate the impact of these particles on the decay rate of the field. Our approach will follow the reduced density matrix formalism used in quantum mechanics to address the influence of the environment on a given quantum process [274–277].[1] In this scheme, the information related to the system is extracted by integrating out the external degrees of freedom. Applied to our case, the decaying field is considered as the system of interest while the environment corresponds to the external bath of created particles.

7.1 Motivation from Higgs vacuum stability

Our analysis will be restricted to its simplest form, namely the backreaction of scalar particles in flat space-time. However, it should be possible to extend this formalism to include spinor, vector fields and even gravitational effects. It would then be interesting to study how such backreaction affects the stability of the current SM electroweak vacuum. This is related to a peculiarity of the SM that we have not discussed in Chapter 3. Since the discovery of the Higgs boson, all the parameters of the SM are known and the theory can be extrapolated to high energies. Assuming the absence of new physics, state-of-the-art calculations indicate that the Universe is lying at the edge between stability and metastability [278–282]. In the latter case, the Higgs potential becomes negative at an instability scale around $\Lambda_I \approx 10^{11}$ GeV and thus develops a global minimum at large field values. In this context, the decay probability of the electroweak vacuum may become a crucial parameter to probe both the fate and the history of our Universe. In particular, it has to agree with the observation that the Higgs field has not yet decayed during the early stage of the Universe or during its subsequent evolution.

[1] This formalism was actually proposed to describe the environment-induced decoherence which attempts to explain why the world looks classical despite its quantum nature.

The usual starting point to evaluate such a false vacuum decay rate in flat space-time is the instanton method of Coleman [217] that we introduced and used in Section 5.2.1. The decay probability per unit time per unit volume is computed at the lowest order of the semi-classical approximation: $\Gamma \approx e^{-S}$, where S is the Euclidean action evaluated along the bounce trajectory. The precision of this result can then be improved including one-loop quantum corrections [218] or finite temperature effects [219, 220]. When gravitational effects cannot be neglected, e.g. during inflation, it is well known that the decay can take place either through the Coleman-de Luccia instanton [283], which is the analogue of bubble nucleation in flat space-time, or through the Hawking-Moss instanton [284] which is a homogeneous process allowed when the geometry of the Universe is closed.

Such computations have been applied to the SM and they indicate that the lifetime of the current electroweak vacuum is much longer than the age of the Universe by many orders of magnitude, both at the semi-classical [281] and one-loop [285, 286] level. Thus, it does not contradict any observation. However, the situation is more intriguing during the early Universe assuming a period of inflation. Several investigations suggest that the survival of the electroweak vacuum during this epoch implies stringent constraints on the Hubble rate and the top quark mass depending on the details of the process, like for example the coupling of the Higgs field to gravity [287–296]. It also appears that the temperature of the Universe during the reheating process following inflation influences the stability of the SM [296–298]. In addition to this, some other effects that could change our knowledge of the Higgs decay rate have also been considered including modifications from Planck scale higher-dimensional operators [286, 299–301], the presence of an impurity in the metastable phase [302] or the influence of black holes as nucleation seeds [303, 304].

7.2 Particle production during vacuum decay

7.2.1 Semi-classical decay rate

We explained how to compute the decay probability of a scalar field in Section 5.2.1. It is worth illustrating again how this works at zero temperature in order to see that there actually exist two different types of process that can take place depending on the geometry of the Universe. Consider a real scalar field σ in Minkowski space-time (with metric $(+,-,-,-)$):

$$\mathcal{L}_\sigma = \frac{1}{2}\partial_\mu\sigma\partial^\mu\sigma - V(\sigma). \tag{7.1}$$

We assume that the potential V has a local minimum at σ_F (false vacuum) and a global minimum at σ_T (true vacuum). In the semi-classical approximation, the decay probability per unit time per unit volume of a field initially trapped near σ_F is given by [217]

$$\Gamma = A\, e^{-\frac{S_B}{\hbar}}\,(1 + O(\hbar)) \tag{7.2}$$

The semi-classical exponent S_B corresponds to the Euclidean action S_E computed along the bounce trajectory: $S_E = \int d\tau d^3\mathbf{x}\left[\frac{1}{2}\left(\partial_\tau\sigma\right)^2 + \frac{1}{2}\left(\partial_i\sigma\right)^2 + V(\sigma)\right]$, with $\tau = it$ the usual Euclidean time. The bounce $\sigma_B(\mathbf{x},\tau)$ is the Euclidean trajectory which minimizes S_E with the conditions that it starts from σ_F at $\tau = -\infty$, evolves under the barrier until it reaches the boundary with the classically allowed region at $\tau = 0$

and then bounces back to σ_F at $\tau = +\infty$. In equations, it satisfies

$$(\partial_\tau^2 + \partial_i^2)\sigma = \frac{\partial V}{\partial \sigma}, \quad \sigma(\tau, \mathbf{x}) \xrightarrow{\tau \to \pm\infty} \sigma_F, \quad \left.\frac{\partial \sigma}{\partial \tau}\right|_{(\tau=0,\mathbf{x})} = 0. \tag{7.3}$$

According to Equation (7.2), the decay process is exponentially suppressed for large values of S_B. It means that the field cannot decay homogeneously in an open universe. This restricts our attention to two cases of interest: a homogeneous decay taking place in a finite volume $\mathcal{V}$ or the nucleation of a bubble of true vacuum σ_T. In the former case, Equation (7.3) reduces to $\partial_\tau^2 \sigma = \frac{\partial V}{\partial \sigma}$ with the same boundary conditions. The Euclidean action also simplifies to

$$S_{E,hom} = \mathcal{V} \int d\tau \left[\frac{1}{2} (\partial_\tau \sigma)^2 + V(\sigma) \right]. \tag{7.4}$$

In the latter case, Coleman proved that there always exists an $O(4)$ symmetric solution $\sigma_B(\tilde{r})$, where $\tilde{r} = \sqrt{\tau^2 + \mathbf{x}^2}$, satisfying[2]

$$\frac{d^2\sigma}{d\tilde{r}^2} + \frac{3}{\tilde{r}} \frac{d\sigma}{d\tilde{r}} = \frac{\partial V}{\partial \sigma}, \quad \sigma(\tilde{r} \to +\infty) = \sigma_F, \quad \left.\frac{d\sigma}{d\tilde{r}}\right|_{\tilde{r}=0} = 0. \tag{7.5}$$

The Euclidean action then becomes

$$S_{E,O(4)} = 2\pi^2 \int_0^{+\infty} d\tilde{r}\, \tilde{r}^3 \left[\frac{1}{2} \left(\frac{d\sigma}{d\tilde{r}} \right)^2 + V(\sigma) \right]. \tag{7.6}$$

The above set of formulae is obviously completely similar to the set of Equations (5.16-5.20) at $T = 0$. It gives all the information to compute the decay rate at the lowest order of the semi-classical approximation. On the other hand, the prefactor A in Equation (7.2) corresponds to the one-loop quantum corrections. Using a path integral formulation, Callan and Coleman showed in [218] that it reduces to the computation of a functional determinant. In practice, this is often a difficult task since this quantity is UV divergent and requires renormalization techniques. Physically, this prefactor corresponds to the smallest fluctuations of the tunnelling field around the bounce trajectory. Thus, roughly speaking, it represents the effect of virtual particles on the decay rate. Our aim in this Chapter is actually to derive a new correction factor related to the production of real particles during false vacuum decay.

7.2.2 Particle production

Formally, the phenomenon of particle creation takes place once we add another field to the Lagrangian (7.1). We restrict our attention to an external scalar field ϕ coupled to σ in the following way:

$$\mathcal{L}_{tot} = \mathcal{L}_\sigma + \underbrace{\frac{1}{2}\partial_\mu \phi \partial^\mu \phi - \frac{1}{2} m^2(\sigma)\phi^2}_{\mathcal{L}_\phi}, \tag{7.7}$$

where $m^2(\sigma)$ represents an arbitrary coupling between the fields. It is worth mentioning that this model allows us to consider the self-excitation of the tunnelling

[2]Note that the last condition in Equation (7.5) is not a consequence of (7.3) but is added to avoid any singular solution at the origin.

field around its bounce solution if we write $\sigma = \sigma_B + \phi$ and if $m^2(\sigma)$ is replaced by $V''(\sigma_B)$.

We now review the formalism of Rubakov [270] who proved that some ϕ particles are created during the decay process of σ. The state vector of the total system $|\Psi\rangle$ satisfies the stationary Schrödinger equation

$$\left(H_\sigma + H_\phi\right)|\Psi\rangle = E\,|\Psi\rangle\,, \tag{7.8}$$

where H_σ and H_ϕ are the Hamiltonians associated to the Lagrangians $\mathcal{L}_\sigma$ and $\mathcal{L}_\phi$. In the absence of ϕ, the model is well approximated by the quasiclassical bounce trajectory $\sigma_B(\mathbf{x},\tau)$ described in the previous section. In that case, the wave functional associated to the state $|\Psi\rangle$ becomes parametrized, in the field representation, by the Euclidean time τ as $\langle\sigma_B(\tau)|\Psi\rangle = \Psi[\sigma_B(\tau)] \approx e^{-S_E[\sigma_B(\tau)]}$ where

$$S_E[\sigma_B(\tau)] = \int_{-\infty}^{\tau} d\tau' \int d^3\mathbf{x}\left[\frac{1}{2}\left(\partial_{\tau'}\sigma_B\right)^2 + \frac{1}{2}\left(\partial_i\sigma_B\right)^2 + V(\sigma_B)\right]. \tag{7.9}$$

Then, we assume that the addition of the new field ϕ does not significantly change this behavior. In other words, we study the field ϕ in the background of the semi-classical tunnelling bounce σ_B without taking into account the action of the former on the latter. This is actually the purpose of Section 7.3 to investigate this effect. Under this assumption, we can parametrize the total state for the two fields as

$$|\Psi(\tau)\rangle \approx e^{-S_E(\tau)}\,|\phi(\tau)\rangle\,, \tag{7.10}$$

where the state $|\phi(\tau)\rangle := |\phi[\sigma_B(\tau)]\rangle$ encodes all the information related to the fluctuating field ϕ along the Euclidean trajectory (for convenience we simply wrote the dependence in τ instead of $\sigma_B(\tau)$). Before tunnelling, we ask for this state to be an eigenstate of H_ϕ according to

$$H_\phi[\sigma_F]\,|\phi[\sigma_F]\rangle = \mathcal{E}\,|\phi[\sigma_F]\rangle\,, \tag{7.11}$$

where the Hamiltonian is also parametrized as a function of the bounce:

$$H_\phi[\sigma_B(\tau)] = \int d^3\mathbf{x}\left[\frac{1}{2}\pi_\phi^2 + \frac{1}{2}\partial_i\phi\partial_i\phi + \frac{1}{2}m^2\left(\sigma_B(\mathbf{x},\tau)\right)\phi^2\right]. \tag{7.12}$$

Even in the Schrödinger picture (with time-independent operators $\phi(\mathbf{x})$ and $\pi_\phi(\mathbf{x})$), we note that the Hamiltonian has an explicit τ dependence coming from $m^2(\mathbf{x},\tau) := m^2\left(\sigma_B(\mathbf{x},\tau)\right)$. This is a typical signature of systems exhibiting particle production like the well-known examples of particle creation by an external electromagnetic field [305] or by a curved space-time background [306] (with the important difference that our system evolves in Euclidean time rather than in physical time).

From the above considerations, Rubakov showed that the stationary equation (7.8) with the boundary condition (7.11) reduces to a Euclidean Schrödinger equation for ϕ:

$$\frac{\partial\,|\phi(\tau)\rangle}{\partial\tau} = -\left(H_\phi(\tau) - \mathcal{E}\right)|\phi(\tau)\rangle\,. \tag{7.13}$$

Since we are only concerned here with ϕ initially in its vacuum state, we set $\mathcal{E} = 0$

and $|\phi[\sigma_F]\rangle = |O_{\tau_-}\rangle$.[3] For convenience, we write the initial instant as τ_- remembering that the limit $\tau_- \to -\infty$ has to be taken at the end of the calculation. As usual in the Schrödinger picture, the solution of the previous equation can be expressed from the evolution operator

$$\mathcal{U}_\tau = T \exp\left(-\int_{\tau_-}^{\tau} H_\phi(\tau')d\tau'\right) \tag{7.14}$$

as

$$|\phi(\tau)\rangle = \mathcal{U}_\tau |O_{\tau_-}\rangle , \tag{7.15}$$

where T is the time ordering operator. In contrast with quantum field theory in Minkowski space-time, this operator is not unitary: $\mathcal{U}_\tau^{-1} \neq \mathcal{U}_\tau^\dagger$ (note the absence of the imaginary factor i in the exponent since we are working in Euclidean time).

We now introduce the set of creation-annihilation operators $b_\alpha^\dagger$, b_α which diagonalize the initial Hamiltonian $H_\phi(\tau_-)$ and satisfy $b_\alpha |O_{\tau_-}\rangle = 0$ (α represents a generic set of quantum numbers and $\sum_\alpha$ shall either refer to summation or integration). Since H_ϕ is explicitly time dependent, the vacuum state is not conserved. In other words, at a given instant τ, the vacuum is defined by a new set of operators $a_{\alpha,\tau}^\dagger$, $a_{\alpha,\tau}$ as $a_{\alpha,\tau}|O_\tau\rangle = 0$. The two sets of operators at different times are related by a time-dependent unitary Bogoliubov transformation $a_{\alpha,\tau} = \mathcal{W}_\tau^\dagger b_\alpha \mathcal{W}_\tau$, where the unitary operator $\mathcal{W}_\tau$ has the property to relate the different vacuum states through $|O_{\tau_-}\rangle = \mathcal{W}_\tau |O_\tau\rangle$. Combining this expression with Equation (7.15), we observe that the state of ϕ at any given instant can be expressed from the vacuum at this moment according to

$$|\phi(\tau)\rangle = \mathcal{U}_\tau \mathcal{W}_\tau |O_\tau\rangle := \mathcal{X}_\tau |O_\tau\rangle . \tag{7.16}$$

Starting from the vacuum, the field has evolved to an excited state whose spectrum is encompassed in the nonunitary operator $\mathcal{X}_\tau$. The main result of Rubakov was to explicitly write this operator in terms of the creation-annihilation operators $a_{\alpha,\tau}^\dagger$, $a_{\alpha,\tau}$, thus acting directly on their related vacuum state $|O_\tau\rangle$. He used the method of nonunitary (resp. unitary) Bogoliubov transformations to compute $\mathcal{U}_\tau$ (resp. $\mathcal{W}_\tau$). We do not give the details of this calculation and directly present the prescription to find $\mathcal{X}_\tau$.

At any instant τ, the state of ϕ is given by[4]

$$|\phi(\tau)\rangle = \mathcal{X}_\tau |O_\tau\rangle = C(\tau) \exp\left(\frac{1}{2}\sum_{\alpha,\beta} D_{\alpha\beta}(\tau) a_{\alpha,\tau}^\dagger a_{\beta,\tau}^\dagger\right) |O_\tau\rangle \tag{7.17}$$

and the number of particles in a given mode α is then

$$N_\alpha(\tau) = \frac{\langle\phi(\tau)|a_{\alpha,\tau}^\dagger a_{\alpha,\tau}|\phi(\tau)\rangle}{\langle\phi(\tau)|\phi(\tau)\rangle} = \left(\frac{D^2(\tau)}{\mathbb{1} - D^2(\tau)}\right)_{\alpha\alpha} , \tag{7.18}$$

where $C(\tau)$ is a τ dependent c-number[5] and D is a real symmetric matrix defined as follows. The two key ingredients to compute D are the sets of functions $\{\xi_\tau^\alpha(\mathbf{x})\}$ and $\{h_\alpha(\mathbf{x},\tau)\}$. At each instant τ, the ξ_τ^α form the complete set of real wave functions of

[3] For the interesting discussion of an initially excited state, we refer to Rubakov's original paper [270].

[4] We stress that this formula is only valid if $|\phi(\tau_-)\rangle = |O_{\tau_-}\rangle$. Rubakov [[270], Equation (3.16)] gave the more complete expression for an initially excited state.

[5] This prefactor C cannot be computed from the Bogoliubov transformations, but as we will discuss later we do not need it to extract the backreaction of particle production.

the ϕ particles in the background of the bounce. So, they satisfy

$$\left[-\partial_i^2 + m^2(\mathbf{x},\tau)\right] \xi_\tau^\alpha(\mathbf{x}) = (\omega_\tau^\alpha)^2\, \xi_\tau^\alpha(\mathbf{x}) \tag{7.19}$$

with the normalization condition

$$\left(\xi_\tau^\alpha, \xi_\tau^\beta\right) := \int d^3\mathbf{x}\; \xi_\tau^\alpha(\mathbf{x})\, \xi_\tau^\beta(\mathbf{x}) = (2\omega_\tau^\alpha)^{-1}\, \delta_{\alpha\beta}. \tag{7.20}$$

On the other hand, the h_α form the set of real Euclidean mode functions similar to the positive-frequency functions in Minkowski space-time. So, they satisfy the Euclidean field equation

$$\left[-\partial_\tau^2 - \partial_i^2 + m^2(\mathbf{x},\tau)\right] h_\alpha(\mathbf{x},\tau) = 0 \tag{7.21}$$

with the condition that they exponentially decrease to zero for $\tau \to -\infty$. The last step is to construct the above matrix as

$$D = VZ^{-1}, \tag{7.22}$$

where

$$\begin{aligned} V_{\alpha\beta}(\tau) &= \left(\omega_\tau^\alpha \xi_\tau^\alpha, h_\beta\right) - \left(\xi_\tau^\alpha, \partial_\tau h_\beta\right) \\ Z_{\alpha\beta}(\tau) &= \left(\omega_\tau^\alpha \xi_\tau^\alpha, h_\beta\right) + \left(\xi_\tau^\alpha, \partial_\tau h_\beta\right) \end{aligned}. \tag{7.23}$$

In summary, the spectrum of created particles described by Equations (7.17) and (7.18) is entirely defined by the solutions of the differential Equations (7.19) and (7.21). However, the computation of the matrix D can be a very difficult task since it requires us to invert a generally infinite-dimensional matrix. In the case of a homogeneous decay, we shall see in Section 7.4 that this computation can be performed straightforwardly because the above matrices are diagonal. However, this often becomes impossible in the case of bubble nucleation. In order to avoid this problem, Rubakov actually provided an iterative way to estimate D. Before presenting this method in the next section, it is worth making some remarks on the above result.

First, the number of created particles (7.18) only has a physical meaning at $\tau = 0$ when the bubble materializes. Second, we observe that this result diverges if the matrix $\mathbb{1} - D^2$ has a zero eigenvalue. According to Rubakov, this problem could occur for the self-excitation of the tunnelling field σ itself. So we should remember this remark if we want to consider such a case. However, it is important to realize that this divergence is not related to the common UV divergences of QFT. Actually, Rubakov proved that the total number of created particles per bubble $N = \sum_\alpha N_\alpha$ is UV finite. As this result will be important for our own discussion regarding the backreaction of these particles, we shall discuss the reason of this fact below.

7.2.3 Weak particle production and UV finiteness

Let us now present how the matrix D can be approximated without inverting an infinite-dimensional matrix. It relies on the observation that D satisfies the following matrix differential equation:

$$\partial_\tau D = -(ED + DE) + B + (AD - DA) - DBD \tag{7.24}$$

where E, A and B are some matrices given by Rubakov ([270], Section 3.3.3):

$$E_{\alpha\beta} = \omega^\alpha_\tau \delta_{\alpha\beta},\ A_{\alpha\beta} = \begin{cases} 0,\ \alpha = \beta \\ \frac{1}{\omega^\alpha_\tau - \omega^\beta_\tau}\left(\xi^\alpha_\tau, \partial_\tau m^2 \xi^\beta_\tau\right),\ \alpha \neq \beta \end{cases},\ B_{\alpha\beta} = \frac{1}{\omega^\alpha_\tau + \omega^\beta_\tau}\left(\xi^\alpha_\tau, \partial_\tau m^2 \xi^\beta_\tau\right). \quad (7.25)$$

We note that D is now uniquely specified by the wave functions ξ^α_τ, without reference to h_α. Moreover, when the parameter $\partial_\tau m^2$ is small (typically compared to $(\omega^\alpha_\tau)^3$), the matrices A and B can be considered as a perturbation and Equation (7.24) can be solved iteratively. The lowest order solution of Equation (7.24) is given by the formula (3.28) in [270]:

$$D_{\alpha\beta}(\tau) = e^{-\left(W_\alpha(\tau)+W_\beta(\tau)\right)} \int_{-\infty}^{\tau} e^{\left(W_\alpha(\tau')+W_\beta(\tau')\right)} \frac{\left(\xi^\alpha_{\tau'}, \partial_{\tau'} m^2 \xi^\beta_{\tau'}\right)}{\omega^\alpha_{\tau'} + \omega^\beta_{\tau'}} d\tau', \quad (7.26)$$

where $W_\alpha(\tau) = \int_0^\tau d\tau' \omega^\alpha_{\tau'}$. This limit corresponds to say that the number of created particles is weak and the matrix D is small. Thus, Equation (7.18) for the number of created particles in a given mode and the total number of particles reduce to

$$N_\alpha(\tau) = \left(D^2(\tau)\right)_{\alpha\alpha} \quad \text{and} \quad N = \mathrm{Tr}\, D^2. \quad (7.27)$$

The two previous equations are also useful to prove that the total number of created particles is UV finite. Indeed, $\partial_\tau m^2$ becomes clearly negligible in front of $(\omega^\alpha_\tau)^3$ for high energy particles. Moreover, the m^2 term can be neglected in Equation (7.19), such that the wave functions ξ^α_τ simply become in that sector[6]

$$\xi^\alpha_\tau(\mathbf{x}) = \frac{e^{i\mathbf{k}\mathbf{x}}}{(2\pi)^{3/2}\sqrt{2\omega^{\mathbf{k}}_\tau}} \quad \text{with} \quad \omega^{\mathbf{k}}_\tau = k = |\mathbf{k}|. \quad (7.28)$$

Plugging Equation (7.28) in Equations (7.26) and (7.27), Rubakov [270] concluded that the number of particles in the UV region roughly behaves as

$$N_{UV} = \int d^3\mathbf{k} d^3\mathbf{k}' |D_{\mathbf{k}\mathbf{k}'}|^2 \propto \int d^3\mathbf{k} d^3\mathbf{k}' \frac{1}{kk'(k+k')^4} \left|\widetilde{\partial_\tau m^2}(\mathbf{k}-\mathbf{k}', \tau)\right|^2, \quad (7.29)$$

where $\widetilde{\partial_\tau m^2}$ is the Fourier transform of $\partial_\tau m^2$. The above integral converges if $\widetilde{\partial_\tau m^2}$ rapidly goes to zero when $|\mathbf{k}-\mathbf{k}'| \to +\infty$. This is actually the case since at high momentum $m \ll \omega^{\mathbf{k}}_\tau \approx k$. It means that in the UV sector the system is insensitive to the variations of the background $\partial_\tau m^2$ and this naturally regularizes the expression (7.29).

7.3 Backreaction of particle production

7.3.1 Reduced density matrix formalism

In the previous section, we assumed that the external field ϕ had no impact on the tunnelling process. We propose now an approach to estimate the effect of the created particles on the semi-classical decay rate of σ. The idea is to work with the reduced density matrix which is a tool introduced in the early days of quantum mechanics by Landau [274]. Its use is convenient to investigate the impact of the environment

[6] Although the formalism was built with real wave functions ξ^α_τ, there is no difficulty to consider complex functions in this short discussion.

on a given quantum system. Let us briefly expose how this mechanism works at the general level.

Consider a system S of interest described by a Hilbert space $\mathcal{H}_S$ coupled to an environment $\mathcal{E}$ with the Hilbert space $\mathcal{H}_\mathcal{E}$. The total state vector satisfies $|\Psi\rangle \in \mathcal{H}_S \otimes \mathcal{H}_\mathcal{E}$ and the total density operator is then given by

$$\hat{\rho} = |\Psi\rangle \langle\Psi| . \tag{7.30}$$

We suppose that we are interested in an observable $\hat{A}$ which is only related to the system S and not to the environment $\mathcal{E}$. In other words, we can write it as $\hat{A} = \hat{A}_S \otimes \hat{I}_\mathcal{E}$ where $\hat{A}_S$ acts on $\mathcal{H}_S$ and $I_\mathcal{E}$ is the identity acting on the environment. An important consequence from quantum mechanics is that the measurement of $\hat{A}$ satisfies [276, 277]

$$\langle \hat{A} \rangle_\Psi = \mathrm{Tr}\left(\hat{\rho}\hat{A}\right) = \mathrm{Tr}_{\mathcal{H}_S}\left(\hat{\rho}_S \hat{A}_S\right), \tag{7.31}$$

where $\hat{\rho}_S$ is the reduced density operator obtained by tracing over the environment:

$$\hat{\rho}_S = \mathrm{Tr}_{\mathcal{H}_\mathcal{E}}\left(\hat{\rho}\right). \tag{7.32}$$

The right-hand side of Equation (7.31) tells us that the effect of the environment only enters in the reduced density operator and thus it entirely contains the effect of these external degrees of freedom.

We can now apply this formalism to our situation as well. Indeed, the role of S and $\mathcal{E}$ is played by σ and ϕ respectively. Moreover, since the decay rate is a quantity which is only related to σ, the backreaction of the created ϕ particles is entirely encompassed in the reduced density operator. We shall now explicitly compute it and discuss its impact on Γ. From the expressions (7.10) and (7.17) describing the state vector of the model of the two scalar fields, we can write the density operator as

$$\hat{\rho}(\tau) = |\Psi(\tau)\rangle \langle\Psi(\tau)| = e^{-2S_E[\sigma_B(\tau)]} \left(\mathcal{X}_\tau |O_\tau\rangle \langle O_\tau| \mathcal{X}_\tau^\dagger\right). \tag{7.33}$$

In this context, tracing over the environment means to sum over all possible particle states of the field σ. So we define

$$|\{\alpha\}_n(\tau)\rangle = \prod_{i=1}^{n} a^\dagger_{\alpha_i,\tau} |O_\tau\rangle , \tag{7.34}$$

which describes an unnormalized n-particle state with each particle in a given mode α_i: $\{\alpha\}_n = \{\alpha_1, \alpha_2, \ldots, \alpha_n\}$. As should be the case for bosons, no restriction on $\{\alpha\}_n$ is imposed, meaning that two or more particles can be in the same state, as for example if $\alpha_i = \alpha_j$ for some $i \neq j$. To obtain the reduced density operator, we first apply the state (7.34) on both sides of (7.33) and then we have to sum over all the possible configurations $\{\alpha\}_n$ and all the numbers of particles. Thus,

$$\hat{\rho}_r(\tau) = e^{-2S_E[\sigma_B(\tau)]} \sum_{n=0}^{\infty} \sum_{\{\alpha\}_n} \frac{|\langle \{\alpha\}_n(\tau)|\mathcal{X}_\tau|O_\tau\rangle|^2}{n!}, \tag{7.35}$$

where we have introduced the factor $n!$ to ensure the correct normalization. In this formula, the dependence on the modes appears as a sum and can easily be extended to an integral in the case of a continuous index α. For convenience, we shall keep the summation symbol throughout this section.

The decay rate of σ including the backreaction of the ϕ particles is now given by

$$\Gamma_{\mathrm{Ba}} = \frac{\hat{\rho}_r(0)}{\hat{\rho}_r(-\infty)} = e^{-S_B} \frac{\mathcal{F}(0)}{\mathcal{F}(-\infty)} |C(0)|^2 , \tag{7.36}$$

where we have used $S_B = 2S_E[\sigma_B(\tau = 0)]$ and $\mathcal{F}(\tau)$ is defined as

$$\mathcal{F}(\tau) = \sum_{n=0}^{\infty} \sum_{\{\alpha\}_n} \frac{\left| \langle \{\alpha\}_n (\tau)| \exp\left(\frac{1}{2}\sum_{\alpha,\beta} D_{\alpha\beta}(\tau) a^\dagger_{\alpha,\tau} a^\dagger_{\beta,\tau}\right) |O_\tau\rangle \right|^2}{n!}. \tag{7.37}$$

As expected, we recover in Equation (7.36) the semi-classical exponential and the new correction factor. The main purpose of the next section is to find a convenient expression for $\mathcal{F}(\tau)$.

7.3.2 Explicit computation

Since we shall work at a given instant, we omit the τ dependence in the expression (7.37) for $\mathcal{F}$. As a first step, we want to simplify the matrix element $M_{\{\alpha\}_n} := \langle O| a_{\alpha_1} \dots a_{\alpha_n} \exp\left(\frac{1}{2}\sum_{\alpha,\beta} D_{\alpha\beta} a^\dagger_\alpha a^\dagger_\beta\right)|O\rangle$. Once we expand the exponential as the usual power series, we observe that the only nonvanishing contribution comes from the term which contains the same number of creation operators $a^\dagger$ as the number of annihilation operators a on their left. It implies in particular that the matrix element vanishes for n odd. So with $n = 2k$, we get

$$\begin{aligned} M_{\{\alpha\}_n} = M_{\{\alpha\}_{2k}} &= \frac{1}{2^k k!} \langle O| a_{\alpha_1} \dots a_{\alpha_{2k}} \left(\sum_{\alpha,\beta} D_{\alpha\beta} a^\dagger_\alpha a^\dagger_\beta\right)^k |O\rangle \\ &= \frac{1}{2^k k!} \sum_{\beta_1,\dots,\beta_{2k}} D_{\beta_1\beta_2} \dots D_{\beta_{2k-1}\beta_{2k}} \langle O| a_{\alpha_1} \dots a_{\alpha_{2k}} a^\dagger_{\beta_1} \dots a^\dagger_{\beta_{2k}} |O\rangle , \end{aligned} \tag{7.38}$$

where we have factorized the $D_{\alpha\beta}$ since they are real numbers. The remaining matrix element can be computed straightforwardly from the commutation rules of the bosonic operators ($[a_\alpha, a^\dagger_\beta] = \delta_{\alpha\beta}$ and zero otherwise):

$$\langle O| a_{\alpha_1} \dots a_{\alpha_{2k}} a^\dagger_{\beta_1} \dots a^\dagger_{\beta_{2k}} |O\rangle = \langle O|O\rangle \sum_{\pi \in S_{2k}} \delta_{\beta_1 \alpha_{\pi(1)}} \dots \delta_{\beta_{2k} \alpha_{\pi(2k)}} \tag{7.39}$$

where π is a permutation of the symmetric group S_{2k}. Once (7.39) is introduced into (7.38), each delta symbol selects one term of each sum over the modes β_i and thus

$$M_{\{\alpha\}_{2k}} = \langle O|O\rangle \frac{1}{2^k k!} \sum_{\pi \in S_{2k}} \prod_i^k D_{\alpha_{\pi(2i-1)} \alpha_{\pi(2i)}}. \tag{7.40}$$

The initial expression (7.37) actually involves $\left| M_{\{\alpha\}_{2k}} \right|^2$. As D is a real matrix, it reduces to take the square of Equation (7.40). As usual, the square of a sum can be written as a double sum and we find

$$\mathcal{F} = |\langle O|O\rangle|^2 \sum_{k=0}^{+\infty} \frac{1}{(2k)!(k!)^2 2^{2k}} \sum_{\{\alpha\}_{2k}} \sum_{\pi,\sigma \in S_{2k}} \prod_{i=1}^k D_{\alpha_{\pi(2i-1)} \alpha_{\pi(2i)}} D_{\alpha_{\sigma(2i-1)} \alpha_{\sigma(2i)}}. \tag{7.41}$$

Thanks to the summation over $\{\alpha\}_{2k}$, we can relabel the dummy indices in the previous equation as $\alpha_{\pi(i)} \to \alpha_i$ and $\alpha_{\sigma(i)} \to \alpha_{\pi^{-1}(\sigma(i))}$. It allows us to factorize the product $\prod_{i=1}^{k} D_{\alpha_{2i-1}\alpha_{2i}}$ in front of the summation over π and σ and then to use the identity

$$\sum_{\pi,\sigma\in S_{2k}} \prod_{i=1}^{k} D_{\alpha_{\pi^{-1}(\sigma(2i-1))}\alpha_{\pi^{-1}(\sigma(2i))}} = (2k)! \sum_{\lambda\in S_{2k}} \prod_{i=1}^{k} D_{\alpha_{\lambda(2i-1)}\alpha_{\lambda(2i)}}. \tag{7.42}$$

This equality holds because for each one of the $(2k)!$ permutations π, the sum over σ is always the same up to the order of the terms. The reason behind this statement comes from the group property of S_{2k}: when π is fixed and σ runs over all the elements of the symmetric group, $\pi^{-1}\circ\sigma$ covers the whole group as well. So, we have reduced the expression to a single sum over the permutations and moreover the two factors $(2k)!$ cancel out:

$$\mathcal{F} = |\langle O|O\rangle|^2 \sum_{k=0}^{\infty} \underbrace{\frac{1}{(k!)^2 2^{2k}} \sum_{\{\alpha\}_{2k}} \sum_{\lambda\in S_{2k}} \prod_{i=1}^{k} D_{\alpha_{2i-1}\alpha_{2i}} D_{\alpha_{\lambda(2i-1)}\alpha_{\lambda(2i)}}}_{:=A_k}. \tag{7.43}$$

To understand how to further simplify this expression, it is worth writing the first terms A_k explicitly. Since the matrix D is symmetric, the summation over the modes $\alpha_1, \alpha_2, \ldots$ gives the trace of an even power of the matrix D, as for instance

$$\sum_{\alpha_1,\alpha_2} D_{\alpha_1\alpha_2} D_{\alpha_1\alpha_2} = \sum_{\alpha_1,\alpha_2} D_{\alpha_1\alpha_2} D_{\alpha_2\alpha_1} = \sum_{\alpha_1} \left(D^2\right)_{\alpha_1\alpha_1} = \mathrm{Tr}\left(D^2\right). \tag{7.44}$$

So a straightforward computation gives us the first four terms:

$$\begin{aligned} A_0 &= 1 \\ A_1 &= \tfrac{1}{2}\,\mathrm{Tr}\left(D^2\right) \\ A_2 &= \tfrac{1}{8}\,\mathrm{Tr}\left(D^2\right)^2 + \tfrac{1}{4}\,\mathrm{Tr}\left(D^4\right) \\ A_3 &= \tfrac{1}{48}\,\mathrm{Tr}\left(D^2\right)^3 + \tfrac{1}{8}\,\mathrm{Tr}\left(D^2\right)\mathrm{Tr}\left(D^4\right) + \tfrac{1}{6}\,\mathrm{Tr}\left(D^6\right). \end{aligned} \tag{7.45}$$

It is clear from both (7.43) and (7.45) that each term A_k is a sum of products of the following form: $\mathrm{Tr}(D^2)^{j_1}\,\mathrm{Tr}(D^4)^{j_2}\ldots\mathrm{Tr}(D^{2k})^{j_k}$, where the integers j_i satisfy $j_1 + 2j_2 + \ldots + kj_k = k$. Such a set $\{j_i\}_k$ is called a partition of k. Thus, A_k can be written as a sum over all the partitions of k as

$$A_k = \sum_{\{j_i\}_k} \frac{C_{\{j_i\}_k}}{(k!)^2 2^{2k}} \prod_{i=1}^{k} \mathrm{Tr}\left(D^{2i}\right)^{j_i}, \tag{7.46}$$

where each coefficient $C_{\{j_i\}_k}$ counts the number of permutations $\lambda \in S_{2k}$ in (7.43) which lead to the partition $\{j_i\}_k$. In particular, they satisfy $\sum_{\{j_i\}_k} C_{\{j_i\}_k} = (2k)!$. According to a combinatorial argument given in [5] Appendix A, we find an explicit formula for them:

$$C_{\{j_i\}_k} = \frac{(k!)^2 2^{2k}}{\prod_{i=1}^{k} j_i!\,(2i)^{j_i}}. \tag{7.47}$$

This result significantly simplifies A_k and $\mathcal{F}$. Indeed, if we insert it in (7.46) and define for convenience the variables $a_i := \mathrm{Tr}\left(D^{2i}\right) i!/(2i)$, we find that A_k actually

corresponds to a complete Bell polynomial $B_k(a_1,\dots,a_k)$ [307]:

$$A_k = \sum_{\{j_i\}_k} \prod_{i=1}^{k} \frac{1}{j_i!}\left(\frac{a_i}{i!}\right)^{j_i} = \frac{1}{k!}B_k(a_1,a_2,\dots,a_k). \tag{7.48}$$

It is a well-known fact in combinatorics that these polynomials give an exponential formula for any formal series $a_1 x + \cdots + \frac{a_n}{n!}x^n + \cdots$ [308]:

$$\sum_{k=0}^{+\infty} \frac{B_k(a_1,\dots,a_k)}{k!}x^k = \exp\left(\sum_{k=1}^{+\infty}\frac{a_k}{k!}x^k\right). \tag{7.49}$$

If we set $x = 1$, the left-hand side of this equation is exactly the sum over the terms A_k. So it is now straightforward to conclude that $\mathcal{F}$ is given by the following expressions

$$\begin{aligned}\mathcal{F} &= |\langle O|O\rangle|^2 \exp\left(\sum_{k=1}^{\infty}\frac{\mathrm{Tr}\left(D^{2k}\right)}{2k}\right)\\ &= |\langle O|O\rangle|^2 \exp\left(-\frac{1}{2}\,\mathrm{Tr}\ln\left(\mathbb{1}-D^2\right)\right)\\ &= |\langle O|O\rangle|^2 \frac{1}{\sqrt{\mathrm{Det}\left(\mathbb{1}-D^2\right)}}.\end{aligned} \tag{7.50}$$

From this result, we can now derive a convenient expression for the backreaction factor $\frac{\mathcal{F}(0)}{\mathcal{F}(-\infty)}$ in Equation (7.36). Since $D(\tau=-\infty)=0$ and $\langle O_{\tau=-\infty}|O_{\tau=-\infty}\rangle = \langle O_\tau|\mathcal{W}_\tau^\dagger\mathcal{W}_\tau|O_\tau\rangle = \langle O_\tau|O_\tau\rangle$, we obtain the modified decay rate as follows:

$$\Gamma_{\mathrm{Ba}} = \frac{|C_{\tau=0}|^2 e^{-S_B}}{\sqrt{\mathrm{Det}\left(\mathbb{1}-D^2_{\tau=0}\right)}} = |C_{\tau=0}|^2 e^{-S_B-\frac{1}{2}\mathrm{Tr}\ln\left(\mathbb{1}-D^2_{\tau=0}\right)}. \tag{7.51}$$

In this expression, the backreaction of the real ϕ particles produced during the decay of the field σ is encompassed in the prefactor $\left[\mathrm{Det}\left(\mathbb{1}-D^2_{\tau=0}\right)\right]^{-1/2}$. On the other hand, the coefficient $|C_{\tau=0}|^2$ can be evaluated from the well-known path integral method of Callan and Coleman [218], corresponding to one-loop quantum fluctuations of ϕ. We shall now exclusively focus our attention on the properties of the new backreaction factor.

7.3.3 Interpretation of the backreaction factor

Without considering any particular model, Equation (7.51) gives interesting information on the effect of particle production during tunnelling. The first remark is to realize that our derivation has been formal and that we should pay attention to potential divergences. As was already the case for the number of particles (7.18), we observe again a problematic behavior when $\mathbb{1}-D^2$ has a zero eigenvalue. As already explained, this has nothing to do with the usual UV divergences and this problem should be treated on a case-by-case basis. More interestingly, we can show that the backreaction factor is UV finite. The reason is clear if we look at the first line of Equation (7.50). Indeed, we already showed in Equation (7.29) that the first term $\mathrm{Tr}\,D^2$ is finite. It is then straightforward to extrapolate the argument to each following term, $\mathrm{Tr}\left(D^{2k}\right)$ for $k=2,3,\dots$, since they will converge faster and faster.

We conclude, in contrast with one-loop quantum corrections, that the backreaction factor does not require any renormalization technique in order to be computed.

The second remark is related to the weak particle production limit. As we explained in Section 7.2.3, the total number of created particles is given in this approximation by $N \approx \mathrm{Tr}\, D^2$ since D is small. For the same reason, the terms $\mathrm{Tr}\left(D^{2k}\right)$ with $k > 2$ appearing in Equations (7.50) and (7.51) are negligible in front of the dominant term $\mathrm{Tr}\, D^2$. It means that in this limit, the modified decay rate becomes $\Gamma_{\mathrm{Ba}} \approx e^{-S_B+\frac{1}{2}N}$. In other words, we see that the backreaction is directly given by one half of the total number of produced particles. This is a useful result if we are interested in an approximated value of the backreaction, since its evaluation does not require us to perform any computation in addition to Rubakov's prescription to find N.

The third observation of interest is that the backreaction of scalar particle production enhances the semi-classical decay probability in this given framework. Looking at Equation (7.51) or at the approximate formula we just discussed, $\Gamma_{\mathrm{Ba}} \approx e^{-S_B+\frac{1}{2}N}$, we observe that the backreaction contribution is positive compared to the semi-classical $(-S_B)$ contribution. At first sight, this result might seem surprising. During tunnelling, the field σ transfers some amount of energy to the environment ϕ which consequently exhibits a spectrum of particles. We may have expected that this dissipation from the system to the surrounding bath slows down the decay process. However, the created particles are fluctuations of the field ϕ which in turn reacts on σ. We are actually facing a situation which has some similarities with the fluctuation-dissipation relation in statistical physics [309]. Both the system and the environment interact with each other in a nontrivial way and eventually Equation (7.51) tells us that the tunnelling process is enhanced in this particular case. This kind of behavior has already been discussed in a variety of situations. The investigation of the impact of the environment on the tunnelling of a quantum mechanical particle was initiated by Caldeira and Leggett in [310]. By considering a dissipative interaction with a bath of harmonic oscillators, they derived a friction term suppressing the decay rate. On the other hand, [311, 312] subsequently described systems for which the impact of the environment results in an enhancement of the tunnelling probability of the quantum particle. More closely related to our case, [313, 314] also reported an enhanced decay rate for a quantum field interacting with some external degrees of freedom.

Our next objective is to quantitatively estimate the contribution of the backreaction in comparison to the semi-classical decay exponent S_B. This requires us to explicitly evaluate the formula (7.51) and thus to consider some specific models.

7.4 A toy model potential

In order to illustrate the mechanism of particle production and the related backreaction, we consider the following tractable potential:

$$V(\sigma) = \frac{\lambda}{8}\left(\sigma^2 - v^2\right)^2 - \frac{\epsilon}{2v}(\sigma + v), \tag{7.52}$$

where λ, v and ϵ are three parameters with dimension $[\lambda] = E^0$, $[v] = E^1$ and $[\epsilon] = E^4$. This model is widely used in the literature since the bounce solution can be computed analytically in the limit of small ϵ. In particular, Coleman [217] introduced it to show how to compute the semi-classical decay rate S_B and Rubakov

[270] used it to illustrate its prescription of particle production. Our aim is now to extend these investigations by estimating the backreaction of the created particles.

As already discussed in Section 7.2.1, we can focus on two different types of decay, namely the nucleation of an $O(4)$ bubble or a homogeneous process in a finite volume $\mathcal{V}$. We shall consider both these cases in the approximation that the energy difference between the two vacua of the potential $V(\sigma)$ is much smaller than the height of the barrier. It is not difficult to show that it corresponds to a small value of ϵ. Indeed, in that case, the vacua are approximately located at $\sigma_{T/F} \approx \pm v$, the energy difference becomes $\Delta V = |V(\sigma_F) - V(\sigma_T)| \approx \epsilon$ and the barrier height is given by $V_B \approx V(0) \approx \frac{1}{8}\lambda v^4$. As expected, the requirement $\Delta V \ll V_B$ is fulfilled for

$$\epsilon \ll \frac{1}{8}\lambda v^4. \tag{7.53}$$

We compute the semi-classical decay exponent S_B in the two cases of interest:

1. Thin-wall (TW) bounce

   Let us focus first on the bubble nucleation under the condition (7.53). The bounce satisfying Equation (7.5) is well approximated by the kink

   $$\sigma(\tilde{r}) = v \tanh\left(\frac{1}{2}v\sqrt{\lambda}(R - \tilde{r})\right), \tag{7.54}$$

   where R is the radius of the bubble at the nucleation time $\tau = 0$. The value of this parameter which minimizes the action (7.6) is given by

   $$R^\star = \frac{2\sqrt{\lambda}v^3}{\epsilon}. \tag{7.55}$$

   The semi-classical decay exponent is then computed by evaluating the action (7.6) along the solution (7.54) with this value of $R^\star$. This gives

   $$S_{B,TW} = \frac{8}{3}\pi^2\frac{\lambda^2 v^{12}}{\epsilon^3}. \tag{7.56}$$

   We now understand why this solution is called a thin-wall bubble. Under the approximation of small ϵ, its radius (7.55) is large while the transition wall between the false and true vacua is thin because of the tanh shape of Equation (7.54).

2. Homogeneous bounce

   We consider a spatially homogeneous solution $\sigma_B(\tau)$ of Equation (7.3) in a sphere of radius R_H. For a small ϵ, the result is again the kink:

   $$\sigma(\tau) = v \tanh\left(\frac{1}{2}v\sqrt{\lambda}\tau + C\right). \tag{7.57}$$

   The constant C is chosen in order to satisfy the condition that the field emerges under the barrier at $\tau = 0$. Since the escape point is given by $\sigma_{esc} = v - \frac{1}{v}\sqrt{\frac{2\epsilon}{\lambda}} + O(\epsilon)$, we have

   $$\tanh(C) \approx 1 - \frac{1}{v^2}\sqrt{\frac{2\epsilon}{\lambda}}. \tag{7.58}$$

We can evaluate the Euclidean action (7.4) along the bounce taking into account the above value of C and the volume $\mathcal{V} = \frac{4}{3}\pi R_H^3$.[7] In the limit of vanishing ϵ, we get

$$S_{B,hom} = \frac{16}{9}\pi R_H^3 \sqrt{\lambda} v^3. \tag{7.59}$$

Looking at the tanh form of the bounce, we observe that the field is nearly constant in Euclidean time until it suddenly endures a rapid transition from its false vacuum to the escape point beyond the barrier. This change occurs around the moment $\tilde{\tau} < 0$ corresponding to the center of the kink:

$$\sigma(\tilde{\tau}) = 0 \Rightarrow \tilde{\tau} = -\frac{2C}{v\sqrt{\lambda}}. \tag{7.60}$$

Now that we have explicitly computed the semi-classical exponents in both cases, we rewrite them in terms of dimensionless parameters. First we introduce $\alpha = \frac{\lambda v^4}{\epsilon}$ such that the approximation (7.53) of small ϵ reduces to $\alpha \gg 8$. Another useful quantity is the ratio $\beta = \frac{R_H}{R^\star}$ between the size of the homogeneous bounce and the radius of the thin-wall bubble. It is straightforward to see that the semi-classical decay exponents reduce to

$$S_{B,TW} = \frac{8\pi^2}{3}\frac{\alpha^3}{\lambda} \qquad S_{B,hom} = \frac{128\pi}{9}\frac{\alpha^3\beta^3}{\lambda}. \tag{7.61}$$

From this parametrization, we can give a few remarks. First, the thin-wall exponent is generally large and leads to a highly suppressed decay probability. Indeed, for the minimal acceptable value $\alpha \sim 10$ and for λ of order one, $S_{B,TW}$ is already of order four. On the other hand, there is more freedom for the homogenous factor $S_{B,hom}$, because of the parameter β entering in it. When $\beta = 1$, namely when the bounces are of the same size, we observe that the two types of decay have a similar probability to occur. Since the radius $R^\star$ of the thin-wall bubble is very large, it is reasonable to also consider a homogeneous tunnelling taking place in a smaller volume. In that case, the decay probability would be more significant. For instance, when $\alpha = 10$, $\beta = 0.1$ and $\lambda = 1$, we find $S_{B,hom} \approx 45$ and $e^{-S_{B,hom}} \approx 10^{-20}$. We shall make use of this discussion to investigate how the backreaction of particle production modifies these results.

7.4.1 Backreaction during a homogeneous bounce

We consider the production of ϕ particles during the homogeneous tunnelling process. As described in Section 7.2.2, the key parameter to introduce is the coupling $m^2(\sigma)$ between the two fields σ and ϕ. Since the homogeneous bounce (7.57) is almost a step function, we approximate this coupling in the following way:

$$m^2(\sigma) = m^2(\tau) = \begin{cases} m_-^2 & \text{for} \quad \tau < \tilde{\tau} \\ m_+^2 & \text{for} \quad \tau > \tilde{\tau} \end{cases}, \tag{7.62}$$

where $m_\pm$ are the masses of the ϕ particles in the true and false vacua, respectively. We remind that the transition occurs at the instant $\tilde{\tau}$ given by Equation (7.60) and that $\tilde{\tau} < 0$.

[7] Note that the solution (7.57) only covers one half of the bounce ($\tau < 0$) and that $\sigma(-\tau)$ gives the $\tau > 0$ part.

In this model, Rubakov's prescription to compute the matrix D can be performed easily. According to the spherical background geometry, the indices of this matrix are given by the discrete radial momentum $k = \frac{n}{R_H}$ ($n = 0, 1, 2, \ldots$) and the usual angular momentum (l, m) ($0 \leq l \leq n$, $-l \leq m \leq l$). According to a computation detailed in [5] Appendix B, we note that D is diagonal and does not depend on (l, m). Omitting these indices, the diagonal part of this matrix reads

$$D_{nn}(\tau = 0) = \frac{\omega_+ - \omega_-}{\omega_+ + \omega_-} e^{2\omega_+ \tilde{\tau}}, \tag{7.63}$$

where

$$\omega_\pm = \sqrt{k^2 + m_\pm^2} = \sqrt{\frac{n^2}{R_H^2} + m_\pm^2}. \tag{7.64}$$

It is worth directly rewriting this expression in terms of dimensionless quantities. In addition to the two parameters α, β already introduced above, we define $\delta_\pm = R_H m_\pm$. From the previous equation for D_{nn} and expression (7.60) for $\tilde{\tau}$, it is straightforward to show that

$$D_{nn} = \frac{\sqrt{n^2 + \delta_+^2} - \sqrt{n^2 + \delta_-^2}}{\sqrt{n^2 + \delta_+^2} + \sqrt{n^2 + \delta_-^2}} e^{-2\frac{\sqrt{n^2+\delta_+^2}}{\tilde{\alpha}\beta}}, \tag{7.65}$$

where $\tilde{\alpha} := \frac{\alpha}{\operatorname{arctanh}\left(1 - \sqrt{\frac{2}{\alpha}}\right)}$.

In this way, the backreaction is entirely determined by the four parameters (α, β, $\delta_\pm$). We can now compute the correction factor entering in Equation (7.51). Since D is diagonal, the logarithm of $\mathbb{1} - D^2$ is just the logarithm of each diagonal element and we get

$$\frac{1}{2} \operatorname{Tr} \ln\left(\mathbb{1} - D^2\right) = \frac{1}{2} \sum_{n=0}^{+\infty} \sum_{l=0}^{n} \sum_{m=-l}^{l} \ln\left(1 - D_{nn}^2\right) = \frac{1}{2} \sum_{n=0}^{+\infty} (n+1)^2 \ln\left(1 - D_{nn}^2\right). \tag{7.66}$$

For consistency with our discussion in Section 7.3.3, we explicitly check that this series is convergent. Indeed, its asymptotic expansion is given by

$$\frac{1}{2}(n+1)^2 \ln\left(1 - D_{nn}^2\right) \xrightarrow[n\to\infty]{} \left[-\frac{1}{32n^2}\left(\delta_+^2 - \delta_-^2\right)^2 + O\left(\frac{1}{n^3}\right)\right] e^{-4\frac{n}{\tilde{\alpha}\beta}}, \tag{7.67}$$

meaning that the backreaction is exponentially suppressed at high momentum. It is also clear that the dominant part in Equation (7.66) comes from the $n = 0$ term and so the computation of this leading contribution will already tell us if the backreaction is negligible or significant compared to $S_{B,hom}$. For simplicity, we restrict this analysis to two limiting cases, namely a small and a large mass difference.

- Small mass difference: $\Delta\delta^2 := \delta_+^2 - \delta_-^2 \ll \delta_+^2$.
  In this limit, the $n = 0$ term in the series (7.66) becomes

$$\frac{1}{2} \ln\left(1 - D_{00}^2\right) = -\frac{1}{32}\left(\frac{\Delta\delta^2}{\delta_+^2}\right)^2 e^{-4\frac{\delta_+}{\tilde{\alpha}\beta}} + O\left(\left(\frac{\Delta\delta^2}{\delta_+^2}\right)^3\right). \tag{7.68}$$

and we directly conclude that this contribution is small. Indeed, the exponential is bounded by 1 and $\frac{\Delta\delta^2}{\delta_+^2} \ll 1$ because of the small mass difference assumption. Thus we conclude that the backreaction is negligible in front of values of $S_{B,hom}$ which are typically bigger than order one.

- Large mass difference: $\delta_- \ll \delta_+$.
  Under this assumption, we obtain

$$\frac{1}{2}\ln\left(1-D_{00}^2\right) = \frac{1}{2}\ln\left(1-e^{-4\frac{\delta_+}{\tilde{\alpha}\tilde{\beta}}}\right) + O\left(\frac{\delta_-}{\delta_+}\right), \tag{7.69}$$

  where the leading term corresponds to directly take $\delta_- = 0$. In contrast with the previous case, this contribution can be arbitrarily large when $\frac{\delta_+}{\tilde{\alpha}\tilde{\beta}}$ becomes small. Thus we should investigate if the backreaction could become of the order of $S_{B,hom}$ for some reasonable values of these parameters. It turns out that the expression (7.69) grows very slowly because of the logarithm. Hence the backreaction would unlikely be significant in front of large values of $S_{B,hom}$. For instance for $(\alpha,\beta) = (10,1)$, we saw that $S_{B,hom} = O(10^4)$ and so δ_+ should be as small as many thousand orders of magnitude for the backreaction to be non-negligible.
  However the situation is more interesting for smaller decay exponents. When $(\alpha,\beta) = (10,0.1)$ we found $S_{B,hom} \approx 45$ and in this case the correction (7.69) becomes significant for acceptable values of δ_+. Explicitly, we have

$$-\frac{1}{2}\ln\left(1-D_{00}^2\right)\Big|_{(\alpha,\beta,\delta_+)=(10,0.1,\{10^{-1},10^{-4},10^{-10}\})} \approx \{0.8,\ 4.1,\ 11.2\}\,. \tag{7.70}$$

  In terms of the decay probability, this corresponds to corrections respectively of order $e^{0.8} = O(1)$, $e^{4.1} = O(10^2)$ and $e^{11.2} = O(10^5)$, in front of $e^{-S_B} \approx 10^{-20}$. It confirms that in this case the backreaction enhances the decay rate by some orders of magnitude.

Although we have not investigated the entire range of parameters of this toy model, the two above cases already give us useful information. The first remark is that large semi-classical decay exponents would generally be insensitive to the production of particles. However, we were also able to exhibit a choice of parameters leading to weaker values of $S_{B,hom}$ which are significantly modified by the particle backreaction.

7.4.2 Backreaction during a thin-wall bounce

We want to perform the same kind of analysis as above but during the nucleation process of the thin-wall bubble. Since the bounce solution (7.54) is again almost a step function, the system is also well described by the two quantities m_+, m_- corresponding to the masses of the ϕ particles in the background of the true and false vacua, respectively.

In contrast to the homogeneous case, the matrix D is not diagonal. A tractable way to compute it is the use of the weak particle production limit described in Section 7.2.3. Under this approximation, we saw in Section 7.3.3 that the backreaction correction is given by one half of the total number of created particles as $\frac{1}{2}\,\mathrm{Tr}\,D^2$. Fortunately for us, Rubakov ([270], Section 5) already computed this quantity since he was interested in the number of created particles in this model. He proved that the

main contribution to the number of produced particles comes from the case $m_- \ll (R^\star)^{-1} \ll m_+$ and from particles with radial momentum $m_- \ll p \ll m_+$ and angular momentum $l = m = 0$. In these conditions, he found that $N = \mathrm{Tr}\, D^2 = O(10^{-2})$. It means that the number of particles is small (at the best roughly one particle produced per 100 bubbles) whatever the values of the parameters. Remembering that $S_{B,TW}$ in Equation (7.61) is at least of order $O(10^4)$, it is clear that the backreaction factor $\frac{1}{2}\,\mathrm{Tr}\, D^2$ is completely negligible.

7.5 Chapter summary

We have presented an approach to compute the backreaction of particle production on the decay rate of a false vacuum. We explicitly derived a formula which corrects the usual semi-classical decay probability, in the case of a tunnelling field coupled to a scalar environment in flat space-time. Starting from Rubakov's formalism describing the spectrum of created particles, the main idea of this work was to integrate out this external bath of particles using the reduced density matrix prescription.

As a first consequence, we found that the correction factor is UV finite. Hence its computation does not require any renormalization techniques in contrast with the calculation of one-loop quantum corrections. We also showed that scalar particle production enhances the decay probability in the context of this formalism. It may be interpreted as the sign that the dissipation of the tunnelling field into the environment is compensated by the external fluctuations. Another important observation is the fact that the backreaction is given by one half of the total number of created particles, in the approximation that they are weakly produced. In other words, Rubakov's prescription gives directly both the spectrum of particles and their backreaction in this limit.

These general remarks would not be of particular importance if the backreaction were always negligible compared to the semi-classical decay rate. That is why we explicitly computed this effect for a toy model potential. We found a negligible impact in the case of the thin-wall bubble nucleation. However, when the field decays homogeneously in a finite volume, we computed a significant correction for a reasonable choice of parameters. Therefore, it would be relevant to apply this formalism to more realistic systems in the future. One of the most interesting scenarios to investigate seems to be the decay of the Higgs field during inflation through the Hawking-Moss instanton which is indeed a homogeneous process (see e.g. [288]). This would require to extend the formalism presented in this Chapter to include possible gravitational effects.

Chapter 8

Conclusion

This thesis has been the occasion to investigate various topics at the interplay between particle physics and cosmology. More particularly, we studied three main subjects. Chapter 4 proposed first to probe the quantum nature of space-time with gravitational waves produced from a black hole merger. We modelled the effect of a hypothetical non-commutative space-time through a modification of the energy-momentum tensor describing the two inspiraling black holes. We then made use of the post-Newtonian formalism to get an analytic prediction for the waveform produced by these co-rotating bodies. We showed that the leading non-commutative correction compared to general relativity appears at 2PN order, namely at order $(v/c)^4$. Whereas such a correction is usually small for slow-moving systems in weak gravitational fields, it plays a more important role when considering almost relativistic black hole binaries. Indeed, by comparing our theoretical prediction to the signal GW150914 detected by LIGO/Virgo, we were able to extract the most stringent constraint to date on the scale of non-commutativity, improving previous bounds by several orders of magnitude.

The second topic, which has been investigated in details in Chapters 5 and 6, is the production of a stochastic GW background from beyond the standard model cosmological phase transitions. We explicitly considered two different particle physics models that exhibit non standard PT dynamics. The first model was based on a non-linear realization of the electroweak gauge group. In this scenario, electroweak symmetry breaking does not rely on the existence of a scalar electroweak doublet. The physical Higgs field can therefore be treated as a singlet allowing the appearance of BSM interactions without new particles. We considered in particular the addition of a Higgs cubic coupling having the advantage to force the electroweak PT to be first-order. We found an interesting range of parameters for which the PT is long-lasting and supercooled, thus resulting in the production of low-frequency GWs potentially detectable by pulsar timing arrays.

The second theory we considered was a scale-invariant extension of the standard model containing a dilaton field. Phenomenological considerations predict a very light dilaton particle with a mass as small as 10^{-8} eV. We emphasized that the electroweak symmetry breaking cannot happen by itself unless it is triggered by the chiral QCD transition occurring at a temperature around $T \sim 130$ MeV. It was particularly interesting to realize that the chiral transition is expected to be first-order since all the quarks are still massless at that period. Low frequency GWs are therefore also expected to be produced in this scenario.

These two analyses also showed that it is not a trivial task to obtain accurate GW predictions from the knowledge of a particle physics model. For example, we had to perform several approximations at various stages of our computations. We pointed out that future investigations and the development of new tools (such as new numerical simulations) could allow physicists to get more accurate theoretical results.

Despite these limitations, our overall conclusion is that the study of the stochastic GW background should provide relevant information about particle physics which is complementary to collider physics.

The last topic we considered was the study of the backreaction of particle production on false vacuum decay. We argued that quantum tunnelling of metastable fields is an important process as it appears in various domains of physics, such as phase transitions. It is therefore important to clearly investigate all the effects that could influence the decay rate of these fields. In our case of interest, we investigated how (real) particles produced during the tunnelling of a scalar field in flat spacetime influence the decay rate of the process. By using a density matrix formalism, we were able to explicitly compute a correction factor accounting for this new effect. We then used a toy model potential to investigate the significance of this correction factor compared to the usual semi-classical decay rate. We predicted negligible effects if the transition occurs through bubble nucleation, as only very few particles are produced per bubbles. However, we saw that backreaction can be significant for homogeneous transitions occurring in a finite volume. This motivates us to try to expand this formalism in the future and to apply it to scenarios of homogeneous transitions that could occur during inflation.

Overall, an important conceptual conclusion we can draw from our study is that some intriguing relationships between microscopic and macroscopic phenomena exist, which seem a priori completely unrelated taking into account the different scales at which they occur. A second aspect which has attracted our interest during the past few years is that the interplay between particle physics and cosmology is one of the fields of research which has the best potential to cast doubt on our knowledge and to show the limits of our understanding of nature.

Appendix A

Appendix

A.1 Finite temperature potential with non-linearly realized electroweak gauge group

We give here the detailed expression of the finite temperature potential (5.6) of Section 5.1.1 and which was used in [3, 198]. The Coleman-Weinberg contribution $V_{CW}^{(1)}$ at $T = 0$ is given by:

$$V_{CW}^{(1)}(\rho) = \sum_{i=W,Z,t,h} n_i \frac{m_i^4(\rho)}{64\pi^2}\left(\ln\left(\frac{m_i^2(\rho)}{v^2}\right) - \frac{3}{2}\right) . \tag{A.1}$$

The finite temperature part $V^{(1)}(\rho, T)$ is defined via the thermal function J:

$$\begin{aligned} V^{(1)}(\rho, T) &= \frac{T^4}{2\pi^2}\sum_{i=W,Z,t,h} n_i J\left[\frac{m_i^2(\rho)}{T^2}\right], \\ J[m_i^2\beta^2] &:= \int_0^\infty dx\, x^2 \ln\left[1 - (-1)^{2s_i+1} e^{-\sqrt{x^2+\beta^2 m_i^2}}\right], \end{aligned} \tag{A.2}$$

where s_i corresponds to the spin and n_i to the number of degrees of freedom of the particle species i. The field-dependent masses $m_i(\rho)$ are given by

$$\begin{aligned} n_h &= 1, & m_h^2(\rho) &= 3\lambda\rho^2 + 2\kappa\rho - \mu^2 \\ n_Z &= 3, & m_Z^2(\rho) &= \frac{g_2^2 + g_1^2}{4}\rho^2, \\ n_W &= 6, & m_W^2(\rho) &= \frac{g_2^2}{4}\rho^2, \\ n_t &= -12, & m_t^2(\rho) &= \frac{y_t^2}{2}\rho^2. \end{aligned} \tag{A.3}$$

The correction from Daisy terms can be described by a shift in the longitudinal components of the respective boson masses by their Debye correction (cf. e.g. [165, 315]):

$$\begin{aligned} m_h^2 \to m_h^2(\rho, T) &= m_h^2(\rho) + \frac{1}{4}\lambda T^2 + \frac{1}{8}g_2^2 T^2 + \frac{1}{16}(g_2^2 + g_1^2)T^2 + \frac{1}{4}y_t^2 T^2, \\ m_{W_L}^2(\rho) \to m_{W_L}^2(\rho, T) &= m_W^2(\rho) + \frac{11}{6}g_2^2 T^2, \\ m_{Z_L}^2(\rho) \to m_{Z_L}^2(\rho, T) &= \frac{1}{2}\left[m_Z^2(\rho) + \frac{11}{6}\left(g_2^2 + g_1^2\right)T^2 + \Delta(\rho, T)\right], \\ m_{\gamma_L}^2(\rho) \to m_{\gamma_L}^2(\rho, T) &= \frac{1}{2}\left[m_Z^2(\rho) + \frac{11}{6}\left(g_2^2 + g_1^2\right)T^2 - \Delta(\rho, T)\right], \end{aligned} \tag{A.4}$$

where:

$$\Delta^2(\rho, T) := \left(m_Z^2(\rho) + \frac{11}{6}(g_2^2 + g_1^2)T^2\right)^2 - g_1^2 g_2^2 \frac{11}{3} T^2 \left(\frac{11}{3}T^2 + \rho^2\right). \tag{A.5}$$

The number of degrees of freedom is then:

$$g_{W_L} = 2g_{Z_L} = 2g_{\gamma_L} = 2, \qquad g_{W_T} = 2g_{Z_T} = 2g_{\gamma_T} = 4. \tag{A.6}$$

A.2 Calculation of the finite temperature effective potential with scale invariance

This appendix shows how to compute the thermal effective potential that we are using in Section 5.2.2 to characterize the PT that take place in the scale invariant model of Section 5.1.2. The contribution of a scalar field with field-dependent mass, $m(h)$, to the thermal effective potential with a 4-dimensional cut-off, $\omega_n^2 + \vec{p}^2 \leq \Lambda^2$ is given by:

$$V_T(h) = \frac{1}{2\beta} \int_{|\vec{p}|\leq\Lambda} \frac{d^3p}{(2\pi)^3} \sum_{n=-N}^{N} \ln\left(1 + \frac{m^2(h)}{\omega_n^2 + \vec{p}^2}\right), \tag{A.7}$$

where $N = \left\lfloor \frac{\beta}{2\pi}\sqrt{\Lambda^2 - \vec{p}^2} \right\rfloor$, $\beta = \frac{1}{T}$ and $\omega_n = \frac{2n\pi}{\beta}$. Define

$$v(y) = \sum_{n=-N}^{N} \ln(n^2 + y^2) \tag{A.8}$$

and $\omega^2 = p^2 + m^2(h)$. The one-loop contribution then becomes

$$V_T(h) = \frac{1}{2\beta} \int_{|\vec{p}|\leq\Lambda} \frac{d^3p}{(2\pi)^3} v\left(\frac{\beta\omega}{2\pi}\right) - \frac{1}{2\beta} \int_{|\vec{p}|\leq\Lambda} \frac{d^3p}{(2\pi)^3} v\left(\frac{\beta p}{2\pi}\right). \tag{A.9}$$

The difference of these integrals can thus be found by evaluating the first integral and discarding any m-indepenedent terms. By using the fact that $\ln(n^2 + y^2) = \ln(n + iy) + \ln(n - iy)$, it can be shown using the properties of Gamma functions as well as the Euler reflection formula that:

$$v(y) = 2\ln\sinh \pi y + 4\Re \ln\Gamma(1 + N + iy) + m\text{-independent terms.} \tag{A.10}$$

The first term of Equation A.10, when integrated, yields:

$$\begin{aligned} &\frac{1}{2\beta} \int_{|\vec{p}|\leq\Lambda} \frac{d^3p}{(2\pi)^3} \left(2\ln\sinh\left(\frac{\beta\omega}{2}\right) - 2\ln\sinh\left(\frac{\beta p}{2}\right)\right) \\ &= \frac{1}{2\pi^2}\left[\frac{1}{8}m^2\Lambda^2 + \left(\frac{1}{4} - \ln 2 - \ln\frac{\Lambda}{m}\right)\frac{m^4}{16} + \frac{1}{\beta^4} J_B(m^2\beta^2)\right] \end{aligned} \tag{A.11}$$

where terms with negative powers of Λ are ignored and

$$J_B(m^2\beta^2) = \int_0^\infty dx x^2 \ln\left[1 - e^{-\sqrt{x^2 + \beta^2 m^2}}\right].$$

(In the above we take the upper integral limit to infinity, as contributions for large x to the integral decay exponentially.) Using the Schwarz reflection principle and the

Stirling formula, the second term of Equation A.10 can be expanded as

$$4\Re \ln \Gamma(1+z) = 4\Re z \ln z + 2\Re \ln z + \frac{1}{3}\Re\frac{1}{z} + O\left(\frac{1}{z^3}\right) + m\text{-independent terms.} \tag{A.12}$$

where $z = N + iy$. Integrating this, one finds that the corresponding contribution to Equation A.9 is

$$\frac{2\ln 2 - 1}{64\pi^2}m^4 - \frac{1}{32\pi^2}m^2\Lambda^2 + O\left(\frac{1}{\beta\Lambda}\right) + O\left(\frac{m}{\Lambda}\right). \tag{A.13}$$

The integration process is rather arduous, as N must be split into a continuous function and a sawtooth function. One then takes advantage of the fact that the sawtooth function has a small period to extract relevant terms of positive powers of Λ. Hence, adding equations A.11 and A.13 together, one obtains:

$$V_T(h) = \frac{1}{32\pi^2}m^2\Lambda^2 - \frac{1}{128\pi^2}m^4 - \frac{1}{32\pi^2}\ln\frac{\Lambda}{m}m^4 + \frac{1}{2\pi^2}T^4 J_B(m^2/T^2) \tag{A.14}$$

Similarly, for a fermion field, one obtains the contribution:

$$V_T(h) = -\frac{1}{32\pi^2}m^2\Lambda^2 + \frac{1}{128\pi^2}m^4 + \frac{1}{32\pi^2}\ln\frac{\Lambda}{m}m^4 + \frac{1}{2\pi^2}T^4 J_F(m^2/T^2) \tag{A.15}$$

where

$$J_F(m^2\beta^2) = \int_0^\infty dx x^2 \ln\left[1 + e^{-\sqrt{x^2+\beta^2 m^2}}\right]$$

. Now, as Λ is proportional to χ in a scale invariant model, the first two terms of Equations A.14 and A.15 can be included into the tree level potential through the redefinition of ξ and λ. Hence, the full thermal effective potential is given by:

$$V_T(h,\chi) = \frac{\lambda(\Lambda)}{4}\left[h^2 - \frac{v^2}{v_\chi^2}\chi^2\right]^2 + \sum_i n_i(-1)^{2s_i+1}\left[\frac{m_i^4}{32\pi^2}\ln\frac{\alpha\chi}{m_i} - \frac{1}{2\pi^2}T^4 J_i(m_i^2/T^2)\right] \tag{A.16}$$

where i runs over all relativistic particles, n_i is the number of degrees of freedom of the corresponding particle, s_i is the spin and $J_i(y)$ is $J_B(y)$ for bosons and $J_F(y)$ for fermions.

Bibliography

[1] A. Kobakhidze, C. Lagger, and A. Manning. "Constraining noncommutative spacetime from GW150914". In: *Phys. Rev.* D94.6 (2016), p. 064033. DOI: 10.1103/PhysRevD.94.064033. arXiv: 1607.03776 [gr-qc].

[2] A. Kobakhidze, C. Lagger, and A. Manning. "Probing the quantum fuzziness of space and time with gravitational waves". In: *Int. J. Mod. Phys.* D26.12 (2017), p. 1743005. DOI: 10.1142/S0218271817430052.

[3] A. Kobakhidze, C. Lagger, A. Manning, and J. Yue. "Gravitational waves from a supercooled electroweak phase transition and their detection with pulsar timing arrays". In: *Eur. Phys. J.* C77.8 (2017), p. 570. DOI: 10.1140/epjc/s10052-017-5132-y. arXiv: 1703.06552 [hep-ph].

[4] S. Arunasalam, A. Kobakhidze, C. Lagger, S. Liang, and A. Zhou. "Low temperature electroweak phase transition in the Standard Model with hidden scale invariance". In: *Phys. Lett.* B776 (2018), pp. 48–53. DOI: 10.1016/j.physletb.2017.11.017. arXiv: 1709.10322 [hep-ph].

[5] C. Lagger. "Backreaction of particle production on false vacuum decay". In: *Phys. Rev.* D93.2 (2016). [Erratum: Phys. Rev.D93,no.8,089902(2016)], p. 025024. DOI: 10.1103/PhysRevD.93.025024. arXiv: 1511.05256 [hep-th].

[6] G. Aad et al. "Observation of a new particle in the search for the Standard Model Higgs boson with the ATLAS detector at the LHC". In: *Phys. Lett.* B716 (2012), pp. 1–29. DOI: 10.1016/j.physletb.2012.08.020. arXiv: 1207.7214 [hep-ex].

[7] S. Chatrchyan et al. "Observation of a new boson at a mass of 125 GeV with the CMS experiment at the LHC". In: *Phys. Lett.* B716 (2012), pp. 30–61. DOI: 10.1016/j.physletb.2012.08.021. arXiv: 1207.7235 [hep-ex].

[8] B. P. Abbott et al. "Observation of Gravitational Waves from a Binary Black Hole Merger". In: *Phys. Rev. Lett.* 116.6 (2016), p. 061102. DOI: 10.1103/PhysRevLett.116.061102. arXiv: 1602.03837 [gr-qc].

[9] I. Newton, A. Motte, and N. W. Chittenden. *Newton's Principia: The Mathematical Principles of Natural Philosophy*. Daniel Adee, 45 Liberty Street., 1846. URL: https://books.google.com.au/books?id=f7PjjwEACAAJ.

[10] M. von Laue. *History of Physics*. Academic Press, 1950. URL: https://books.google.com.au/books?id=UehJvgAACAAJ.

[11] S. Hawking and R. Penrose. *The Nature of Space and Time*. Princeton University Press, 1996.

[12] A. Janiak. "Kant's Views on Space and Time". In: *The Stanford Encyclopedia of Philosophy*. Ed. by Edward N. Zalta. Winter 2016. Metaphysics Research Lab, Stanford University, 2016.

[13] K. Popper. *The Logic of Scientific Discovery*. Routledge Classics. Taylor & Francis, 2002. ISBN: 9780203994627. URL: https://books.google.com.au/books?id=T76Zd20IYlgC.

[14] T. S. Kuhn. *The Structure of Scientific Revolutions*. ISSR collection. University of Chicago Press, 1996. ISBN: 9780226458083. URL: https://books.google.com.au/books?id=xnjS401VuFMC.

[15] G. Galilei and S. Drake. *Dialogue Concerning the Two Chief World Systems, Ptolemaic and Copernican*. Modern Library Classics. Modern Library, 2001. ISBN: 9780375757662. URL: https://books.google.com.au/books?id=c-nIrKjBqOwC.

[16] C. A. Coulomb. "Premier mémoire sur l'électricité et le magnétisme". In: *Histoire de l'Academie royale des sciences*. Ed. by Académie royale des sciences Paris. De l'imprimerie royale, 1788, pp. 569–577. URL: https://books.google.com.au/books?id=by5EAAAAcAAJ&pg=PA569&redir_esc=y#v=onepage&q&f=false.

[17] C. A. Coulomb. "Second mémoire sur l'électricité et le magnétisme". In: *Histoire de l'Academie royale des sciences*. Ed. by Académie royale des sciences Paris. De l'imprimerie royale, 1788, pp. 578–611. URL: https://books.google.com.au/books?id=by5EAAAAcAAJ&pg=PA578&redir_esc=y#v=onepage&q&f=false.

[18] C. D. Murray and S. F. Dermott. *Solar System Dynamics*. Cambridge University Press, 1999. ISBN: 9780521575973. URL: https://books.google.com.au/books?id=aU6vcy5L8GAC.

[19] U. Le Verrier. "Lettre de M. Le Verrier à M. Faye sur la théorie de Mercure et sur le mouvement du périhélie de cette planète". In: *Comptes rendus hebdomadaires des séances de l'Académie des sciences*. Paris: Académie des sciences, 1859, pp. 379–383. URL: https://archive.org/stream/comptesrendusheb49acad#page/378/mode/2up.

[20] P. G. Roll, R. Krotkov, and R. H. Dicke. "The equivalence of inertial and passive gravitational mass". In: *Annals of Physics* 26 (1964), pp. 442–517. DOI: 10.1016/0003-4916(64)90259-3.

[21] S. Ducheyne. "Newton on action at a distance". In: *JOURNAL OF THE HISTORY OF PHILOSOPHY* 52.4 (2014), pp. 675–702. ISSN: 0022-5053. URL: https://biblio.ugent.be/publication/5782803.

[22] J. C. Maxwell. "A dynamical theory of the electromagnetic field". In: *Philosophical Transactions of the Royal Society of London* 155 (1865), pp. 459–513. DOI: 10.1098/rstl.1865.0008.

[23] A. A. Michelson and E. W. Morley. "On the Relative Motion of the Earth and the Luminiferous Ether". In: *Am. J. Sci.* 34 (1887), pp. 333–345. DOI: 10.2475/ajs.s3-34.203.333.

[24] A. Einstein. "On the electrodynamics of moving bodies". In: *Annalen Phys.* 17 (1905). [Annalen Phys.14,194(2005)], pp. 891–921. DOI: 10.1002/andp.200590006.

[25] O. Darrigol. "The Genesis of the Theory of Relativity". In: *Einstein, 1905–2005*. Ed. by T. Damour, O. Darrigol, B. Duplantier, and Vincent R. Vol. 47. Birkhäuser Basel: Progress in Mathematical Physics, 2005.

[26] A. Einstein. "Über das Relativitätsprinzip und die aus demselben gezogenen Folgerungen". In: *Jahrbuch der Radioaktivität und Elektronik* 4 (1908).

[27] A. Einstein. "On The influence of gravitation on the propagation of light". In: *Annalen Phys.* 35 (1911). [Annalen Phys.14,425(2005)], pp. 898–908. DOI: 10.1002/andp.200590033.

[28] A. Einstein. "The Field Equations of Gravitation". In: *Sitzungsber. Preuss. Akad. Wiss. Berlin (Math. Phys.)* 1915 (1915), pp. 844–847. URL: https://einsteinpapers.press.princeton.edu/vol6-trans/129.

[29] S. M. Carroll. *Spacetime and geometry: An introduction to general relativity*. Addison-Wesley, 2004. ISBN: 0805387323. URL: http://www.slac.stanford.edu/spires/find/books/www?cl=QC6:C37:2004.

[30] A. Einstein. "The Foundation of the General Theory of Relativity". In: *Annalen Phys.* 49.7 (1916). [Annalen Phys.354,no.7,769(1916)], pp. 769–822. DOI: 10.1002/andp.200590044.

[31] F. W. Dyson, A. S. Eddington, and C. Davidson. "A Determination of the Deflection of Light by the Sun's Gravitational Field, from Observations Made at the Total Eclipse of May 29, 1919". In: *Philosophical Transactions of the Royal Society of London Series A* 220 (1920), pp. 291–333. DOI: 10.1098/rsta.1920.0009.

[32] B. Pullman and A.R. Reisinger. *The Atom in the History of Human Thought*. Oxford University Press, 2001. ISBN: 9780195150407. URL: https://books.google.com.au/books?id=IQs5hur-BpgC.

[33] E.R. Scerri. *The Periodic Table: Its Story and Its Significance*. Oxford University Press, 2006. ISBN: 9780195345674. URL: https://books.google.com.au/books?id=yPtSszJMOOOC.

[34] M. Planck. "Ueber das Gesetz der Energieverteilung im Normalspectrum". In: *Annalen der Physik* 309 (1901), pp. 553–563. DOI: 10.1002/andp.19013090310.

[35] A. Einstein. "Über einen die Erzeugung und Verwandlung des Lichtes betreffenden heuristischen Gesichtspunkt". In: *Annalen der Physik* 322 (1905), pp. 132–148. DOI: 10.1002/andp.19053220607.

[36] E. Rutherford. "The scattering of alpha and beta particles by matter and the structure of the atom". In: *Phil. Mag. Ser.6* 21 (1911), pp. 669–688. DOI: 10.1080/14786440508637080.

[37] N. Bohr. "On the Constitution of Atoms and Molecules". In: *Phil. Mag. Ser.6* 26 (1913), pp. 1–24. DOI: 10.1080/14786441308634955.

[38] L. V. de Broglie. "Ondes et quanta". In: *Comptes Rendus Mathématique* 177 (1923), pp. 507–510. URL: https://www.academie-sciences.fr/pdf/dossiers/Broglie/Broglie_pdf/CR1923_p507.pdf.

[39] M. Born. "Zur Quantenmechanik der Stoßvorgänge". In: *Zeitschrift für Physik* 37.12 (1926), pp. 863–867. DOI: 10.1007/BF01397477. URL: https://doi.org/10.1007/BF01397477.

[40] E. Schrödinger. "Quantisierung als Eigenwertproblem". In: *Annalen der Physik* 384.4 (1926), pp. 361–376. DOI: 10.1002/andp.19263840404.

[41] Niels Bohr. "Discussion with Einstein on Epistemological Problems in Atomic Physics". In: *The Library of Living Philosophers, Volume 7. Albert Einstein: Philosopher-Scientist*. Ed. by Paul Arthur Schilpp. Open Court, 1949, pp. 199–241.

[42] W. Heisenberg. "Über quantentheoretische Umdeutung kinematischer und mechanischer Beziehungen." In: *Zeitschrift für Physik* 33.1 (1925), pp. 879–893. DOI: 10.1007/BF01328377.

[43] M. Born, W. Heisenberg, and P. Jordan. "Zur Quantenmechanik. II." In: *Zeitschrift für Physik* 35.8 (1926), pp. 557–615. ISSN: 0044-3328. DOI: 10.1007/BF01379806.

[44] W. Heisenberg. "Über den anschaulichen Inhalt der quantentheoretischen Kinematik und Mechanik". In: *Zeitschrift für Physik* 43.3 (1927), pp. 172–198. ISSN: 0044-3328. DOI: 10.1007/BF01397280.

[45] W. Pauli. "Über den Zusammenhang des Abschlusses der Elektronengruppen im Atom mit der Komplexstruktur der Spektren". In: *Zeitschrift fur Physik* 31 (1925), pp. 765–783. DOI: 10.1007/BF02980631.

[46] W. Gerlach and O. Stern. "Der experimentelle Nachweis der Richtungsquantelung im Magnetfeld". In: *Zeitschrift für Physik* 9.1 (1922), pp. 349–352. ISSN: 0044-3328. DOI: 10.1007/BF01326983. URL: https://doi.org/10.1007/BF01326983.

[47] P. A. M. Dirac. "The Quantum Theory of the Emission and Absorption of Radiation". In: *Proceedings of the Royal Society of London Series A* 114 (1927), pp. 243–265. DOI: 10.1098/rspa.1927.0039.

[48] P. A. M. Dirac. "The Quantum Theory of the Electron". In: *Proceedings of the Royal Society of London Series A* 117 (1928), pp. 610–624. DOI: 10.1098/rspa.1928.0023.

[49] P. A. M. Dirac. "The Quantum Theory of the Electron. Part II". In: *Proceedings of the Royal Society of London Series A* 118 (1928), pp. 351–361. DOI: 10.1098/rspa.1928.0056.

[50] C. D. Anderson. "The Positive Electron". In: *Phys. Rev.* 43 (6 1933), pp. 491–494. DOI: 10.1103/PhysRev.43.491.

[51] T. Y. Cao. *Conceptual Developments of 20th Century Field Theories*. Cambridge University Press, 1997, p. 451.

[52] A. Friedman. "Über die Krümmung des Raumes". In: *Zeitschrift für Physik* 10.1 (1922), pp. 377–386. ISSN: 0044-3328. DOI: 10.1007/BF01332580.

[53] G. Lemaître. "Un Univers homogène de masse constante et de rayon croissant rendant compte de la vitesse radiale des nébuleuses extra-galactiques". In: *Annales de la Société Scientifique de Bruxelles* 47 (1927), pp. 49–59.

[54] H. P. Robertson. "Kinematics and World-Structure". In: *Astrophys. J.* 82 (1935), p. 284. DOI: 10.1086/143681.

[55] A. G. Walker. "On Milne's Theory of World-Structure". In: *Proceedings of the London Mathematical Society, (Series 2) volume 42, p. 90-127* 42 (1937), pp. 90–127. DOI: 10.1112/plms/s2-42.1.90.

[56] V. M. Slipher. "Radial velocity observations of spiral nebulae". In: *The Observatory* 40 (1917), pp. 304–306.

[57] E. Hubble. "A Relation between Distance and Radial Velocity among Extra-Galactic Nebulae". In: *Proceedings of the National Academy of Science* 15 (1929), pp. 168–173. DOI: 10.1073/pnas.15.3.168.

[58] A. G. Riess et al. "Observational evidence from supernovae for an accelerating universe and a cosmological constant". In: *Astron. J.* 116 (1998), pp. 1009–1038. DOI: 10.1086/300499. arXiv: astro-ph/9805201 [astro-ph].

[59] S. Perlmutter et al. "Measurements of Omega and Lambda from 42 high redshift supernovae". In: *Astrophys. J.* 517 (1999), pp. 565–586. DOI: 10.1086/307221. arXiv: astro-ph/9812133 [astro-ph].

[60] A. A. Penzias and R. W. Wilson. "A Measurement of Excess Antenna Temperature at 4080 Mc/s." In: *Astrophys. J.* 142 (1965), pp. 419–421. DOI: 10.1086/148307.

[61] R. H. Dicke, P. J. E. Peebles, P. G. Roll, and D. T. Wilkinson. "Cosmic Black-Body Radiation." In: *Astrophys. J.* 142 (1965), pp. 414–419. DOI: 10.1086/148306.

[62] R. Durrer. "The cosmic microwave background: the history of its experimental investigation and its significance for cosmology". In: *Class. Quant. Grav.* 32.12 (2015), p. 124007. DOI: 10.1088/0264-9381/32/12/124007. arXiv: 1506.01907 [astro-ph.CO].

[63] S. Hossenfelder. *Lost in Math: How Beauty Leads Physics Astray*. Basic Books, 2018. ISBN: 9780465094264. URL: https://books.google.com.au/books?id=OvI3DwAAQBAJ.

[64] J. Butterfield. "Lost in Math? A review of 'Lost in Math: How Beauty Leads Physics Astray', by Sabine Hossenfelder". In: arXiv:1902.03480 (2019), arXiv:1902.03480. arXiv: 1902.03480 [physics.hist-ph].

[65] F. Zwicky. "Die Rotverschiebung von extragalaktischen Nebeln". In: *Helvetica Physica Acta* 6 (1933), pp. 110–127.

[66] F. Zwicky. "On the Masses of Nebulae and of Clusters of Nebulae". In: *Astrophys. J.* 86 (1937), p. 217. DOI: 10.1086/143864.

[67] V. C. Rubin and W. K. Ford. "Rotation of the Andromeda Nebula from a Spectroscopic Survey of Emission Regions". In: *Astrophys. J.* 159 (1970), p. 379. DOI: 10.1086/150317.

[68] K. Freese. "Review of Observational Evidence for Dark Matter in the Universe and in upcoming searches for Dark Stars". In: *EAS Publ. Ser.* 36 (2009), pp. 113–126. DOI: 10.1051/eas/0936016. arXiv: 0812.4005 [astro-ph].

[69] V. Sahni. "Dark matter and dark energy". In: *Lect. Notes Phys.* 653 (2004). [,141(2004)], pp. 141–180. DOI: 10.1007/b99562,10.1007/978-3-540-31535-3_5. arXiv: astro-ph/0403324 [astro-ph].

[70] S. Dodelson. "The Real Problem with MOND". In: *Int. J. Mod. Phys.* D20 (2011), pp. 2749–2753. DOI: 10.1142/S0218271811020561. arXiv: 1112.1320 [astro-ph.CO].

[71] J. Martin. "Everything You Always Wanted To Know About The Cosmological Constant Problem (But Were Afraid To Ask)". In: *Comptes Rendus Physique* 13 (2012), pp. 566–665. DOI: 10.1016/j.crhy.2012.04.008. arXiv: 1205.3365 [astro-ph.CO].

[72] M. E. Peskin and D. V. Schroeder. *An Introduction to quantum field theory*. Reading, USA: Addison-Wesley, 1995. ISBN: 9780201503975. URL: http://www.slac.stanford.edu/~mpeskin/QFT.html.

[73] M. D. Schwartz. *Quantum Field Theory and the Standard Model*. Cambridge University Press, 2014. ISBN: 1107034736. URL: http://www.cambridge.org/us/academic/subjects/physics/theoretical-physics-and-mathematical-physics/quantum-field-theory-and-standard-model.

[74] S. Carlip. "Quantum gravity: A Progress report". In: *Rept. Prog. Phys.* 64 (2001), p. 885. DOI: 10.1088/0034-4885/64/8/301. arXiv: gr-qc/0108040 [gr-qc].

[75] Joseph Polchinski. *String Theory*. Vol. 1. Cambridge Monographs on Mathematical Physics. Cambridge University Press, 1998. DOI: 10.1017/CBO9780511816079.

[76] C. Rovelli. "Loop quantum gravity". In: *Living Rev. Rel.* 1 (1998), p. 1. DOI: 10.12942/lrr-1998-1. arXiv: gr-qc/9710008 [gr-qc].

[77] D. Baumann. "Inflation". In: *Physics of the large and the small, TASI 09, proceedings of the Theoretical Advanced Study Institute in Elementary Particle Physics, Boulder, Colorado, USA, 1-26 June 2009*. 2011, pp. 523–686. DOI: 10.1142/9789814327183_0010. arXiv: 0907.5424 [hep-th].

[78] V. A. Kuzmin, V. A. Rubakov, and M. E. Shaposhnikov. "On the Anomalous Electroweak Baryon Number Nonconservation in the Early Universe". In: *Phys. Lett.* B155 (1985), p. 36. DOI: 10.1016/0370-2693(85)91028-7.

[79] M. Fukugita and T. Yanagida. "Baryogenesis Without Grand Unification". In: *Phys. Lett.* B174 (1986), pp. 45–47. DOI: 10.1016/0370-2693(86)91126-3.

[80] J. W. F. Valle. "Neutrino physics overview". In: *J. Phys. Conf. Ser.* 53 (2006), pp. 473–505. DOI: 10.1088/1742-6596/53/1/031. arXiv: hep-ph/0608101 [hep-ph].

[81] J. L. Cervantes-Cota, S. Galindo-Uribarri, and G-F. Smoot. "A Brief History of Gravitational Waves". In: *Universe* 2.3 (2016), p. 22. DOI: 10.3390/universe2030022. arXiv: 1609.09400 [physics.hist-ph].

[82] R. A. Hulse and J. H. Taylor. "Discovery of a pulsar in a binary system". In: *Astrophys. J.* 195 (1975), pp. L51–L53. DOI: 10.1086/181708.

[83] J. H. Taylor, L. A. Fowler, and P. M. McCulloch. "Measurements of general relativistic effects in the binary pulsar PSR 1913+16". In: *Nature* 277 (1979), pp. 437–440. DOI: 10.1038/277437a0.

[84] M. C. Guzzetti, N. Bartolo, M. Liguori, and S. Matarrese. "Gravitational waves from inflation". In: *Riv. Nuovo Cim.* 39.9 (2016), pp. 399–495. DOI: 10.1393/ncr/i2016-10127-1. arXiv: 1605.01615 [astro-ph.CO].

[85] A. Vilenkin. "Cosmic Strings and Domain Walls". In: *Phys. Rept.* 121 (1985), pp. 263–315. DOI: 10.1016/0370-1573(85)90033-X.

[86] T. Damour and A. Vilenkin. "Gravitational wave bursts from cosmic strings". In: *Phys. Rev. Lett.* 85 (2000), pp. 3761–3764. DOI: 10.1103/PhysRevLett.85.3761. arXiv: gr-qc/0004075 [gr-qc].

[87] B. P. Abbott et al. "Prospects for Observing and Localizing Gravitational-Wave Transients with Advanced LIGO, Advanced Virgo and KAGRA". In: *Living Rev. Rel.* 21.1 (2018), p. 3. DOI: 10.1007/s41114-018-0012-9. arXiv: 1304.0670 [gr-qc].

[88] K. Somiya. "Detector configuration of KAGRA: The Japanese cryogenic gravitational-wave detector". In: *Class. Quant. Grav.* 29 (2012), p. 124007. DOI: 10.1088/0264-9381/29/12/124007. arXiv: 1111.7185 [gr-qc].

[89] H. Audley et al. "Laser Interferometer Space Antenna". In: (2017). arXiv: 1702.00786 [astro-ph.IM].

[90] C. Cutler and D. E. Holz. "Ultra-high precision cosmology from gravitational waves". In: *Phys. Rev.* D80 (2009), p. 104009. DOI: 10.1103/PhysRevD.80.104009. arXiv: 0906.3752 [astro-ph.CO].

[91] S. Kawamura et al. "The Japanese space gravitational wave antenna: DECIGO". In: *Class. Quant. Grav.* 28 (2011), p. 094011. DOI: 10.1088/0264-9381/28/9/094011.

[92] G. Hobbs et al. "The International Pulsar Timing Array project: using pulsars as a gravitational wave detector". In: *Classical and Quantum Gravity* 27.8, 084013 (2010), p. 084013. DOI: 10.1088/0264-9381/27/8/084013. arXiv: 0911.5206 [astro-ph.SR].

[93] R. van Haasteren et al. "Placing limits on the stochastic gravitational-wave background using European Pulsar Timing Array data". In: *Mon. Not. Roy. Astron. Soc.* 414.4 (2011). [Erratum: Mon. Not. Roy. Astron. Soc.425,no.2,1597(2012)], pp. 3117–3128. DOI: 10.1111/j.1365-2966.2011.18613.x. arXiv: 1103.0576 [astro-ph.CO].

[94] R. M. Shannon et al. "Gravitational-wave Limits from Pulsar Timing Constrain Supermassive Black Hole Evolution". In: *Science* 342.6156 (2013), pp. 334–337. DOI: 10.1126/science.1238012. arXiv: 1310.4569 [astro-ph.CO].

[95] P. B. Demorest et al. "Limits on the Stochastic Gravitational Wave Background from the North American Nanohertz Observatory for Gravitational Waves". In: *The Astrophysical Journal* 762.2 (2013), p. 94. URL: http://stacks.iop.org/0004-637X/762/i=2/a=94.

[96] P. E. Dewdney, P. J. Hall, R. T. Schilizzi, and T. J. L. W. Lazio. "The Square Kilometre Array". In: *Proceedings of the IEEE* 97.8 (2009), pp. 1482–1496. ISSN: 0018-9219. DOI: 10.1109/JPROC.2009.2021005.

[97] N. Yunes, K. Yagi, and F. Pretorius. "Theoretical Physics Implications of the Binary Black-Hole Mergers GW150914 and GW151226". In: *Phys. Rev.* D94.8 (2016), p. 084002. DOI: 10.1103/PhysRevD.94.084002. arXiv: 1603.08955 [gr-qc].

[98] D. Blas, M. M. Ivanov, I. Sawicki, and S. Sibiryakov. "On constraining the speed of gravitational waves following GW150914". In: *JETP Lett.* 103.10 (2016). [Pisma Zh. Eksp. Teor. Fiz.103,no.10,708(2016)], pp. 624–626. DOI: 10.1134/S0021364016100040. arXiv: 1602.04188 [gr-qc].

[99] M. Sasaki, T. Suyama, T. Tanaka, and S. Yokoyama. "Primordial Black Hole Scenario for the Gravitational-Wave Event GW150914". In: *Phys. Rev. Lett.* 117.6 (2016). [erratum: Phys. Rev. Lett.121,no.5,059901(2018)], p. 061101. DOI: 10.1103/PhysRevLett.121.059901. arXiv: 1603.08338 [astro-ph.CO].

[100] S. Hossenfelder. "Minimal Length Scale Scenarios for Quantum Gravity". In: *Living Rev. Rel.* 16 (2013), p. 2. DOI: 10.12942/lrr-2013-2. arXiv: 1203.6191 [gr-qc].

[101] H. S. Snyder. "Quantized space-time". In: *Phys. Rev.* 71 (1947), pp. 38–41. DOI: 10.1103/PhysRev.71.38.

[102] A. Connes. "Non-commutative differential geometry". In: *Publications Mathématiques de l'Institut des Hautes Études Scientifiques* 62.1 (1985), pp. 41–144. ISSN: 1618-1913. DOI: 10.1007/BF02698807. URL: http://dx.doi.org/10.1007/BF02698807.

[103] F. Ardalan, H. Arfaei, and M. M. Sheikh-Jabbari. "Noncommutative geometry from strings and branes". In: *JHEP* 02 (1999), p. 016. DOI: 10.1088/1126-6708/1999/02/016. arXiv: hep-th/9810072 [hep-th].

[104] N. Seiberg and E. Witten. "String theory and noncommutative geometry". In: *JHEP* 09 (1999), p. 032. DOI: 10.1088/1126-6708/1999/09/032. arXiv: hep-th/9908142 [hep-th].

[105] M. R. Douglas and N. A. Nekrasov. "Noncommutative field theory". In: *Rev. Mod. Phys.* 73 (2001), pp. 977–1029. DOI: 10.1103/RevModPhys.73.977. arXiv: hep-th/0106048 [hep-th].

[106] R. J. Szabo. "Quantum field theory on noncommutative spaces". In: *Phys. Rept.* 378 (2003), pp. 207–299. DOI: 10.1016/S0370-1573(03)00059-0. arXiv: hep-th/0109162 [hep-th].

[107] I. Mocioiu, M. Pospelov, and R. Roiban. "Low-energy limits on the antisymmetric tensor field background on the brane and on the noncommutative scale". In: *Phys. Lett.* B489 (2000), pp. 390–396. DOI: 10.1016/S0370-2693(00)00928-X. arXiv: hep-ph/0005191 [hep-ph].

[108] M. Chaichian, M. M. Sheikh-Jabbari, and A. Tureanu. "Hydrogen atom spectrum and the Lamb shift in noncommutative QED". In: *Phys. Rev. Lett.* 86 (2001), p. 2716. DOI: 10.1103/PhysRevLett.86.2716. arXiv: hep-th/0010175 [hep-th].

[109] S. M. Carroll, J. A. Harvey, V. A. Kostelecky, C. D. Lane, and T. Okamoto. "Noncommutative field theory and Lorentz violation". In: *Phys. Rev. Lett.* 87 (2001), p. 141601. DOI: 10.1103/PhysRevLett.87.141601. arXiv: hep-th/0105082 [hep-th].

[110] X. Calmet. "What are the bounds on space-time noncommutativity?" In: *Eur. Phys. J.* C41 (2005), pp. 269–272. DOI: 10.1140/epjc/s2005-02226-9. arXiv: hep-ph/0401097 [hep-ph].

[111] B. P. Abbott et al. "Tests of general relativity with GW150914". In: *Phys. Rev. Lett.* 116.22 (2016). [Erratum: Phys. Rev. Lett.121,no.12,129902(2018)], p. 221101. DOI: 10.1103/PhysRevLett.116.221101. arXiv: 1602.03841 [gr-qc].

[112] K. Kajantie, M. Laine, K. Rummukainen, and M. E. Shaposhnikov. "Is there a hot electroweak phase transition at m(H) larger or equal to m(W)?" In: *Phys. Rev. Lett.* 77 (1996), pp. 2887–2890. DOI: 10.1103/PhysRevLett.77.2887. arXiv: hep-ph/9605288 [hep-ph].

[113] Y. Aoki, G. Endrodi, Z. Fodor, S. D. Katz, and K. K. Szabo. "The Order of the quantum chromodynamics transition predicted by the standard model of particle physics". In: *Nature* 443 (2006), pp. 675–678. DOI: 10.1038/nature05120. arXiv: hep-lat/0611014 [hep-lat].

[114] J.B. Hartle. *Gravity: An Introduction to Einstein's General Relativity*. Addison-Wesley, 2003. ISBN: 9780805386622. URL: https://books.google.com.au/books?id=ZHgpAQAAMAAJ.

[115] M. Maggiore. *Gravitational Waves: Volume 1: Theory and Experiments*. Gravitational Waves. OUP Oxford, 2008. ISBN: 9780198570745. URL: https://books.google.com.au/books?id=AqVpQgAACAAJ.

[116] M. Maggiore. *Gravitational Waves: Volume 2: Astrophysics and Cosmology*. OUP Oxford, 2018. ISBN: 9780191074479. URL: https://books.google.com.au/books?id=FGdRDwAAQBAJ.

[117] L. Blanchet. "Gravitational Radiation from Post-Newtonian Sources and Inspiralling Compact Binaries". In: *Living Rev. Rel.* 17 (2014), p. 2. DOI: 10.12942/lrr-2014-2. arXiv: 1310.1528 [gr-qc].

[118] A. Buonanno and T. Damour. "Effective one-body approach to general relativistic two-body dynamics". In: *Phys. Rev.* D59 (1999), p. 084006. DOI: 10.1103/PhysRevD.59.084006. arXiv: gr-qc/9811091 [gr-qc].

[119] E. Berti, V. Cardoso, and A. O. Starinets. "Quasinormal modes of black holes and black branes". In: *Class. Quant. Grav.* 26 (2009), p. 163001. DOI: 10.1088/0264-9381/26/16/163001. arXiv: 0905.2975 [gr-qc].

[120] L. Lehner and F. Pretorius. "Numerical Relativity and Astrophysics". In: *Ann. Rev. Astron. Astrophys.* 52 (2014), pp. 661–694. DOI: 10.1146/annurev-astro-081913-040031. arXiv: 1405.4840 [astro-ph.HE].

[121] B. P. Abbott et al. "Multi-messenger Observations of a Binary Neutron Star Merger". In: *Astrophys. J.* 848.2 (2017), p. L12. DOI: 10.3847/2041-8213/aa91c9. arXiv: 1710.05833 [astro-ph.HE].

[122] B. P. Abbott et al. "GW170817: Measurements of neutron star radii and equation of state". In: *Phys. Rev. Lett.* 121.16 (2018), p. 161101. DOI: 10.1103/PhysRevLett.121.161101. arXiv: 1805.11581 [gr-qc].

[123] G. D. Birkhoff and R. E. Langer. *Relativity and modern physics*. 1923.

[124] K. Schwarzschild. "On the gravitational field of a mass point according to Einstein's theory". In: *Sitzungsber. Preuss. Akad. Wiss. Berlin (Math. Phys.)* 1916 (1916), pp. 189–196. arXiv: physics/9905030 [physics].

[125] C. M. Will. "The Confrontation between General Relativity and Experiment". In: *Living Rev. Rel.* 17 (2014), p. 4. DOI: 10.12942/lrr-2014-4. arXiv: 1403.7377 [gr-qc].

[126] K. Akiyama et al. "First M87 Event Horizon Telescope Results. I. The Shadow of the Supermassive Black Hole". In: *Astrophys. J.* 875.1 (2019), p. L1. DOI: 10.3847/2041-8213/ab0ec7.

[127] L. Blanchet and G. Faye. "Lorentzian regularization and the problem of point - like particles in general relativity". In: *J. Math. Phys.* 42 (2001), pp. 4391–4418. DOI: 10.1063/1.1384864. arXiv: gr-qc/0006100 [gr-qc].

[128] L. Blanchet and G. Faye. "Hadamard regularization". In: *J. Math. Phys.* 41 (2000), pp. 7675–7714. DOI: 10.1063/1.1308506. arXiv: gr-qc/0004008 [gr-qc].

[129] L. Blanchet and G. Faye. "General relativistic dynamics of compact binaries at the third postNewtonian order". In: *Phys. Rev.* D63 (2001), p. 062005. DOI: 10.1103/PhysRevD.63.062005. arXiv: gr-qc/0007051 [gr-qc].

[130] P. C. Peters and J. Mathews. "Gravitational radiation from point masses in a Keplerian orbit". In: *Phys. Rev.* 131 (1963), pp. 435–439. DOI: 10.1103/PhysRev.131.435.

[131] P. C. Peters. "Gravitational Radiation and the Motion of Two Point Masses". In: *Phys. Rev.* 136 (1964), B1224–B1232. DOI: 10.1103/PhysRev.136.B1224.

[132] V. C. de Andrade, L. Blanchet, and G. Faye. "Third postNewtonian dynamics of compact binaries: Noetherian conserved quantities and equivalence between the harmonic coordinate and ADM Hamiltonian formalisms". In: *Class. Quant. Grav.* 18 (2001), pp. 753–778. DOI: 10.1088/0264-9381/18/5/301. arXiv: gr-qc/0011063 [gr-qc].

[133] L. Bernard, L. Blanchet, G. Faye, and T. Marchand. "Center-of-Mass Equations of Motion and Conserved Integrals of Compact Binary Systems at the Fourth Post-Newtonian Order". In: *Phys. Rev.* D97.4 (2018), p. 044037. DOI: 10.1103/PhysRevD.97.044037. arXiv: 1711.00283 [gr-qc].

[134] T. Damour, B. R. Iyer, and B. S. Sathyaprakash. "A Comparison of search templates for gravitational waves from binary inspiral". In: *Phys. Rev.* D63 (2001). [Erratum: Phys. Rev.D72,029902(2005)], p. 044023. DOI: 10.1103/PhysRevD.63.044023,10.1103/PhysRevD.72.029902. arXiv: gr-qc/0010009 [gr-qc].

[135] T. Damour and A. Nagar. "An Improved analytical description of inspiralling and coalescing black-hole binaries". In: *Phys. Rev.* D79 (2009), p. 081503. DOI: 10.1103/PhysRevD.79.081503. arXiv: 0902.0136 [gr-qc].

[136] P. Ajith et al. "Inspiral-merger-ringdown waveforms for black-hole binaries with non-precessing spins". In: *Phys. Rev. Lett.* 106 (2011), p. 241101. DOI: 10.1103/PhysRevLett.106.241101. arXiv: 0909.2867 [gr-qc].

[137] L. Santamaria et al. "Matching post-Newtonian and numerical relativity waveforms: systematic errors and a new phenomenological model for non-precessing black hole binaries". In: *Phys. Rev.* D82 (2010), p. 064016. DOI: 10.1103/PhysRevD.82.064016. arXiv: 1005.3306 [gr-qc].

[138] S. Khan, S. Husa, M. Hannam, F. Ohme, M. Pürrer, X. Jiménez F., and A. Bohé. "Frequency-domain gravitational waves from nonprecessing black-hole binaries. II. A phenomenological model for the advanced detector era". In: *Phys. Rev.* D93.4 (2016), p. 044007. DOI: 10.1103/PhysRevD.93.044007. arXiv: 1508.07253 [gr-qc].

[139] C. P. Burgess and G. D. Moore. *The standard model: A primer*. Cambridge University Press, 2006. ISBN: 9780511254857.

[140] M. Laine and A. Vuorinen. "Basics of Thermal Field Theory". In: *Lect. Notes Phys.* 925 (2016), pp.1–281. DOI: 10.1007/978-3-319-31933-9. arXiv: 1701.01554 [hep-ph].

[141] M. Quiros. "Finite temperature field theory and phase transitions". In: *Proceedings, Summer School in High-energy physics and cosmology: Trieste, Italy, June 29-July 17, 1998*. 1999, pp. 187–259. arXiv: hep-ph/9901312 [hep-ph].

[142] D. S. Gorbunov and V. A. Rubakov. *Introduction to the Theory of the Early Universe: Hot Big Bang Theory*. World Scientific Publishing Company, 2011. DOI: 10.1142/7874. URL: https://www.worldscientific.com/doi/abs/10.1142/7874.

[143] D. S. Gorbunov and V. A. Rubakov. *Introduction to the Theory of the Early Universe: Cosmological Perturbations and Inflationary Theory*. World Scientific Publishing Company, 2011. DOI: 10.1142/7873. URL: https://www.worldscientific.com/doi/abs/10.1142/7873.

[144] J. Z. Simon. "Higher-derivative Lagrangians, nonlocality, problems, and solutions". In: *Phys. Rev. D* 41 (12 1990), pp. 3720–3733. DOI: 10.1103/PhysRevD.41.3720. URL: https://link.aps.org/doi/10.1103/PhysRevD.41.3720.

[145] E. Noether. "Invariant variation problems". In: *Transport Theory and Statistical Physics* 1.3 (1971), pp. 186–207. DOI: 10.1080/00411457108231446. arXiv: physics/0503066 [physics.hist-ph].

[146] J. Gomis and S. Weinberg. "Are nonrenormalizable gauge theories renormalizable?" In: *Nucl. Phys.* B469 (1996), pp. 473–487. DOI: 10.1016/0550-3213(96)00132-0. arXiv: hep-th/9510087 [hep-th].

[147] H. Fritzsch, M. Gell-Mann, and H. Leutwyler. "Advantages of the Color Octet Gluon Picture". In: *Phys. Lett.* 47B (1973), pp. 365–368. DOI: 10.1016/0370-2693(73)90625-4.

[148] H. D. Politzer. "Reliable Perturbative Results for Strong Interactions?" In: *Phys. Rev. Lett.* 30 (1973), pp. 1346–1349. DOI: 10.1103/PhysRevLett.30.1346.

[149] D. J. Gross and F. Wilczek. "Ultraviolet Behavior of Nonabelian Gauge Theories". In: *Phys. Rev. Lett.* 30 (1973), pp. 1343–1346. DOI: 10.1103/PhysRevLett.30.1343.

[150] S. L. Glashow. "Partial Symmetries of Weak Interactions". In: *Nucl. Phys.* 22 (1961), pp. 579–588. DOI: 10.1016/0029-5582(61)90469-2.

[151] S. Weinberg. "A Model of Leptons". In: *Phys. Rev. Lett.* 19 (1967), pp. 1264–1266. DOI: 10.1103/PhysRevLett.19.1264.

[152] A. Salam. "Weak and Electromagnetic Interactions". In: *Conf. Proc.* C680519 (1968), pp. 367–377.

[153] F. Englert and R. Brout. "Broken Symmetry and the Mass of Gauge Vector Mesons". In: *Phys. Rev. Lett.* 13 (1964). [,157(1964)], pp. 321–323. DOI: 10.1103/PhysRevLett.13.321.

[154] P. W. Higgs. "Broken Symmetries and the Masses of Gauge Bosons". In: *Phys. Rev. Lett.* 13 (1964). [,160(1964)], pp. 508–509. DOI: 10.1103/PhysRevLett.13.508.

[155] G. S. Guralnik, C. R. Hagen, and T. W. B. Kibble. "Global Conservation Laws and Massless Particles". In: *Phys. Rev. Lett.* 13 (1964). [,162(1964)], pp. 585–587. DOI: 10.1103/PhysRevLett.13.585.

[156] J. Goldstone. "Field theories with Superconductor solutions". In: *Il Nuovo Cimento (1955-1965)* 19.1 (1961), pp. 154–164. ISSN: 1827-6121. DOI: 10.1007/BF02812722.

[157] J. Goldstone, A. Salam, and S. Weinberg. "Broken Symmetries". In: *Phys. Rev.* 127 (1962), pp. 965–970. DOI: 10.1103/PhysRev.127.965.

[158] S. R. Coleman and E. J. Weinberg. "Radiative Corrections as the Origin of Spontaneous Symmetry Breaking". In: *Phys. Rev.* D7 (1973), pp. 1888–1910. DOI: 10.1103/PhysRevD.7.1888.

[159] P. A. R. Ade et al. "Planck 2015 results. XIII. Cosmological parameters". In: *Astron. Astrophys.* 594 (2016), A13. DOI: 10.1051/0004-6361/201525830. arXiv: 1502.01589 [astro-ph.CO].

[160] M. Tanabashi et al. "Review of Particle Physics". In: *Phys. Rev. D* 98 (3 2018), p. 030001. DOI: 10.1103/PhysRevD.98.030001.

[161] S. Weinberg. "Gauge and global symmetries at high temperature". In: *Phys. Rev. D* 9 (12 1974), pp. 3357–3378. DOI: 10.1103/PhysRevD.9.3357. URL: https://link.aps.org/doi/10.1103/PhysRevD.9.3357.

[162] M. E. Carrington. "The Effective potential at finite temperature in the Standard Model". In: *Phys. Rev.* D45 (1992), pp. 2933–2944. DOI: 10.1103/PhysRevD.45.2933.

[163] B.-H. Liu, L. D. McLerran, and N. Turok. "Bubble nucleation and growth at a baryon number producing electroweak phase transition". In: *Phys. Rev.* D46 (1992), pp. 2668–2688. DOI: 10.1103/PhysRevD.46.2668.

[164] M. Dine, R. G. Leigh, P. Y. Huet, Andrei D. Linde, and Dmitri A. Linde. "Towards the theory of the electroweak phase transition". In: *Phys. Rev.* D46 (1992), pp. 550–571. DOI: 10.1103/PhysRevD.46.550. arXiv: hep-ph/9203203 [hep-ph].

[165] P. B. Arnold and O. Espinosa. "The Effective potential and first order phase transitions: Beyond leading-order". In: *Phys. Rev.* D47 (1993). [Erratum: Phys. Rev.D50,6662(1994)], p. 3546. DOI: 10.1103/PhysRevD.47.3546. arXiv: hep-ph/9212235 [hep-ph].

[166] M. Chaichian, P. Presnajder, M. M. Sheikh-Jabbari, and A. Tureanu. "Noncommutative standard model: Model building". In: *Eur. Phys. J.* C29 (2003), pp. 413–432. DOI: 10.1140/epjc/s2003-01204-7. arXiv: hep-th/0107055 [hep-th].

[167] M. Chaichian, A. Kobakhidze, and A. Tureanu. "Spontaneous reduction of noncommutative gauge symmetry and model building". In: *Eur. Phys. J.* C47 (2006), pp. 241–245. DOI: 10.1140/epjc/s2006-02547-1. arXiv: hep-th/0408065 [hep-th].

[168] X. Calmet, B. Jurco, P. Schupp, J. Wess, and M. Wohlgenannt. "The Standard model on noncommutative space-time". In: *Eur. Phys. J.* C23 (2002), pp. 363–376. DOI: 10.1007/s100520100873. arXiv: hep-ph/0111115 [hep-ph].

[169] P. Aschieri, B. Jurco, P. Schupp, and J. Wess. "Noncommutative GUTs, standard model and C,P,T". In: *Nucl. Phys.* B651 (2003), pp. 45–70. DOI: 10.1016/S0550-3213(02)00937-9. arXiv: hep-th/0205214 [hep-th].

[170] P. K. Joby, P. Chingangbam, and S. Das. "Constraint on noncommutative spacetime from PLANCK data". In: *Phys. Rev.* D91.8 (2015), p. 083503. DOI: 10.1103/PhysRevD.91.083503. arXiv: 1412.6036 [astro-ph.CO].

[171] X. Calmet and C. Fritz. "Inflation on a non-commutative space–time". In: *Phys. Lett.* B747 (2015), pp. 406–409. DOI: 10.1016/j.physletb.2015.06.033. arXiv: 1506.04049 [hep-th].

[172] A. H. Chamseddine. "Deforming Einstein's gravity". In: *Phys. Lett.* B504 (2001), pp. 33–37. DOI: 10.1016/S0370-2693(01)00272-6. arXiv: hep-th/0009153 [hep-th].

[173] P. Aschieri, C. Blohmann, M. Dimitrijevic, F. Meyer, P. Schupp, and J. Wess. "A Gravity theory on noncommutative spaces". In: *Class. Quant. Grav.* 22 (2005), pp. 3511–3532. DOI: 10.1088/0264-9381/22/17/011. arXiv: hep-th/0504183 [hep-th].

[174] X. Calmet and A. Kobakhidze. "Noncommutative general relativity". In: *Phys. Rev.* D72 (2005), p. 045010. DOI: 10.1103/PhysRevD.72.045010. arXiv: hep-th/0506157 [hep-th].

[175] P. Aschieri, M. Dimitrijevic, F. Meyer, and J. Wess. "Noncommutative geometry and gravity". In: *Class. Quant. Grav.* 23 (2006), pp. 1883–1912. DOI: 10.1088/0264-9381/23/6/005. arXiv: hep-th/0510059 [hep-th].

[176] A. Kobakhidze. "Theta-twisted gravity". In: *Int. J. Mod. Phys.* A23 (2008), pp. 2541–2545. DOI: 10.1142/S0217751X08041190. arXiv: hep-th/0603132 [hep-th].

[177] R. J. Szabo. "Symmetry, gravity and noncommutativity". In: *Class. Quant. Grav.* 23 (2006), R199–R242. DOI: 10.1088/0264-9381/23/22/R01. arXiv: hep-th/0606233 [hep-th].

[178] X. Calmet and A. Kobakhidze. "Second order noncommutative corrections to gravity". In: *Phys. Rev.* D74 (2006), p. 047702. DOI: 10.1103/PhysRevD.74.047702. arXiv: hep-th/0605275 [hep-th].

[179] P. Mukherjee and A. Saha. "A Note on the noncommutative correction to gravity". In: *Phys. Rev.* D74 (2006), p. 027702. DOI: 10.1103/PhysRevD.74.027702. arXiv: hep-th/0605287 [hep-th].

[180] A. Kobakhidze. "Noncommutative corrections to classical black holes". In: *Phys. Rev.* D79 (2009), p. 047701. DOI: 10.1103/PhysRevD.79.047701. arXiv: 0712.0642 [gr-qc].

[181] N. E. J. Bjerrum-Bohr, J. F. Donoghue, and B. R. Holstein. "Quantum corrections to the Schwarzschild and Kerr metrics". In: *Phys. Rev.* D68 (2003). [Erratum: Phys. Rev.D71,069904(2005)], p. 084005. DOI: 10.1103/PhysRevD.68.084005,10.1103/PhysRevD.71.069904. arXiv: hep-th/0211071 [hep-th].

[182] J. E. Moyal. "Quantum mechanics as a statistical theory". In: *Proc. Cambridge Phil. Soc.* 45 (1949), pp. 99–124. DOI: 10.1017/S0305004100000487.

[183] A. P. Balachandran, T. R. Govindarajan, C. Molina, and P. Teotonio-Sobrinho. "Unitary quantum physics with time-space noncommutativity". In: *JHEP* 10 (2004), p. 072. DOI: 10.1088/1126-6708/2004/10/072. arXiv: hep-th/0406125 [hep-th].

[184] O. Aharony, J. Gomis, and T. Mehen. "On theories with lightlike noncommutativity". In: *JHEP* 09 (2000), p. 023. DOI: 10.1088/1126-6708/2000/09/023. arXiv: hep-th/0006236 [hep-th].

[185] L. Blanchet, G. Faye, and B. Ponsot. "Gravitational field and equations of motion of compact binaries to 5/2 postNewtonian order". In: *Phys. Rev.* D58 (1998), p. 124002. DOI: 10.1103/PhysRevD.58.124002. arXiv: gr-qc/9804079 [gr-qc].

[186] L. Blanchet, T.t Damour, and B. R. Iyer. "Gravitational waves from inspiralling compact binaries: Energy loss and wave form to second postNewtonian order". In: *Phys. Rev.* D51 (1995). [Erratum: Phys. Rev.D54,1860(1996)], p. 5360. DOI: 10.1103/PhysRevD.51.5360,10.1103/PhysRevD.54.1860. arXiv: gr-qc/9501029 [gr-qc].

[187] M. S. Turner and F. Wilczek. "Relic gravitational waves and extended inflation". In: *Phys. Rev. Lett.* 65 (1990), pp. 3080–3083. DOI: 10.1103/PhysRevLett.65.3080.

[188] A. Kosowsky, M. S. Turner, and R. Watkins. "Gravitational radiation from colliding vacuum bubbles". In: *Phys. Rev.* D45 (1992), pp. 4514–4535. DOI: 10.1103/PhysRevD.45.4514.

[189] A. Kosowsky, M. S. Turner, and R. Watkins. "Gravitational waves from first order cosmological phase transitions". In: *Phys. Rev. Lett.* 69 (1992), pp. 2026–2029. DOI: 10.1103/PhysRevLett.69.2026.

[190] A. Kosowsky and M. S. Turner. "Gravitational radiation from colliding vacuum bubbles: envelope approximation to many bubble collisions". In: *Phys. Rev.* D47 (1993), pp. 4372–4391. DOI: 10.1103/PhysRevD.47.4372. arXiv: astro-ph/9211004 [astro-ph].

[191] M. Kamionkowski, A. Kosowsky, and M. S. Turner. "Gravitational radiation from first order phase transitions". In: *Phys. Rev.* D49 (1994), pp. 2837–2851. DOI: 10.1103/PhysRevD.49.2837. arXiv: astro-ph/9310044 [astro-ph].

[192] S. Coleman, J. Wess, and Bruno Zumino. "Structure of Phenomenological Lagrangians. I". In: *Phys. Rev.* 177 (5 1969), pp. 2239–2247. DOI: 10.1103/PhysRev.177.2239.

[193] C. G. Callan, S. Coleman, J. Wess, and B. Zumino. "Structure of Phenomenological Lagrangians. II". In: *Phys. Rev.* 177 (5 1969), pp. 2247–2250. DOI: 10.1103/PhysRev.177.2247.

[194] D. Binosi and A. Quadri. "Scalar Resonances in the Non-linearly Realized Electroweak Theory". In: *JHEP* 02 (2013), p. 020. DOI: 10.1007/JHEP02(2013)020. arXiv: 1210.2637 [hep-ph].

[195] A. Kobakhidze. "Standard Model with a distorted Higgs sector and the enhanced Higgs diphoton decay rate". In: (2012). arXiv: 1208.5180 [hep-ph].

[196] A. Kobakhidze, L. Wu, and J. Yue. "Electroweak Baryogenesis with Anomalous Higgs Couplings". In: *JHEP* 04 (2016), p. 011. DOI: 10.1007/JHEP04(2016)011. arXiv: 1512.08922 [hep-ph].

[197] J. T. S. Yue. "Higgs Properties at the LHC: Implications for the Standard Model and for Cosmology". PhD thesis. Sydney U., 2016.

[198] A. Kobakhidze, A. Manning, and J. Yue. "Gravitational waves from the phase transition of a nonlinearly realized electroweak gauge symmetry". In: *Int. J. Mod. Phys.* D26.10 (2017), p. 1750114. DOI: 10.1142/S0218271817501140. arXiv: 1607.00883 [hep-ph].

[199] C. T. Lu, J. Chang, K. Cheung, and J. S. Lee. "An exploratory study of Higgs-boson pair production". In: *JHEP* 08 (2015), p. 133. DOI: 10.1007/JHEP08(2015)133. arXiv: 1505.00957 [hep-ph].

[200] C. Wetterich. "Fine Tuning Problem and the Renormalization Group". In: *Phys. Lett.* 140B (1984), pp. 215–222. DOI: 10.1016/0370-2693(84)90923-7.

[201] W. A. Bardeen. "On naturalness in the standard model". In: *Ontake Summer Institute on Particle Physics Ontake Mountain, Japan, August 27-September 2, 1995*. 1995. URL: http://lss.fnal.gov/cgi-bin/find_paper.pl?conf-95-391.

[202] A. Kobakhidze and K. L. McDonald. "Comments on the Hierarchy Problem in Effective Theories". In: *JHEP* 07 (2014), p. 155. DOI: 10.1007/JHEP07(2014)155. arXiv: 1404.5823 [hep-ph].

[203] K. A. Meissner and H. Nicolai. "Conformal Symmetry and the Standard Model". In: *Phys. Lett.* B648 (2007), pp. 312–317. DOI: 10.1016/j.physletb.2007.03.023. arXiv: hep-th/0612165 [hep-th].

[204] R. Foot, A. Kobakhidze, and R. R. Volkas. "Electroweak Higgs as a pseudo-Goldstone boson of broken scale invariance". In: *Phys. Lett.* B655 (2007), pp. 156–161. DOI: 10.1016/j.physletb.2007.06.084. arXiv: 0704.1165 [hep-ph].

[205] A. Kobakhidze and S. Liang. "Standard Model with hidden scale invariance and light dilaton". In: (2017). arXiv: 1701.04927 [hep-ph].

[206] A. Kobakhidze and S. Liang. "Scale Invariant Top Condensate". In: (2017). arXiv: 1707.05942 [hep-ph].

[207] M. Shaposhnikov and D. Zenhausern. "Quantum scale invariance, cosmological constant and hierarchy problem". In: *Phys. Lett.* B671 (2009), pp. 162–166. DOI: 10.1016/j.physletb.2008.11.041. arXiv: 0809.3406 [hep-th].

[208] R. Foot, A. Kobakhidze, and R. R. Volkas. "Cosmological constant in scale-invariant theories". In: *Phys. Rev.* D84 (2011), p. 075010. DOI: 10.1103/PhysRevD.84.075010. arXiv: 1012.4848 [hep-ph].

[209] "First combination of Tevatron and LHC measurements of the top-quark mass". In: (2014). arXiv: 1403.4427 [hep-ex].

[210] A. Kobakhidze and A. Spencer-Smith. "Neutrino Masses and Higgs Vacuum Stability". In: *JHEP* 08 (2013), p. 036. DOI: 10.1007/JHEP08(2013)036. arXiv: 1305.7283 [hep-ph].

[211] R. D. Newman, E. C. Berg, and P. E. Boynton. "Tests of the gravitational inverse square law at short ranges". In: *Space Sci. Rev.* 148 (2009), pp. 175–190. DOI: 10.1007/s11214-009-9540-7.

[212] R. Foot, A. Kobakhidze, K. L. McDonald, and R. R. Volkas. "A Solution to the hierarchy problem from an almost decoupled hidden sector within a classically scale invariant theory". In: *Phys. Rev.* D77 (2008), p. 035006. DOI: 10.1103/PhysRevD.77.035006. arXiv: 0709.2750 [hep-ph].

[213] R. Foot, A. Kobakhidze, K. L. McDonald, and R. R. Volkas. "Renormalization-scale independence of the physical cosmological constant". In: *Phys. Lett.* B664 (2008), pp. 199–200. DOI: 10.1016/j.physletb.2008.05.029. arXiv: 0712.3040 [hep-th].

[214] L. Randall and G. Servant. "Gravitational waves from warped spacetime". In: *JHEP* 05 (2007), p. 054. DOI: 10.1088/1126-6708/2007/05/054. arXiv: hep-ph/0607158 [hep-ph].

[215] T. Konstandin, G. Nardini, and M. Quiros. "Gravitational Backreaction Effects on the Holographic Phase Transition". In: *Phys. Rev.* D82 (2010), p. 083513. DOI: 10.1103/PhysRevD.82.083513. arXiv: 1007.1468 [hep-ph].

[216] T. Konstandin and G. Servant. "Cosmological Consequences of Nearly Conformal Dynamics at the TeV scale". In: *JCAP* 1112 (2011), p. 009. DOI: 10.1088/1475-7516/2011/12/009. arXiv: 1104.4791 [hep-ph].

[217] S. Coleman. "The Fate of the False Vacuum. 1. Semiclassical Theory". In: *Phys. Rev.* D15 (1977). [Erratum: Phys. Rev.D16,1248(1977)], pp. 2929–2936. DOI: 10.1103/PhysRevD.15.2929.

[218] C. G. Callan and S. R. Coleman. "The Fate of the False Vacuum. 2. First Quantum Corrections". In: *Phys. Rev.* D16 (1977), pp. 1762–1768. DOI: 10.1103/PhysRevD.16.1762.

[219] I. Affleck. "Quantum Statistical Metastability". In: *Phys. Rev. Lett.* 46 (1981), p. 388. DOI: 10.1103/PhysRevLett.46.388.

[220] A. D. Linde. "Decay of the False Vacuum at Finite Temperature". In: *Nucl. Phys.* B216 (1983). [Erratum: Nucl. Phys.B223,544(1983)], p. 421. DOI: 10.1016/0550-3213(83)90293-6.

[221] A. Salvio, A. Strumia, N. Tetradis, and A. Urbano. "On gravitational and thermal corrections to vacuum decay". In: *JHEP* 09 (2016), p. 054. DOI: 10.1007/JHEP09(2016)054. arXiv: 1608.02555 [hep-ph].

[222] A. Ferrera. "Bubble nucleation in phi**4 models at all temperatures". In: *Phys. Rev.* D52 (1995), pp. 6717–6729. DOI: 10.1103/PhysRevD.52.6717. arXiv: hep-ph/9510379 [hep-ph].

[223] M. S. Turner, E. J. Weinberg, and L. M. Widrow. "Bubble nucleation in first order inflation and other cosmological phase transitions". In: *Phys. Rev.* D46 (1992), pp. 2384–2403. DOI: 10.1103/PhysRevD.46.2384.

[224] L. Leitao, A. Megevand, and A. D. Sanchez. "Gravitational waves from the electroweak phase transition". In: *JCAP* 1210 (2012), p. 024. DOI: 10.1088/1475-7516/2012/10/024. arXiv: 1205.3070 [astro-ph.CO].

[225] L. Leitao and A. Megevand. "Gravitational waves from a very strong electroweak phase transition". In: *JCAP* 1605.05 (2016), p. 037. DOI: 10.1088/1475-7516/2016/05/037. arXiv: 1512.08962 [astro-ph.CO].

[226] V. K. S. Shante and S. Kirkpatrick. "An introduction to percolation theory". In: *Advances in Physics* 20 (1971), pp. 325–357. DOI: 10.1080/00018737100101261.

[227] C. Caprini et al. "Science with the space-based interferometer eLISA. II: Gravitational waves from cosmological phase transitions". In: *JCAP* 1604.04 (2016), p. 001. DOI: 10.1088/1475-7516/2016/04/001. arXiv: 1512.06239 [astro-ph.CO].

[228] D. Bodeker and G. D. Moore. "Can electroweak bubble walls run away?" In: *JCAP* 0905 (2009), p. 009. DOI: 10.1088/1475-7516/2009/05/009. arXiv: 0903.4099 [hep-ph].

[229] D. Bodeker and G. D. Moore. "Electroweak Bubble Wall Speed Limit". In: *JCAP* 1705.05 (2017), p. 025. DOI: 10.1088/1475-7516/2017/05/025. arXiv: 1703.08215 [hep-ph].

[230] G. F. Mazenko, Robert M. Wald, and W. G. Unruh. "Does a Phase Transition in the Early Universe Produce the Conditions Needed for Inflation?" In: *Phys. Rev.* D31 (1985), pp. 273–282. DOI: 10.1103/PhysRevD.31.273.

[231] D. S. Goldwirth and T. Piran. "Inhomogeneity and the Onset of Inflation". In: *Phys. Rev. Lett.* 64 (1990), pp. 2852–2855. DOI: 10.1103/PhysRevLett.64.2852.

[232] D. S. Goldwirth and T. Piran. "Initial conditions for inflation". In: *Phys. Rept.* 214 (1992), pp. 223–291. DOI: 10.1016/0370-1573(92)90073-9.

[233] R. Brandenberger. "Initial conditions for inflation ? A short review". In: *Int. J. Mod. Phys.* D26.01 (2016), p. 1740002. DOI: 10.1142/S0218271817400028. arXiv: 1601.01918 [hep-th].

[234] E. Witten. "Cosmological Consequences of a Light Higgs Boson". In: *Nucl. Phys.* B177 (1981), pp. 477–488. DOI: 10.1016/0550-3213(81)90182-6.

[235] W. Buchmuller and D. Wyler. "The Effect of dilatons on the electroweak phase transition". In: *Phys. Lett.* B249 (1990), pp. 281–285. DOI: 10.1016/0370-2693(90)91256-B.

[236] S. Iso, P. D. Serpico, and K. Shimada. "QCD-Electroweak First-Order Phase Transition in a Supercooled Universe". In: *Phys. Rev. Lett.* 119.14 (2017), p. 141301. DOI: 10.1103/PhysRevLett.119.141301. arXiv: 1704.04955 [hep-ph].

[237] J. Gasser and H. Leutwyler. "Light Quarks at Low Temperatures". In: *Phys. Lett.* B184 (1987), pp. 83–88. DOI: 10.1016/0370-2693(87)90492-8.

[238] R. D. Pisarski and F. Wilczek. "Remarks on the Chiral Phase Transition in Chromodynamics". In: *Phys. Rev.* D29 (1984), pp. 338–341. DOI: 10.1103/PhysRevD.29.338.

[239] H. Gausterer and S. Sanielevici. "Can the Chiral Transition in QCD Be Described by a Linear σ Model in Three-dimensions?" In: *Phys. Lett.* B209 (1988), pp. 533–537. DOI: 10.1016/0370-2693(88)91188-4.

[240] M. Crawford and D. N. Schramm. "Spontaneous Generation of Density Perturbations in the Early Universe". In: *Nature* 298 (1982). [,333(1982)], pp. 538–540. DOI: 10.1038/298538a0.

[241] G. Servant. "Baryogenesis from Strong *CP* Violation and the QCD Axion". In: *Phys. Rev. Lett.* 113.17 (2014), p. 171803. DOI: 10.1103/PhysRevLett.113.171803. arXiv: 1407.0030 [hep-ph].

[242] C. Delaunay, C. Grojean, and J. D. Wells. "Dynamics of Non-renormalizable Electroweak Symmetry Breaking". In: *JHEP* 04 (2008), p. 029. DOI: 10.1088/1126-6708/2008/04/029. arXiv: 0711.2511 [hep-ph].

[243] J. Kehayias and S. Profumo. "Semi-Analytic Calculation of the Gravitational Wave Signal From the Electroweak Phase Transition for General Quartic Scalar Effective Potentials". In: *JCAP* 1003 (2010), p. 003. DOI: 10.1088/1475-7516/2010/03/003. arXiv: 0911.0687 [hep-ph].

[244] M. Kakizaki, S. Kanemura, and T. Matsui. "Gravitational waves as a probe of extended scalar sectors with the first order electroweak phase transition". In: *Phys. Rev.* D92.11 (2015), p. 115007. DOI: 10.1103/PhysRevD.92.115007. arXiv: 1509.08394 [hep-ph].

[245] K. Hashino, M. Kakizaki, S. Kanemura, and T. Matsui. "Synergy between measurements of gravitational waves and the triple-Higgs coupling in probing the first-order electroweak phase transition". In: *Phys. Rev.* D94.1 (2016), p. 015005. DOI: 10.1103/PhysRevD.94.015005. arXiv: 1604.02069 [hep-ph].

[246] K. Hashino, M. Kakizaki, S. Kanemura, P. Ko, and T. Matsui. "Gravitational waves and Higgs boson couplings for exploring first order phase transition in the model with a singlet scalar field". In: *Phys. Lett.* B766 (2017), pp. 49–54. DOI: 10.1016/j.physletb.2016.12.052. arXiv: 1609.00297 [hep-ph].

[247] F. P. Huang, Y. Wan, D.-G. Wang, Y.-F. Cai, and X. Zhang. "Hearing the echoes of electroweak baryogenesis with gravitational wave detectors". In: *Phys. Rev.* D94.4 (2016), p. 041702. DOI: 10.1103/PhysRevD.94.041702. arXiv: 1601.01640 [hep-ph].

[248] V. Vaskonen. "Electroweak baryogenesis and gravitational waves from a real scalar singlet". In: (2016). arXiv: 1611.02073 [hep-ph].

[249] W. Chao, H.-K. Guo, and J. Shu. "Gravitational Wave Signals of Electroweak Phase Transition Triggered by Dark Matter". In: (2017). arXiv: 1702.02698 [hep-ph].

[250] C. Balazs, A. Fowlie, A. Mazumdar, and G. White. "Gravitational waves at aLIGO and vacuum stability with a scalar singlet extension of the Standard Model". In: *Phys. Rev.* D95.4 (2017), p. 043505. DOI: 10.1103/PhysRevD.95.043505. arXiv: 1611.01617 [hep-ph].

[251] A. Beniwal, M. Lewicki, J. D. Wells, M. White, and A. G. Williams. "Gravitational wave, collider and dark matter signals from a scalar singlet electroweak baryogenesis". In: (2017). arXiv: 1702.06124 [hep-ph].

[252] R.-G. Cai, Z. Cao, Z.-K. G., S.-J. Wang, and T. Yang. "The Gravitational Wave Physics". In: (2017). arXiv: 1703.00187 [gr-qc].

[253] M. Maggiore. "Gravitational wave experiments and early universe cosmology". In: *Phys. Rept.* 331 (2000), pp. 283–367. DOI: 10.1016/S0370-1573(99)00102-7. arXiv: gr-qc/9909001 [gr-qc].

[254] S. J. Huber and T. Konstandin. "Gravitational Wave Production by Collisions: More Bubbles". In: *JCAP* 0809 (2008), p. 022. DOI: 10.1088/1475-7516/2008/09/022. arXiv: 0806.1828 [hep-ph].

[255] C. Caprini, R. Durrer, and G. Servant. "Gravitational wave generation from bubble collisions in first-order phase transitions: An analytic approach". In: *Phys. Rev.* D77 (2008), p. 124015. DOI: 10.1103/PhysRevD.77.124015. arXiv: 0711.2593 [astro-ph].

[256] M. Hindmarsh, S. J. Huber, K. Rummukainen, and D. J. Weir. "Gravitational waves from the sound of a first order phase transition". In: *Phys. Rev. Lett.* 112 (2014), p. 041301. DOI: 10.1103/PhysRevLett.112.041301. arXiv: 1304.2433 [hep-ph].

[257] M. Hindmarsh, S. J. Huber, K. Rummukainen, and D. J. Weir. "Numerical simulations of acoustically generated gravitational waves at a first order phase transition". In: *Phys. Rev.* D92.12 (2015), p. 123009. DOI: 10.1103/PhysRevD.92.123009. arXiv: 1504.03291 [astro-ph.CO].

[258] J. T. Giblin and J. B. Mertens. "Vacuum Bubbles in the Presence of a Relativistic Fluid". In: *JHEP* 12 (2013), p. 042. DOI: 10.1007/JHEP12(2013)042. arXiv: 1310.2948 [hep-th].

[259] J. T. Giblin and J. B. Mertens. "Gravitational radiation from first-order phase transitions in the presence of a fluid". In: *Phys. Rev.* D90.2 (2014), p. 023532. DOI: 10.1103/PhysRevD.90.023532. arXiv: 1405.4005 [astro-ph.CO].

[260] C. Caprini and R. Durrer. "Gravitational waves from stochastic relativistic sources: Primordial turbulence and magnetic fields". In: *Phys. Rev.* D74 (2006), p. 063521. DOI: 10.1103/PhysRevD.74.063521. arXiv: astro-ph/0603476 [astro-ph].

[261] T. Kahniashvili, A. Kosowsky, G. Gogoberidze, and Y. Maravin. "Detectability of Gravitational Waves from Phase Transitions". In: *Phys. Rev.* D78 (2008), p. 043003. DOI: 10.1103/PhysRevD.78.043003. arXiv: 0806.0293 [astro-ph].

[262] T. Kahniashvili, L. Campanelli, G. Gogoberidze, Y. Maravin, and B. Ratra. "Gravitational Radiation from Primordial Helical Inverse Cascade MHD Turbulence". In: *Phys. Rev.* D78 (2008). [Erratum: Phys. Rev.D79,109901(2009)], p. 123006. DOI: 10.1103/PhysRevD.78.123006, 10.1103/PhysRevD.79.109901. arXiv: 0809.1899 [astro-ph].

[263] T. Kahniashvili, L. Kisslinger, and T. Stevens. "Gravitational Radiation Generated by Magnetic Fields in Cosmological Phase Transitions". In: *Phys. Rev.* D81 (2010), p. 023004. DOI: 10.1103/PhysRevD.81.023004. arXiv: 0905.0643 [astro-ph.CO].

[264] C. Caprini, Ruth D., and G. Servant. "The stochastic gravitational wave background from turbulence and magnetic fields generated by a first-order phase transition". In: *JCAP* 0912 (2009), p. 024. DOI: 10.1088/1475-7516/2009/12/024. arXiv: 0909.0622 [astro-ph.CO].

[265] R. Jinno and M. Takimoto. "Gravitational waves from bubble collisions: analytic derivation". In: *Phys. Rev.* D95.2 (2017), p. 024009. DOI: 10.1103/PhysRevD.95.024009. arXiv: 1605.01403 [astro-ph.CO].

[266] C. J. Moore, R. H. Cole, and C. P. L. Berry. "Gravitational-wave sensitivity curves". In: *Class. Quant. Grav.* 32.1 (2015), p. 015014. DOI: 10.1088/0264-9381/32/1/015014. arXiv: 1408.0740 [gr-qc].

[267] D. Cutting, M. Hindmarsh, and D. J. Weir. "Gravitational waves from vacuum first-order phase transitions: from the envelope to the lattice". In: *Phys. Rev.* D97.12 (2018), p. 123513. DOI: 10.1103/PhysRevD.97.123513. arXiv: 1802.05712 [astro-ph.CO].

[268] J. Ellis, M. Lewicki, J. M. No, and V. Vaskonen. "Gravitational wave energy budget in strongly supercooled phase transitions". In: (2019). arXiv: 1903.09642 [hep-ph].

[269] C. Caprini, R. Durrer, and X. Siemens. "Detection of gravitational waves from the QCD phase transition with pulsar timing arrays". In: *Phys. Rev.* D82 (2010), p. 063511. DOI: 10.1103/PhysRevD.82.063511. arXiv: 1007.1218 [astro-ph.CO].

[270] V. A. Rubakov. "Particle creation during vacuum decay". In: *Nucl. Phys.* B245 (1984), p. 481. DOI: 10.1016/0550-3213(84)90443-7.

[271] G. V. Lavrelashvili, V. A. Rubakov, and P. G. Tinyakov. "Production of Fermion Pairs Associated With Decay of a Metastable Vacuum". In: *Theor. Math. Phys.* 66 (1986). [Teor. Mat. Fiz.66,66(1986)], pp. 44–52. DOI: 10.1007/BF01028937.

[272] T. Vachaspati and A. Vilenkin. "Quantum state of a nucleating bubble". In: *Phys. Rev.* D43 (1991), pp. 3846–3855. DOI: 10.1103/PhysRevD.43.3846.

[273] T. Tanaka, M. Sasaki, and K. Yamamoto. "Field theoretical description of quantum fluctuations in the multidimensional tunneling approach". In: *Phys. Rev.* D49 (1994), pp. 1039–1046. DOI: 10.1103/PhysRevD.49.1039.

[274] L. Landau. "Das Dämpfungsproblem in der Wellenmechanik". In: *Zeitschrift fur Physik* 45 (May 1927), pp. 430–441. DOI: 10.1007/BF01343064.

[275] E. Joos and H. D. Zeh. "The Emergence of classical properties through interaction with the environment". In: *Z. Phys.* B59 (1985), pp. 223–243. DOI: 10.1007/BF01725541.

[276] W. H. Zurek. "Decoherence, einselection, and the quantum origins of the classical". In: *Rev. Mod. Phys.* 75 (2003), pp. 715–775. DOI: 10.1103/RevModPhys.75.715.

[277] M. Schlosshauer. "Decoherence, the measurement problem, and interpretations of quantum mechanics". In: *Rev. Mod. Phys.* 76 (2004), pp. 1267–1305. DOI: 10.1103/RevModPhys.76.1267. arXiv: quant-ph/0312059 [quant-ph].

[278] G. Degrassi, S. Di Vita, J. Elias-Miro, J. R. Espinosa, G. F. Giudice, et al. "Higgs mass and vacuum stability in the Standard Model at NNLO". In: *JHEP* 1208 (2012), p. 098. DOI: 10.1007/JHEP08(2012)098. arXiv: 1205.6497 [hep-ph].

[279] F. Bezrukov, M. Y. Kalmykov, B. A. Kniehl, and M. Shaposhnikov. "Higgs Boson Mass and New Physics". In: *JHEP* 1210 (2012), p. 140. DOI: 10.1007/JHEP10(2012)140. arXiv: 1205.2893 [hep-ph].

[280] A. Spencer-Smith. "Higgs Vacuum Stability in a Mass-Dependent Renormalisation Scheme". In: (2014). arXiv: 1405.1975 [hep-ph].

[281] D. Buttazzo, G. Degrassi, P. P. Giardino, G. F. Giudice, F. Sala, et al. "Investigating the near-criticality of the Higgs boson". In: *JHEP* 1312 (2013), p. 089. DOI: 10.1007/JHEP12(2013)089. arXiv: 1307.3536 [hep-ph].

[282] A. V. Bednyakov, B. A. Kniehl, A. F. Pikelner, and O. L. Veretin. "Stability of the Electroweak Vacuum: Gauge Independence and Advanced Precision". In: *Phys. Rev. Lett.* 115.20 (2015), p. 201802. DOI: 10.1103/PhysRevLett.115.201802. arXiv: 1507.08833 [hep-ph].

[283] S. Coleman and F. De Luccia. "Gravitational Effects on and of Vacuum Decay". In: *Phys. Rev.* D21 (1980), p. 3305. DOI: 10.1103/PhysRevD.21.3305.

[284] S. W. Hawking and I. G. Moss. "Supercooled Phase Transitions in the Very Early Universe". In: *Phys. Lett.* B110 (1982), p. 35. DOI: 10.1016/0370-2693(82)90946-7.

[285] G. Isidori, G. Ridolfi, and A. Strumia. "On the metastability of the standard model vacuum". In: *Nucl. Phys.* B609 (2001), pp. 387–409. DOI: 10.1016/S0550-3213(01)00302-9. arXiv: hep-ph/0104016 [hep-ph].

[286] V. Branchina, E. Messina, and M. Sher. "Lifetime of the electroweak vacuum and sensitivity to Planck scale physics". In: *Phys. Rev.* D91 (2015), p. 013003. DOI: 10.1103/PhysRevD.91.013003. arXiv: 1408.5302 [hep-ph].

[287] A. Kobakhidze and A. Spencer-Smith. "Electroweak Vacuum (In)Stability in an Inflationary Universe". In: *Phys. Lett.* B722 (2013), pp. 130–134. DOI: 10.1016/j.physletb.2013.04.013. arXiv: 1301.2846 [hep-ph].

[288] A. Kobakhidze and A. Spencer-Smith. "The Higgs vacuum is unstable". In: (2014). arXiv: 1404.4709 [hep-ph].

[289] A. Hook, J. Kearney, B. Shakya, and K. M. Zurek. "Probable or Improbable Universe? Correlating Electroweak Vacuum Instability with the Scale of Inflation". In: *JHEP* 01 (2015), p. 061. DOI: 10.1007/JHEP01(2015)061. arXiv: 1404.5953 [hep-ph].

[290] J. Kearney, H. Yoo, and K. M. Zurek. "Is a Higgs Vacuum Instability Fatal for High-Scale Inflation?" In: *Phys. Rev.* D91.12 (2015), p. 123537. DOI: 10.1103/PhysRevD.91.123537. arXiv: 1503.05193 [hep-th].

[291] M. Fairbairn and R. Hogan. "Electroweak Vacuum Stability in light of BICEP2". In: *Phys. Rev. Lett.* 112 (2014), p. 201801. DOI: 10.1103/PhysRevLett.112.201801. arXiv: 1403.6786 [hep-ph].

[292] K. Enqvist, T. Meriniemi, and S. Nurmi. "Higgs Dynamics during Inflation". In: *JCAP* 1407 (2014), p. 025. DOI: 10.1088/1475-7516/2014/07/025. arXiv: 1404.3699 [hep-ph].

[293] M. Herranen, T. Markkanen, S. Nurmi, and A. Rajantie. "Spacetime curvature and the Higgs stability during inflation". In: *Phys. Rev. Lett.* 113.21 (2014), p. 211102. DOI: 10.1103/PhysRevLett.113.211102. arXiv: 1407.3141 [hep-ph].

[294] M. Herranen, T. Markkanen, S. Nurmi, and A. Rajantie. "Spacetime curvature and Higgs stability after inflation". In: (2015). arXiv: 1506.04065 [hep-ph].

[295] A. Shkerin and S. Sibiryakov. "On stability of electroweak vacuum during inflation". In: *Phys. Lett.* B746 (2015), pp. 257–260. DOI: 10.1016/j.physletb.2015.05.012. arXiv: 1503.02586 [hep-ph].

[296] Jose R. Espinosa, Gian F. Giudice, Enrico Morgante, Antonio Riotto, Leonardo Senatore, Alessandro Strumia, and Nikolaos Tetradis. "The cosmological Higgstory of the vacuum instability". In: *JHEP* 09 (2015), p. 174. DOI: 10.1007/JHEP09(2015)174. arXiv: 1505.04825 [hep-ph].

[297] J. R. Espinosa, G. F. Giudice, and A. Riotto. "Cosmological implications of the Higgs mass measurement". In: *JCAP* 0805 (2008), p. 002. DOI: 10.1088/1475-7516/2008/05/002. arXiv: 0710.2484 [hep-ph].

[298] L. Delle Rose, C. Marzo, and A. Urbano. "On the fate of the Standard Model at finite temperature". In: (2015). arXiv: 1507.06912 [hep-ph].

[299] V. Branchina and E. Messina. "Stability, Higgs Boson Mass and New Physics". In: *Phys. Rev. Lett.* 111 (2013), p. 241801. DOI: 10.1103/PhysRevLett.111.241801. arXiv: 1307.5193 [hep-ph].

[300] V. Branchina, E. Messina, and A. Platania. "Top mass determination, Higgs inflation, and vacuum stability". In: *JHEP* 09 (2014), p. 182. DOI: 10.1007/JHEP09(2014)182. arXiv: 1407.4112 [hep-ph].

[301] V. Branchina and E. Messina. "Stability and UV completion of the Standard Model". In: (2015). arXiv: 1507.08812 [hep-ph].

[302] B. Grinstein and C. W. Murphy. "Semiclassical Approach to Heterogeneous Vacuum Decay". In: (2015). arXiv: 1509.05405 [hep-ph].

[303] P. Burda, R. Gregory, and I. G. Moss. "Gravity and the stability of the Higgs vacuum". In: *Phys. Rev. Lett.* 115 (2015), p. 071303. DOI: 10.1103/PhysRevLett.115.071303. arXiv: 1501.04937 [hep-th].

[304] P. Burda, R. Gregory, and I. Moss. "Vacuum metastability with black holes". In: *JHEP* 08 (2015), p. 114. DOI: 10.1007/JHEP08(2015)114. arXiv: 1503.07331 [hep-th].

[305] J. S. Schwinger. "On gauge invariance and vacuum polarization". In: *Phys. Rev.* 82 (1951), pp. 664–679. DOI: 10.1103/PhysRev.82.664.

[306] L. Parker. "Quantized fields and particle creation in expanding universes. 1." In: *Phys. Rev.* 183 (1969), pp. 1057–1068. DOI: 10.1103/PhysRev.183.1057.

[307] E. T. Bell. "Partition Polynomials". In: *Annals of Mathematics*. Second Series 29.1/4 (1927), pp. 38–46. URL: http://www.jstor.org/stable/1967979.

[308] L. Comtet. *Advanced Combinatorics: The art of finite and infinite expansions*. Springer Science & Business Media, 1974.

[309] H. B. Callen and T. A. Welton. "Irreversibility and Generalized Noise". In: *Phys. Rev.* 83 (1 1951), pp. 34–40. DOI: 10.1103/PhysRev.83.34. URL: http://link.aps.org/doi/10.1103/PhysRev.83.34.

[310] A. O. Caldeira and A. J. Leggett. "Quantum tunneling in a dissipative system". In: *Annals Phys.* 149 (1983), pp. 374–456. DOI: 10.1016/0003-4916(83)90202-6.

[311] R. Bruinsma and Per Bak. "Quantum tunneling, dissipation, and fluctuations". In: *Phys. Rev. Lett.* 56 (5 1986), pp. 420–423. DOI: 10.1103/PhysRevLett.56.420. URL: http://link.aps.org/doi/10.1103/PhysRevLett.56.420.

[312] K. Fujikawa, S. Iso, M. Sasaki, and H. Suzuki. "Quantum tunneling with dissipation: Possible enhancement by dissipative interactions". In: *Phys. Rev. B* 46 (16 1992), pp. 10295–10309. DOI: 10.1103/PhysRevB.46.10295. URL: http://link.aps.org/doi/10.1103/PhysRevB.46.10295.

[313] E. Calzetta, A. Roura, and E. Verdaguer. "Vacuum decay in quantum field theory". In: *Phys. Rev.* D64 (2001), p. 105008. DOI: 10.1103/PhysRevD.64.105008. arXiv: hep-ph/0106091 [hep-ph].

[314] C. Kiefer, F. Queisser, and A. A. Starobinsky. "Cosmological Constant from Decoherence". In: *Class. Quant. Grav.* 28 (2011), p. 125022. DOI: 10.1088/0264-9381/28/12/125022. arXiv: 1010.5331 [astro-ph.CO].

[315] J. R. Espinosa and M. Quiros. "The Electroweak phase transition with a singlet". In: *Phys. Lett.* B305 (1993), pp. 98–105. DOI: 10.1016/0370-2693(93)91111-Y. arXiv: hep-ph/9301285 [hep-ph].